

9-30-1999

Final Technical Report For The Enhancement Of Autonomous Marine Vehicle Testing In The South Florida Testing Facility Range

South Florida ocean Measurement Center (SFOMC) Partners

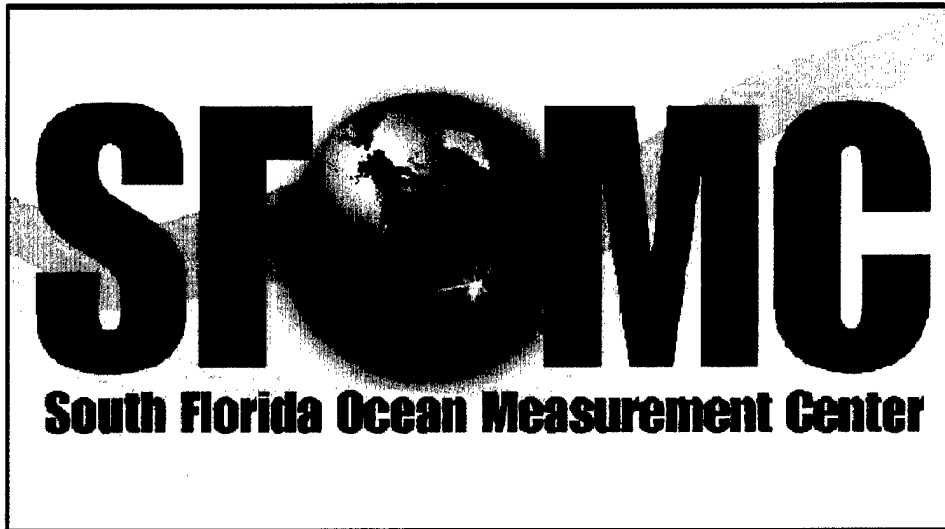
Find out more information about [Nova Southeastern University](#) and the [Halmos College of Natural Sciences and Oceanography](#).

Follow this and additional works at: https://nsuworks.nova.edu/occ_facreports



Part of the [Marine Biology Commons](#), and the [Oceanography and Atmospheric Sciences and Meteorology Commons](#)

Final Technical Report
 for
 The Enhancement of Autonomous
 Marine Vehicle Testing in the
 South Florida Testing Facility Range



19991019 029

Sponsored by:



DTIC QUALITY INSPECTED 4

DISTRIBUTION STATEMENT A
 Approved for Public Release
 Distribution Unlimited

FINAL TECHNICAL REPORT
FOR
**THE ENHANCEMENT OF AUTONOMOUS MARINE
VEHICLE TESTING IN THE SOUTH FLORIDA
TESTING FACILITY RANGE**

Prepared For:

Office of Naval Research
Ballston Centre Tower One
800 North Quincy Street
Arlington, VA. 22217-5660

Prepared By;

South Florida Ocean Measurement Center
101 North Beach Road
Dania Beach, FL. 33004

Under ONR Grant Number: N00014-98-1-0861

September 30, 1999

DISTRIBUTION STATEMENT A
Approved for Public Release
Distribution Unlimited

TABLE OF CONTENTS

| | |
|--|-----------|
| EXECUTIVE SUMMARY | 1 |
| 1. INTRODUCTION..... | 4 |
| 1.1 Goals | 4 |
| 1.2 Approach – The SFOMC | 4 |
| 1.3 Specific Objectives..... | 4 |
| 1.4 Outline of Report..... | 5 |
| 2. THE SOUTH FLORIDA OCEAN MEASUREMENT CENTER (SFOMC)..... | 6 |
| 2.1 Definition | 6 |
| 2.2 SFOMC Site Justification | 6 |
| 2.3 Project Management | 6 |
| 2.4 Expected Impact of the SFOMC..... | 6 |
| 2.5 Resource Sharing..... | 7 |
| 2.6 South Florida Testing Facility Support and Improvements | 8 |
| 2.6.1 Experiments to Evaluate AUV Capabilities | 9 |
| 2.6.2 Adverse Weather and 4-Dimensional Current Experiments..... | 10 |
| 2.6.3 Environmental Array and Data Analysis | 11 |
| 2.6.4 Very Long Range Shallow Water Acoustic Propagation | 11 |
| 2.6.5 Biological And Geological Inventory And Assessment | 12 |
| 2.6.6 Miscellaneous Support..... | 13 |
| 2.7 Shallow Water Multiplexer (MUX) Installation | 13 |
| 2.7.1 Background..... | 13 |
| 2.7.2 Mechanics and Structure..... | 14 |
| 2.7.2.1 Pressure Vessel..... | 14 |
| 2.7.3 Power and Electronics | 16 |
| 2.7.4 Data Communication | 18 |
| 2.7.5 Safety | 20 |
| 2.7.6 Testing & Deployment..... | 21 |
| 2.7.7 References..... | 26 |
| 2.8 SFOMC Workshop | 27 |

| | |
|--|------------|
| 3. RESEARCH ACTIVITIES..... | 28 |
| 3.1 Mine Hunting Experiment (Experiment 1)..... | 28 |
| 3.1.1 Results of an Experiment Using Auvs for Shallow Water Mine Reconnaissance | 28 |
| 3.1.2 Development of a 1.2 Mhz Chirp Sidescan Sonar for Mine Classification by AUVs..... | 40 |
| 3.2 Adverse Weather Experiment (Experiment 2)..... | 46 |
| 3.2.1 Adverse Weather Experiment (Experiment 2) | 47 |
| 3.2.2 Measurements of the Ambient Acoustic Environment of the SFTF Range using the Ambient Noise Sonar..... | 61 |
| 3.2.3 Docking System For Fau Ocean Explorer Class Auvs Using A Low Cost, High Accuracy Short Baseline Positioning System..... | 70 |
| 3.2.4 Acoustic Communication using SFOMC Shallow Water Multiplexer | 78 |
| 3.3 Four-Dimensional Current Experiment (Experiment 3) | 82 |
| 3.3.1 Goals..... | 82 |
| 3.3.2 Motivations | 82 |
| 3.3.3 Long Term Objectives | 82 |
| 3.3.4 Accomplishments..... | 83 |
| 3.3.5 Results: | 89 |
| 3.3.6. Summary | 93 |
| 3.4 Environmental Array and Data Analysis (Experiment 4) | 95 |
| 3.5 Development of a Natural Laboratory for the Study of Low Frequency Shallow Water Acoustic Propagation, Reverberation and Ambient Noise (Experiment 5) | 104 |
| 3.6 Bio/Geological Inventory and Assessment (Experiment 6)..... | 128 |
| 3.6.1 Introduction..... | 128 |
| 3.6.2. Environmental (Biological/Geological) Goals..... | 128 |
| 3.6.3. Project Tasks..... | 129 |
| 4. SUMMARY..... | 141 |
| APPENDICES..... | 143 |
| Appendix 2.7..... | 144 |
| Appendix 3.2.3..... | 152 |
| Appendix 3.6..... | 164 |

Final Technical Report for the Enhancement of Autonomous Marine Vehicle Testing in the South Florida Testing Facility Range

EXECUTIVE SUMMARY

Of critical importance to the US Navy is the enhancement of littoral war fighting capability. Clandestine rapid environmental assessment and mine reconnaissance are two significant aspects of that capability. Autonomous Underwater Vehicles (AUVs) can be important to the successful performance of these tasks. This report describes the research and development of several related technologies such as; sampling methodologies; sensor and navigation performance; and operational envelopes including range, sea state, and mission duration.

This report is submitted by the South Florida Ocean Measurement Center (SFOMC). The SFOMC partnership involves the Naval Surface Warfare Center, Carderock Division (NSWCCD), Florida Atlantic University (FAU), University of South Florida (USF), University of Miami Rosenstiel School of Marine and Atmospheric Science (UM-RSMAS), Nova Southeastern University Oceanographic Center (NSUOC), National Oceanic and Atmospheric Administration-Atlantic Oceanographic and Meteorological Laboratory (NOAA-AOML) and the Harbor Branch Oceanographic Institution (HBOI). The Center was established for collaborative research efforts in ocean engineering and oceanography in South Florida. In response to ONR, collaborative marine vehicle research has been conducted at the NSWCCD South Florida Testing Facility (SFTF) over the past year. The objectives of these experiments were to carry out a series of specific experiments to further Navy ocean technology and scientific capabilities, as well as to provide the scientific community with a natural ocean laboratory.

Six scientific experiments were carried out in the SFTF Range. The existing infrastructure at the range was enhanced to achieve the scientific goals of these experiments. However, this resulted in a well instrumented, calibrated site that will be utilized for oceanographic and engineering studies using marine vehicles well into the future.

The six initial experiments conducted under this ONR task were:

1. An AUV coastal mine reconnaissance and surveillance tasks experiment.
2. An experiment to evaluate the reliability of deploying and operating AUVs in shallow water during adverse weather conditions.
3. An investigation into the performance of AUV-based sensor systems combined with surface radar systems for mapping surface and subsurface currents.
4. An evaluation of physical-oceanographic variability as it effects AUV operations and Navy missions.
5. An experiment to quantify range-dependent variations of the environment on long-range transmission of sound in the littoral ocean.

6. A baseline survey of the biological, ecological and geological environmental conditions of the SFTF to enhance environmental stewardship and optimize sampling by the AUV and other sensors, coupled with preliminary evaluation of direct AUV biological assessment.

The six experiments were carried out with significant effort and to a high degree of success, demonstrating the versatility of mobile AUV platforms for carrying out MCM missions and for coastal oceanography. The experience gained during the MCM experiment will help to establish procedures for post processing data and determining environmental conditions. The Adverse Weather and 4-D Current experiments demonstrated how AUV-based measurements can be used in conjunction with ship-based and fixed measurements to characterize complex physical processes in a shallow water environment. The 3-D environmental array is in place and together with the OSCAR formed the basis of the fixed measurement system on the range. Significant data have been collected during the experiments and are currently being analyzed. The analysis will form the basis of long-term studies of air-sea interaction and of the impact of the Florida Current meanders on the coastal environment. The acoustic transceivers are in place and are expected to be utilized extensively during the next phase for determining acoustic propagation characteristics in a complex environment. Bio/Geological surveys of the range focused on determining the biodiversity of the in-water laboratory and it is expected to examine the seasonal variations during the next phase.

Improvements to the SFTF infrastructure accomplished to support these experiments included:

1. Development of an AUV and sensor support station hard wired to shore.
2. Deployment of multiple permanent environmental monitoring arrays.
3. Improvements to existing offshore node in 200m of water to support acoustic experiments.

The shallow water MUX was designed, fabricated and installed on the range and provided power and shore-based communication link to the instruments during the summer experiments. The design and preliminary tests have been completed in the development of the Docking Station and further work is expected during the next phase. The 200m node was refurbished and re-installed to interface with three new acoustic receiving arrays.

Successes were realized throughout the planning, construction, installation and experimentation phases. Some problems were encountered and are discussed in the text. However, most were overcome and did not significantly impact the results. An overview of what was conducted and a significant amount of preliminary data is presented in this report. Independent reports for each experiment will be published in appropriate journals as analysis is completed.

These studies are of importance to the Navy because they improve the understanding of AUV mounted sensor system performance for shallow water mine hunting and surveillance tasks, assess AUV performance as oceanographic sensor platforms in adverse weather, and demonstrate the use of AUVs when integrated with other ocean sensor systems. In addition, the project has

improved the understanding of the physical and biological oceanography in shallow water environments and has demonstrated how AUVs can be used to improve environmental monitoring. The physical oceanographic measurements also provided important information on how AUV shallow water mine hunting and surveillance programs can be optimized by taking into consideration the environmental conditions in the area of interest.

Final Technical Report for the Enhancement of Autonomous Marine Vehicle Testing in the South Florida Testing Facility Range

1. INTRODUCTION

This report is submitted by the South Florida Ocean Measurement Center (SFOMC) for collaborative marine vehicle research at the Naval Surface Warfare Center Carderock Division (NSWCCD) South Florida Testing Facility (SFTF).

1.1 Goals

The goal of this research project was to evaluate the performance of marine vehicles by carrying out a number of scientific experiments at the SFTF Range. Central to this theme was the characterization of the influence of physical, acoustic, biological and geological processes in the ocean on operational aspects of Autonomous Underwater Vehicles (AUVs). These vehicles are a new and important technology for the Navy because they provide the ability to survey shallow water regions in a systematic manner, using a number of small, inexpensive, unmanned vehicles.

A key aspect of the effort was the integration of AUV technology with other observing techniques to study various properties of the coastal ocean. The SFTF range is an excellent location for this purpose because it provides a domain rich in oceanic variability, a domain that is therefore adequate to assess a wide range of environmental conditions on AUV operations.

1.2 Approach – The SFOMC

The SFOMC partnership involves the Naval Surface Warfare Center Carderock Division (NSWCCD), Florida Atlantic University (FAU), University of South Florida (USF), University of Miami Rosenstil School of Marine and Atmospheric Science (UM-RSMAS), Nova Southeastern University Oceanographic Center (NSUOC), the National Oceanic and Atmospheric Administration-Atlantic Oceanographic and Meteorological Laboratory (NOAA-AOML) and The Harbor Branch Oceanographic Institution (HOBi). This Center was established for collaborative research efforts in ocean engineering and oceanography in South Florida. One objective of the Center is to provide the scientific community with a natural ocean laboratory within the existing SFTF range operated by NSWCCD. More details about the Center can be found in section 2 of this report.

1.3 Specific Objectives

This report describes six scientific experiments that were carried out in the SFTF Range. To achieve the scientific goals of these experiments the existing infrastructure at the range was enhanced with the specific objective of providing a calibrated site for oceanographic and engineering studies for underwater marine vehicles. The central theme of the oceanographic experiments was to understand and calibrate the underwater environment with respect to the physics, acoustics, geology, and biology of the range. As part of these studies extensive oceanographic measurement equipment was installed enabling long term observations that did and will support these and future experiments. A central theme in the engineering studies is to

improve the understanding of AUV performance capabilities. These studies included the development of a permanent AUV underwater docking facility so that multiple AUV sampling schemes can be carried out. This will enable AUVs to operate over extended periods and, in the longer term, provide a facility for ongoing AUV research.

The scientific objectives of the six experiments were:

1. To characterize the remote sampling performance of AUVs and sensor systems for coastal mine reconnaissance and surveillance tasks; and to evaluate the impact of the environment on navigation, communications, and object detection/classification sensors.
2. To evaluate the reliability of deploying and operating AUVs in stormy weather and high sea states including the quantification of the effects on AUV navigation, communication and control performances. In addition an extensive data set was collected on the environmental properties of the shallow water column during high sea states, including the effect of reverberation on the acoustic sensors.
3. To investigate the performance of AUV-based sensor systems combined with surface radar systems for mapping the subsurface submesoscale dynamics associated with small-scale eddies and internal waves on the shelf circulation influenced by tides, low-frequency flows, current, and surface winds, and the net impact of these processes on AUV performance and acoustic propagation.
4. To provide a detailed description of the physical-oceanographic variability that takes place within the SFTF Range on time scales from hourly to seasonal, and to identify the processes that cause this variability.
5. To quantify range-dependent variations in bathymetry and inhomogeneous bottom properties and variability in the sound speed profiles induced by internal waves on long-range transmission of sound in the littoral ocean.
6. To conduct a baseline survey of the biological, ecological and geological environmental conditions of the SFTF to optimize sampling by the AUV and other sensors, coupled with preliminary evaluation of direct AUV biological assessment

The six experiments described above were conducted in the SFTF over the past year utilizing the enhanced infrastructure for marine vehicle research activities.

1.4 Outline of Report

Section 2 provides an overview of the site and improvements affected to support these experiments. This includes support provided by the Navy and a detailed description of the FAU multiplexer used as the hub for the suite of AUV support sensors. Section 3 gives detailed descriptions of the six experiments which were conducted and results to date. Section 4 provides summary information.

2. THE SOUTH FLORIDA OCEAN MEASUREMENT CENTER (SFOMC)

2.1 Definition

While the need to develop technology for future naval forces and to better understand the ocean environment remains paramount, the need to do so in a cost effective manner has taken on increased importance. Creating partnerships that bring together complementary strengths and interests will play a key role in addressing the Navy's technology and science needs in a cost effective manner. With this objective a consortium of academic and government entities have come together to form the SFOMC; building on their respective technical strengths, assets, and shared interests. The SFOMC couples Navy ocean measurement range assets with university science and engineering expertise, technology and measurement equipment.

The partnership involves the Naval Surface Warfare Center Carderock Division (NSWCCD), Florida Atlantic University (FAU), University of South Florida (USF), University of Miami Rosenstil School of Marine and Atmospheric Science (UM-RSMAS), Nova Southeastern University Oceanographic Center (NSUOC), The National Oceanic and Atmospheric Administration-Atlantic Oceanographic and Meteorological Laboratory (NOAA-AOML), and The Harbor Branch Oceanographic Institution (HOBI).

2.2 SFOMC Site Justification

Lying on the southeast coast of Florida, at a point closest to the continental shelf edge and Florida Current, (see figure 2.2.1) the SFOMC was build on the existing SFTF range. This brought together a rich sensor system to measure the atmosphere, sea surface, and the ocean in 4 dimensional aspects. Real-time data links are hardwired to shore increasing the infrastructure of fixed and mobile sensor suites. This has facilitated the development of an autonomous real-time Internet observatory for continuously monitoring the effects of wind stress, upper layer mixing, wave effects on gas transfer and climate change, wave/coastal boundary region interaction, inlet/continental shelf interactions, and internal wave-driven currents and eddies.

2.3 Project Management

NSWCCD and FAU have been sharing the coordination role to insure the various elements of the SFOMC effort were carried out in a timely and productive fashion. The multi institutional SFOMC, which was formed by MOUs between the partners, met on at least a monthly basis in support of these projects. These meetings are anticipated to continue as the Center continues contributing to the scientific community.

2.4 Expected Impact of the SFOMC

1. Provide scientific and technical expertise for the US Navy in handling mine countermeasure operations in hostile and adverse weather conditions.
2. Leverage extensive, existing and developing infrastructure and resources to provide considerable increased capability for a relatively small investment.

3. Enhance existing partnerships among NSWCCD, NOAA, and Florida universities; and provide a basis for expanding the partnership in the future to organizations and academic institutions beyond the State.
4. Create an opportunity for a broad range of science and engineering research on a more cost-effective basis.
5. Coalesce range capabilities, systems and instrumentation of the partners into one location to enhance research for the scientific community.
6. Contribute to the transfer of science and technology to education, application and commercialization.

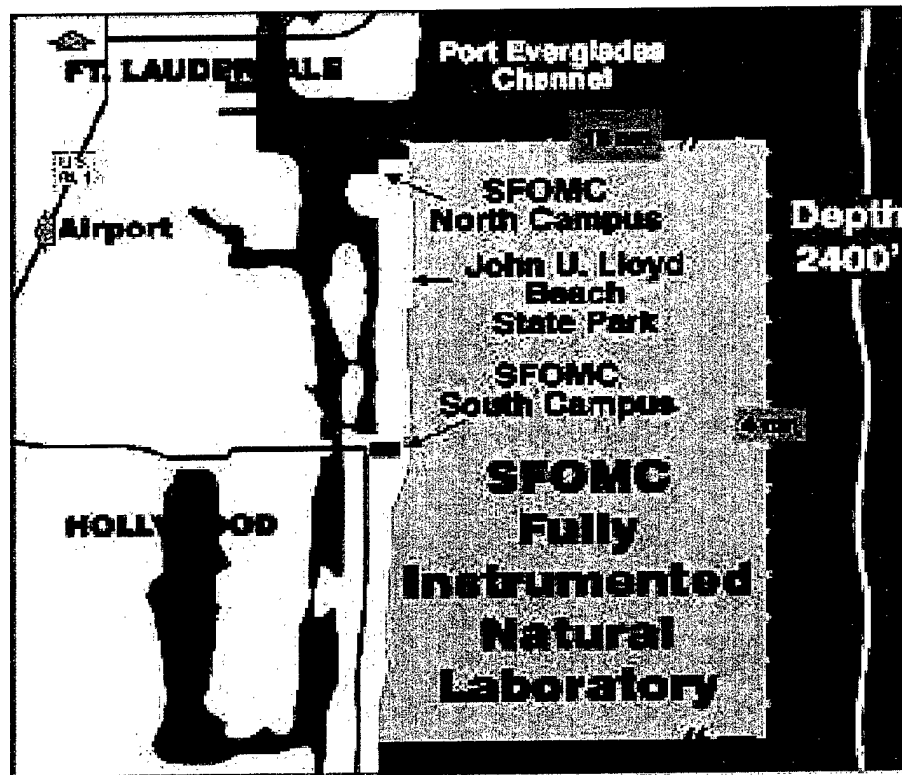


Figure 2.2.1 South Florida Ocean Measurement Center Site

2.5 Resource Sharing

The SFOMC encompasses several major features that are associated with combining resources and capabilities. First, the SFOMC capitalized on an existing ocean measurement range at the Navy's South Florida Testing Facility that provides access to both shallow and deep water near land. The site is ideal for the cost effective development of capabilities for the future Navy. In addition, the confluence of nearby academic institutions with their pool of scientific and

technical talent and physical assets that span the range of relevant engineering and science issues identified as being central to the Navy's future serve to provide a resident technical staff that can cost effectively employ the unique features of the ocean measurement range. Importantly, these institutions were already significantly involved in ongoing research for the Navy. The result is a natural ocean laboratory unusually well suited to support and drive the advancement of naval technology and science capabilities for now and into the future.

Shared resources include:

1. NSWCCD - SFTF in water range and shore based support infrastructure, 2 ADCPs, vessels, radar and tracking systems, cables and \$2.7M for new shore-side support construction.
2. FAU - Lab space in Sea-Tech. Support for information dissemination on the SFOMC Web site and FAU research vessel time. FAU is also providing a long-term \$1/year lease to the Navy in order to co-locate a new Navy building next to the FAU SeaTech laboratory, thus providing greater space and functionality for the SFOMC affiliates.
3. University of Miami 3-d Hydrophone array (128 elements) and mooring components, two self recording 12 element thermister arrays, and The Miami Sound Machine - an autonomous moored, high-power, broad-band and low-frequency sound projector (frequency range 100 to 3200 Hz), and the Ocean Surface Current Radar (OSCR) system for 1 month.
4. NSUOC - small boats, measurements, analysis, lab equipment.
5. NOAA-AOML - 1 ADCP.

2.6 South Florida Testing Facility Support and Improvements

W Venezia, T Metz (SFTF)

The SFTF range, with over 300 miles of existing in-water fiber optic and electrical cables and a wide variety of in-water measurement and tracking systems, is the primary in-water testing facility for the South Florida Ocean Measurement Center (SFOMC) projects and programs. The site offshore Fort Lauderdale was originally selected by the Naval Ordnance Laboratory to develop and test the CAPTOR mine because it provides deep water close to shore. The SFTF range, where 600 feet of water is found just three miles off the beach, is located at the narrowest point of the continental shelf and provides easy access for surface ships and submarines with relatively low cost for cabling to all water depths of interest in a littoral environment. Until 1994 the range was used primarily to support various mine warfare development programs including SLIMM, SUBSTRIKE, and CAPTOR. Many mine research programs were also conducted such as Propelled Rocket Ascent Mine (PRAM), Intermediate Water Depth (IWD) mine, Advanced Sea Mine (ASM), and currently Littoral Sea Mine (LSM) testing. The work requires a seafloor space under Navy control and the ability to control the air and sea surface as needed. The range maintains a restricted bottom anchorage area and, as needed, can control the surface (Navy Range

Control) and air (designated Water Bug air space). The history of the range includes underwater, surface and air test operations. Underwater testing includes shooting of exercise torpedoes and controlled maneuvers over signature gathering sensors. Surface testing includes signature measurements on surface ships and submarine in water depth from 60 to 600 feet. Air operations include, but are not limited to, In Service Engineering (ISE) mine tests, which vary from high altitude (>20,000 feet) airdrops to higher speed (>500 knots) lower altitude (<500 feet) mine deployments. In 1994 operation was turned over to NSWCCD. Subsequently, several range upgrades were affected, adding the ability to support more littoral warfare programs. Emphasis was placed on ship and underwater vehicle detection issues (i.e. tracking, signature measurement and control).

At the onset of this proposal the range had enhanced underwater, surface and air tracking capabilities; enhanced surface ship and submerged electromagnetic and new acoustic measurement systems; mine fields in various water depths; and ADCP current measurements in 60 and 600-foot water depths. Real-time data from these sensors along with wind direction and speed, were available on the SFTF website. Also, one of the two existing tracking towers was modified to accommodate radar antennas from the NSWCCD Radar Image Measurement System (RIMS). Coupled with the deep water close to shore, this allows precision submarine Radar Cross Section (RCS) near surface measurements at very close ranges.

The extensive expertise of the personnel at SFTF in developing, planting and operating in-water systems, along with the significant in-water resources and support equipment, was used to help ensure the success of the University Principal Investigators. A leadership role was taken in coordinating the development of the complex systems used in these experiments and in establishing the techniques to plant these systems. In addition, all anchoring subsystems and bedplates were designed and built by SFTF personnel. Highlights of the SFTF contributions follow:

2.6.1 Experiments to Evaluate AUV Capabilities

Part of this experiment encompassed coastal mine reconnaissance tasks. Six moored mines, ten bottom mines, and one dummy torpedo were selected from the SFTF inventory. All units were refurbished and new anchor systems installed. SFTF personnel provided detailed AutoCAD charts of the range area; identifying deployment sites that met the mine hunting experiment requirements, while not interfering with other range operations, the natural reef system, nor planned experiments. After completing a survey of these areas, a final selection was made of a 30-foot depth site. SFTF chartered the University of Miami CALANUS to affect the

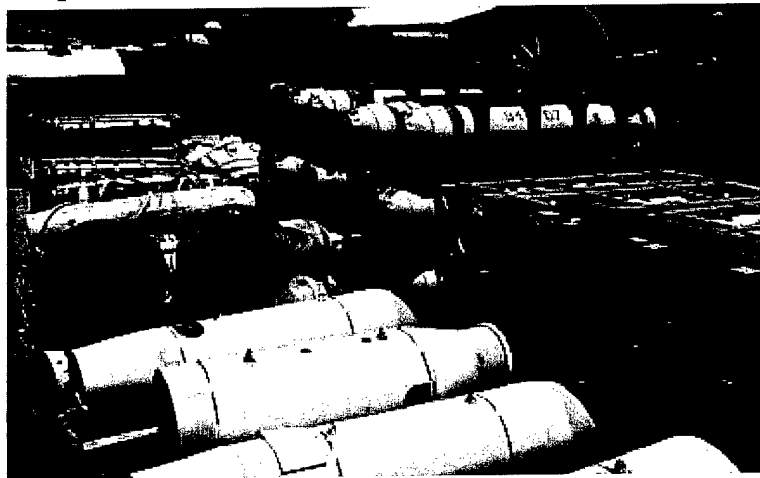


Figure 2.6.1-Part of the SFTF mine inventory used to support the experiment to evaluate AUV capabilities. Units selected were refurbished and attached to new anchoring systems before deployment.

deployment. Navy equipment was installed and used by SFTF engineers to deploy the selected mine units.

After the initial mine-hunting experiment was complete, the moored units were removed. These moored mines were reconditioned as appropriate and replanted in new locations to support further experimentation. Four of the original 10 bottom mines were also repositioned. This second deployment was accomplished using divers and the R/V SEWARD JOHNSON from the Harbour Branch Oceanographic Institution. The SEWARD JOHNSON was made available during a two-day window when deep-water acoustic propagation experiment work was awaiting project materials.

2.6.2 Adverse Weather and 4-Dimensional Current Experiments

Both of these experiments used the same suite of instrumentation in conjunction with independent AUV measurements. At the selected 65-foot water-depth site, several instruments were called for. At the center was a new shallow water multiplexer (MUX) designed and built to control these instruments and transmit the data to shore through a fiber optic cable. The multiplexer was configured to interface with a 5-head ADCP, cyclesconde, modem receiver, modem source, ambient noise array, AUV docking station, and one of 4 environmental arrays.

At the commencement of the work funded by ONR, SFTF personnel established a milestone chart to insure that all the components came together in a timely fashion. Monthly reviews were established where the responsible personnel reported subsystem status and presented any problems meeting agreed upon milestones. The PERT chart was maintained and updated by SFTF personnel after each meeting.

SFTF personnel also took the lead in establishing the requirement for integrated testing (IT). IT was to be completed before installation of the in-water components. An IT agenda was prepared by SFTF and oversight was provided during the testing phase. Each subsystem was evaluated for proper function, operating individually through the multiplexer and shore cabling and again concurrently with all components as a total system. This process was conducted dry

and repeated wet alongside a dock area. Over the course of the IT, several problems were detected. Some were corrected by the respective PIs. Others could not be resolved in time to meet the deployment schedule, so workarounds were developed such that the experiment requirements could still be met.

Before the shallow water multiplexer could be installed, a new cable needed to be run from shore to support the instrumented test site. To accomplish this task a 96-foot

long commercial vessel was chartered by SFTF. Navy winches, deck fittings, and handling equipment were

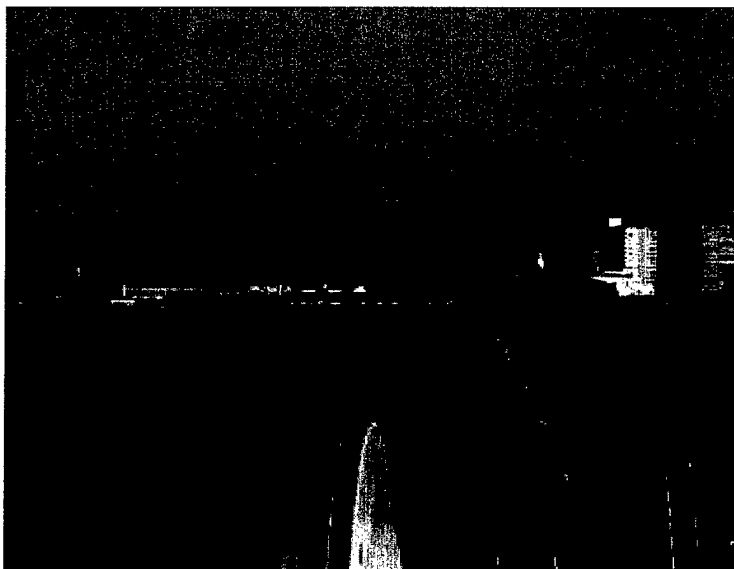


Figure 2.6.2-Picture from the ship; cable is being laid from SFTF to the 65-foot site.

installed per SFTF design. SFTF provided appropriate, load cells, floats and day shapes. A practice lay was conducted using SFTF cable. The next day, 14,000 ft. of fiber optic and copper cable was successfully laid. Divers were used to survey the route prior to and after the deployment. The route survey was to ensure that no damage would or did occur to the live reef system in the area of the lay.

In the 65-foot water depth site, SFTF personnel installed a series of 6 strategically placed permanent anchors. These allow easy use of the small boats operated by FAU for installing, retrieving and maintaining system components. These anchors were placed after a diver survey to ensure no damage to the reef.

One of the important components of these experiments was the University of Miami OSCAR system that was used to make surface current measurements over the areas of the instrumentation and AUV operations. The availability of OSCAR set the outer time limit of when the other installations had to be completed. SFTF provided the site, power, and telephone line for the OSCAR installation on the SFTF property.

SFTF personnel provided range control and coordinated operations for the conduct of these experiments. SFTF also provided a CTD that was used by FAU on the R/V STEPHAN while the AUV's were being deployed.

2.6.3 Environmental Array and Data Analysis

Four arrays were to be provided by USF, 2 surface (i.e. buoyed) and 2 bottomed mounted. The latter were to be connected, 1 each, to the new shallow and deep multiplexer. Appropriate designs and deployment techniques were developed by SFTF personnel to accommodate all of the installations. The surface arrays were installed by FAU using the STEPHAN. SFTF personnel conducted safety checks, loaded the vessel and reinforced equipment as necessary to support that task.

2.6.4 Very Long Range Shallow Water Acoustic Propagation

A substantial amount of SFTF resources were provided to support the University of Miami propagation experiment. An existing 35,000 ft fiber optic and copper cable was supplied that ran from shore out to the nominal 500-foot water depth site selected for the 3 large receive arrays. Broken fibers in the cable were repaired at sea by SFTF personnel. 8,000 feet of cable and feed-through boxes were provided for jumpers between the UM deep water multiplexer and the three-receiver/array units. SFTF personnel conceived and executed the scheme used successfully to deploy the arrays and associated in-water electronic

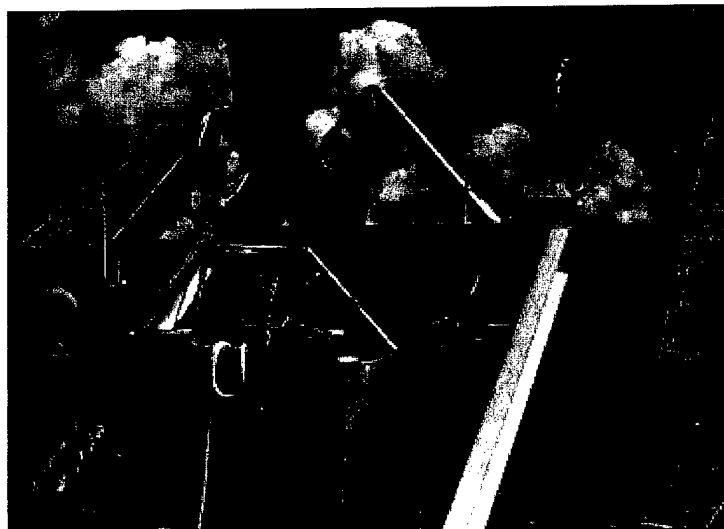


Figure 2.6.3-Picture of new bedplate with baskets and jumper cables to be deployed from RV SEWARD JOHNSON using TONGS in 500 feet of water.

packages. The resulting 12-foot by 12-foot by 10-foot bedplate with 3 large baskets was designed and built by SFTF personnel. Also needed to support the installation were a 40,000-pound working load bail, which was designed, build and tested by SFTF, along with two 2,000-pound anchors and one 6,000-pound anchor for the vertical array. Strong backs were also designed and built for each of the three receivers to safely hold the fiber optic array interfaces.

The entire system was successfully deployed using the SEWARD JOHNSON, which was provided by ONR under UNOLS, along with the SFTF remote operated vehicle TONGS (Television Observation Nautical Grappling System). This included retrieving and attaching the shore cable to the new multiplexer and bedplate and lowering the unit with jumper cables coiled in the baskets (see Figure 2.6.3). The jumper cables were then taken out of

the baskets using TONGS (see figure 2.6.4). The vertical array with sub-surface buoy was attached to one leg. One kilometer long east to west and north to south bottom arrays were attached to the other two.



Figure 2.6.4- Picture from TONGS camera as it approaches one of the cable baskets (upper left) to pull out the jumper cable for vertical array. Note the empty basket on the left (used for east bottom array) and the partially full basket on right (used for south array).

Initially, the plan was to perform this installation in two periods. The SEWARD JOHNSON and TONGS were to be used first to retrieve existing equipment on the cable being dedicated to this project and to prepare the cable ends with new bails. The bedplate already deployed was to be retrieved and modified to use with the new system. Because the SEWARD JOHNSON had a generator failure on the first day at sea, the initial work had to be cancelled. Due to the time constraints it was decided to quickly design and build a new bedplate and perform all operations during the second time period, which was extended to accommodate the new schedule. This redesigned deployment scheme worked very well, although there was substantial cost associated with building a new bedplate.

This experiment involves the use of a large UM sound source ("Miami Sound Machine"). As a condition of running this experiment an environmental assessment (EA) was required. SFTF personnel took the lead in preparing this EA and guiding it through the review cycle. The study and resulting document considered all marine mammals and sea turtles in the area and the impact on human divers. The resulting information was provided to the United States Fish and Wildlife Service and National Marine Fisheries Service. All issues were resolved satisfactorily and reviewed by NAVSEA General Counsel. A FONSI (Finding of No Significant Impact) was signed by NAVSEA.

2.6.5 Biological And Geological Inventory And Assessment

Although SFTF personnel are providing little direct support in this endeavor, SFTF has been working with NAVOCEANO to get detailed bathymetry measurements that are needed to

support this project. Bathymetry and coring over a larger area are also needed to support the very long-range shallow water acoustic propagation experiment. SFTF now has a commitment from NAVOCEANO to provide these measurements in the near future.

2.6.6 Miscellaneous Support

Initially, the plan was to put all the shore-side instrumentation in the SFTF range house, which is where all the sea connections terminate and range control, is maintained. This caused some problems due to limited access necessitated by security considerations. This problem was resolved when SFTF provided a 40-foot air-conditioned trailer that was set up adjacent to the range house. Appropriate interface cables, power and communications were provided to the trailer, allowing the dry-end equipment associated with these experiments to be housed. This now allows the PIs unlimited access to their equipment.

Also, because of a move of the SFTF offices, the original T-1 line to the range house was lost. To provide reasonably fast rate remote access to the equipment by FAU, SFTF personnel installed 6 telephone lines and a proxy server. This proxy server allowed FAU and others to “remote control” experiments from outside the Range House. Replacement of the T-1 line is expected in the near future.

2.7 Shallow Water Multiplexer (MUX) Installation

Edgar An, Robert Coulson, Doug Williams, John Webb, Rob Reibman (FAU)

This section presents the design, development and installation of the South Florida Ocean Measurement Center (SFOMC) shallow water node instrumentation. A new underwater telemetry node (or multiplexer) which interconnects a number of at-sea ocean instruments has been deployed continuously for six weeks since the end of June of 1999. This node provided to the attached instruments necessary power, monitored the internal operational status, and relayed the instrument data back to shore in real time via fiber optic communication. The instruments which have been or will be connected to the MUX include an AUV docking station (Florida Atlantic University, FAU), an environmental array (University of South Florida), a passive acoustic ambient noise array (FAU), Cyclesonde (University of Miami), and an acoustic modem source and receiver (FAU). As each of these instruments requires unique data and power requirement, ranging from LonTalk, RS422, to Ethernet / Fast Ethernet connection, there was a great deal of effort spent on the node design with regard to scalability and reconfigurability issues. That is, maximizing the node’s utility in order to support a wide variety of instruments now and in the future. Besides the modularity constraint, the safety issue has been rigorously addressed in the design given that the node installation site is in shallow water and is within diver’s reach. This underwater node was utilized to support two major scientific experiments (adverse weather experiments and 4D current measurement experiments described in Sections 3.2 and 3.3 respectively) that were carried out during the month of July of 1999.

2.7.1 Background

Development and enhancement of rapid littoral environment assessment capability is of critical importance to both the US Navy and scientific community. A coherent mapping and

characterization of relevant environmental attributes is required to properly model and predict ocean processes of varying magnitudes of temporal and spatial scale [1,2]. Data acquisition must be carried out not only in a timely manner but also spatial sampling must be well distributed in such a way that any environmental change can be synoptically captured [3]. To characterize the assessment performance, a well-calibrated environment consisting of distributed independent sensors is required.

The shallow water portion of the SFOMC experiments were centered around an underwater node or multiplexer (MUX), see Figure 2.7.1. Seven instrumentation packages are configured to connect to the MUX so that they could be powered, monitored and controlled from the shore station. The seven packages which can be connected to the MUX for power and data transfer are:

1. UM Cyclesonde Autonomous Vertical Profiler
2. FAU Ambient Noise Sonar (Peacock)
3. USF Environmental Array
4. FAU Acoustic Modem Receiver
5. FAU Acoustic Modem Source
6. FAU 5-Head Acoustic Doppler Current Profiler
7. FAU AUV Docking Station

Each of these packages has its own power, data, cabling, connector, mooring and installation requirements. These information are summarized in Table 2.7.1 and their relative co-ordinates with respect to the MUX is shown in Figure 2.7.2. This MUX was installed between the second and third reefs, in about 65 feet of water, in the South Florida Testing Facility's range. A 14,000 ft. electro-optic cable was laid from the NSWC-CD range house, which is adjacent to Port Everglades Inlet, to the MUX in order to supply about 1.5 kW of usable power and to allow real time fiber optic communications between the MUX and shore. The MUX was designed to simultaneously support a maximum of 7 instrument packages; one of which will be an AUV docking station.

2.7.2 Mechanics and Structure

The MUX module is made up of two distinct assemblies. First there is an external structure which consists of a pressure vessel with its associated bulkhead connectors, a stand on which the vessel is mounted and a 4'x 8' oval concrete bed-plate to secure the stand and cabling on the ocean floor, see Figure 2.7.3. There is also a fiberglass cover which encloses both the vessel and stand to protect it against damage from anchors, fishing tackle, critters and vandalism. The second assembly corresponds to the internal components of the MUX, consisting of a heat exchanging split aluminum ring onto which all the DC-DC converters are mounted and a rack for the fiber modules, relays, iso-meters etc.

2.7.2.1 Pressure Vessel

The pressure vessel is made from a 60" piece of 14" OD stainless steel schedule 40 pipe with standard slip-on flanges welded to the ends. An o-ring groove was machined into each flange for a face seal. The end caps are machined from matching standard blind flanges and have two bore o-ring seals each and the inside ends of the pipe are machined to accommodate these bore seals. The vessel is clamped into a stand whose feet have through holes that fit over studs that

protrude from an 8' x 4' x 1.5' oval fiber reinforced concrete slab. The pipe, flanges, stand and mounting hardware are all made from 316L stainless steel. Finite element analysis showed that the vessel and end cap assemblies could withstand the environment at a depth of 60 ft with a safety factor of at least 10.

2.7.2.2 Cables & Connectors

Cables: The electro-optic cable that runs from the NSWC-CD site to the MUX was made by Rochester Corporation. It is 14,000 ft long, and is made of 6 single-mode optical fibers and 6 14-AWG copper conductors, see Appendix 2.7. To mechanically strengthen the cable and prolong the cable's lifespan, the conductors are enclosed within a double steel armor and HDPE belt and jacket.

In contrast to the Rochester cable, the instrument cables are made of multiple shielded twisted pairs of copper conductors. The USF environment array cable consists of 6 #14 AWG wires for power and 5 #24 AWG twisted shielded pairs for RS422 data transfer. The shields for the twisted pairs are connected to two of the pins so that 4 of the #24 AWG wire will have a common shield for one RS422 link and the other 4 will have a common shield for the other link. This cable is mated to a 16 pin wet-mateable connector with #14 AWG pins (Impulse Titan series MKS(W) 7-16) so that it cannot be accidentally connected to the wrong bulkhead connector on the MUX.

All other instruments, with the exception of the Acoustic Modem Receiver, will have a standard cable and connector specification. Three supplemental power cable and connectors are provided for the three AUV Docking Stations. The standard cable contains 6 #14 AWG wires for power and 5 #24 AWG twisted shielded pairs for data. Two of the shields for these pairs are connected to one pin for a RS422 link, two shields are connected to one pin for an Ethernet link, and the remaining twisted pair shields are connected to individual pins for a LonTalk link. This wire hook-up requires 19 pins which are provided with an Impulse Titan series connector, MKS(W) 7-19. Three supplemental power cables for the AUV docks consists of 4 #12 AWG wires connected to an Impulse connector, HD-4, with 4 #12 AWG pins. All the instrument cables used were manufactured by Falmat Inc.

Connectors: With the exception of the fiber optic connector, all connections to the Mux can be made underwater. The shore power and fiber optic cable termination and matching bulk head connectors were furnished by Ocean Design Inc. Their design uses a fluid filled, pressure balanced, Field Installable Termination Assembly (FITA), that splits the optics from the power, two pressure compensated jumper hoses, a Nautilus series 6 way power plug and bulk-head assembly and a six way Hybrid Dry Mate optical plug and bulkhead assembly. The bulkhead connectors are shown in Appendix 2.7, Figure 2.7.4a. The complete FITA/bulkhead assembly is manufactured from 316L stainless steel.

The other 5 connectors shown in this figure are underwater pluggable molded neoprene Impulse connectors. Three of these are for power to the AUV docking stations, another is an auxiliary shore power connection for a future power upgrade. The fifth smaller connector supplies power to a strobe light that mounts on the fiberglass MUX cover to indicate when shore power is present.

Appendix 2.7, Figure 2.7.4b shows the other end cap with 10 Impulse Titan series stainless steel wet pluggable bulkhead connectors. Nine of these are 19 pin generic instrument

hookups and one is a 16 pin for the USF array. This end cap also contains a vacuum port and plug. Figures 2.7.5 and 2.7.6, of Appendix 2.7, detail the pinouts of the two connector types.

2.7.2.3 Internal Components

The internal components of the MUX are separated into two assemblies, and are shown in figure 2.7.7 of Appendix 2.7. Since the maximum power transfer to the MUX is approximately 1.4kW, there can be a significant amount of heat dissipated in all the DC-DC converters within the pressure vessel. These converters are thus mounted on flat surfaces milled into an aluminum ring as shown in figure 2.7.7a. This ring is split along its length and has an expansion joint allowing it to be securely pressed up against the stainless steel wall of the pressure vessel. A thermal film was added underneath the DC-DC converters and between the ring and the pressure vessel to ensure a good thermal path to the surrounding seawater. The assembly is securely wedged in place within the sleeve. A two-dimensional thermodynamic model was used to predict the internal heating under various operating conditions, and the results showed that the internal temperature under full load would not exceed 54 degrees Centigrade. Subsequent wet testing showed this model were accurate to within 2 or 3 degrees.

The second assembly within the MUX is an aluminum chassis built around a 19" rack containing the fiber optic multiplexer modules. The chassis, shown in Appendix 2.7, figure 2.7.7b, holds Ethernet multiplexers/media converters, Echelon LonPoint Routers, RS-422 media converters, RS-422 isolation modules, ground fault detection/isolation devices, associated mechanical relays, Coactive LonTalk routers and an auto-sensing networking hub. The complete assembly is shown in figure 2.7.7c. This assembly is friction secured within the pressure vessel, using three 3 pivoting "Jacking Pads" that wedge the chassis in place.

2.7.3 Power and Electronics

Although AC power from the shore to the MUX would provide power more efficiently, the transformer required in the MUX would be large in size and would potentially cause electrical and acoustical interference. By using DC power from shore to the MUX, there will be no transformer hum and the physical size required by the DC-DC converters is less than that required by a transformer and an AC to DC power supply. We have chosen for power transmission to use DC-DC converters, which provide total isolation between the shore and the instruments. Based on the available components in the market at the design time, the maximum voltage that 48v (nominal) DC-DC converters can operate at is 425 VDC. An analysis of power loss across the shore cable to the MUX was performed. With 3 pairs of 14 AWG wire at 14000 ft plus service the resistance of the cable is 27 ohms. By applying 425 VDC at the shore and having an estimated load of 6.4 amps at the MUX, 173 volts will be dropped across the cable. This will provide 252 Vdc and 1.6 kW at the MUX. The DC-DC converters inside the MUX are 90 % efficient so the total usable power at the MUX will be 1.44kW.

A fully operational system requires a shore-based station capable of providing a 425Vdc source of power and a fiber-optic coupled data terminal device connected by way of an underwater cable system to the MUX. The shore power in the Navy's range house is regulated via two UPS, having 208Vac as their inputs. Their outputs are then fed to two Sorrensen power supplies stacked in parallel, generating 425VDC isolated outputs @ 6.2A maximum. A ground fault circuit interrupter GFI (Bender IRDH265-4921) for ungrounded DC systems is used to detect whether there is any ground fault occurring between the positive and negative lines. If so, a

triggering signal will then be sent to a 2-pole contactor that in turn shuts down the power to the MUX. There are a total of ten instrument ports at the MUX. Three of them are used to interface with AUV docks that require heavier gauge wires, whereas the remaining seven ports are used to interface with low-power oceanographic instruments. A functional block diagram which illustrates the operation at shore is shown in Appendix 2.7, Figure 2.7.8.

Within the MUX, there is a main power board that converts incoming 425Vdc to individual 5, 12, 24 and 48Vdc output sources required for all the internal electronics. Figure 2.7.9 shows a block diagram of the internal power conversion using a Vicor DC-DC converter @ 600W. The converted 48Vdc output is passed through a High-Performance Standard Node (HPSN) which monitors the current and voltage usage, ground fault status, water leakage level as well as ambient temperature setting. This HPSN is considered as the main switchboard within the MUX because it can be used to turn each of the instrument's power on or off via software commands sent remotely from the shore. The HPSN is a LonTalk device that can communicate with other LonTalk devices via a variety of media channels. In our applications, only two channels were used: FTT10 (free topology) and TP1250 (high-speed 1.25Mbps). As illustrated in the figure, all the HPSNs inside the MUX communicate over TP1250 for fast response. To communicate with instrument's LonTalk devices, we chose FTT10 channel interface because of its range flexibility. Thus, a TP1250-to-FTT10 router is needed to interface between the internal HPSNs and instrument's LonTalk devices. Each of these connections is coupled through a LonTalk opto-isolated repeater such that one failed LonTalk node from some instrument will not bring down the entire LonTalk system.

For each of the ten ports, a separate power board which regulates the instrument power and monitors for any ground fault was designed and built. Similar to the shore setting, a GFI was used to detect and interrupt any ground fault. In addition to the hardware interrupt, the GFI also sends a serial RS485 message continuously to the HPSN with regard to the health status of the connection. This message can be monitored and logged at the shore computer via LonTalk communication. If there is a ground fault, the GFI will trip the instrument's relay, which in turn shuts down its power. Notice that once the GFI has been tripped, it can be reset from shore via one of the HPSN TTL outputs. For each of the AUV docks, a special power circuitry was designed because of its high-power requirement. As shown in Appendix 2.7, Figure 2.7.10, the power board for an AUV port consists of two DC-DC converters stacked in parallel, giving an isolated output of 52Vdc. The power board layouts for the remaining seven instrument ports are similar to those of the AUV docks, except that only one DC-DC converter is needed. The detailed power consumption and cable length requirements for each of the instruments are listed in the following table.

| | AUV Docking Station | Peacock | USF Environmental Array | Acoustic Modem (Bambam) | Acoustic Modem (GP) | 5-head ADCP | Cycle-sonde |
|-------------------|---------------------|---------|-------------------------|-------------------------|---------------------|-------------|-------------|
| Cable Length (ft) | 350 | 405 | 2000 | 150 | 900 | 660 | 175 |
| Wire Gauge (AWG) | 2 x 12 | 3 x 14 | 3 x 14 | 3 x 14 | 3 x 14 | 3 x 14 | 3 x 14 |
| Cable | 0.364 | 1.07 | 1.07 | 1.07 | 1.07 | 1.07 | 1.07 |

| | | | | | | | |
|---------------------------------------|--------|--------|-------|--------|-------|-------|--------|
| Resistance/kft (ohm) | | | | | | | |
| Power at Instrument (W) | 700.43 | 100.53 | 50.31 | 178.07 | 70.42 | 6.22 | 202.01 |
| Voltage at MUX (V) | 52 | 52 | 52 | 52 | 52 | 52 | 52 |
| Voltage at Instrument (minimum) | 48.31 | 50.27 | 47.46 | 50.88 | 49.25 | 51.83 | 50.50 |
| Voltage at Instrument (maximum V) | 51.9 | 51.9 | 51.9 | 51.9 | 51.9 | 51.9 | 51.9 |
| Current at Instrument (maximum A) | 14.5 | 2.0 | 1.06 | 3.5 | 1.43 | 0.12 | 4.0 |
| Power at MUX (W) | 754 | 104 | 55.12 | 182 | 74.36 | 6.24 | 208 |
| Power loss From MUX to instrument (W) | 53.57 | 3.47 | 4.81 | 3.93 | 3.94 | 0.02 | 5.99 |

Table 2.7.1. Summary of SFOMC Instrument power and distance requirements from the MUX

To ensure the compatibility of the MUX-instrument interface, we have provided the following table of system parameters to which any of the future instruments must be adhered. In addition, all electrical circuits including power circuits as well as signal circuits shall be isolated from the power feed. All circuits shall be isolated from earth.

| Interface Parameter | Value |
|---|--|
| Maximum current (A) | |
| Generic port | 8 |
| Power port | 14.5 |
| Maximum voltage (V) | 51.9 |
| Minimum voltage (V) | 51.9 – 2.58 L (L = cable length in kft) |
| Resistance between instrument powerground and chassis (ohm) | 5Mega |
| DC-DC converter peak-peak ripple voltage (V) | 100mV |
| DC-DC converter ripple frequency (Hz) | TBD |

Table 2.7.2. MUX-Instrument Interface Parameters

2.7.4 Data Communication

Data supported by the SFOMC shallow water MUX consist of LonTalk, RS422 and 10BT/100BT Ethernet data formats. The multiplexer consists of a 19” rack with add/drop plug-in

fiber-optic transeiver cards that support 1 dedicated 100BT channel, 1 dedicated 10BT channel, 1 shared 10BT/100BT channel and 16 RS422 channels operated at a maximum of 38.4Kbaud. To maximize the modularity of the MUX interface, we have adopted a generic connector interface such that seven of the ports can handle shared Ethernet, RS422 and LonTalk formats. One of the ports is dedicated to handle only 2 RS422 channels (with 16 pin configuration), and one other port dedicated to handle a 100BT channel.

The fiber-optic transceivers are off-the-shelf single-mode components and were purchased from T.C. Communication Inc. A block diagram of the interconnection of the shared 100BT and 10BT Ethernet cards between the shore and the MUX is shown in Appendix 2.7, Figure 2.7.11. Wavelength-multiplexers (WDM) are used to combine the transmit and receive link onto a single physical fiber, thereby reducing the total number of needed optical fibers to four. The two remaining fibers in the Rochester cable are allocated for redundancy and/or expansion purposes.

2.7.4.1 Lontalk

The LonTalk communication operates over FTT-10 and TP1250 channels both at shore and instrument ends, and is dedicated solely for control and monitoring purposes. Thus, high-bandwidth LonTalk data communication other than for control purpose is currently not supported. A network topology for all LonTalk devices is depicted in Appendix 2.7, Figure 2.7.12, using Echelon LonMaker for Windows API at the shore end to monitor and control high-level network variables. There is for each of the instrument ports a HPSN which monitors its ambient temperature and power required by its corresponding instruments. These HPSNs were designed in-house at FAU, each providing two high-speed serial ports with 64 byte FIFO, 16 analog input and 4 analog output channels. A more detailed description of the HPSN functionality can be found in [4]. These HPSNs are depicted in the figure as MUX1 through MUX10, whereas MUX0 represents the main HPSN node which turns each of the instrument's power on or off individually. With this configuration, a faulty instrument can be isolated without affecting the rest of the system. As part of the monitoring and control devices, MUX0 through MUX10 are mounted on the aluminum ring inside the pressure vessel, and communicate to each other over the TP1250 channel. To aid troubleshooting, monitored information from these MUXes are sent back to shore and logged automatically at a regular time interval. Besides the internal HPSNs, the MUX also can handle instruments' LonTalk communication via INTR1 through INTR10 over the FTT-10 channel. Each of the instruments LonTalk connection is electrically isolated using an opto-coupled repeater. With reference to Figure 2.7.12, the LonTalk communication is taken place over the 10BT channel where a Coactive router translates between the LonTalk and Ethernet protocol at both the shore and MUX end.

2.7.4.2 Asynchronous RS422

The RS422 data capability is provided to support most of the underwater instruments that have serial data interface, such as the mainstream ADCP and CTD. Based on our current design, the maximum data bandwidth provided for each of the serial instruments by the MUX is 38,400 baud, without any handshaking facility (e.g DTR). As part of the RS422 standard, the maximum range is 1,000 meters although the farthest instrument (USF array) that is connected to the MUX is 600meters, see Figure 2.7.2. Each of the instrument interface to the MUX is via an RJ11 socket at the shore end inside the NSWC SFTF range house.

2.7.4.3 Ethernet

The Ethernet communication is mainly provided to support the AUV docking station, Peacock ambient noise array and the acoustic modem receiver. As mentioned previously, there are shared Ethernet channels and dedicated Ethernet channels in the MUX. The shared Ethernet bandwidth is non-deterministic, as expected for a varied number of instruments. For a quick reference, a typical data rate estimate for dedicated Ethernet communication is approximately 30% of full bandwidth. In addition, all the shared Ethernet instruments are connected together via an auto-sensing hub, and thus an Ethernet switch with a dedicated 100BT uplink must be required at least at one of the ends (in this case the shore end since a standard off-the-shelf switch would take up too much space within the MUX). Instrument interface to the MUX is via an RJ45 socket at the shore end. As part of the Ethernet standard, the maximum range is 100 meters although the farthest Ethernet instrument to the MUX is 50m. Apart from the shared channel, there is a dedicated 100BT channel specifically provided for the FAU acoustic modem receiver because of its high-throughput requirement. There is also a dedicated 10BT channel specifically provided for supporting the LonTalk communication so that control and data transmission are not mutually interfered.

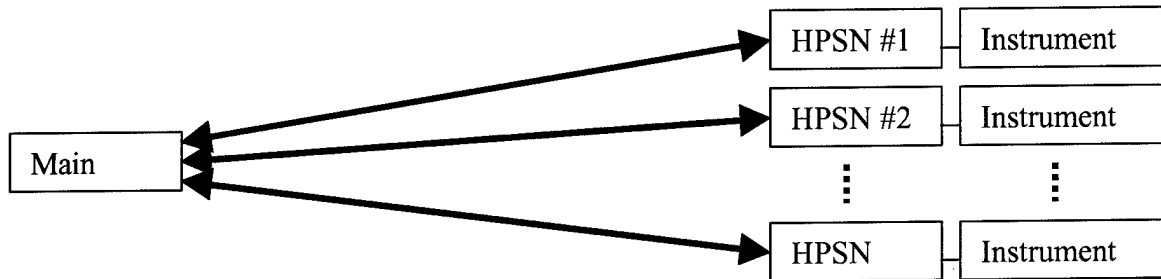
2.7.5 Safety

As the MUX's operational location is within diver depth, and the fact that high voltage is sent from the shore to the MUX, personnel safety was rigorously addressed. The secondary side of the 425Vdc shore power supply is electrically isolated and is equipped with a DC ground fault circuit interrupter (GFI) made by Bender. With this configuration, it requires two ground faults and a failed GFI to constitute a safety hazard. The GFI was designed to follow UL guidelines for ungrounded systems, and will trip within a second when there is a fault in one of the power conductors. Thus, it is highly unlikely that an unintentional diver will be in such a situation that he or she is within 5 meters from the cable and 2 ground faults happen simultaneously within 1 second. In addition to the GFI, a lightning arrester is also placed at the cable entrance into the range house. This provides both personnel and equipment safety when lightning occurs.

With regard to the safety at the MUX, it is sheltered by a fiberglass shroud so that any unintentional diver cannot physically be in contact with the MUX within 1 meter, and disconnect any of the connectors. Similarly, the entire MUX and instrument power output are electrically isolated, thus providing safety protection all the way to the primary side of each of the instrument's power. In addition, each of the instrument ports is equipped with the same GFI such that any ground fault will automatically trip the circuit interrupter within 1 second. Again, only the power associated with the faulty line will be shut down, leaving the rest of the instruments unaffected. Reasons for having a ground fault could be bad cable / connector / connection, or instrument not electrically isolated from its chassis. Note that once any of these GFIs is tripped, its alarm will be activated, and stayed on until it is reset either via its panel display button or software programming. To avoid opening up the MUX during remote operations, we have implemented a software reset utility via LonTalk messages such that any GFI can be reset and power resumed from the shore computer for any faulty instrument once it is repaired and tested.

A strobe light is mounted on top of the MUX, which indicates whether there is power coming from the shore. This provides an additional safety measure for any operating diver who is to retrieve or service the MUX. High-voltage danger signs are also located outside the shroud to warn and discourage curious recreational divers.

Inside the SFOMC MUX, there is a main LonTalk High-Performance Standard Node (HPSN) which monitors and independently controls the power activity of each of the active instruments. To do so, each instrument is interfaced with a unique HPSN that in turn communicates individually with the main HPSN.



To allow automatic power control, each of the instrument's HPSNs continuously monitors its current and voltage drawn, as well as monitors the insulation resistance of its cable. If some instrument's power status exceeds the power interface requirements (described in earlier subsection) or its cable insulation resistance falls below a UL approved level, there are two levels of automatic operations. Firstly, the instrument power will be shut off at a hardware level. In addition, its HPSN will report it to the main HPSN which in turn shuts the instrument's power off. In an event the CPU in some instrument crashes, the main HPSN can recycle that instrument's power. By having this design, one faulty instrument will NOT bring down the entire system. The main HPSN also logs the internal operating status within the MUX, such as its ambient temperature, leakage, voltage and current at a regular time interval.

2.7.6 Testing & Deployment

Once the MUX was assembled, it was tested, both dry and wet, with the intended instruments. The entire testing and debugging period lasted for two months, starting at the beginning of May of 1999.

2.7.6.1 Dry Test

The dry test was carried out in the Corrosion Lab at SeaTech in Dania Beach during the month of May of 1999. During that time, each of the instruments was tested with the MUX for power and data transfer. Before testing with the dedicated instruments, the MUX was self-tested with a laptop simulating both an RS422 and Ethernet device. All ten ports in the MUX were each tested with the following steps (without the Rochester cable):

1. recycle power
2. test internal LonTalk communication
3. read GFM status messages
4. read instrument voltage and current levels
5. intentionally trip the GFI
6. reset the GFI trip from shore laptop
7. test RS422 communication with a laptop
8. test Ethernet communication with a laptop
9. test instrument LonTalk communication

At one point in the self-test, the MUX was subjected to 120% of maximum power load, and was able to perform satisfactorily. During the initial self-test, there appeared to be some internal heating problem inside the MUX which caused the LonTalk communication to fail. Additional fans were thus installed inside the pressure vessel in order to increase the heat flow, and this appeared to have solved the heating problem. At the end of the self-test period, it was found that all ten ports functioned properly, except that 1) in Port #3 the GFI readings were incorrect, and 2) instruments Lontalk communication was not established for all the ports. A careful decision was made in proceeding to the remaining dry test based on the fact that there are redundant ports to support the 4D current and adverse weather experiments (leaving Port #3 unused), and none of the instruments required LonTalk communication. It was decided that once the experiments are complete, the MUX would be retrieved and the above-mentioned problems fixed. This quick retrieval also provides us good insights into the effect of corrosion and bio-fouling on the MUX function, thus allowing quick diagnosis to be carried out, and prompt action taken.

To finish the dry test, all the instruments were tested with the MUX, except the AUV dock and 5-head ADCP because they were unavailable at the time. Among these instruments, we experienced significant noise problem between the MUX and the acoustic modem receiver. A great deal of effort was spent on reducing the noise level by relocating wires properly and building a better ground plane, and the resulting 100BT communication still appeared unreliable. There were two possible explanations at the time: the Ethernet device inside the modem receiver and the Ethernet transceiver inside the MUX are not compatible, and/or additional noise source existed due to the instrument cable and connector. Other than this problem, the majority of the dry-test debugging with other instruments was due to mislabeled wiring diagrams, which were easily resolved by the end of the dry test period.

The fiber-optic transceivers were also tested against potential power loss due to fiber splicing and connector interface. Each of the fibers was tested together with the Rochester cable using a power meter. The following table presents the power loss results measured at both the shore and off-shore end. In addition, an optical attenuator (up to 10db) was inserted into the system, and it was found that the system remained functional.

| Fiber Color | Offshore (db loss) | Shore (db loss) |
|-------------|--------------------|-----------------|
| BRN | 1.64 | 1.86 |
| BLU | 2 | 2.02 |
| WHT | 1.45 | 1.37 |
| RED | 2.11 | 1.78 |
| ORG | 2.25 | 1.58 |
| GRY | 2.21 | 1.76 |

Table 2.7.3 Optical fiber power loss test from both shore and offshore

2.7.6.2 Wet Test

The wet test was carried out at the dock outside the SeaTech facility. During the wet test, all the instruments, including the MUX, were placed on the bottom in about 8 feet of warm brackish water, and power was run from the lab to the dock site. On the first wet test day, the MUX failed to communicate with the shore laptop over the LonTalk channel. This was due to the

fact that some of the optical fibers were pinched against the heavier gauge copper wires, and were bent excessively. In addition, the Coactive router was found to work properly only if the server unit was powered up prior to the client unit.

Once these problems were corrected, Peacock, USF arrays and modem source were lowered into the water, followed by the MUX. Individual data communication and power were tested successfully for these instruments. Internal MUX temperature readings indicate that heating was not a problem because of the light load. In addition, a resistive load of about 520W was applied to the MUX as if it was an AUV dock, and ran for a whole afternoon. The results, with close to 100% power load, indicated that the internal temperature reading reached a steady value of about 51 degree C, which was acceptable for all the internal electronics, see Figure 2.7.13, Appendix 2.7. In this wet test, the MUX was submerged in 8 ft of warm water, and it is expected that it should perform better in the chosen installation site, 60ft of water with currents, where better cooling and circulation conditions can be expected.

Towards the end of the wet test period, the instruments and the MUX were left in the water over-night. During the retrieval, corrosion was discovered on the RS422 drain pin on all the ports that were used during the test. This included the Cyclesonde and USF array. This might have contributed to the fact that the connectors did not exclude all the salt water as well as the RS422 drain was tied to the signal reference inside the MUX. This problem could be eliminated by requiring all the connections to be carried out in air.

After the wet test, SFTF teamed with FAU and successfully installed the 14 thousand foot fiber-optic cable in the 60 foot area of the SFTF Range. A practice cable was laid to work out some installation bugs. The entire deployment took 3 days to complete, and the off-shore cable end position is now within 50 yards of the planned termination point. The electrical check out on the cable shows all cable fibers working properly. During the deployment process, the optical fibers and copper conductors were monitored continuously using OTDR and TDR. The actual optical loss from shore to the cable end was approximately 1db, leaving a significant loss margin for the MUX.

After the shore cable was laid, individual concrete bedplates for the MUX and other instruments were then laid one at a time. The heaviest bedplate is close to 5000lb, which was built for the MUX. On June 28 of 1999, it was finally deployed to the chosen site. The MUX was given a final self-test while it was on the surface. All steps were checked successfully, and the MUX was then lowered into the water. To enable dry connection, the instrument cables for the Cyclesonde and USF array were already connected to the MUX at one end, leaving the other end capped. Once the MUX was on the ocean bottom, it was re-tested for the first four steps as described in Section 2.6.1. These tests were successful.

On the following day, the Cyclesonde was deployed and tested successfully together with the MUX. The internal operational record was continuously logged onto a file using the laptop at shore. On July 14 of 1999, Peacock was scheduled to be connected to the MUX for power and data. When connecting the Peacock cable, the diver discovered a significant amount of corrosion on the connector pins at the Peacock port. This was due to the fact that the dummy plug used on that port was not completely watertight. During the final test, only the power was successfully relayed to Peacock. There appeared to be corrosion-related problem which subsequently caused the data communication to fail. At the time, it was decided not to fix the problem until the experiments were completed. The USF array was never connected to the MUX in open ocean. Subsequent testing at-sea indicated that the array would have operated successfully had it been

connected to the MUX right from the start of the deployment. The acoustic modem receiver was never tested successfully in water. As its role in both the 4D current and adverse weather experiments was not critical, it was decided to further investigate the problem(s) after the experiments were completed.

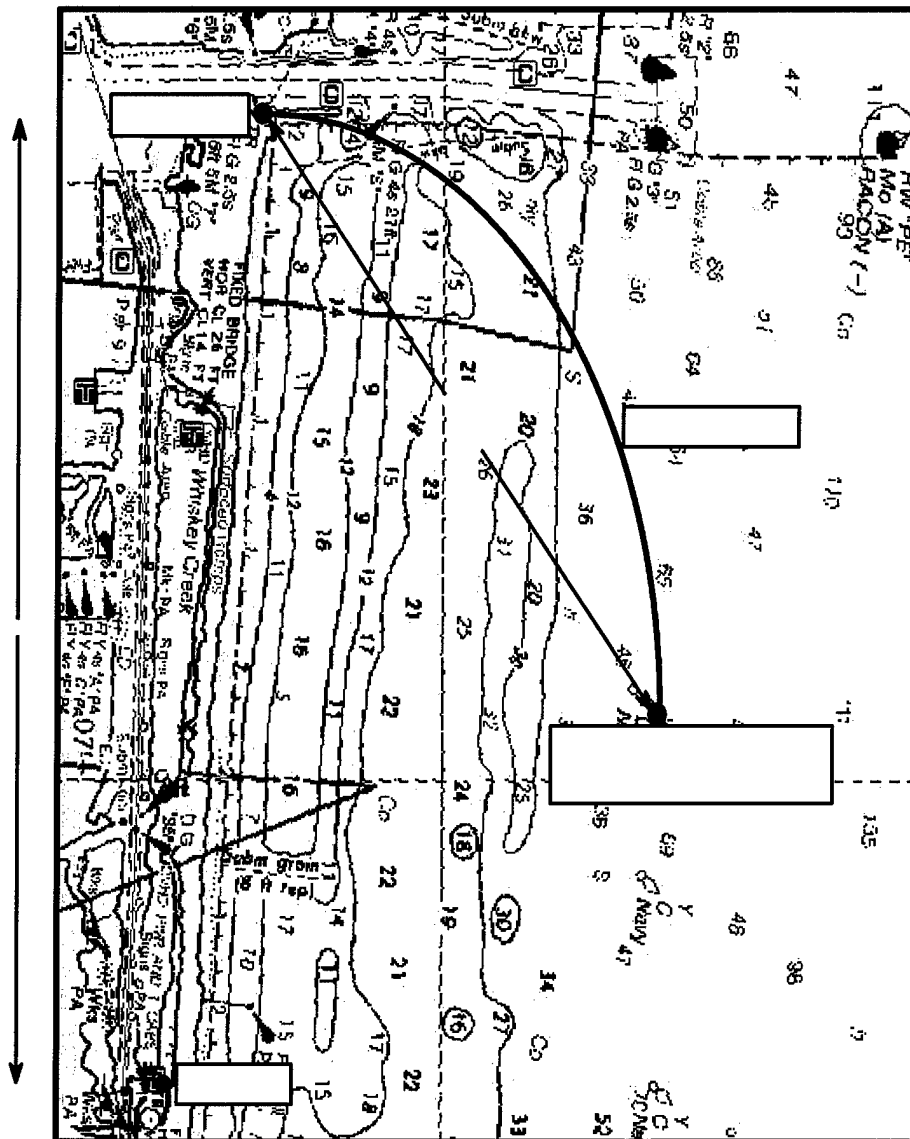


Figure 2.7.1 SFOMC MUX site

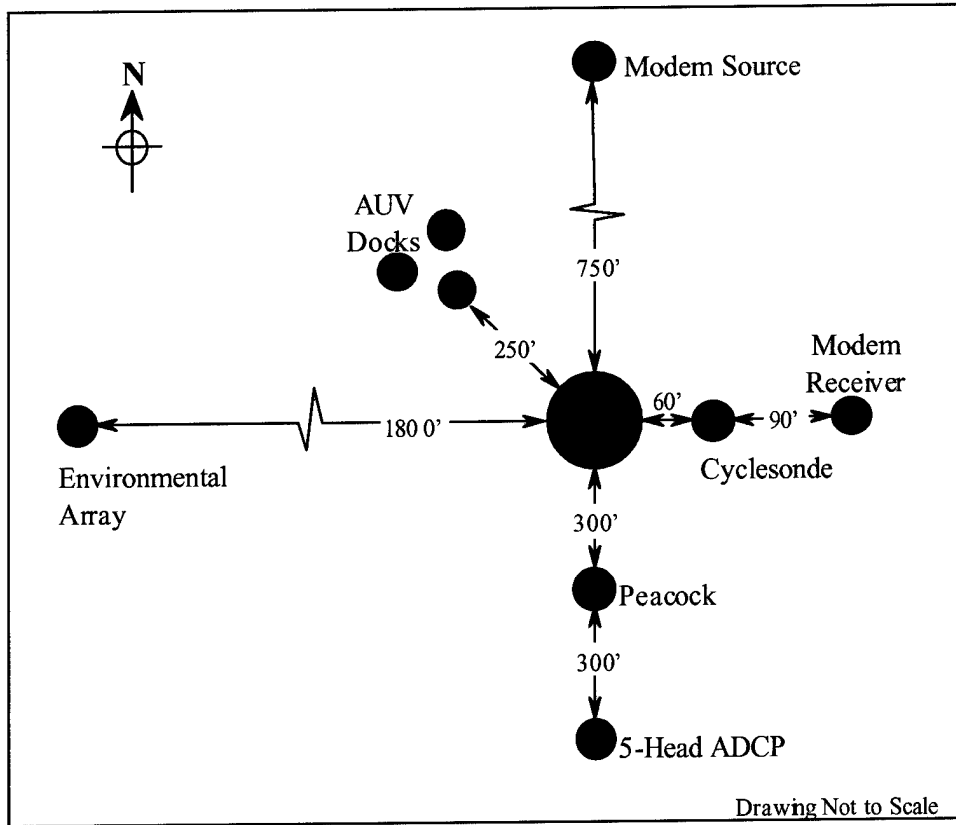


Figure 2.7.2 Instruments co-ordinates relative to the MUX

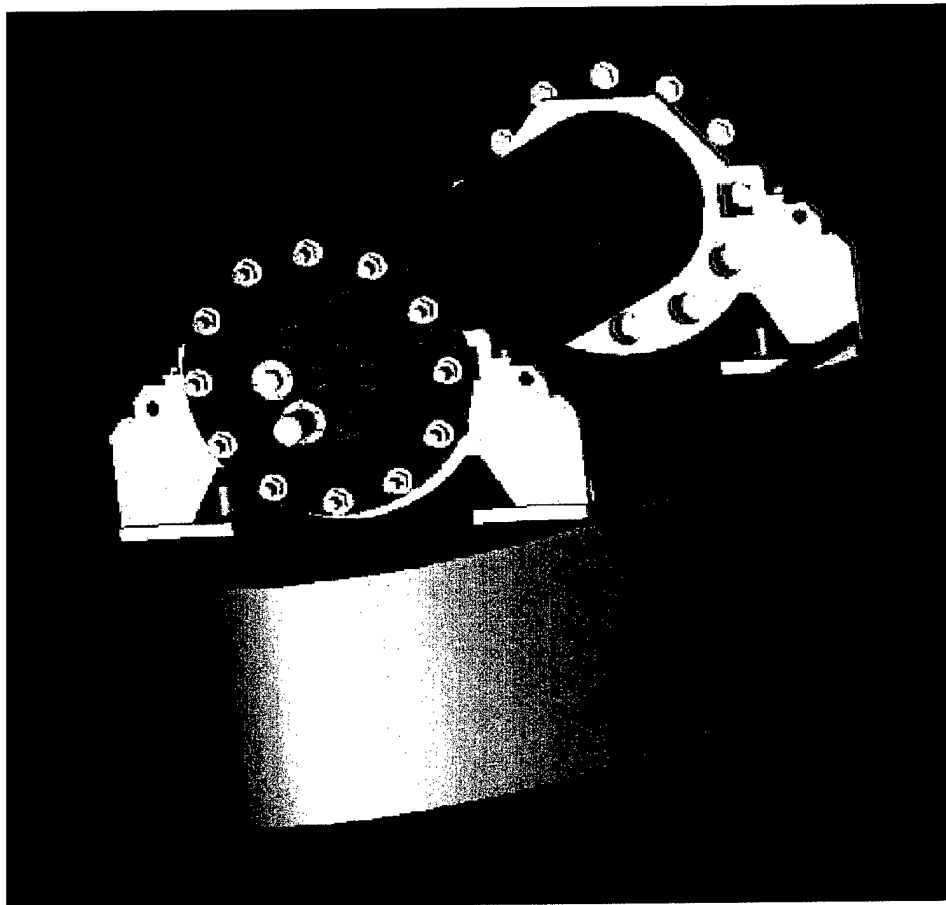


Figure 2.7.3 SFOMC MUX outfit

2.7.7 References

1. **Coastal Oceanography Using a Small AUV**, P.E. An, M. Dhanak, N. Shay, J.Van Leer, Sam Smith, *submitted to* Journal of Atmospheric and Oceanic Technology, September, 1998.
2. **Flow Measurements in an Atmospherically Forced Shallow Water Column During the Passage of a Cold Front** Conference, pp.93-97, Nova Scotia.**Using A Small AUV**, P.E. An, M. Dhanak, N. Shay, J.Van Leer, 13th Symposium on Boundary Layers and Turbulence, January, 1999.
3. **A Fiber Optic Telemetry System for Multiple Oceanographic Platforms**, R.G. Goldsborough III, Oceans 97
4. **The High Performance Standard Node Specification**, Internal Report, Department of Ocean Engineering, Florida Atlantic University.
5. **High Performance Standard Node Library Definitions, version 1.0**, Eric Heatzig, Ocean Engineering internal report, FAU, June 18, 1998.
6. **LonMaker for Windows Users Guide**, Echelon Corporation, 1999.
7. Safety Review of the South Florida Ocean Measurement Center, design review by Ned Forrester, April, 1999.

2.8 SFOMC Workshop

A workshop on the future of the SFTF Range was held in February 1999 and hosted by the SFOMC. The proceedings of this workshop are published in the following report:

PROCEEDINGS OF THE SFOMC WORKSHOP

February 24 - 26, 1999

Establishment of a Center for Innovative Oceanography in the 21st Century



**Edited by
Manhar Dhanak, Norman Caplan and Stanley Dunn**

**Sponsored by the National Science Foundation, and
Hosted by the Department of Ocean Engineering,
Florida Atlantic University**

This report is available online at: <http://www.sfomc.org/Workshop99/index.html>

3. RESEARCH ACTIVITIES

To realize the Navy's needs in the area of marine vehicle research activities, two major scientific and technological experiments were conducted beginning in the Fall of 1998 and continuing through the Summer of 1999. The focus of these experiments was to demonstrate the capabilities and limitations of deploying multiple AUVs and multiple sensor systems for mine hunting operations and operations in adverse weather conditions. The South Florida Testing Facility (SFTF) range was utilized because of the existing infrastructure of power supply and fiber-optic data links to shore at desired water depth enabling continuous monitoring of the environment offshore. In addition the SFTF provides a secure environment in which to deploy and calibrate the chosen suite of sensors, and to install calibrated targets for mine-hunting purposes.

3.1 Mine Hunting Experiment (Experiment 1)

The main goals of this experiment were to both characterize the remote sampling performance of multiple small AUVs/sensor systems for coastal mine reconnaissance tasks, and to characterize the effect of environment on navigation, communications, and object detection/classification sensors. Specific goals included: 1) quantify the optimized multiple vehicle synoptic and pseudo synoptic search detection and mapping capabilities for mine like objects based on on-line feedback cooperative sampling and modeling of environment and vehicle conditions; and 2) quantify the performance of the sensor systems and platforms, including cameras, and side scan sonar systems, in relation to environmental conditions and sea states.

3.1.1 Results of an Experiment Using Auvs for Shallow Water Mine Reconnaissance

Samuel M. Smith, Edgar An, Reed Christensen, John Kloske, Scott Snowden, Dave Kronen, and Larry Marquis (FAU)

The objective of this experiment was to quantify the performance of the Ocean Explorer AUV for mine reconnaissance tasks such as rapid environmental assessment, remote search, remote classification and remote identification of mine like objects both moored in the water column and laying on the sea floor.

AUV Description

The Ocean Explorer AUV hull is a flooded modified Gertler fiberglass fairing. The maximum OD is 21". The Ocean Explorer AUV (OEX) is divided into two sections fore and aft. The aft section is 4.5 feet long and houses the main propulsion, rudder, stern plane, main computer, batteries, CTD, and navigation sensors. Dry sections consist of aluminum or fiberglass pressure vessels with wet cabling. The OEX B has a direct drive propeller and independent actuators for each of the 4 control surfaces. The thruster and servo section is vibration isolated with rubber mounts. Important sensors housed in the tail include an RDI 1200 Khz DVL/ADCP,

a popup DGPS/RF modem antennae, an Edgetech Acoustic Modem, and a Falmouth CTD or Applied Microsystems CTD. The tail also houses an ORE USBL tracking beacon. The DVL provides water velocity and ground velocity of the AUV from which current shear can be calculated. It also provides bottom altitude. The batteries consist of NiCad D cells. These are mounted in eight cans and have built in charges and monitoring circuitry. All systems are connected by an eight pin cable that includes communications and power buses. The fore and aft sections meet at the 21" diameter. The fore section is left free for mission payloads and may vary in length from 3 to 6.5 feet where the additional length is a parallel 21" section. A quick mounting set of pins and standard 8 pin cable connect the two ends. This modular arrangement facilitates the pre configuration of various payloads with in the field attachment. Standard payloads configurations must include an intelligent drop weight system and RF beacon/optical strobe. Additional batteries may be housed in the nose. A diagram of the Ocean Explorer is shown in Figure 3.1.1.

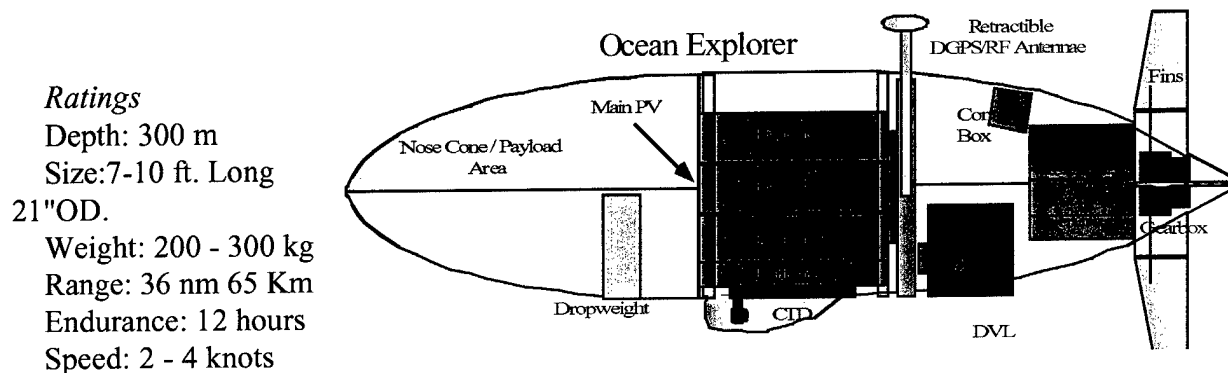


Figure 3.1.1 Ocean Explorer Autonomous Underwater Vehicle base configuration

Distributed Architecture

The primary motivation for the Ocean Explorer architecture was ease of reconfiguration to support multiple payloads. Ease of reconfiguration requires not only structural modularity but electrical and control as well. To this end an intelligent distributed control system (IDCS) architecture was used. The IDCS is based on the LONTalk protocol and Neuron chip. All the sensors and actuators on the vehicle are connected on a single serial network. A standard connector with power and network wires is daisy-chained to each of the pressure vessels and devices. Adding devices to the vehicle consists of plugging into this network. Software rewrites are minimized because network communications is at a high level. The IDCS is also used to implement health monitors in each of the pressure vessels and the intelligent battery system. The IDCS approach also facilitates upgrading of system components or adding functionality.

Control Capabilities

A simple text based mission file allows complete specification of mission plans without recompilation of code. The mission file supports macros for repetitive maneuvers. Mission commands can be sent over a remote acoustic or RF link. The high level control system has an Event Manager that has a rule base of failure conditions and responses. The Event Manager can also generate mission commands.

The vehicle control system has an autopilot that can be configured to control heading, depth, altitude, pitch, and speed. Open loop control of the control actuators is permitted. The guidance system can follow way points by homing or tracking, or docking. Combinations of control can all be configured on a mission to mission basis. The high level control system consists of a shared memory based multi process architecture running on a VME VxWorks processor. This system is highly scalable. All sensor and control values and parameters are stored in shared memory.

An independent data logging process transparently logs anything in shared memory. A text file is used to configure the logger on a mission by mission basis. Items can be logged by frequency or by change in value. Typically payloads have their own stand alone data logging systems.

Payload Configuration

There were four payloads deployed during the Mine Counter Measure (MCM) experiments: 1) Long high frequency side scan (HFSS) payload; 2) Short high frequency side scan payload; 3) Forward Look Sonar (FLS, or Barney); and 4) Laser line scanner (ROBOT). Both of the HFSS payloads were operated and supported by the AUV group. Each was equipped with an Edge Tech DF-1000 dual frequency side scan sonar (100 and 390 KHz), Edgetech acoustic modem, video camera, and an Edgetech long base line (LBL) navigation transceiver. The side scan has a custom data logging unit developed at FAU. This unit takes the T-1 data coming out of the side scan and dumps it to a pair of 4.5 Gb hard drives. This provides 12 hours of data storage capacity. The long payload had six additional OEX modular battery packs that extend the range and duration of the AUV missions. The Barney payload was operated by the Forward Look Sonar group from FAU, and the ROBOT payload was operated by the Center for Ocean Technology (COT) group from the University of South Florida. All payloads were interchangeable among the two OEX tail sections: Drake and Magellan. A diagram of the OEX side scan configuration is shown in Figure 3.1.2.

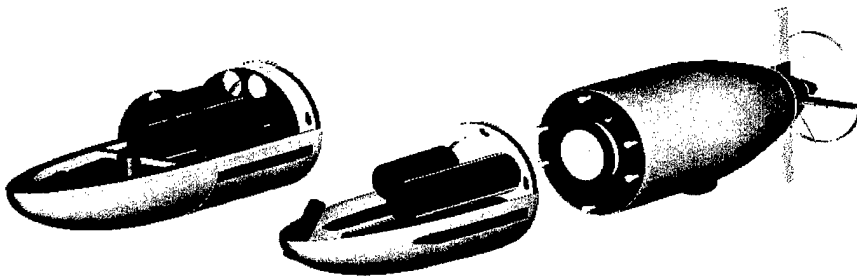


Figure 3.1.2: Cut -away view of the payloads used for the mine reconnaissance experiment along with a tail section. Any payload can attach to any tail section.

Navigation

Although several different Navigation and vehicle positioning systems have been integrated into the OEX only two were employed for this experiment. In one mode of operation the AUV dead reckons under water using DVL based ground speed and heading to calculate its position. The AUV periodically surfaces to obtain DGPS fixes to bound the drift in its position estimate. A retractable DGPS antennae is used when the vehicle is on the surface to obtain the fix. The limiting constraint on this navigation method is compass accuracy. Positional accuracy is on the order of 1 - 5% of distance traveled. The compass is calibrated with a deviation table to within 1 degree. Other errors in the system further decrease the positional accuracy.

The second type of navigation used in the experiment is long base line (LBL) sonar. In LBL, an array of acoustic beacons ping at different frequencies when interrogated by the AUV. The round trip time gives a range to each beacon. The AUV can calculate its position by intersecting the spheres corresponding to each range. This is the most accurate navigation method but also requires a lot of effort to install and calibrate the LBL beacon array. The positioning code has a heuristic sensor fusion algorithm that robustly uses whatever navigation information is available.

Mine Reconnaissance Experiment Objectives

The principle objective of the experiment was to perform remote mine reconnaissance using AUVs. This would explore the issues associated with using AUVs solely as for mine reconnaissance without human or mammals having to visit the mine field. In our case the AUVs serve as a delivery platform for the sensors to go to the site collect the data and return. Detection, classification, and identification of targets is still done off line by humans. As capability improves, future experiments will successively test on line target detection etc. But before we can worry about on-line detection one must solve the sensor, navigation, control, and logistics problems. Secondary objectives include: 1) quantifying the performance of the AUV sensors, navigation, and communications systems; 2) refine logistical issues; 3) investigate performance of search and survey operational and control approaches.

Mine Reconnaissance Approach

The fast brute force way is the single pass approach that is pass over the survey area once at the highest coverage rate with the maximum spacing between transects while detecting, classifying, and identifying mines as you go. This requires imaging sensors with high resolution at long range. These are typically large and expensive. Small AUVs have size, power, computation, and speed limitations that make single pass mine reconnaissance impractical given current technology. However the lower operating and deployment costs for small vehicles makes a multi-pass approach feasible. In this approach one or more AUVs perform repeated surveys. Each survey serves to identify those areas where a more focused higher resolution survey is needed and rule out areas where no further survey is needed. Because spatial resolution of the imaging sensors is a function of range one can get high spatial resolutions if the range is short enough. The hypothesis is that for comparable cost multiple inexpensive vehicles can achieve coverage rate comparable to large vehicles. The remote mine reconnaissance task can be broken down into the following stages.

- a) *Rapid environmental assessment (REA)*. The purpose of REA missions is to collect oceanographic data about the operating environment such as bathymetry, ocean currents, sea floor composition, clutter, visibility, and sound velocity profiles. This data is needed for tactical decision aids for operation in the area and to help plan the next stages of mine reconnaissance. The OEX are equipped with sensors that can measure some of these quantities. The Doppler velocity log measures ground speed, water speed, and altitude. Combined with heading and depth sensors this enables calculations of bathymetry and current shear. The CTD measurements can be used to calculate sound velocity. The side scan sonar gives a direct indication of bottom clutter and an indirect indication of bottom type. The video camera can be used to roughly estimate visibility.
- b) *Mine detection*. The side scan sonar is the primary sensor for detecting mine like objects. This was done using wide area grid surveys. In fact the REA and initial detection missions used the same wide area grid survey pattern. The result of the mine detection stage is a prioritized list of mine like targets and their locations. In this experiment, the detection was done off line by manually viewing the side scan data using visualization software and then calculating the locations of likely objects from the vehicle position and relative location of the target in the side scan image.
- c) *Mine classification*. For this stage close in targeted side scan surveys were used to get multiple hits from multiple viewing angles of the targets detected in the previous stage. The targeted surveys were low altitude, high resolution, multiple pass surveys. This stage classifies the mine like targets as either mines or not. A new list of mine targets is generated for use in the next stage.
- d) *Mine identification*. The primary sensor used for this stage was the downward looking video. The AUV swims over the top of the mine at close range. Given sufficient visibility it is possible to identify the mine type by inspection of the video. Because of positional inaccuracies multiple closely spaced "swim" overs are conducted in the vicinity of the target to guarantee a video hit. This stage produces a list of mines, types, and locations. In addition to the video we experimented with a forward look multi-beam sonar and nighttimes surveys using a laser line scan.
- e) *Mine localization & revisitation*. The multi-pass approach to mine reconnaissance requires that the targets be localized and revisited at each succeeding pass. In a single pass approach this stage is only needed in preparation for mine neutralization.

Mission Descriptions

The 1998 Mine Counter Measure experiments (MCM) took place off Ft. Lauderdale from December 1 to December 12. All missions were conducted from the Research Vessel Sea Diver in the SFTF Range site approximately 2 NM South of Port Everglades Inlet in 20 - 70 ft. of water depth. An LBL array consisting transponders at 9.5 kHz and 11.0 kHz was deployed in the Range. The survey area consisted of a 500 meter by 500 meter box with side roughly aligned to North-South East-West respectively. The mines were deployed in 2 North-south lines near the western (shallow) end of the box. There were a total of 19 mines of various shapes and one torpedo. A picture of 3 of the mine shapes is given in Figure 3.1.2



Figure 3.1.2: Pictures of some of the mine targets placed in the mine field.

During the 1998 MCM Experiment, 22 missions were run with the Drake and Magellan OEX AUVs. All the data collected from these missions is available on computer. Each data log file is indicated by a unique mission identifier. The mission identifier is made up of the year month and day separated by a period from the GMT start time of the mission. The results described in this paper will also follow this convention. For instance Mission 19981202.1954 started December 2, 1998 at 19:54 GMT. Given the 5 hour difference between GMT and EST this translates to 2:54 p.m. EST.

Three basic mission types were used as follows: 1) Wide area grid survey of a 500 meter box with both North-South and East-West legs at 25 meter spacing and at 5 meters altitude; 2) Targeted grid survey of a 50 meter box with both North-South and East-West legs at 10 meter spacing and at 2.5 meter altitude for bottom targets and higher altitude for moored targets. 3) Swim over surveys at 2.5 to 4 meter altitude with 3 - 5 meter spacing parallel to the track line. Several other types of missions were conducted to test navigation and vehicle systems in preparation for the reconnaissance missions. All the missions were run at a water speed of 2.5 knots. The next sections will present the results from 3 of those missions.

Mission 19981204.1433

Mission 19981204.1433 was the first and only run of the third day of the 1998 MCM operation. The purpose of this mission was to conduct a Rapid Environmental Assessment (REA) of the minefield using LBL navigation. The mission lasted approximately 4 hours and 45 minutes. Because of the relatively long duration of the mission, the vehicle was commanded to surface for GPS fixes eight times. This mission surveyed the complete mine field area (a 500 meter square box) at a spacing of 25 meters between transects. Both North-South and East-West transects were flown. A plot of the vehicle trajectory is shown in Figure 3.1.3. A plot of the currents is

given in Figure 3.1.4. Space limitations prevent showing other data such as sound velocity profiles, bathymetry, and side scan data.

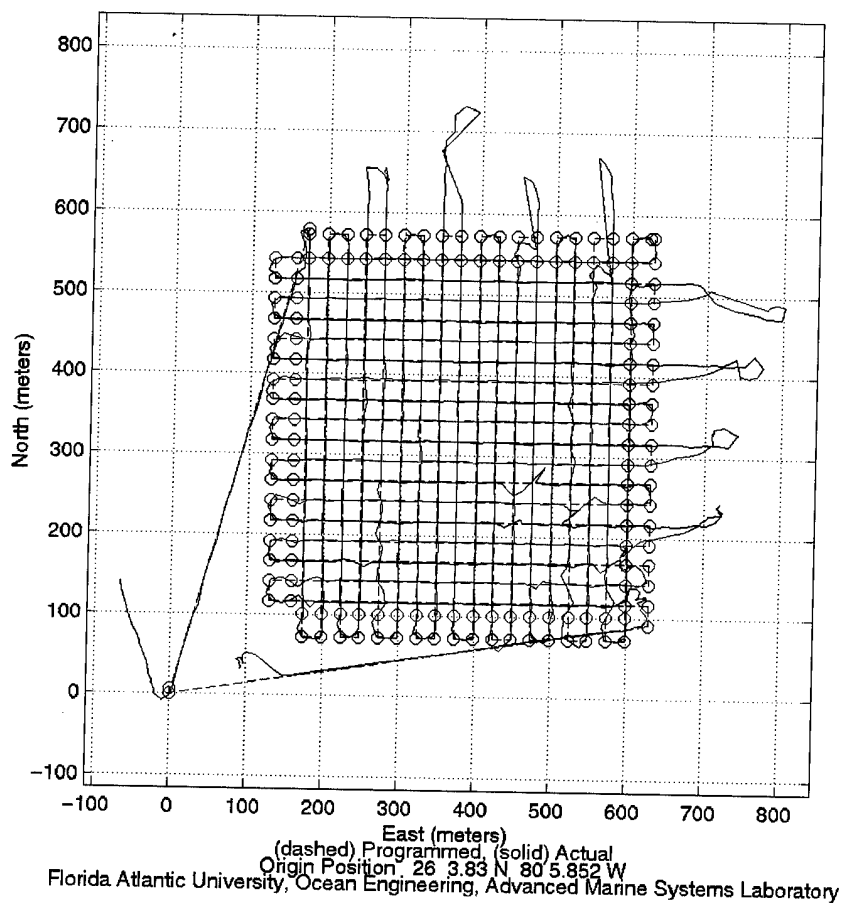


Figure 3.1.3: Plot of the vehicle path for Mission 19981204.1433. Coordinates are in meters relative to origin.

DRAKE (E/W) Water Current (Mean set, drift = 357□6, 0.15 kts.) 19981204.1433

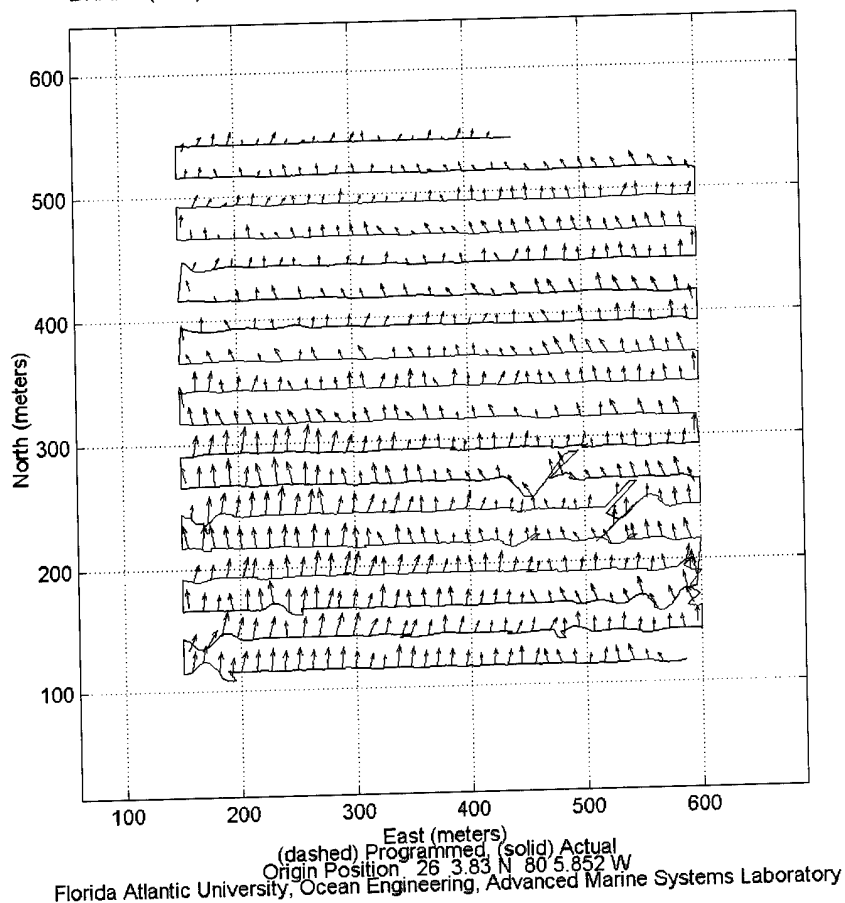


Figure 3.1.4: Current measured on mission 19981204.1433.

Mission 19981210.1959

Mission 19981210.1959 was a targeted survey for mine classification with Magellan using LBL navigation, and collecting high frequency sidescan data, and video. The mission consisted of two 50 meter box grids each overlaid on top of a different mine target. The grid spacing was 10 meters with both North-South and East-West transects. The vehicle altitude was 2.5 meters off the bottom. The mission was successful. Both sidescan and video images were collected. The video was clear enough that the mines could be identified. A plot of the vehicle trajectory as well as one side scan image is shown in Figure 3.1.5.

Mission 19981211.1630

Mission 19981211.1630 was a "fly over" mission for mine classification and identification. The mission collected sidescan and video data, and used LBL navigation and the acoustic modem for status updates. The mission was run at 3m. altitude and with 3 m. spacing between the legs in order to obtain complete video coverage of the area. The mission completed successfully. The mission consisted of two swaths, one over each of the lines of mines. Given that the mine field was laid out in lines, this was deemed the most efficient way to fly over as many mines as possible. A plot of the vehicle trajectory and a sample side scan image are shown in Figure 3.1.6.

This mission passed by each targets multiple times. By post processing and viewing the side scan data, a list was generated of all the hits or targets. These hits are plotted along with the actual locations of the mines. The target plot shows clusters of hits near bottom objects. This confirms the consistency of the survey measurements and gives an indication of the repeatability of the navigation system and the error in positioning a target. This target plot is shown in Figure 3.1.7. A zoomed in more detailed view of a section of the target plot is shown in Figure 2.8. The clusters are under 20 meters in diameter. More work can be done to further calibrate the LBL system and the vehicle navigation systems. The errors are a combination of vehicle positioning inaccuracies and range and bearing errors of the targets from the vehicle. Multiple hits on the mines were also achieved with the video camera. The video camera has a 60 degree aperture. This gives a 1 to 1 ratio between altitude and swath width. So even given the limited swath (3 meters) of the downward pointed camera at 3 meters altitude, revisitation, localization, and positive identification of the mines was possible using multiple closely spaced passes over a 30 meter wide lane centered on the target.

Results

This experiment has demonstrated that small low cost AUVs can be effective for remote shallow water mine reconnaissance tasks using a multiple pass approach. Experiments are planned in 1999 to further refine and enhance capabilities. This will include multiple simultaneous vehicle missions and acoustically remote controlled missions. Eventually we plan to include on-line target detection capability.

References

1. S.E. Dunn, S.M. Smith, P. Betzer, T. Hopkins, "Design of Autonomous Underwater Vehicles for Coastal Oceanography," *Underwater Robotic Vehicles: Design and Control*, J. Yuh Editor, TSI Press, 1994, pp. 299-326,
2. S.M. Smith & J. Park, "Navigational Data Fusion in the Ocean Explorer AUVs", UT 98, 15-17 April, 1998, Tokyo Japan
3. S. Smith, J. Park, J. Rivero, T. Pantelakis, E. Henderson, E. An, "Development of Hydrographic Survey Capabilities on the Ocean Explorer AUV, *Oceanology* 98, 10-13 March 1998, Brighton UK.
4. S.M. Smith, E. An, D. Kronen, K. Ganesan, J. Park, and S.E. Dunn, "The Development of Autonomous Underwater Vehicle Based Survey and Sampling Capabilities for Coastal Exploration." *IEEE Oceans* 1996, Ft. Lauderdale Florida, Sept. 23 -26, 1996.

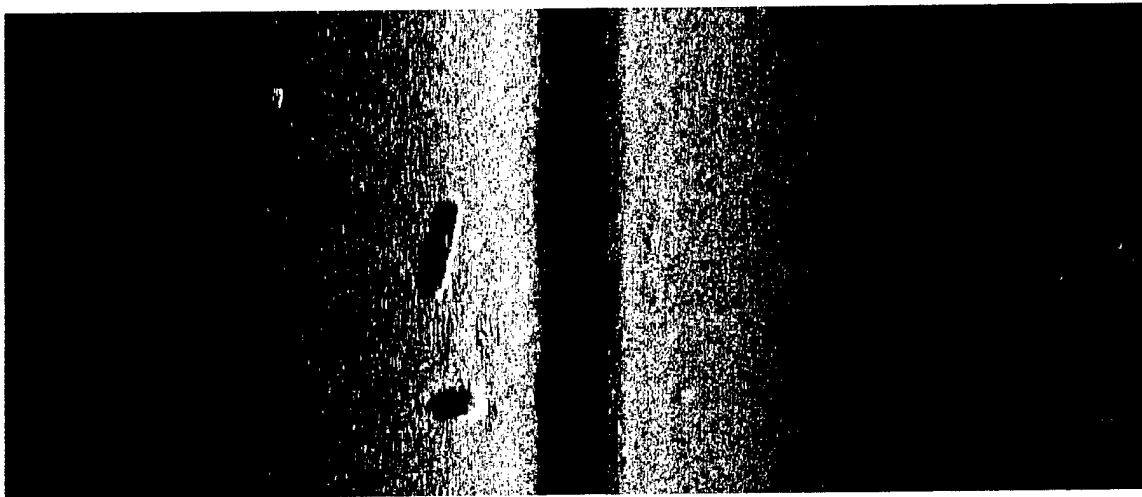
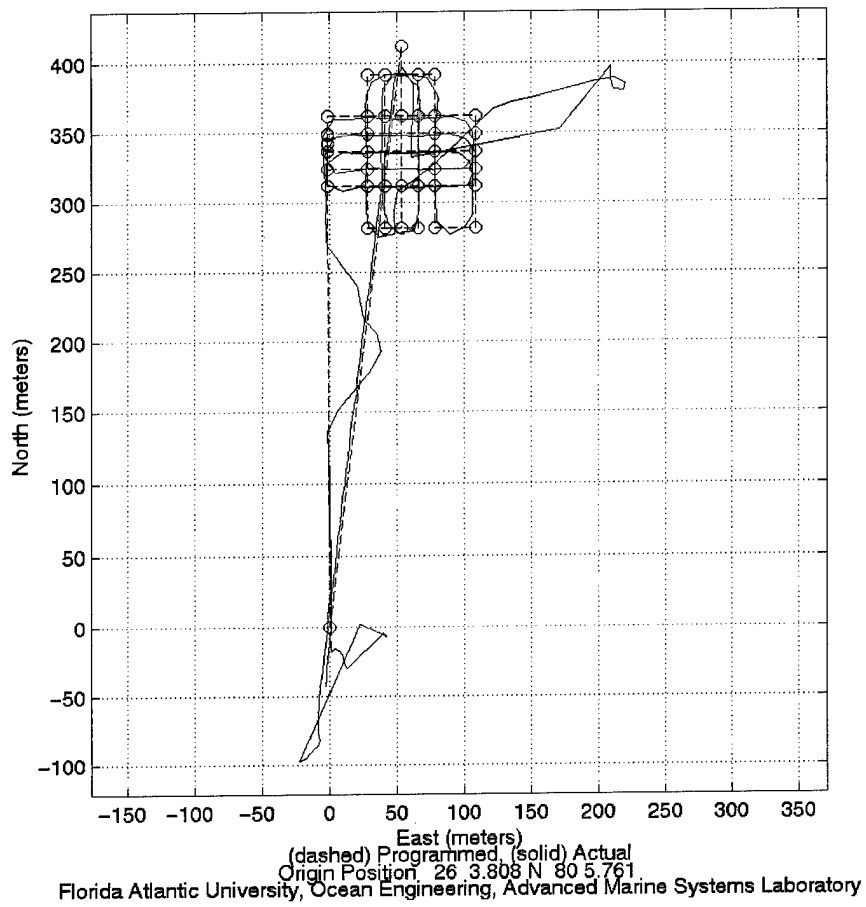
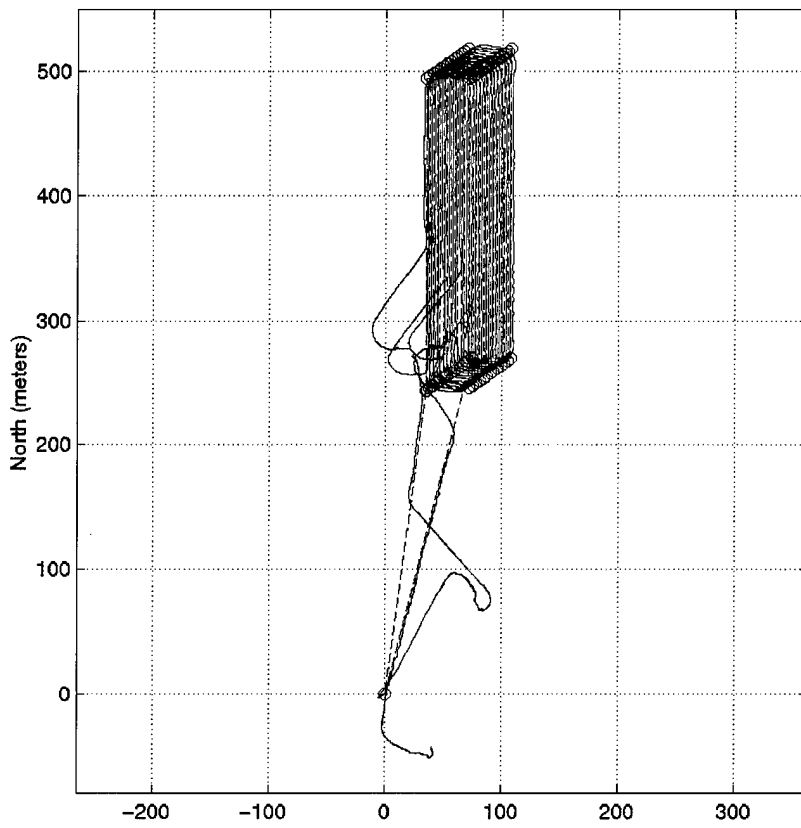


Figure 3.1.5: Mission 19981210.1959 targeted survey. (a) plot of vehicle path during mission. Two small grids over two different targets. (b) side scan image from mission showing mine target in left center (torpedo) and non mine target (concrete block) in left bottom.



(dashed) Programmed, (solid) Actual
 Origin Position 26 3.818 N 80 5.761 W
 Florida Atlantic University, Ocean Engineering, Advanced Marine Systems Laboratory

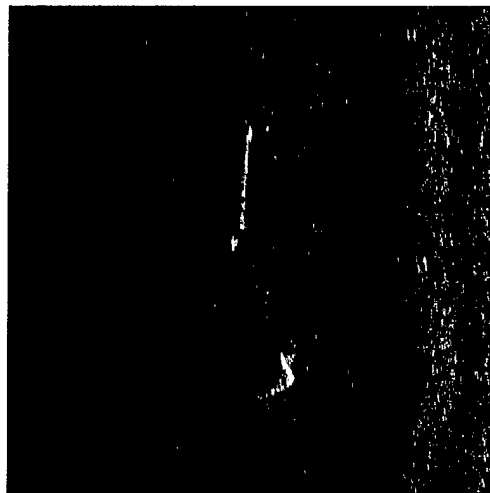


Figure 3.1.6: Mission 19981211.1630. (a) Plot of vehicles path. Starting point is at origin. The AUV transited to the survey site and then surveyed the two lines of mines with a 3 meter spacing between each path. (b) Blow up of a side scan image showing torpedo and concrete block.

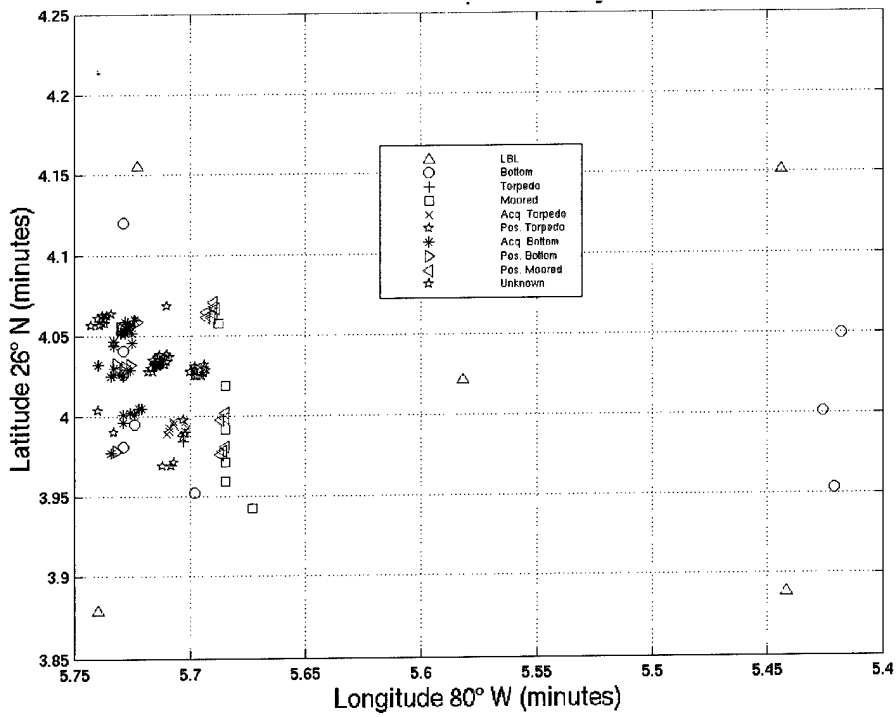


Figure 3.1.7: Mission 19981211.1630. Target plot showing detections and actual locations of targets.

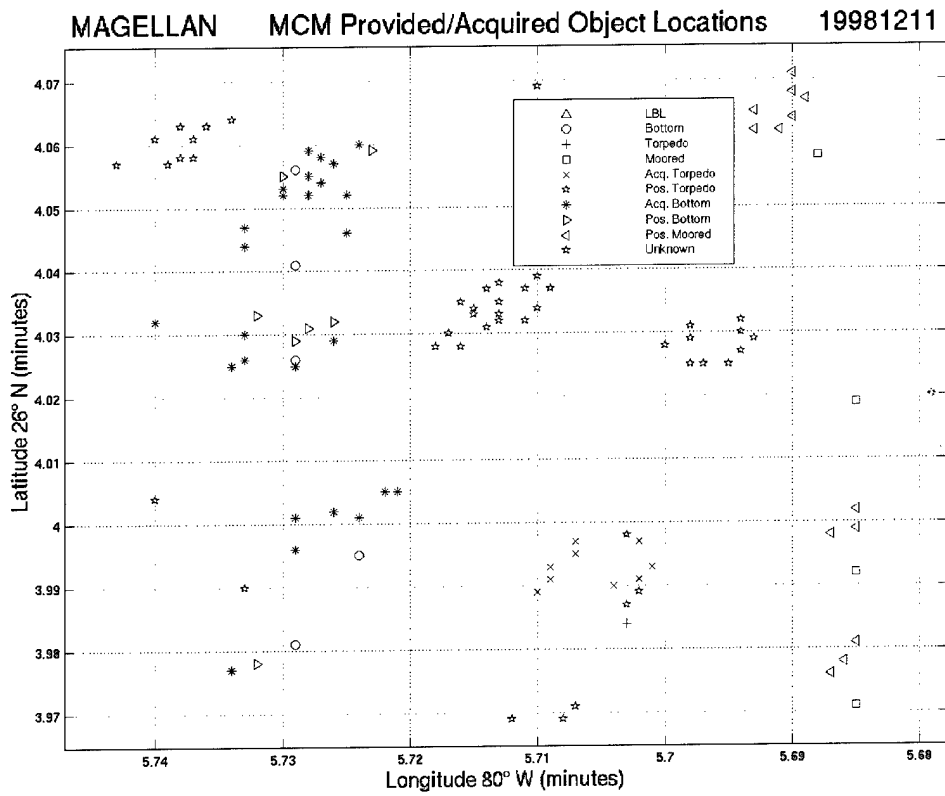


Figure 3.1.8: Mission 19981211.1630. Detailed view of a section of target plot showing clusters of detections.

3.1.2 Development of a 1.2 Mhz Chirp Sidescan Sonar for Mine Classification by AUVs

S. G. Schock, J. Wulf (FAU)

A 1.2 MHz chirp sidescan was developed for AUV mine hunting and classification. The frequency of 1.2 MHz was selected to ensure that scattering could be detected off of surfaces not normal to the acoustic axis of the sonar beampattern. Since the wavelength at 1.2 MHz is approximately 1 mm, the wavelength is near the same order of magnitude as the surface roughness of a mine. Scattering off the surface of the mine allows generation of the imagery suitable for classification. Lower frequency sonars usually only receive echoes off normal surfaces which makes classification difficult if not impossible. For example, a spherical target would generate a single echo or the part of the sphere that is normal to the sonar beam. As shown below the 1.2 MHz chirp sidescan can generate an image of a spherical mine showing the outline of the closest hemisphere by detecting scattering off the sides of the mine.

For the images in this report, the chirp sidescan was transmitting at rates between 40 and 86 pps. The maximum transmission rate is 127 pps. The chirp sidescan has a bandwidth of 50 kHz. The sonar is completely contained in a single canister with the exception of the acoustic arrays and the battery. The bottle contains DSP processor and data acquisition cards, a PC motherboard, 100 Base T Ethernet, a disk for data storage, and transmission and reception circuitry. The A/D converters digitize the data at a rate of 200 kHz. The DSP performs real time correlation processing. The pulse length is 1 msec which is short enough to allow the sonar to operate as close as 1 meter from the seabed.

The sidescan was designed to operate in a towed mode or in an AUV. In the AUV configuration the sonar is powered with 48 VDC. The full power load of the sonar is about 100 Watts.

In the block diagram shown in Figure 3.1.9, a Pentium computer controls a 20 MHz waveform generator which generates a 1 msec long chirp pulse with a center frequency of 1.2 MHz and a bandwidth of 50 kHz. A class B amplifier drives the piezoelectric transmitting array through a matching transformer and T/R switch. The small signal output of the sidescan arrays is amplified by a preamp. The bandpass filter rejects out of band noise before digital conversion. The digitized data is processed with a digital correlator. The correlated data can be stored on disk or sent via 100 Base-T ethernet to a sonar display or processor.

The sidescan was tested in a towed mode over a mine field installed at the SFTF range located just to the south of the Port Everglades inlet. Correlated data was stored. The images in this reports (figures 3.1.10, 3.1.11, 3.1.12 and 3.1.13) were generated from the stored correlated data. During the seatests a real time image of the seabed allowed the sonar operator to confirm that the sonar was passing over the mines. The sonar was connected to the topside via 100 Base-T.

Results

During a sea test over the minefield, the chirp sidescan, operating at 1.2 MHz, demonstrated its ability to generate detailed images of moored and bottom mines. The high frequency allows the measurement of scattering off target surfaces that are not normal to the

sonar beam and provides the ability to generate images of the target shape useful for target classification.

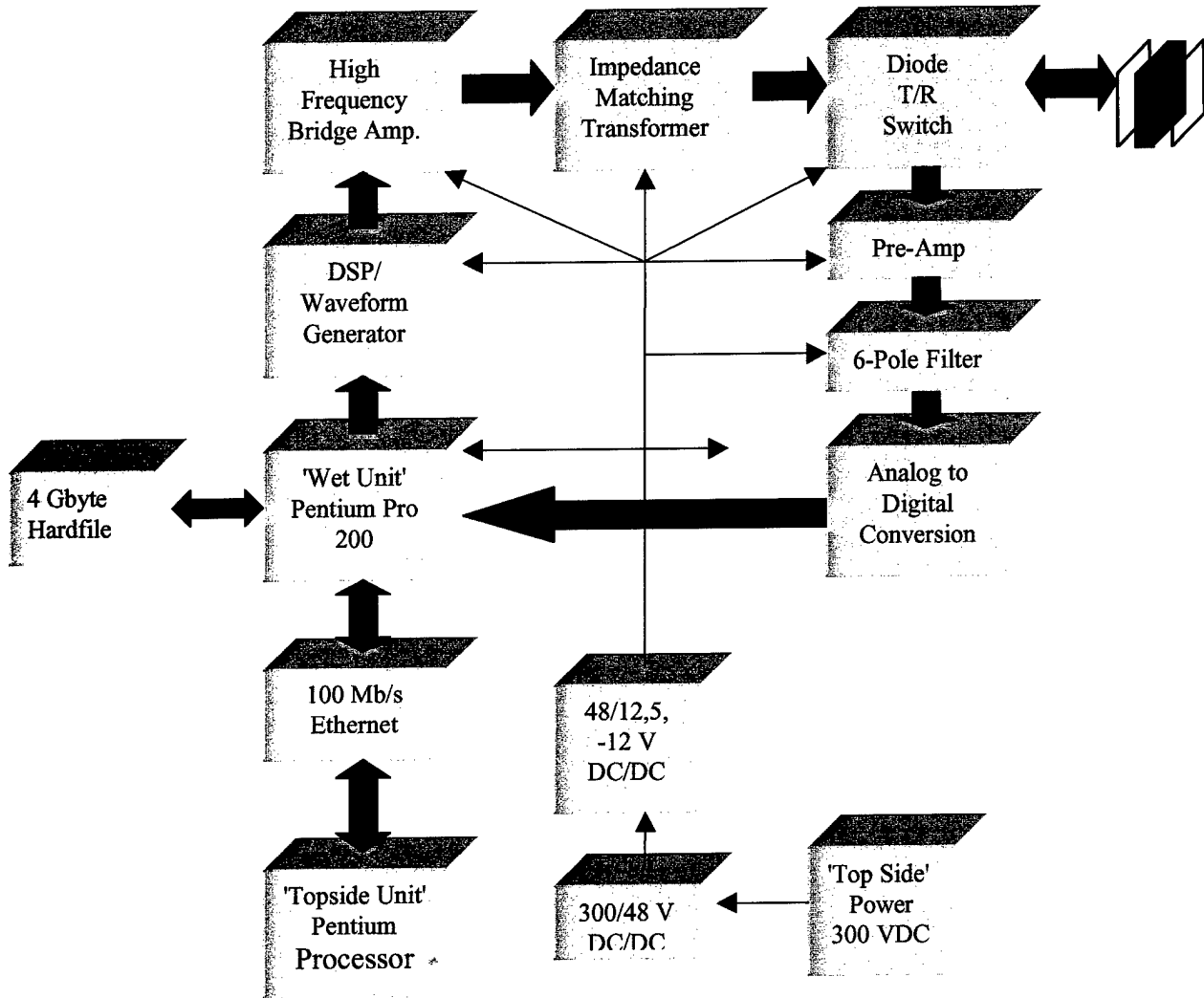


Figure 3.1.9: Block Diagram of 1.2 Mhz Chirp Sidescan Sonar

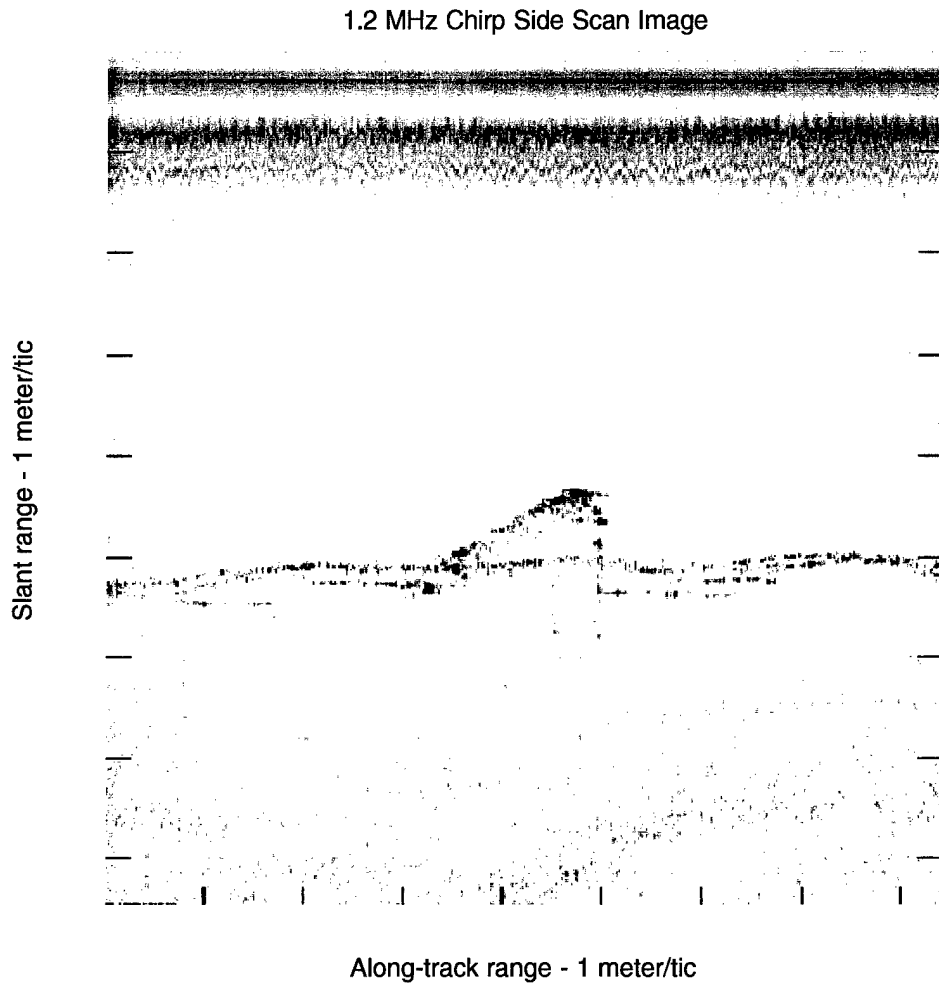


Figure 3.1.10: Chirp sidescan image showing outline and sides of MK 56 cylindrical mine in vicinity of surface multiple reflection.

1.2 MHz Chirp Side Scan Image

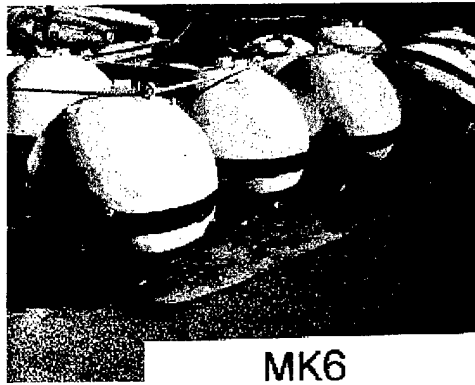
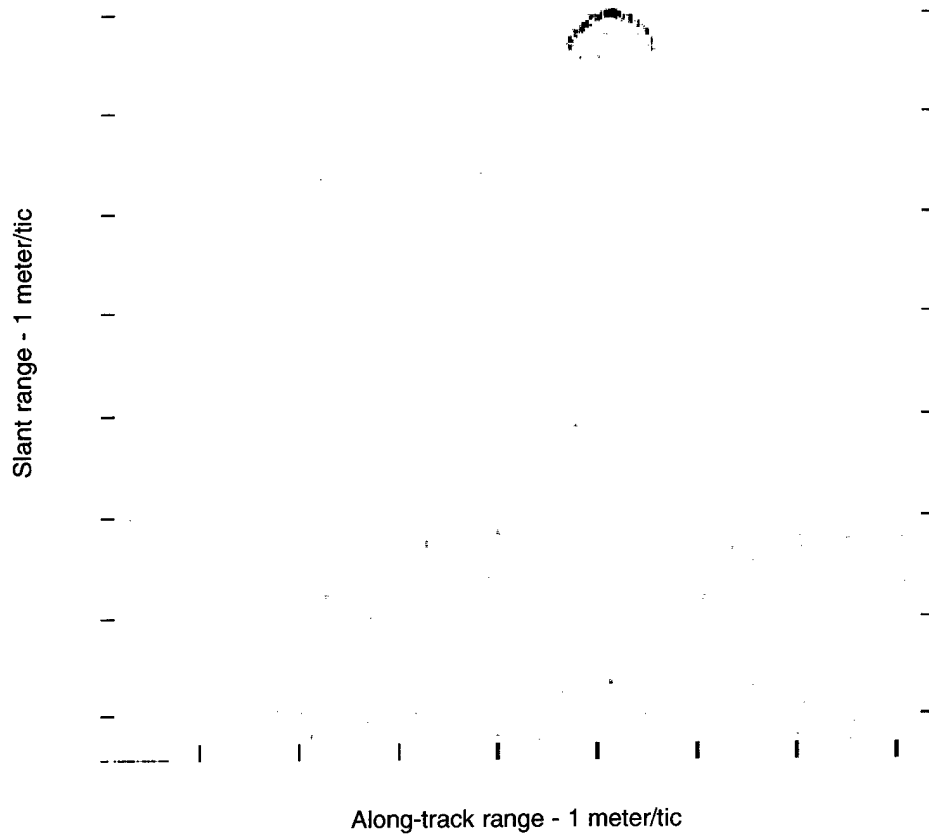
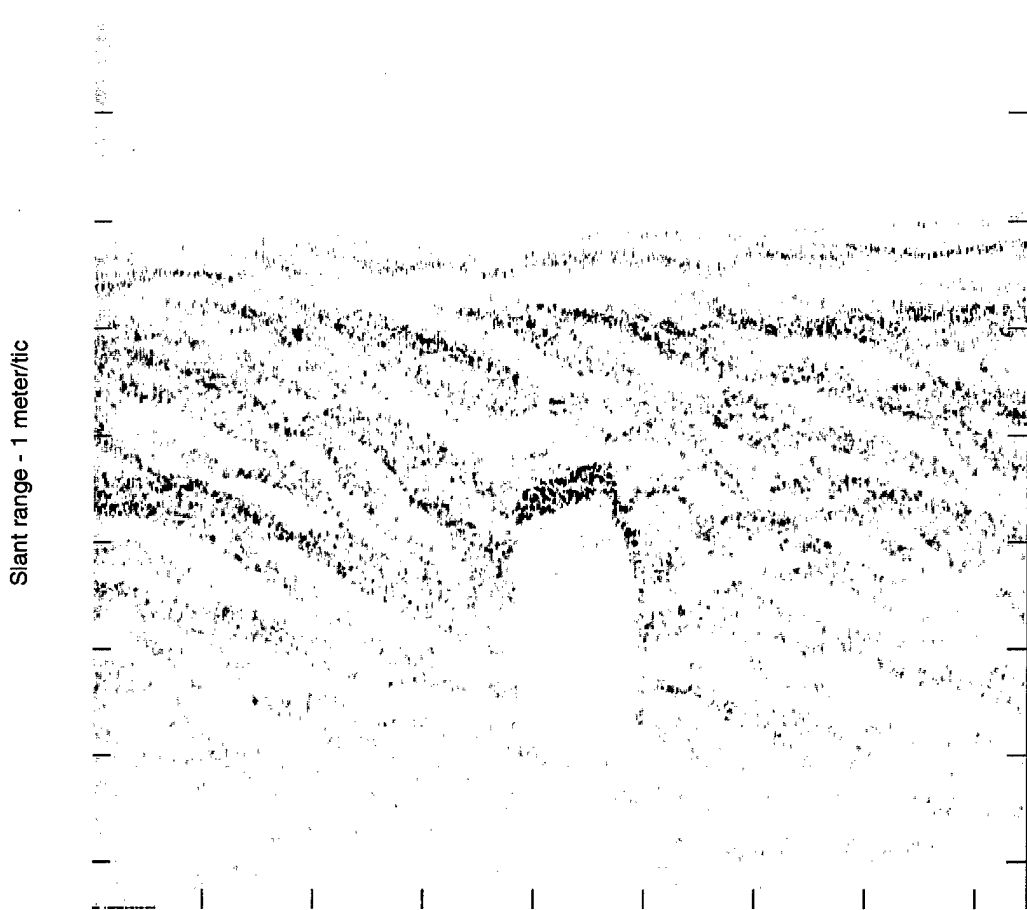


Figure 3.1.11: Chirp Sidescan Image Showing Scattering off Surface of Half a MK 6 Spherical Mine Allowing Measurement of the Mine Diameter

1.2 MHz Chirp Side Scan Image



Along-track range - 1 meter/tic



Figure 3.1.12: Chirp Sidescan Image showing outline of 2 faces and top of 1 meter cube of concrete in a sand wave field. The length of the shadow shows that the height of the cube is 1 meter.

1.2 MHz Chirp Side Scan Image

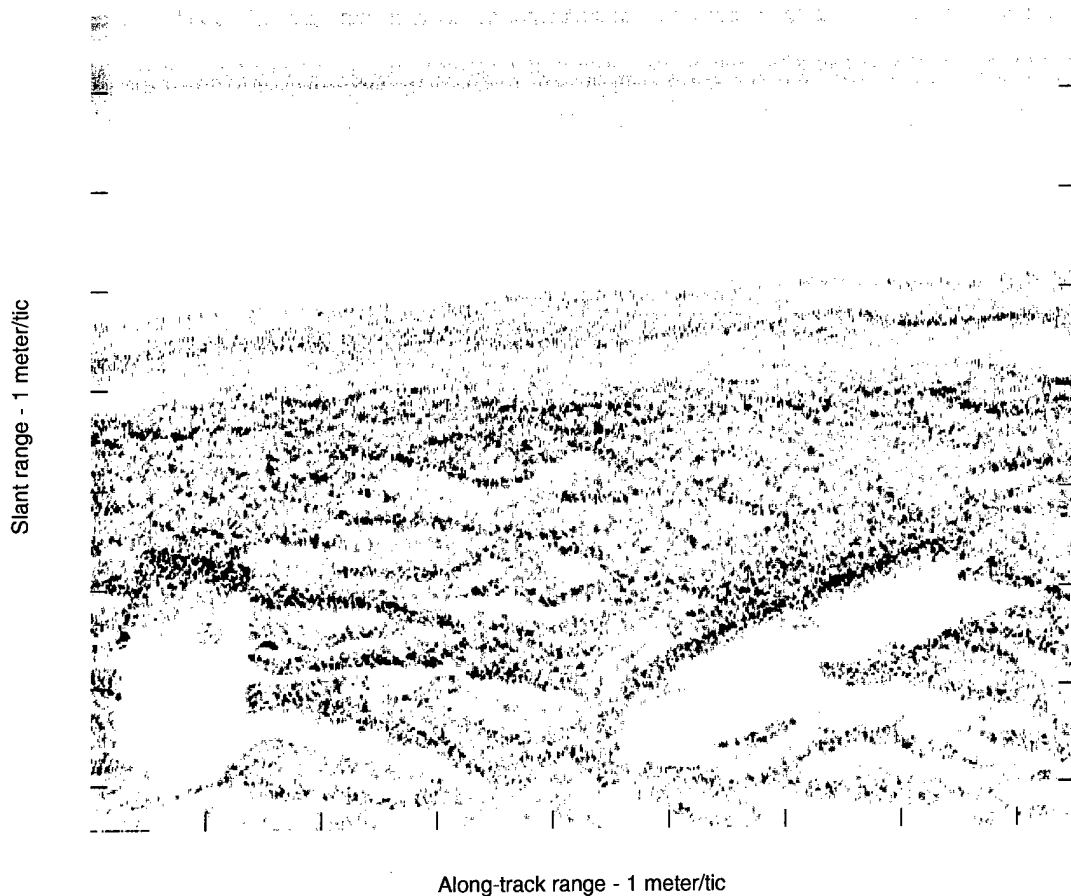


Figure 3.1.13: Sidescan Image showing cylindrical mine (right), lying on the seabed, and 1 meter cube of concrete (left) in field of sandwaves

3.2 Adverse Weather Experiment (Experiment 2)

Adverse weather experiments were carried out in the SFTF range in the Fall of 1998. Typically, in the fall months cold fronts move across South Florida from North to South causing rapidly varying weather conditions, followed by one to three days of strong North Easterly winds and high seas. This experiment evaluated AUV performance during one of these events.

The technical goals of the experiment were:

- 1) To evaluate the reliability aspect of deploying and operating multiple AUVs in stormy weather;
- 2) To quantify the effect of acoustic propagation properties on AUV navigation, communication and control performances;
- 3) To address problems associated with the current docking mechanism and power transfer to be used in high sea-state conditions.

The scientific goals of the experiment were to:

- 1) Initiate a data bank of measurements in the shallow water column during high sea states. This will form the basis for testing and developing dynamic ocean models associated with such events;
- 2) Determine the effect of the adverse weather on the local bathymetry;
- 3) Assess the changes in oceanographic conditions in the water column;
- 4) Test the various acoustic sonars in environments with very high reverberation levels and provide new insights into the turbulence and ambient noise levels in the littoral zone in high sea states.

Specific tasks included:

- 1) Bathymetric surveys over a region of 1 square kilometer, CTD/ADCP surveys of the water column were taken before and after the adverse weather period.
- 2) In-situ measurements using an AUV platform of the three components of turbulent velocity, dynamic pressure and microstructure temperature in the upper mixed layer and in the close-bottom boundary layer.
- 3) During the experiment, side scan sonar measurements using an AUV platform were made of a target in the water column in order to assess the effect of reverberation on a moving sonar in different sea-states.
- 4) Throughout the experiment, ambient noise measurements were made using an ambient noise array.

5) Reverberation measurements were carried out using a static acoustic modem in order to evaluate the effect of sea-states in shallow water on communication systems

3.2.1 Adverse Weather Experiment (Experiment 2)

Manhar Dhanak (PI), Stewart Glegg (PI), Ken Holappa (PI), Rolf Lueck, Steve Monismith, Matt Brenan, Mike Chernys and Rachel Perrie (FAU)

Objectives

The objectives of the experiment were to make measurements of small-scale turbulence, kinetic energy and ambient noise as well as of background current, temperature, salinity and sound velocity profiles in the shallow water column during the passage of a cold front over the warm continental shelf off the East Coast of Florida. The long-term aim is to investigate the impact of such fronts on mixing, air-sea interaction, sediment transport and the noise characteristics in the shallow water column. The technical aims include determining suitability of AUVs as oceanographic measurement platforms and the influence of adverse conditions on acoustic propagation and in turn on navigation, underwater communication and control performance.

Introduction

The passage of a cold atmospheric front over a subtropical continental-shelf region such as southeast Florida is generally preceded by strong cold offshore winds. During this time, air temperatures may drop by over 10° C and the associated rapid surface cooling can lead to significant convective motion [1]. The cold offshore winds do not have sufficient fetch to generate significant waves. However, once the front has passed the region, the wind directions change, blowing onshore, typically leading to white-capping breaking waves. Bubbles generated during breaking waves and entrained into well-mixed turbulent mixing layers are a significant source of ambient noise [2]. The mixed layers can penetrate through the entire shallow water column causing significant exchange of heat, gases and momentum between the upper mixed layer and the bottom boundary layer. The associated turbulent mixing in the bottom boundary layer, during such an episodic event, is of considerable importance to the rate of scour, suspension and deposition of sediments and to the dispersion and dilution of chemicals.

Small autonomous underwater vehicles (AUVs) provide versatile mobile platforms for surveying a shallow water coastal environment at low operational costs. The platforms are uncoupled from the low - frequency vibrations associated with platforms towed from surface ships. Often such vibrations are in the range of flow measurements of interest and may corrupt the data. The AUVs are good platforms for turbulence measurement [3] and for developing regional maps of bathymetry, current profiles, temperature and salinity[4]. The use of AUVs on the SFTF range for making small-scale turbulence measurements and surveying the shallow water column during Fall, 1998 in a coordinated adverse weather experiment is described below.

Procedure

The experiment was conducted in December 1998 on the SFTF range, in the vicinity of the location $26^{\circ} 03.7'N$ and $80^{\circ} 05.56'W$ south of Port Everglades, offshore Dania Beach, Florida. The schematics of the operations are shown in Figure 3.2.1.1. An Ocean Explorer-series AUV (OEX) and a smaller AUV, the MADDOG (Figures 3.2.1.2 and 3.2.1.3, respectively) were used to make in-situ turbulence measurement surveys in the upper mixed layer and the boundary layer during a cold front. The AUVs carried the turbulence package, consisting of two shear probes, a microstructure thermister and a 3-axis accelerometer, developed at FAU, and a self-motion package; the MADDOG also carried a dynamic Pitot tube. The OEX tail section carried a Falmouth CTD package, a 1200kHz ADCP and a GPS navigation system.

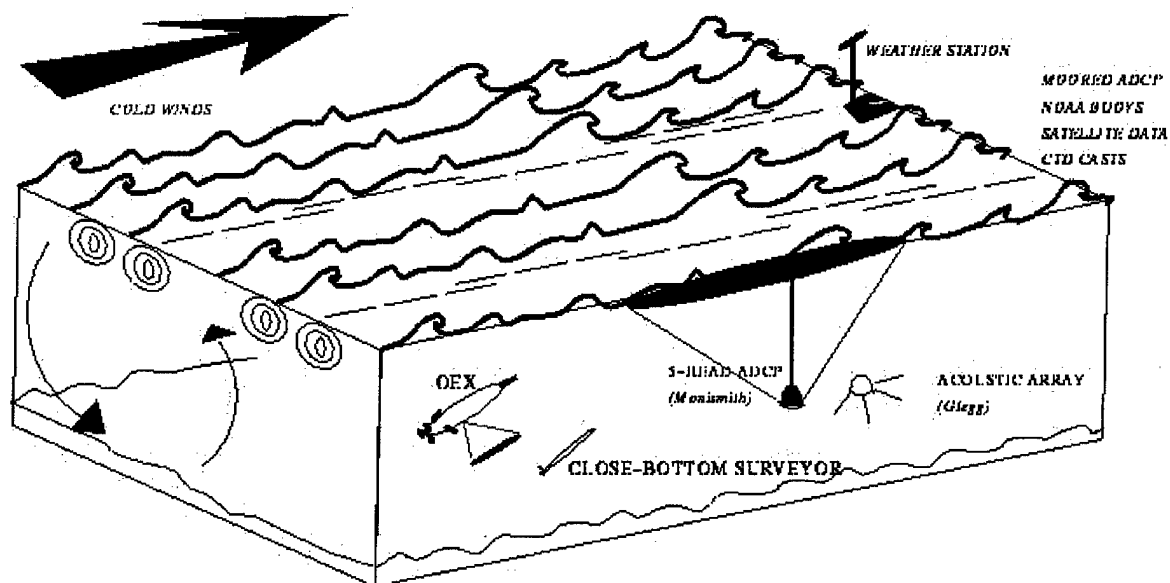


Figure 3.2.1.1.

The Bottom-mounted instruments consisted of (i) PEACOCK, a passive sonar developed at FAU, for measurement of ambient noise from breaking waves when spilling breakers occur. The ambient noise is caused by bubble plumes as they are generated from the air entrapped by the spilling breaker. (ii) A 5-head ADCP, which measured currents and the TKE in the water column during the passage of the cold front. Local wind velocity, air temperature, humidity, solar irradiance was recorded using a MET station mounted on the surface ship.

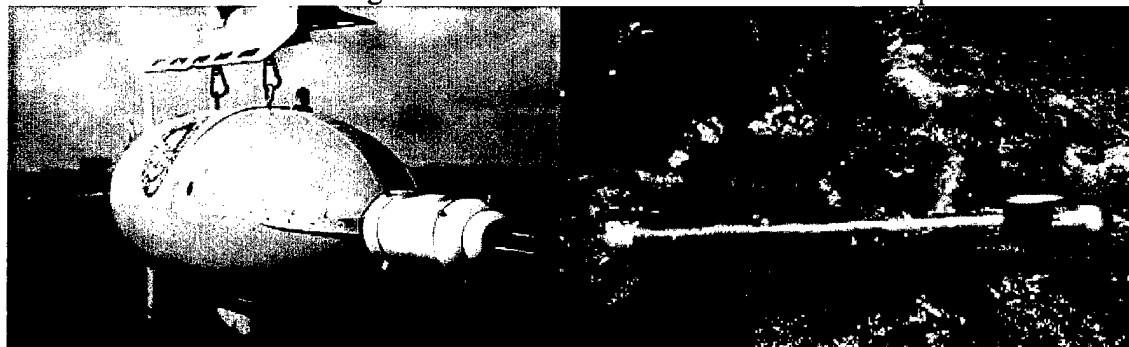


Figure 3.2.1.2.

Figure 3.2.1.3

Atmospheric Conditions: The atmospheric conditions for December, 1998 as recorded at the C-MAN buoy at Fowey Rocks is shown in Figure 3.2.1.4. The figure clearly shows the cold front with the air temperature dropping by about 10° C and wind speeds reaching around 10m/s and undergoing change in direction. The front we were considering weakened once it had moved offshore, so that no breaking waves were observed during its passage. Thus the ambient noise measurements excluded contributions from that source. The ambient noise measurements are described separately below.

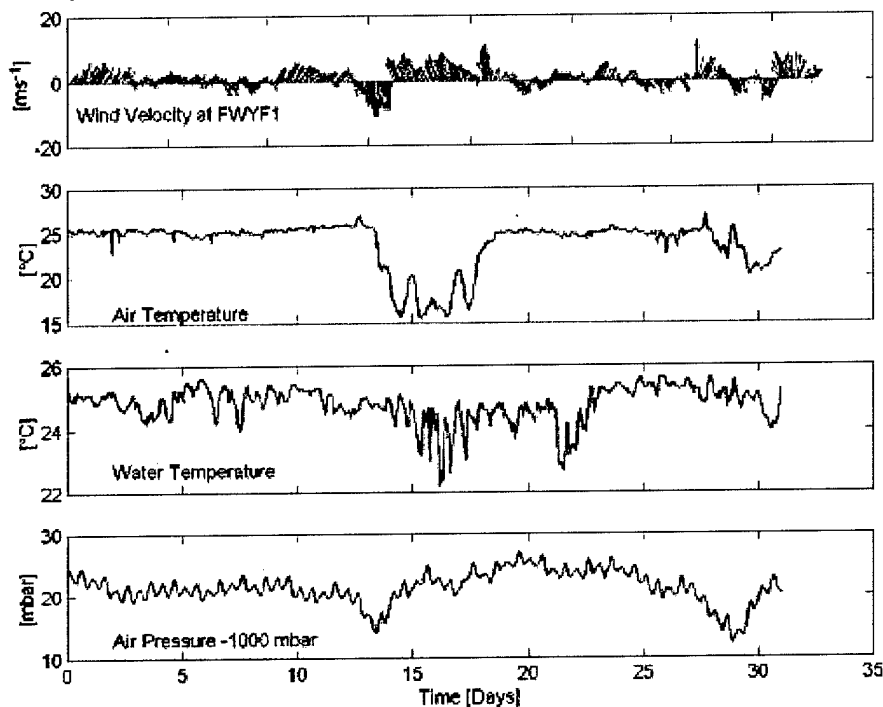


Figure 3.2.1.4. Atmospheric conditions recorded by NOAA C-MAN buoy at Fowey Rocks during December.

Ship-based CTD casts. Half-hourly CTD casts were conducted from the surface support vessel close to the box of AUV operations at $26^{\circ} 3.83'N$, $80^{\circ} 5.68'W$ using a Seabird CTD during Dec. 14 - 18 and on Dec. 21. At the end of each day, CTD measurements along east-west transects were made by the box of AUV operations approximately along the latitude $26^{\circ} 3.8'N$, starting in the vicinity of the above location. From these measurements, composite views have been developed, showing the variation of temperature, salinity and water density during each day and with respect to the offshore distance. Sample results for Dec. 17 and Dec. 21 are shown in Figures 3.2.1.5a-d. Vertical bars on Figures 3.2.1.5a and 3.2.1.5c mark the periods of AUV operations. On Dec. 17 the skies overnight were clear, the weather reports indicating clear skies for 12 hours preceding the measurements. Temperatures vary by 0.5° C, salinity by around 0.3 psu and density by 0.25 kg / m^3 at the location on both the days, indicating well-mixed regions. However, the nature of the variations suggests somewhat more dynamic environment on Dec. 17.

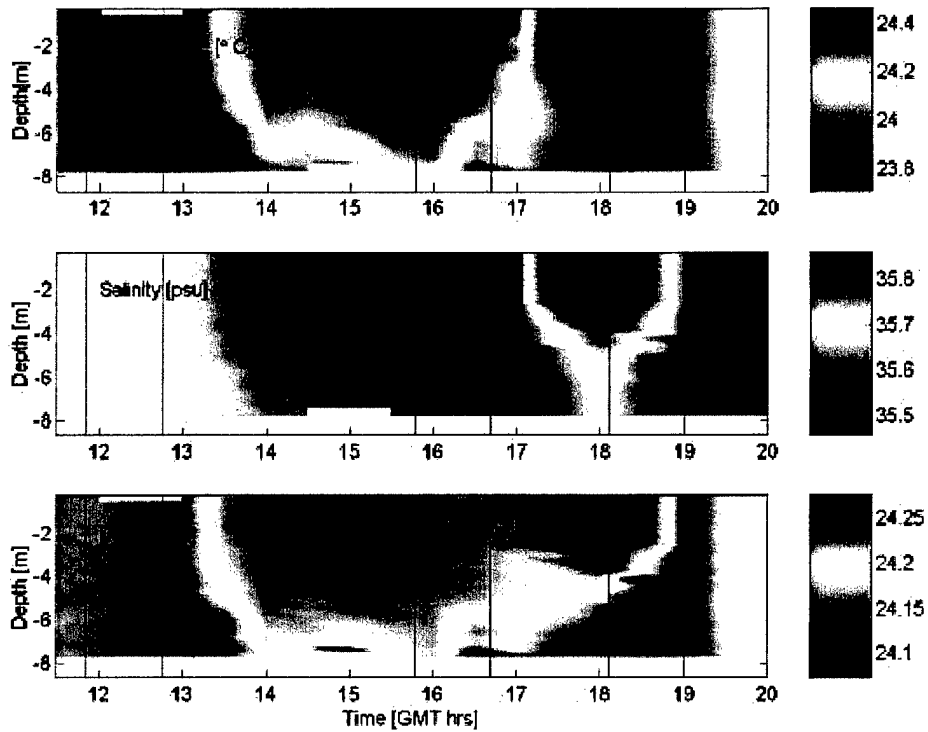


Figure 3.2.1.5a. Composite views of temperature, salinity and density during Dec. 17 at $26^{\circ} 3.83'N 80^{\circ} 5.68'W$.

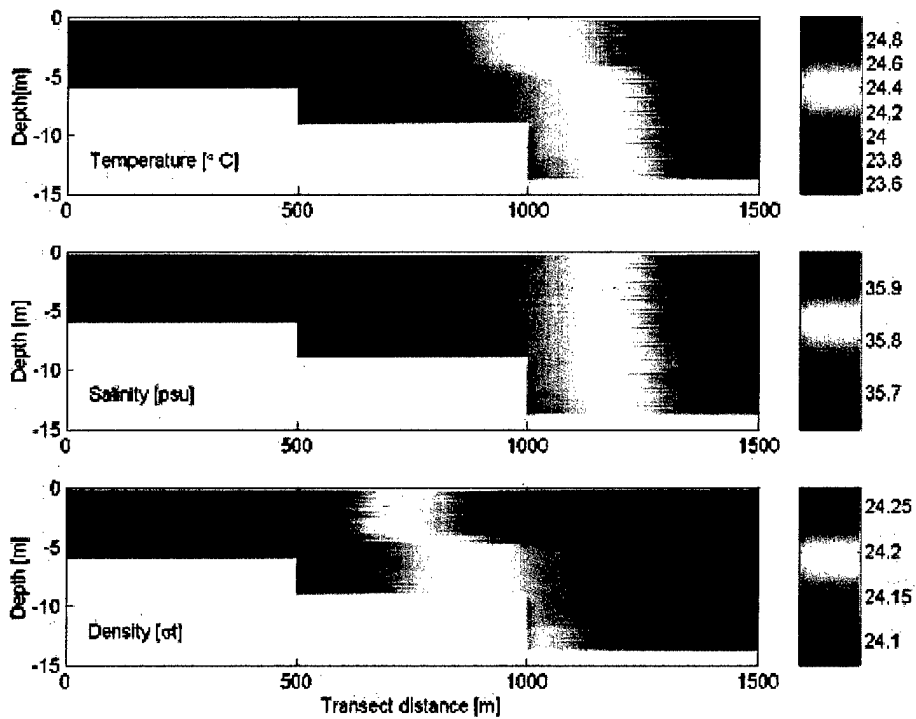


Figure 3.2.1.5b. Composite views of temperature, salinity and density during Dec. 17 over a transect along $26^{\circ} 3.8' N$ starting at $26^{\circ} 3.8'N 80^{\circ} 5.68'W$.

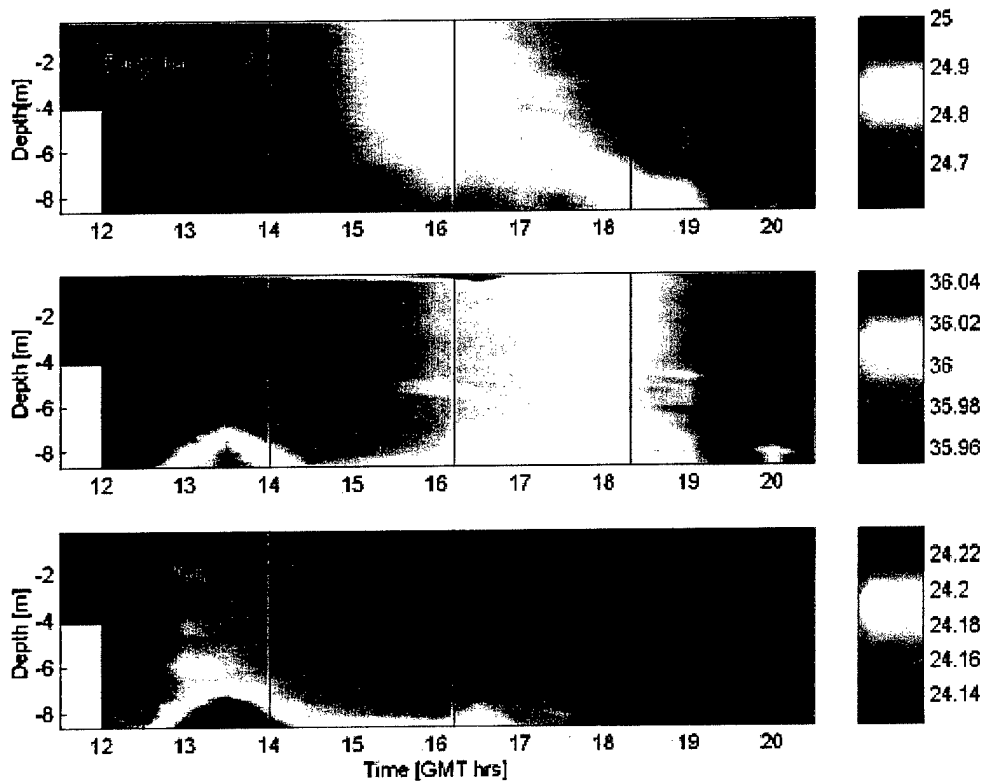


Figure 3.2.1.5c. Composite views of temperature, salinity and density during Dec. 21 at $26^{\circ} 3.83'N 80^{\circ} 5.68'W$.

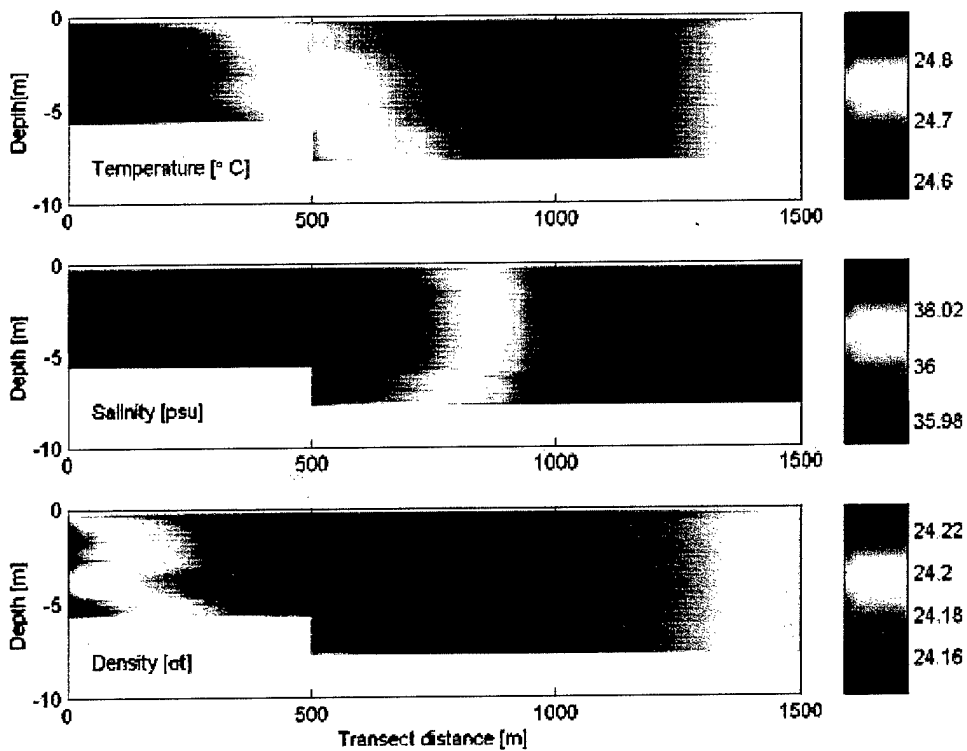


Figure 3.2.1.5d. Composite views of temperature, salinity and density during Dec. 17 over a transect along $26^{\circ} 3.8' N$ starting at $26^{\circ} 3.8'N 80^{\circ} 5.68'W$.

Bottom-mounted 5-Head ADCP Measurements: The five-head ADCP was bottom mounted at $26^{\circ} 3.7' \text{ N}$, $80^{\circ} 5.565' \text{ W}$. The bin sizes are 1m, with the first bin 1.25m above the bottom. Figure 3.2.1.6 shows the distribution of TKE measured by the ADCP.

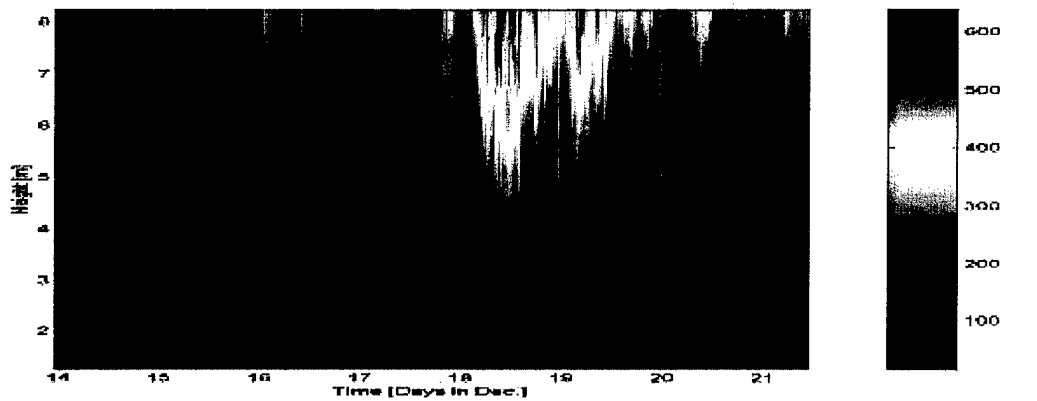


Figure 3.2.1.6: TKE $((\text{cm/s})^2)$ distribution in the water column over the 5-head ADCP during Dec 14 – 22, 1998
(Analysis by Matt Brennan).

Further analysis is being carried out on the data. Much information about the rate of TKE generated in the water is expected. For example the Reynolds stress is much higher near the surface than near the bottom, during the cold front period.

AUV operations: Our measurement missions started at dawn. Clear skies during the night enhanced the cooling, through heat loss by radiation. Figure 3.2.1.5 shows the variability in temperature, salinity and density with depth and time.

The OEX and the MADDOG were launched from the surface vessels and carried out box-pattern surveys over the bottom-mounted, upward-looking 5-head ADCP. The path of the OEX AUV during Dec. 21 operations is shown in Figure 3.2.1.7. Sample turbulence spectra as measured from the mobile AUV platforms are shown in an attached figure 3.2.1.8. The dissipation rate as a function of time is being developed and together with the 5-head ADCP will provide useful information about the energy balance in the water column. Details about the AUV paths, and spatial maps of temperature, salinity, density and sound speed developed from AUV-based measurements are illustrated for measurements on Dec. 17 in Figures 3.2.1.9 - 3.2.1.15 below. Similar results for other days are also available. Figures 3.2.1.16 - 3.2.1.17 illustrate data recorded by sensors on-board the MADDOG. Work is in progress to synthesize the various data for a full analysis of the experiment.

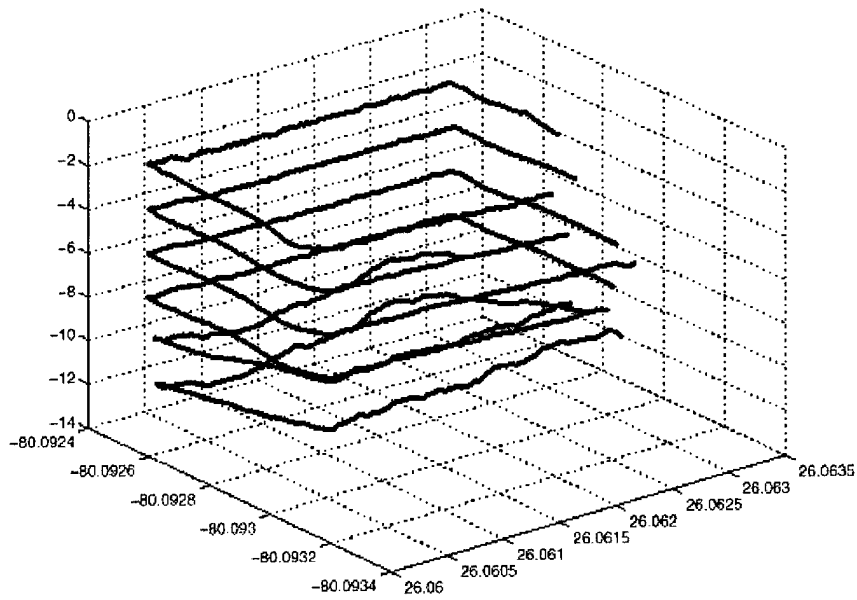


Figure 3.2.1.7

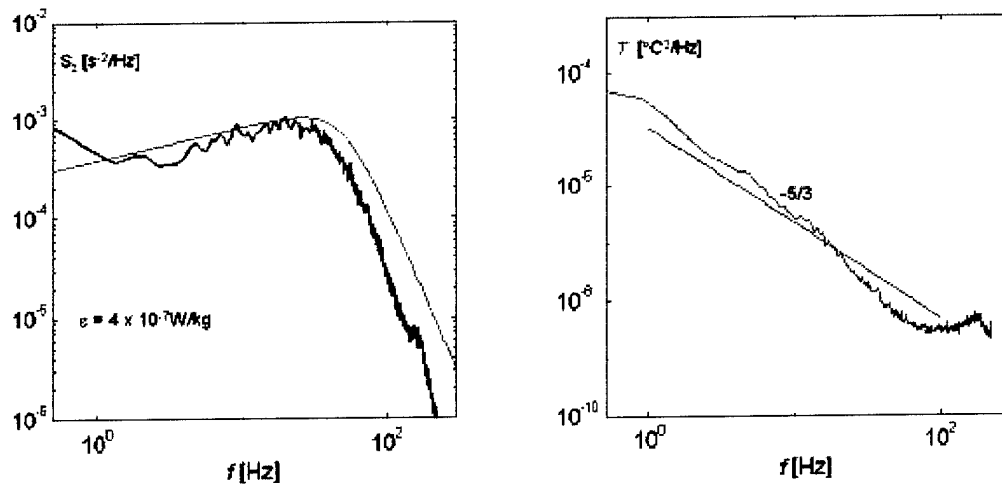


Figure 3.2.1.8: Sample shear and temperature spectra from 2-minute time segment on Dec 21.

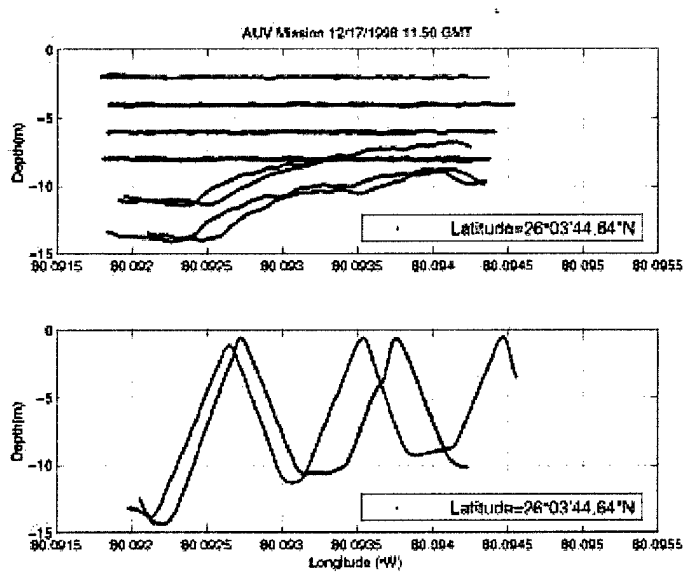


Figure 3.2.1.9. Mission path for the OEX.

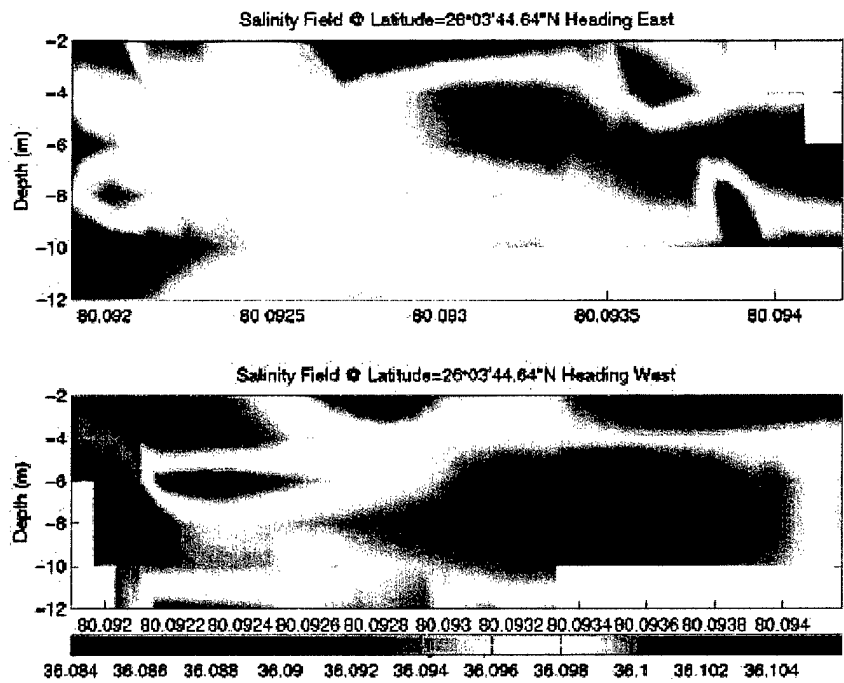


Figure 3.2.1.10. Salinity field at constant latitudes for longitudinal legs. Note variation of salinity $O(0.1 \text{ psu})$.

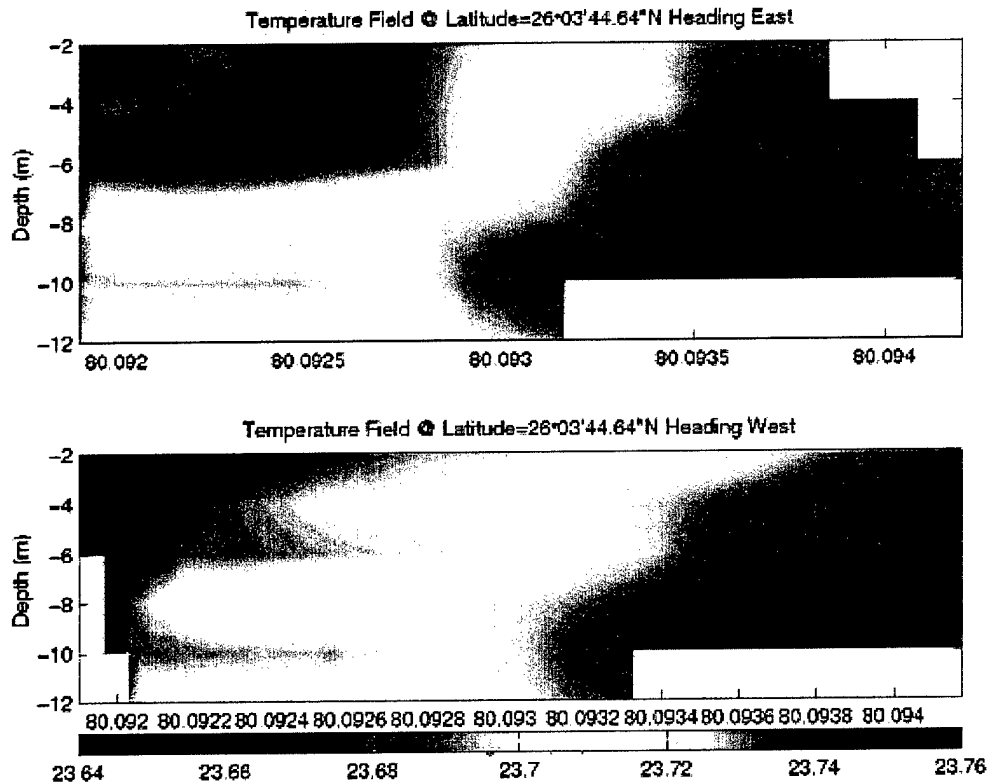


Figure 3.2.1.11. Temperature field, consistent in each direction.

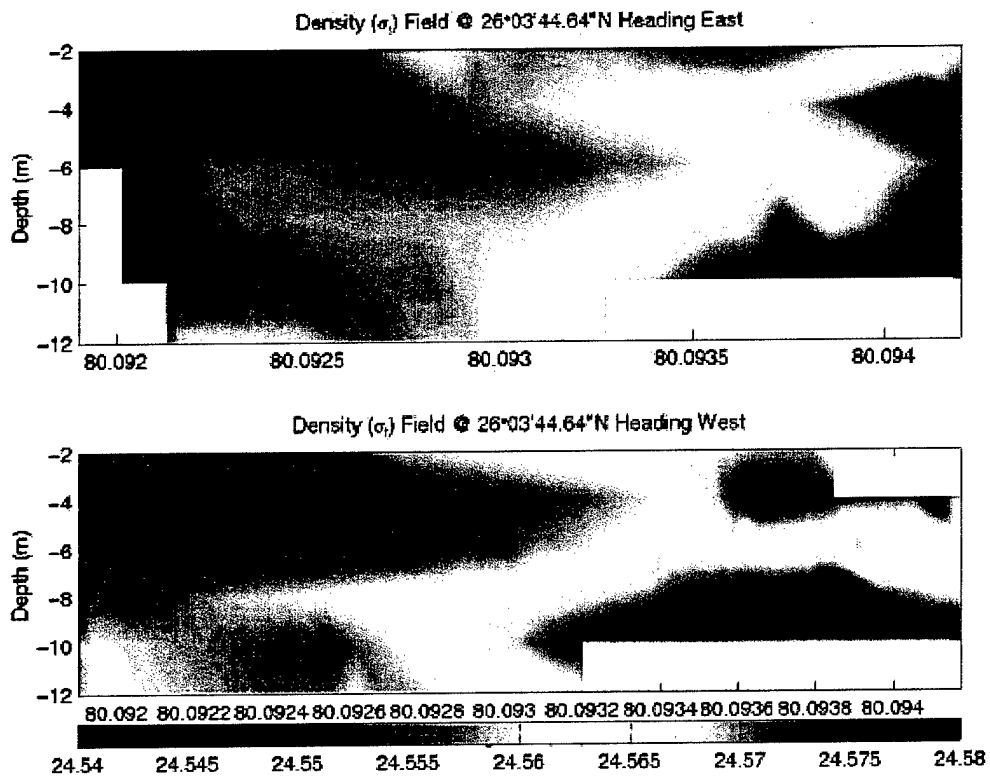


Figure 3.2.1.12. Density field consistent in each direction.

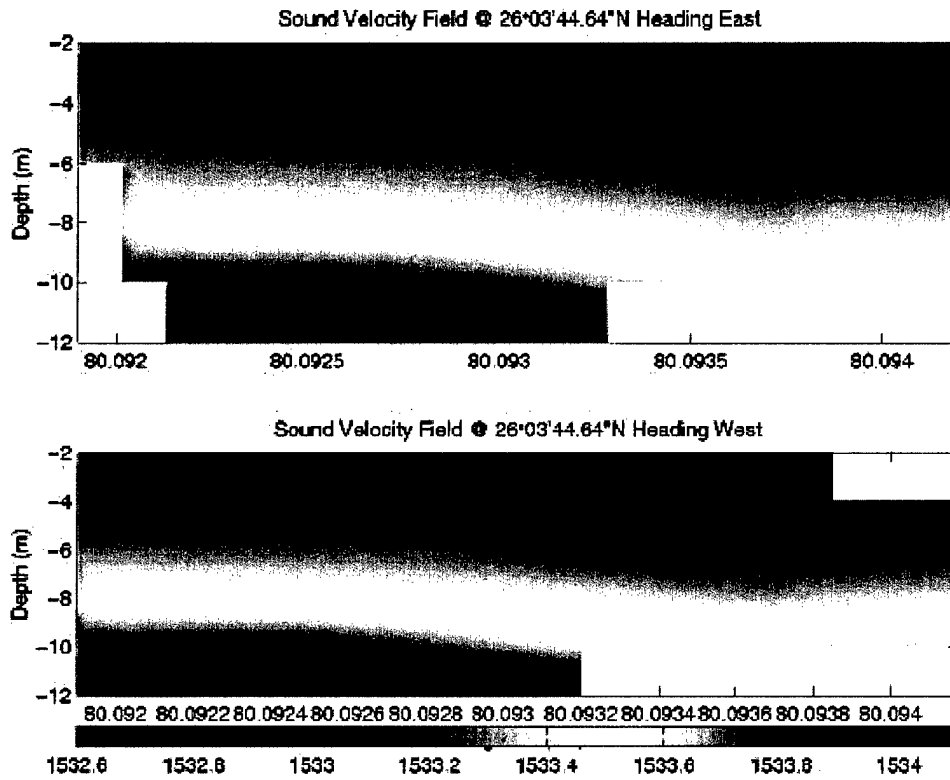


Figure 3.2.1.13. Sample speed of sound; it appears to be mainly a function of depth, since variations in salinity and temperature are small.

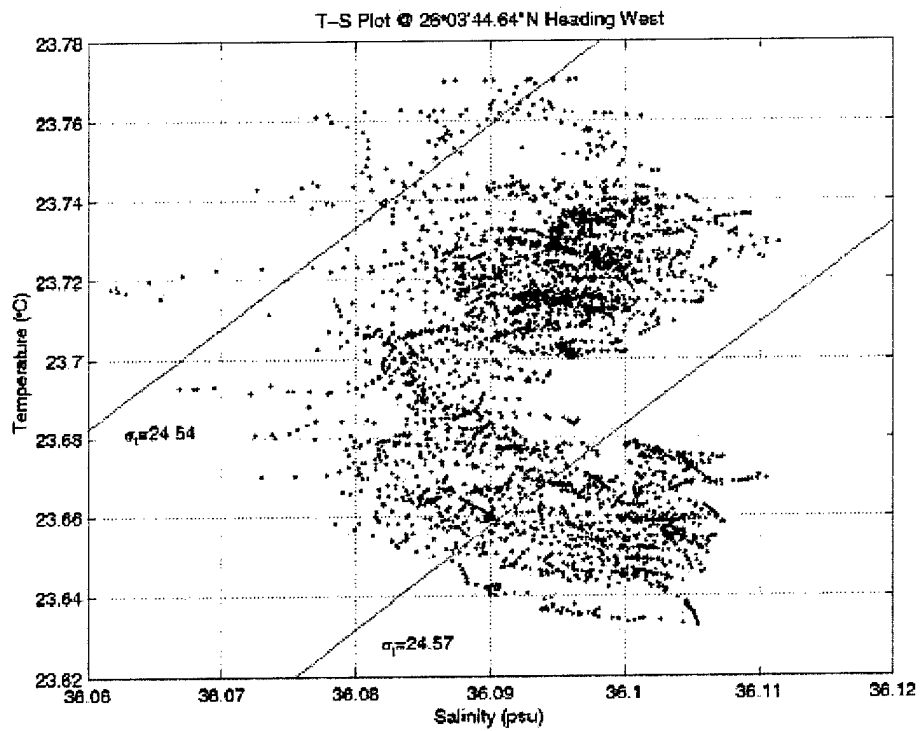
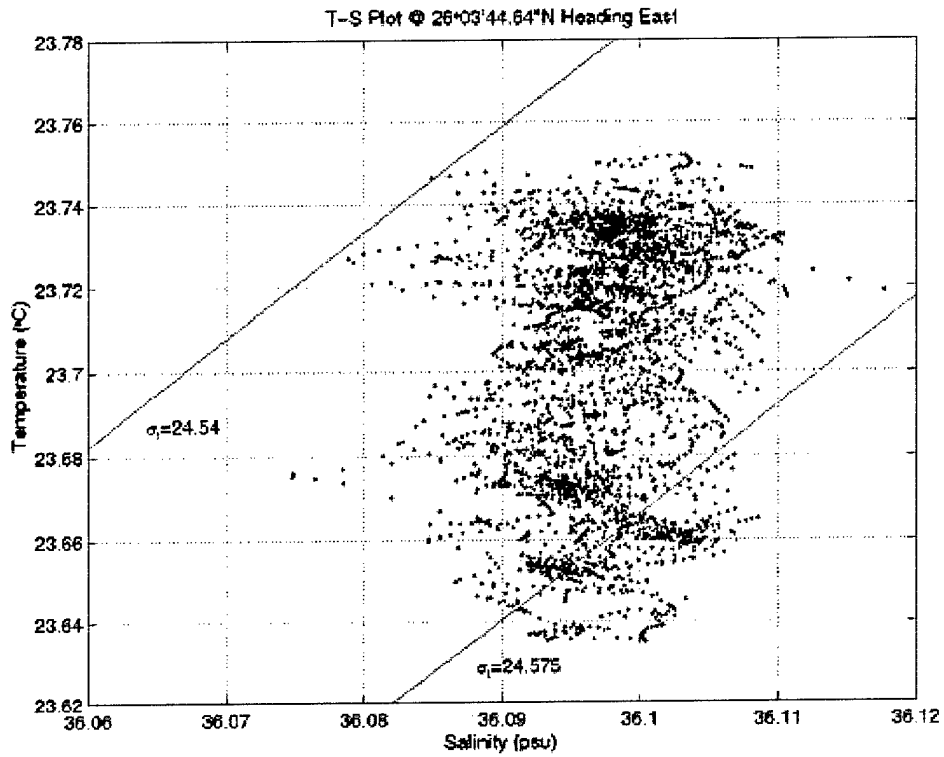


Figure 3.2.1.14. T-S plots early morning on 12/17/99. Note range for comparison to later date.

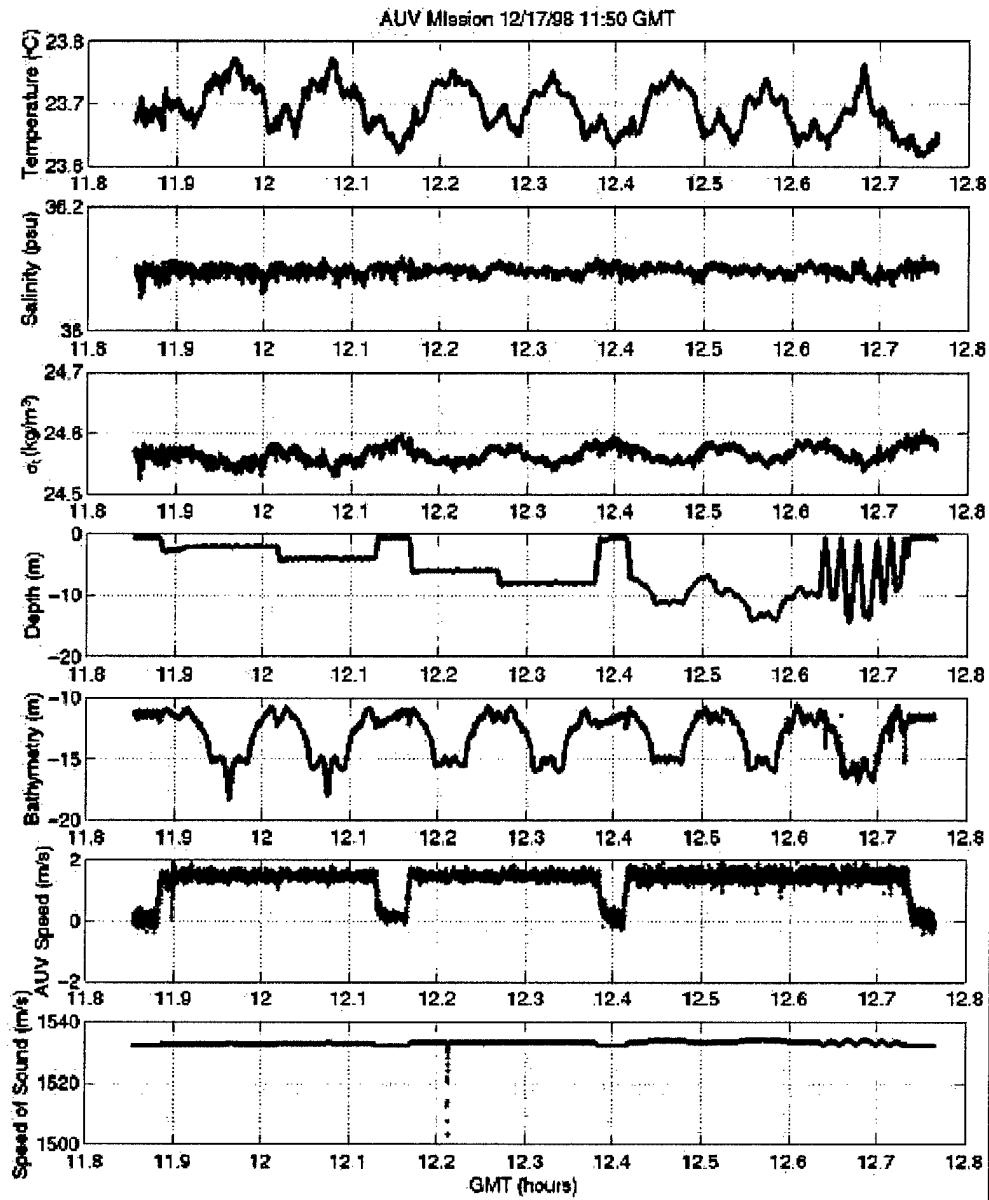


Figure 3.2.1.15. Time series data recorded by the OEX on Dec. 17.

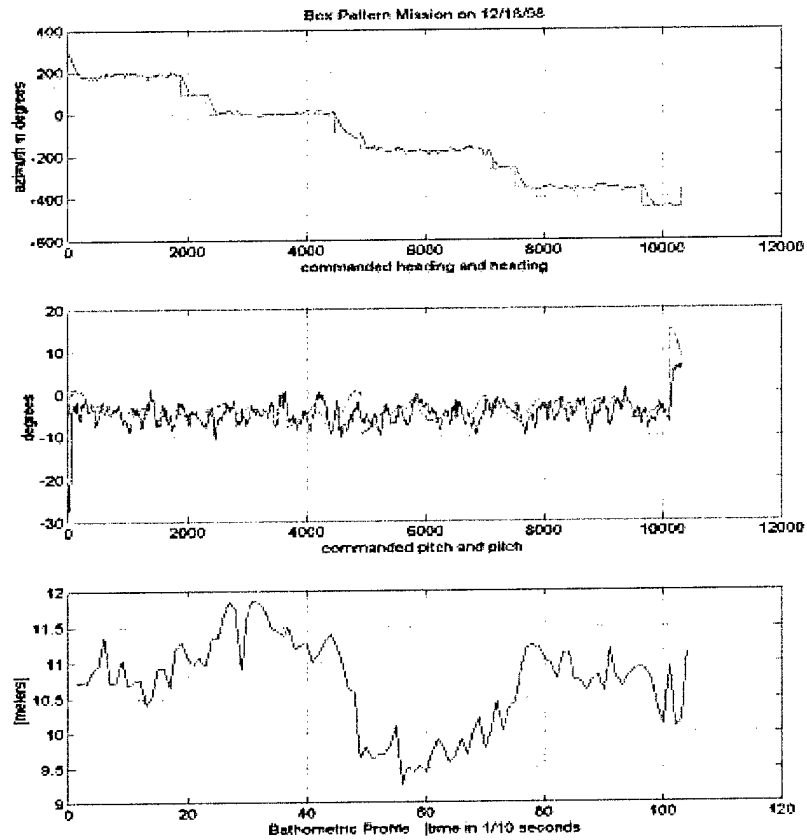


Figure 3.2.1.16. MADD OG AUV data, illustrating its performance.

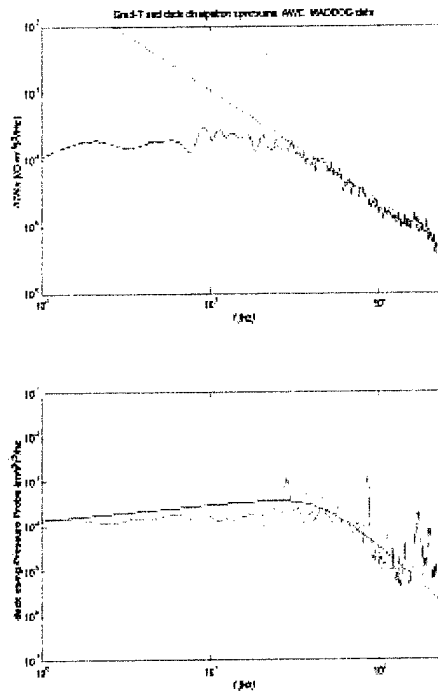


Figure 3.2.1.17. Spectra of Temperature gradient and shear as measured respectively by a fast-response thermistor and a dynamic pressure probe on board the MADD OG.

Summary

A successful, well-coordinated effort was able to capture a cold front event during Fall, 1998. Full results of the work will be published after a detailed analysis of the data. The effort illustrates the nature of process-oriented experiments that are possible at SFOMC and how AUVs can be utilized for profiling, and making in-situ CTD and small-scale turbulence measurements. A region over the 5-head ADCP was surveyed at various depths using the full potential of the mobile AUV platforms. Using appropriate sensors and taking special measures to isolate the sensors from the vibrations induced by the self-propelled vehicle, good quality turbulence measurements were made. The turbulence levels and the associated mixing rates were high, with dissipation rates of $O(10^{-7} \text{ W/kg})$, throughout the shallow water column in response to the cooling of the surface waters, giving rise to fairly homogenous conditions in the water column. Simultaneous CTD and ADCP measurements using the AUV, together with measurement from a bottom-mounted 5-head ADCP and CTD casts from the support ship provided sufficient background information to put the small-scale measurements in proper context and determine implications for mixing rates and rates of energy dissipation. Breaking waves were not observed at the time of the experiment so the ambient noise measurements excluded contributions from this source. Further adverse weather experiments on the SFOMC range are planned.

References

1. Gregg, M. C. 1987. Structures and fluxes in deep mixed layer. In Dynamics of the Oceanic Surface Mixed Layer, ed P. Muller, D. Henderson.
2. Osborn, T., D. M. Farmer, S. Vagle, S. A. Thorpe and M. Cure. 1992. Measurement of bubble plumes and turbulence from a submarine. *Atmos-Ocean* 30, 419-440.
3. M. R. Dhanak and K. Holappa. An Autonomous Ocean Turbulence Measurement Platform. To appear in the special Microstructure Sensors Microstructure Sensors in JOAT.
4. An, E., M. Dhanak, L. K. Shay, S. Smith, J. Van Leer, 1999: Coastal oceanography using autonomous underwater vehicles. *J. Atmos. Oceanogr. Tech.*, (Revised and Resubmitted)

3.2.2 Measurements of the Ambient Acoustic Environment of the SFTF Range using the Ambient Noise Sonar

Stewart A.L. Glegg, Anthony Lavigne, Rachel Pirie (FAU)

Presented here is a summary of the missions accomplished using the Ambient Noise Sonar (ANS) to study the diurnal variations of the shallow water ambient acoustic environment of the SFTF range. This is the first series of measurements to have taken place with connection to the MUX box recently installed at the SFTF, which supplies power and enables data transfer to shore for up to ten separate systems.

The experiment was conducted on the SFTF range in 65ft of water in July 1999. The ANS was moored on top of a concrete block at $26^{\circ} 04.117'N$, $80^{\circ} 05.362'W$. This position was 93 meters, on bearing 188° , away from the shallow water MUX. The system was deployed on Tuesday 13th July and retrieved, almost two weeks later, on Monday 26th July. This was the longest deployment time of the ANS array thus far, enabled by the power supplied by the MUX from shore and not the batteries as previously used. Because the data transfer link could not be established to shore via the MUX, an Ethernet cable was connected directly from the ANS to the laptop computer onboard a boat, and required daily visits to the site to download data.

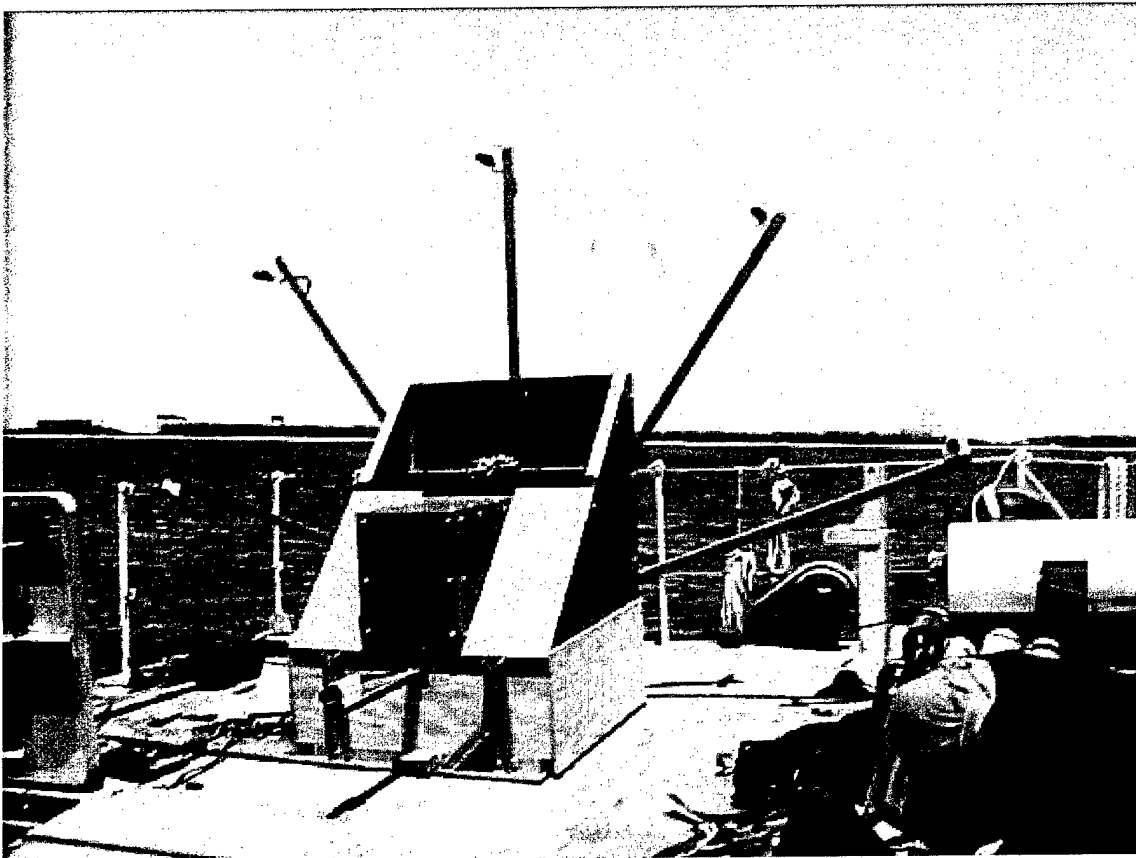


Figure 3.2.2.1: Peacock on deck of RV Stephan, just before deployment.

The objective was to collect data to enable further characterization of the shallow water ambient noise environment of the SFTF range. The main priority was to collect 24-hour data, to see the diurnal changes in ambient noise. Four sets of data acquisition were made.

The dates were: July 15, 1999
 July 19, 1999
 July 21, 1999
 July 22, 1999

The ANS was deployed with the five hydrophones in the vertical plane and the reference hydrophone was positioned at 145°. The bottom type at the deployment site was sandy. A photograph of the ANS, or Peacock, is also shown in Figure 3.2.2.1 just before deployment.

Method of Data Acquisition

The acquisitions that were made took averaged frequency data. The sampling frequency was 51.2 kHz and the number of points used was 4096. Each recorded measurement was an average of 125 measurements, calculated on the SigLab DSP boards. A measurement was recorded approximately every 27 seconds, excluding periods during level checks. The measurements were grouped into cases, each approximately an hour long, containing 154 measurements. A level check was made every 13 measurements.

July 15, 1999

Measurements started at 10:22 and ended at 15:46. Shown here is the spectrogram of that mission.

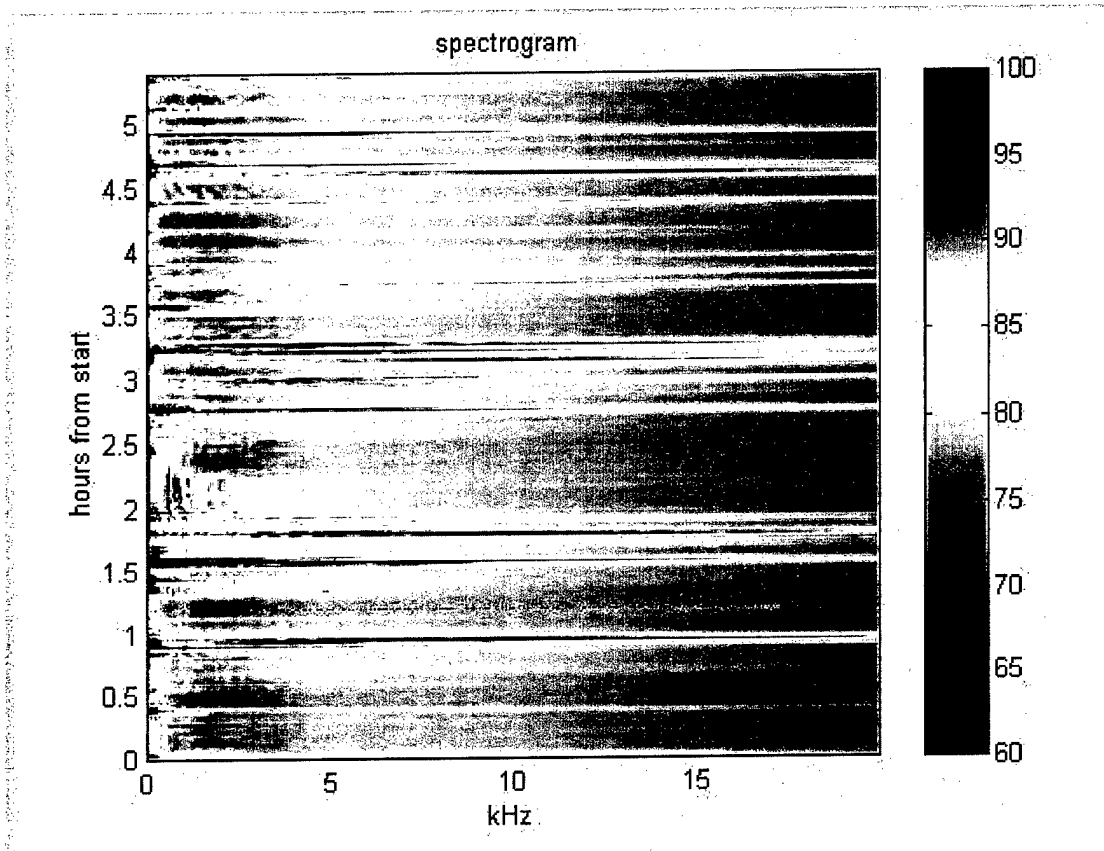


Figure 3.2.2.2: Spectrogram of 07/15/99

July 19, 1999

Measurements started at 14:32 and ended at 19:56. The spectrogram is shown below.

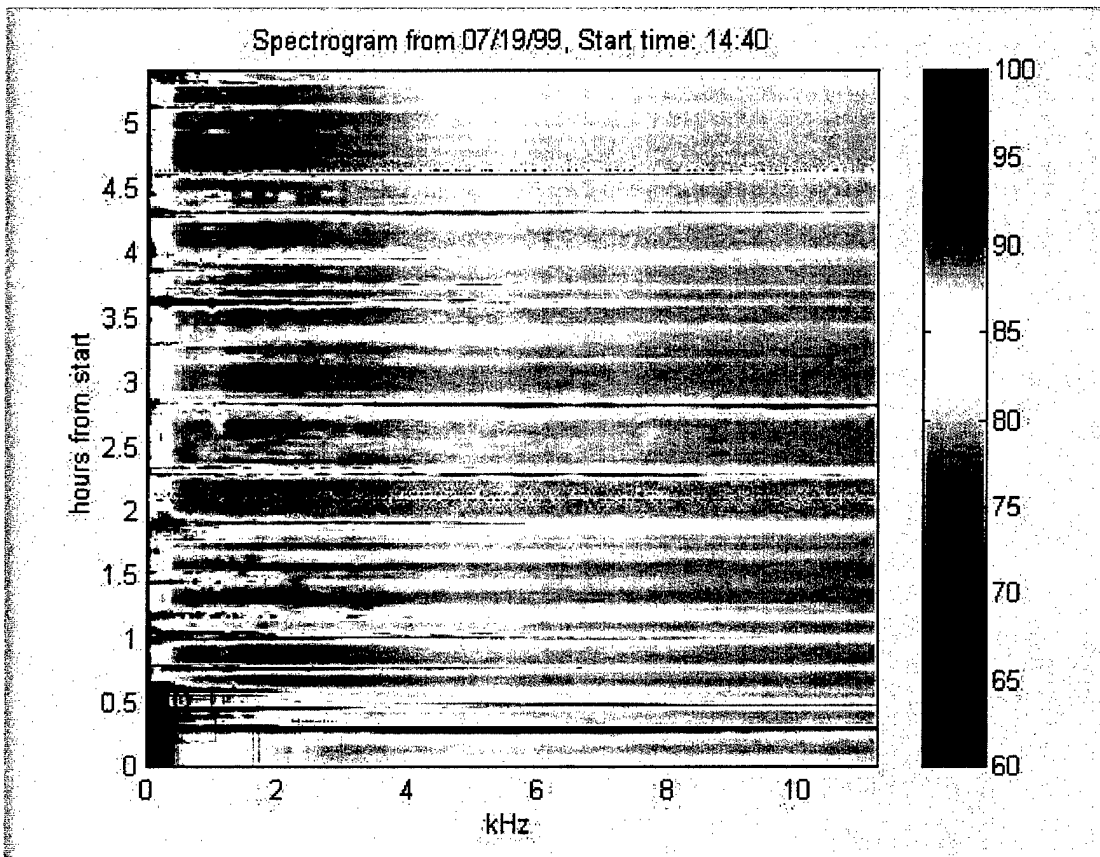


Figure 3.2.2.3: Spectrogram of 07/19/99

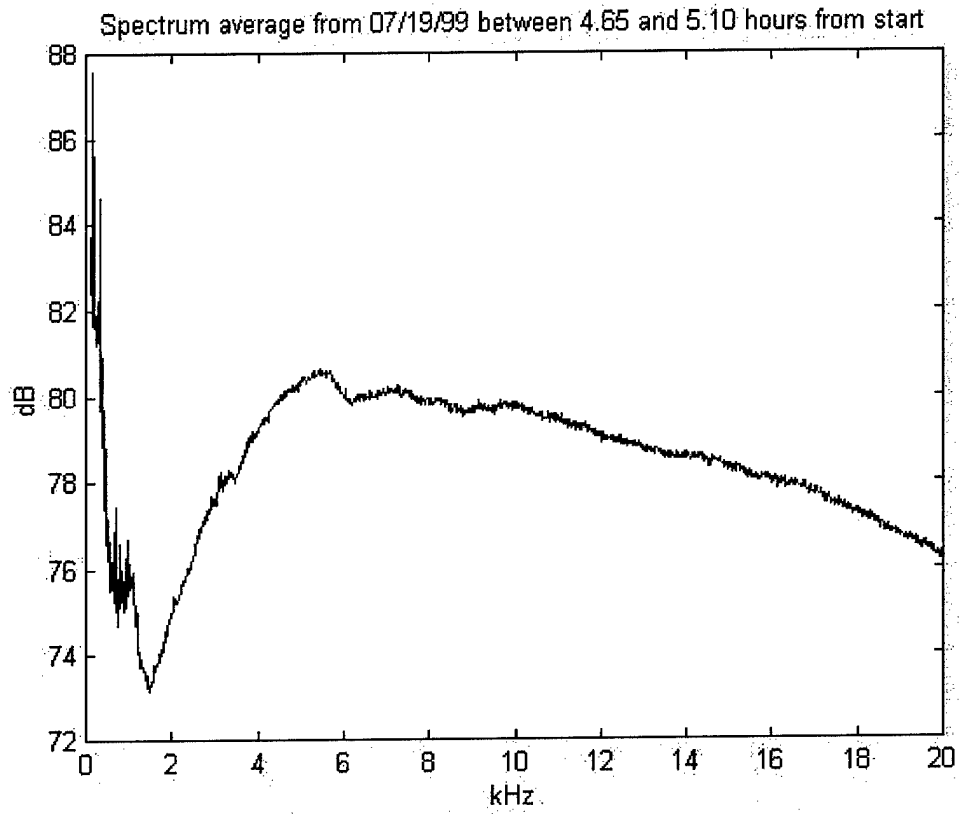


Figure 3.2.2.4: Average spectrogram over a period containing no boat tracks

July 21, 1999

Measurements started on 07/21/99 at 10:53 and ended on 07/22/99 at 10:53. The spectrogram is shown in Figure 3.2.2.5.

Weather data was also recorded every 15 minutes from the USF NE weather buoy situated approximately 1250 meters East of the ANS. A plot shown between the same time as the data acquisition is shown in Figure 3.2.2.6.

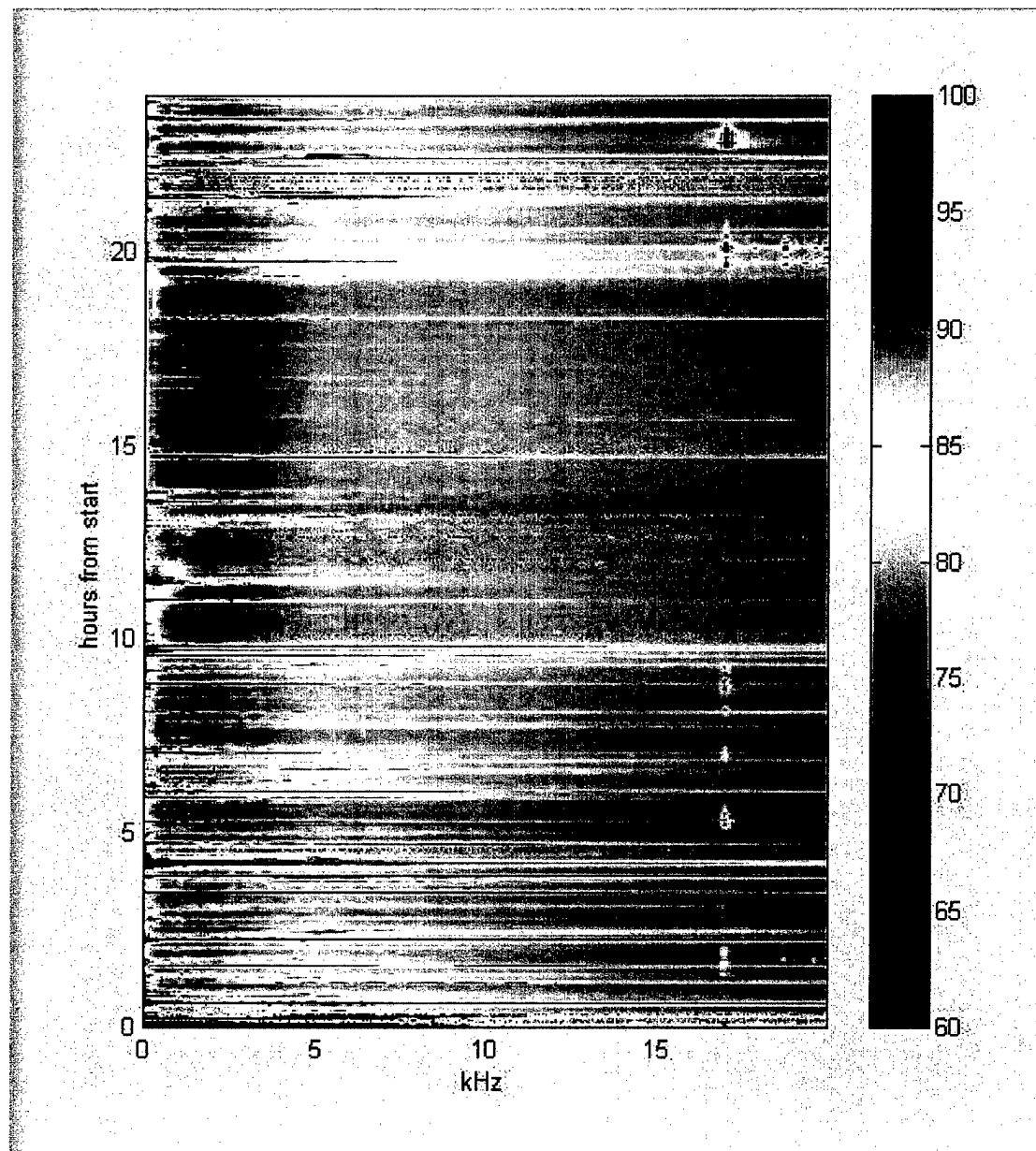


Figure 3.2.2.5: Spectrogram of 07/21/99 - 07/22/99

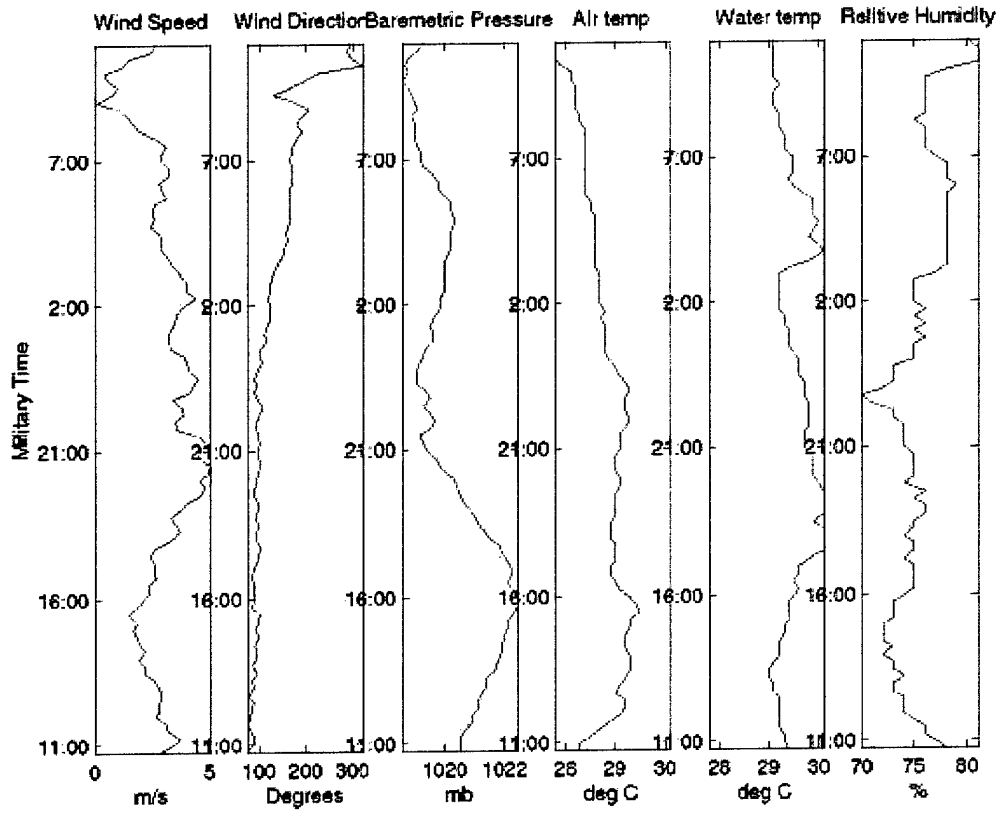


Figure 3.2.2.6: Weather data corresponding to the 24hr mission started on 07/21/99

July 22, 1999

Measurements started on 07/22/99 at 15:29 and ended on 07/23/99 at 18:45. The spectrogram and the weather data are shown in Figures 3.2.2.7 and 3.2.2.8 respectively.

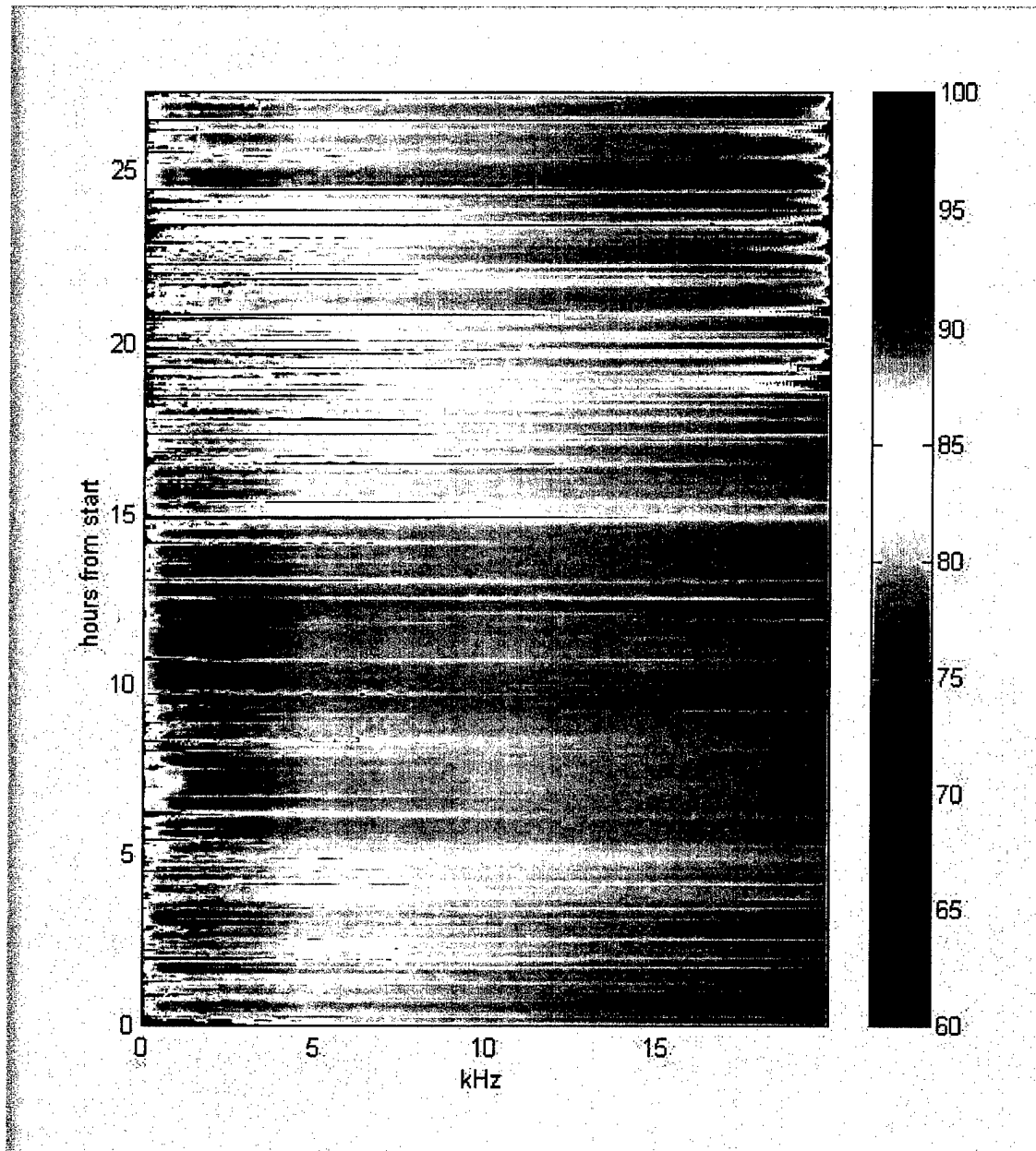


Figure 3.2.2.7: Spectrogram of 07/22/99 - 07/23/99

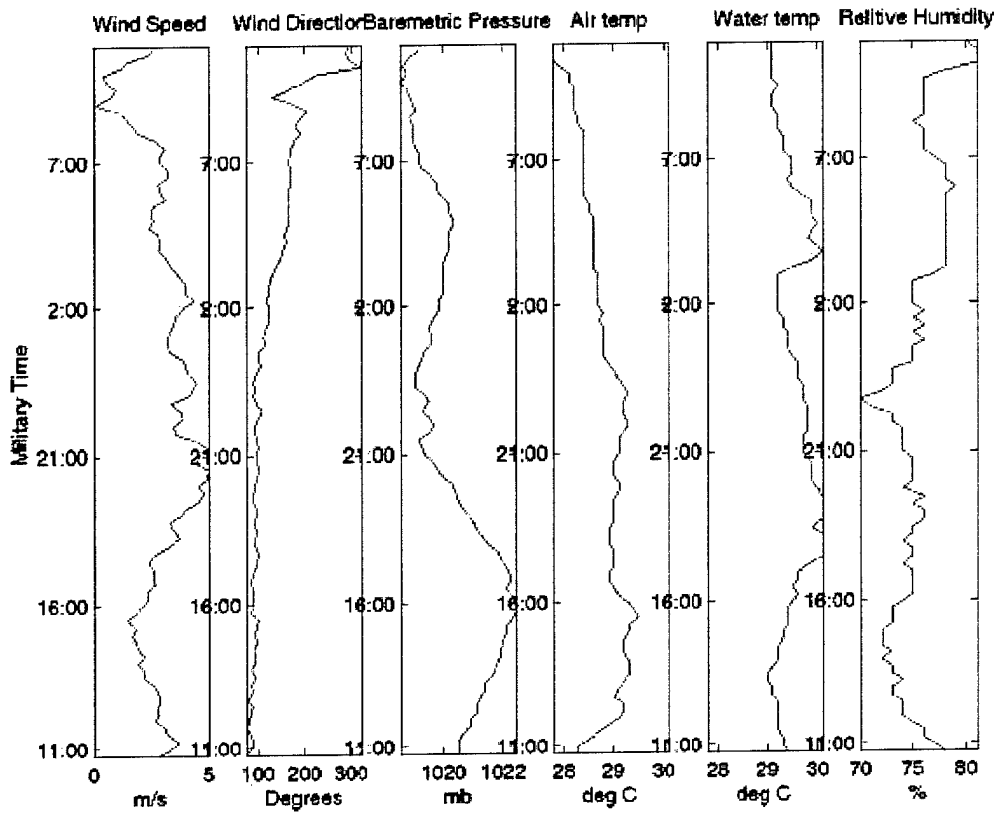


Figure 3.2.2.8: Weather data corresponding to the 27hr mission started on 07/22/99

Results

The objective to acquire 24 hours of data was met. The increased boat traffic as compared to previous measurements made in Boca Raton and Tampa can be seen. The boat noise decreases in the evening, then becomes quiet at night before increasing again just before dawn.

Although the high levels of shrimp noise recorded at other sites in Florida are not seen here, there is still the general curve that peaks at 5kHz that is indicative of shrimp noise. Further processing of the data is being made at this time to investigate the presence of this source. Also seen in the spectrograms from the 21st and 22nd July is what looks like an evening chorus just after sunset.

3.2.3 Docking System For Fau Ocean Explorer Class Auvs Using A Low Cost, High Accuracy Short Baseline Positioning System

Graeme Rae, Sam Smith, David Kronen (FAU)

Summary

This section describes efforts carried out at SeaTech during 1999 to develop a high accuracy underwater navigation system capable of maneuvering an Autonomous Underwater Vehicle to a point that is within the tolerances of a docking and capturing system. A brief description of this docking set-up is provided. The Short Baseline (SBL) Docking/Navigation system is described along with some performance data. Problems encountered with the navigation system and controllers are described and solutions given. Conclusions describe the overall performance of the navigation system.

Introduction

In order for the FAU AUVs to dock with a static base station several goals need to be accomplished.

- Design and implement a mechanical system capable of capturing and releasing an AUV automatically and repeatedly.
- Develop a positioning system capable of locating the vehicle with enough accuracy to reach the docking window.
- Develop and implement a control system capable of navigating the vehicle towards the dock in a manner that will allow the vehicle to successfully couple.

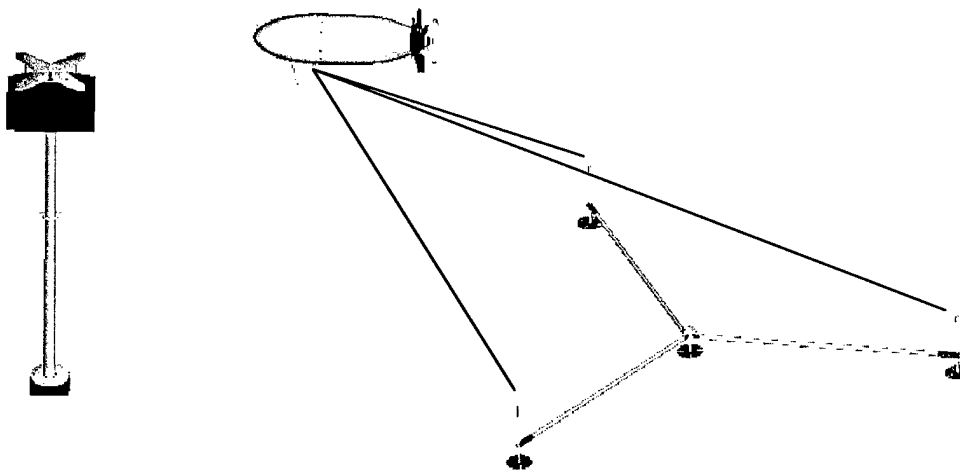


Figure 3.2.3.1 Dock Setup

The mechanical dock has been completed and the thrust of the work presented here is to develop and implement a positioning and control system capable of reaching it. The layout of the transducers and the dock are shown in Figure 3.2.3.1. A complete description of the mechanical dock can be found in [1].

This report describes the implementation and testing of the positioning and navigation systems incorporated onto the FAU AUV 'Magellan'. During the period from May to August of 1999, Magellan operated successfully using SBL navigation on 8 full days at sea and carried out over 70 missions. Although the ultimate goal of this project is to dock with a stationary target only half of these missions were designed to actually attempt to hit a small, stationary ball. In fact, most missions were conducted at a safe distance from the transducer array in order to determine vehicle navigation and control performance. The last thirty missions were conducted using targeting as the aim and these were extremely successful.

SBL Theory and Modifications

The basis of the navigation system is a Desert Star re-configurable Short Baseline Sonar. The base station consists of three transducers that respond to a moving fourth transducer in a sequential manner. Accuracy of 10cm or less was claimed by the manufacturer but it was discovered that this resolution is only achievable with a stationary or very slowly moving vehicle. As Magellan required 1-2 knots of headway in order to maintain maneuvering control the Desert-Star system needed some modification. This speed related accuracy is shown in Figure 3.2.3.2 during the first high speed section of the mission, RMS error averages to 1.3. During the final, slow approach to the dock the RMS error drops to an almost constant 0.8m

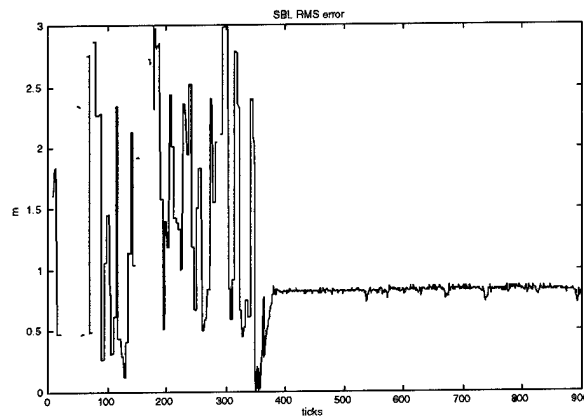


Figure 3.2.3.1: SBL RMS Error

The problem lies in the fact that between pings from the base station the vehicle can move a significant distance, and unless previous localization can be performed the direction of this motion in relation to the base position is unknown. A solution to this problem using artificial movements of the base transducer locations based on vehicle motion was determined and has been implemented in the position-estimating package installed on the Ocean Explorer. A full description of this work is given in [1].

This approach to navigation, i.e. driving the AUV to an absolute point in space where the dock is located, rather than using a homing or sensing system that aims for the dock itself was chosen for a number of reasons:

- The AUV does not need to carry a nose mounted homing system.
- The navigation system provides additional high accuracy positioning near the dock

- Homing is not dependent on environmental conditions such as daylight.
- Long-range missions will be able to dock to a given lat/long coordinate regardless of the power of the homing beacon.
- The dock does not need to be powered

SBL Performance

Several missions have been successfully run using the SBL as an inert payload gathering raw data, as a payload performing inert position fixing and finally a component of position estimation. This early implementation, carried out in May and June of 1999 is described in some detail here.

The position estimator based on the SBL fix uses a novel-seeding algorithm that uses recent dead reckoned position as a basis for the best SBL fix. As with many roundtrip time based navigation systems, problems locating the vehicle on a particular side of a baseline are common. This can be solved either by using redundant transducers or by using seeding. The combination of both methods in the Docking SBL system described here gives a fix rate of approximately 80% of raw returned ranges. An example of a successful mission is shown in Figure 3.2.3.3. The vehicle begins at top left, travels south. A compass calibration error causes a jump in vehicle position but once a fix is re-acquired the vehicle navigates well south, east and finally northwest to the dock. A region in the southwest corner of the dock locale has been shown to contain an acoustic blindspot where few returns from the DiveTracker are received. This is felt to be a feature of the terrain – this area is extremely shallow and rocky.

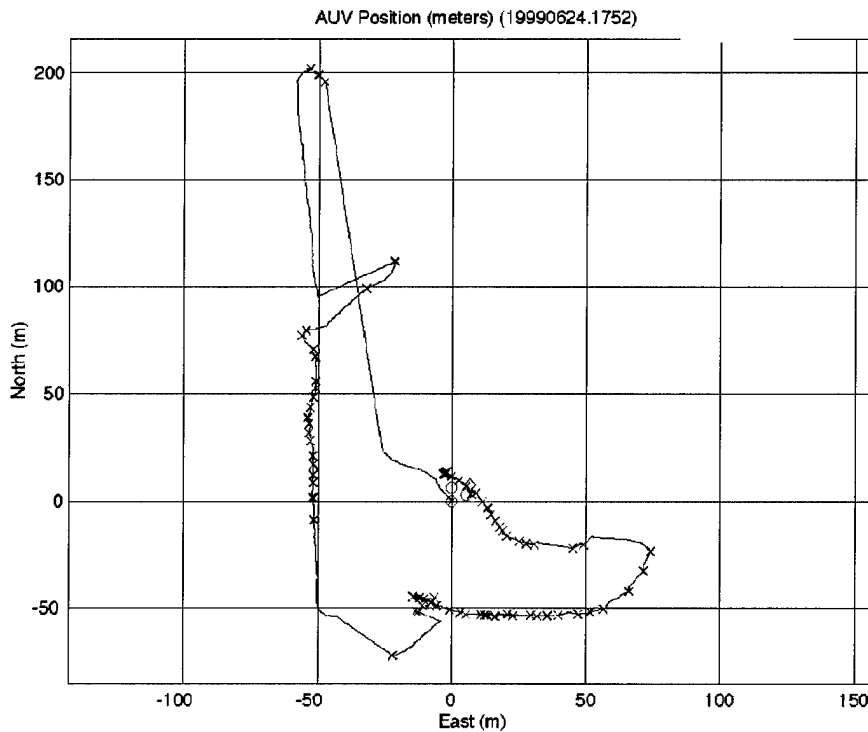


Figure 3.2.3.2 : Docking Run

Control System Performance

The vehicles were originally controlled on docking runs using a PD based trackline controller. This will drive the vehicle towards and then along a corridor drawn between successive waypoints. However the lack of an integrator in the system means that once the vehicle is inside the corridor it will cease trying to achieve the exact trackline and will simply follow its designated heading. This is clearly shown in Figure 3.2.3.4. The AUV cruises by the dock (the small diamond) at a fixed distance.

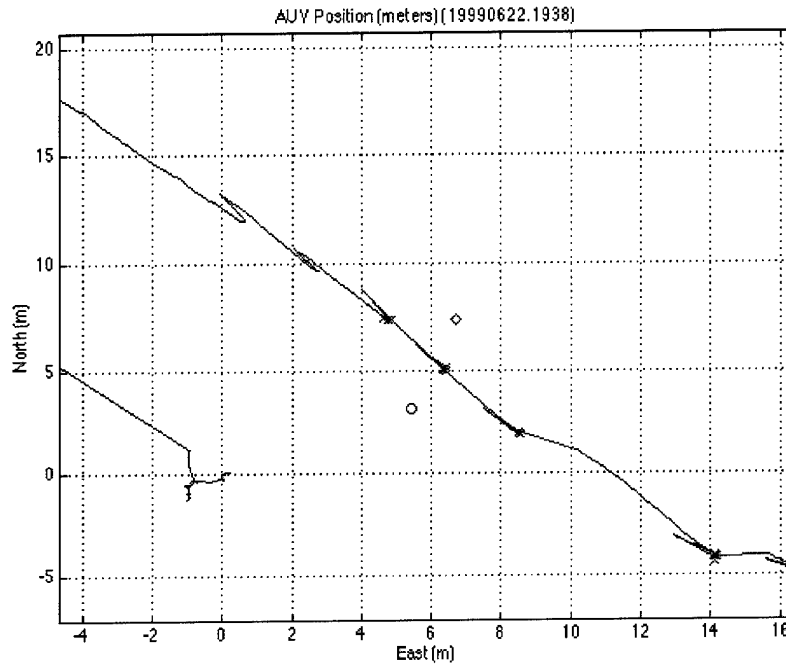


Figure 3.2.3.3: Trackline Error

Although the vehicle is receiving multiple fixes as it approaches the dock position it does not correct its path. As far as the vehicle is concerned it is navigating successfully. This control system is more than adequate for typical AUV missions where positional accuracy on the order of meters is acceptable. However for the purposes of docking this will not suffice. An obvious and simple solution of narrowing the allowable corridor has been tried but as the corridor width is a function of vehicle maneuvering capabilities this does not necessarily have the desired effect. If the AUV loses the trackline it will immediately begin to hunt wildly trying to achieve a trackline that is beyond the turning capability of the rudders. This is shown in Figure 3.2.3.5. This figure also shows the lack of fixes in the bottom left of the docking area. Another solution to this hunting problem, which is in fact a manual version of the fuzzy docking controller that is hoped to be the final implementation, is to provide the vehicle with successively narrower and narrower corridors.

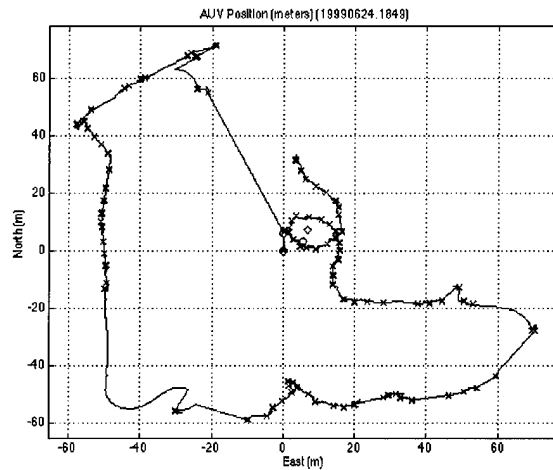


Figure 3.2.3.5: Hunting Error

Second Generation Tracking Controller (TCII)

The implementation of the improved tracking controller made significant differences in the AUV docking performance. This controller uses a fuzzy integrator when it approaches the trackline and thus can reduce and eliminate the trackline error shown in the earlier missions. The dramatically improved performance of this controller is shown in the mission graphs in Appendix 3.2.3.

Depth Control Performance

Depth performance of the docking system is excellent, as shown in Figure 3.2.3.6. The AUV is capable of holding altitude to within a few centimeters. As long as the dock altitude is known with some accuracy before the mission the vehicle is fully capable of reaching and maintaining this required vertical position.

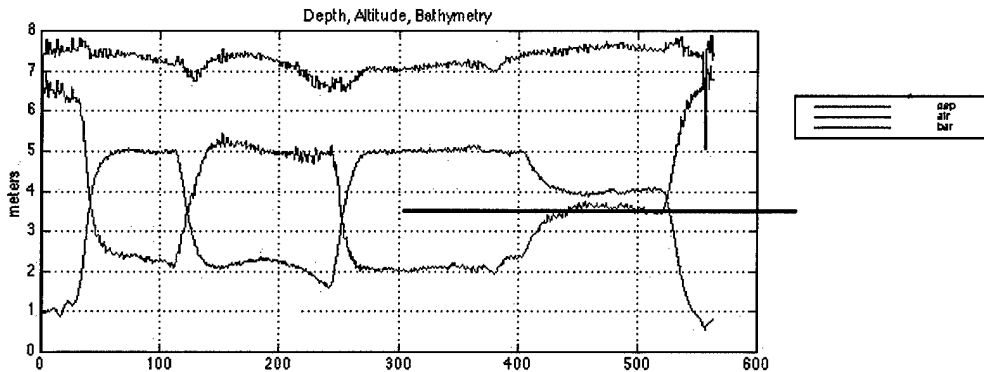


Figure 3.2.3.6 : Depth Performance

Operations

During the first two weeks of August 1999 a total of 24 docking missions were carried out during two days at sea. Each mission lasted approximately 10 minutes and was in most cases a simple 'out and back' configuration, with the return leg oriented to allow the vehicle to

approach the docking balloon from down current. These were all performed using the Magellan AUV operating off the Oceaner IV. Each of these missions was an attempt to navigate the AUV within a pre-defined limit of a tethered buoy floating mid water. The buoy was located approximately 5 m from the fixed seafloor mounted SBL array. A nose-mounted video camera recorded the approach to the dock from onboard the AUV. However many of these taped missions were subsequently discovered to have been missed or over – recorded. This has since been traced to an error in the camera control system.

Mission Summaries of August 13, 1999

Prior missions had determined the cause of many of the problems experienced. Corrections to mission plans and the tracking controller were implemented and several successful missions as listed in table 3.2.3.1 were completed back to back.

1459- failed due to compass calibration error

1528- towed mission to check that the compass calibration was indeed the error.

1550- failed mission – AUV approached from up-current as current had switched. All missions thereafter were also switched

TABLE 3.2.3.1 : 1643-1853 Successful Missions

| Miss ID | D-X | AUV Error | Observed Error | Corrected Error |
|----------------|------------|------------------|-----------------------|------------------------|
| 1643 | 5.4 | 0.4mW | <1mW | <0.8mW |
| 1653 | 5.4 | 0.4mW | <1mW | <0.8mW |
| 1701 | 5.4 | 0.2mW | HIT | <0.2mE |
| 1728 | 6.0 | 0.3mW | <1mE | <0.6mE |
| 1747 | 5.6 | 1mE | <0.2mE | <0.2mE |
| 1756 | 5.6 | 0.5mW | HITW | HITW |
| 1812 | 5.6 | 0.0 | HITW | HITW |
| 1844 | 5.6 | 1.5mE | <0.5mE | <0.5mE |
| 1853 | 5.6 | 0.8mW | <1mW | <1mW |

KEY:

Miss-ID = Mission ID

D-X = East (X) location of dock (apparent)

The dock is not moved, but the AUV is given a corrected target.

AUV Error – approximate minimum cross track error from mission data files

Observed Error – Diver observed error

Corrected Error – Post mission error based on re-localization of docking ball.

In all of these missions the AUV passed within 1m of the buoy. Figure 3.2.3.7 clearly shows that depth accuracy can be achieved within the required limits. For the earlier missions it must be remembered that the AUV is actually aiming at a point some distance from the target ball. The actual location of the ball (by experiment) is found to be at 5.6m East of the dock. If these earlier missions are corrected for this change an overall measure of achievable accuracy can be

computed of approximately 0.45m. That is the AUV is capable of achieving the ball within a +/- 0.45m corridor

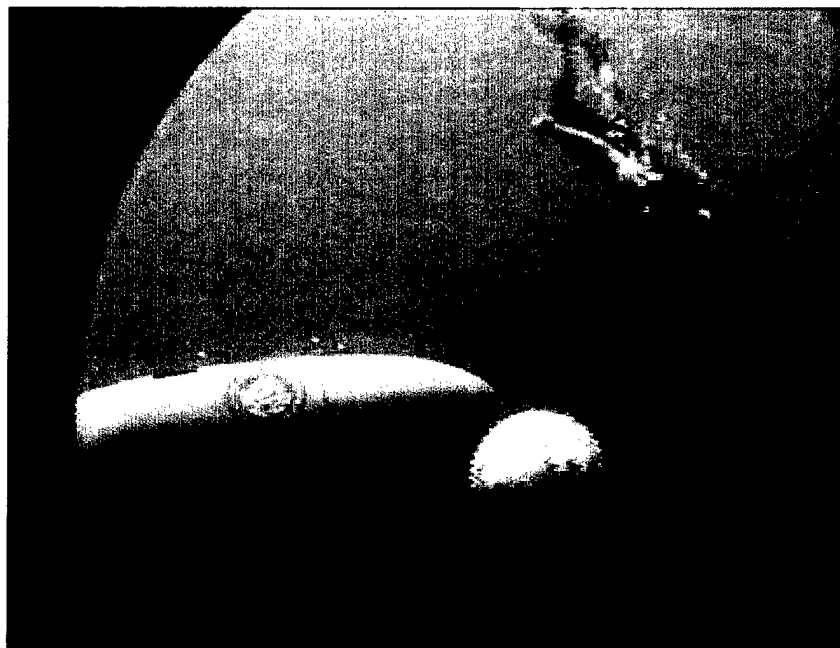


Figure 3.2.3.7 MISSION 1853 (shows depth accuracy)

Mission Summaries of August 25, 1999

In the latter part of August a set of tests were run to determine if some small changes in the TCII were successful. Five Missions were run – four of these hit the ball and in fact from onboard video the sub can be seen to jerk slightly as it catches the balloon. Only one mission missed and that was by approximately 0.2m – which is well within the capture window of the mechanical dock. The graphical output of the runs listed in table 3.2.3.2, are shown in missions 1828-1906 in the attached Appendix 3.2.3.

TABLE 3.2.3.2 : 1828-1906 Successful Missions

| Miss ID | D-X | AUV Error | Observed Error |
|---------|-----|-----------|----------------|
| 1828 | 5.6 | HIT | HIT |
| 1837 | 5.6 | HIT | HIT |
| 1847 | 5.6 | HIT | HIT |
| 1855 | 6.6 | 0.2mE | HIT(E) |
| 1906 | 5.6 | HIT | HIT |

Future Missions and Improvements

Immediate improvements of vehicle performance were achieved with the addition of the next generation trackline controller (TCII). Ongoing missions are being performed to tune this controller to perform optimally for specific vehicles and speeds. Initial tests were hampered by a

problematic DVL altitude and ground velocity sensor. Migrating the entire SBL system to a more stable and newer AUV is anticipated to improve the situation considerably. Ultimately a full fuzzy docking control system will be implemented that uses a cell to cell navigation technique that will drive the vehicle towards the dock with ever increasing but achievable accuracy requirements. This controller also uses a speed controller to ensure that the vehicle reaches the dock at a speed that is sufficient to maintain control but not so fast as to cause a damaging collision.

Compass calibration continues to be a problem, particularly during final approaches if the AUV needs to make major course adjustments. A problem with regional and time varying performance of the SBL needs to be addressed. The SBL seems to operate adequately only in specific but changing regions around the dock. This is thought to be due to changing environmental conditions. Once surface testing is complete and the dock is relocated to a much deeper location this problem should diminish.

The next phase of testing is to include passive (i.e. no power or data transfer) docking with the actual mechanical dock system. This is scheduled for the early part of October 1999.

Conclusions

The SBL system to-date has performed well, and has exceeded our expectations both in terms of accuracy, and in terms of number of successful fixes received. Navigation within the limits of the docking window are achievable and repeatable once the dock has been localized and the position noted. The Tracking Controller has performed well, although tuning it to perform optimally has proved more difficult than originally expected. Simulation work is on-going to model and optimize this system.

References:

- [1] Kronen, D "Docking the Ocean Explorer AUV using a low cost acoustic positioning system and a fuzzy guidance algorithm." Masters Thesis. Florida Atlantic University, Boca Raton FL. 1997
- [2] Langenbach, R. "A Fuzzy Logic Algorithm to Dock an AUV with a Moving Submarine" Masters Thesis. Florida Institute of Technology. April 1996.
- [3] Rae, G. Smith S. "A Fuzzy Rule Based Docking Procedure for AUVs." Proc. IEEE Oceans 92, Newport RI, pp539-546. October 1992.
- [4] Rae, Smith, Kronen, "INTERIM REPORT-SBL Docking System for FAU Ocean Explorer Class AUVs Using a Low Cost, High Accuracy Short Baseline Positioning System." – Internal Report, Florida Atlantic University, July 1999

3.2.4 Acoustic Communication using SFOMC Shallow Water Multiplexer

*Professor Lester R. LeBlanc, Principal Investigator
Pierre-Philippe Beaujean, Project Coordinator (FAU)*

Underwater acoustic communication is vital to the operation of Autonomous Underwater Vehicles (AUV) and transmission of data from remote underwater imaging sensors. Two systems have been developed in the Sonar Laboratory of Ocean Engineering. The first system, called Coherent Path Beamformer (CPB), or Mills-Cross, is a high-performance communication receiver for high data transfer rate at long distance and in very shallow water. The second system, called General Purpose Acoustic Modem (GPM) is a low-cost and very compact transmit/receive system for lower data transfer rate. Very robust and compact, it is used for command, navigation and networking, and is currently installed in every AUV OEX.

The SFOMC Shallow Water MUX experiment is the first long-range experiment scheduled for the MillsCross. Mills-Cross and General Purpose Modem (GPM) are connected to an underwater Multiplexer (MUX) controlled from shore through fiber optics. Using this setup, underwater acoustic data can be collected for weeks at a time and meaningful reliability tests can be run, without the expense of a research vessel.

Scientific And Technical Background

The underwater acoustic channel is characterized with strong time varying multipath conditions. To some degree, each path is independently time delayed and frequency smeared by fluctuations induced by surface and internal waves, turbulence, temperature gradients and other related phenomena. The extent and the independence of these variations place a theoretical upper bound on the information transfer rate in such a medium. In addition to direct multipath, bistatic volume and boundary reverberation from distributed scatterers in the surrounding water column, sea floor and sea surface make it even more difficult to communicate at high baud rate in shallow water. Our strategy is to separate communication systems based on their application. To be more specific, two systems have been developed:

- 1) The Coherent Path Beamformer is a high-performance communication receiver (uplink) using Phase Shift Key processing for high data transfer rate at long distance and in very shallow water. It is mainly used for data transmission at the present time, but also has a very strong potential in network applications. The source is usually installed under a boat or an AUV.
- 2) The general purpose Acoustic Modem is a low-cost and very compact transmit/receive system for lower data transfer rate, based on Multi Frequency Shift Key (MFSK) processing technique. Very robust, it is used for command, navigation and networking, and is currently installed in every AUV OEX.

Experiment Plan

The SFOMC Shallow Water MUX experiment is the first long-range experiment scheduled for the MillsCross. The idea is to attach the Mills-Cross and a General Purpose Modem (GPM) to an underwater Multiplexer (MUX) controlled from shore through fiber optics (see Figure 3.2.4.1). Many other systems are involved in this experiment. Later on, the AUV

OEX's should be deployed to test the new docking station. The water depth is ranging from 10'

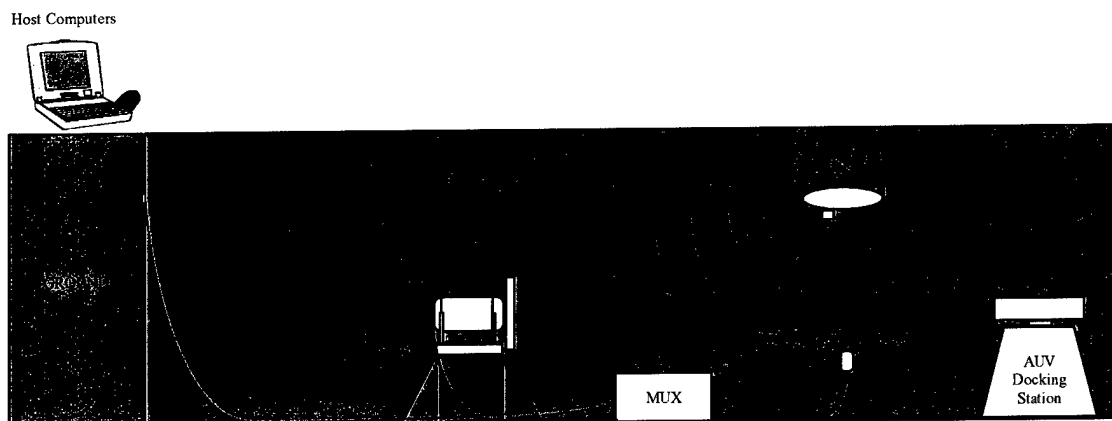


Figure 3.2.4.1. Mechanical Setup for MUX Sea Test

The General Purpose Modem has the following characteristics:

- 1) Controlled through LonWorks and RS422 by host computer on shore.
- 2) Reprogrammable from shore.
- 3) Can be used as a standard MFSK modem in acoustic network.
- 4) Can transmit PSK sequences to the Mills-Cross.
- 5) Can request built-in PSK sequence to be transmitted by AUV to millscross.

The Millscross operates as follows:

- 1) Controlled through LonWorks by host computer on shore.
- 2) Waits for a trigger to start recording sequence.
- 3) Records filtered and decimated data on disk.
- 4) Transfers data upon request to shore.

The major effort is going to be software development and data analysis, as follows:

- 1) Space-Time analysis of acoustic channel.
- 2) Doppler spread study of the acoustic channel.
- 3) Study of acoustic channel capacity for communication.
- 4) Data Transmission Protocol for Maximum Performance.

Results

Both the Mills-Cross and General Purpose Modem have been successfully tested at sea using two boats, as depicted in Figure 3.2.4.2. Figures 3.2.4.3 and 3.2.4.4 show the Mills-Cross and the Modem, respectively. The concrete slabs for each system have also been deployed on the SFTF range in the planned locations. Data has been collected from April to September 1999, and a report on communication performance is in process. Both Mills-Cross and GPM fulfill their expected functions, which are given in table 3.2.4.1.

| Function | General Purpose Modem | MillsCross |
|---------------------------|-----------------------|--------------------|
| Ethernet | None | 100Mbps and 10Mbps |
| Serial | RS422 | None |
| LonWorks | 78kbps | 78kbps |
| Average Power Consumption | 25 Watts | 99 Watts |

Table 3.2.4.1. GPM and MillsCross Functions

During these tests, the MUX was not able to provide either the minimum 10Mbps or the more practical dedicated 100Mbps Ethernet required for the modem tests. However, once the MUX has been refurbished, the additional tests can be conducted.

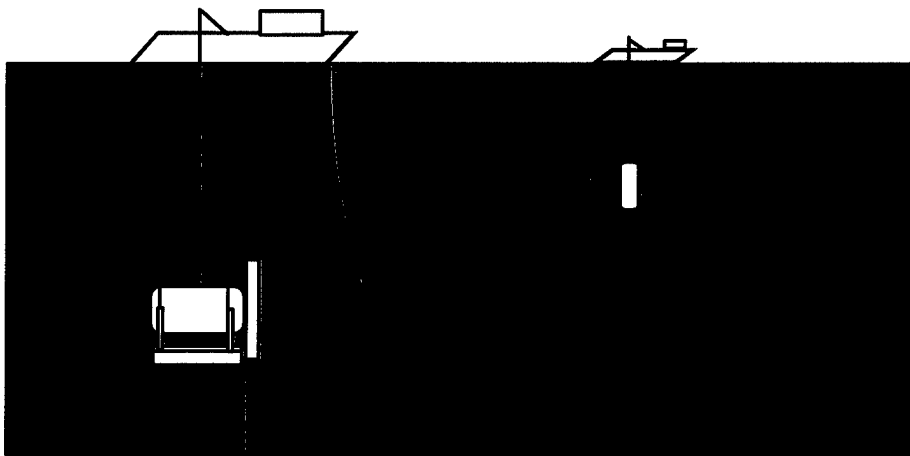


Figure 3.2.4.2. MillsCross and General Purpose Modem test using two boats.



Figure 3.2.4.3. MillsCross on frame during at-sea operation.

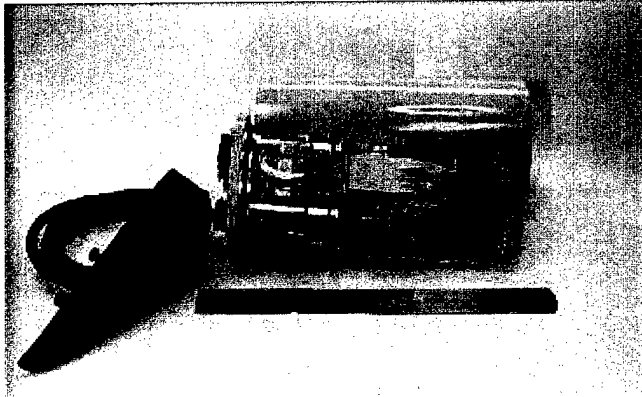


Figure 3.2.4.4. General Purpose Modem.

3.3 Four-Dimensional Current Experiment (Experiment 3)

PIs: Shay (UM), An (FAU), Smith (FAU), Peters (UM), Van Leer (UM), Mariano (UM)

3.3.1 Goals

The goal of the study is to understand the role of small-scale physical processes on coastal ocean variability through high-resolution measurements of the 4-dimensional current variability. For the first time, the approach combines the FAU AUV technology with the UM/RSMAS Ocean Surface Current Radar (OSCR). The engineering part of the research seeks to develop, integrate and test instrumentation designed to measure and characterize the subsurface current structure from AUVs. The working scientific hypothesis is that subsurface and surface currents are dynamically linked such that the four-dimensional physical environment can be reconstructed by integrating AUV, OSCR, shipboard and moored observations. In terms of flow physics, the scientific part of this investigation relates observed current patterns induced by winds (Ekman), low-frequency flows and tides to internal waves in a regime with variable stratification and bottom topography.

3.3.2 Motivations

The coastal ocean exhibits a wide range of physical processes relevant to Navy operations as well as chemical, biological and geological studies. It has been difficult to resolve the complex four-dimensional variability, but significant progress has resulted from synoptic surface current observations with HF radar techniques using OSCR. The utilization of AUVs further widen the range of resolved processes and scales, and an efficient approach of relating subsurface structural variability to surface signals.

3.3.3 Long Term Objectives

Specific engineering and scientific objectives are:

1. Design and implement multiple ADCPs as part of the AUV payload;
2. Relate the aerial estimates of the OSCR-derived surface currents in selected cells to high resolution subsurface current measurements acquired from ADCPs on multiple AUVs as well as from ship- and mooring-based (i.e. Cyclesonde) observations;
3. Isolate low-frequency (subinertial), wind-driven (Ekman), tidal and internal wave signals present in the surface current signals, and to relate them to the vertical structure of subsurface currents and stratification observed by AUVs, ships and moorings within the context of oceanic dynamics;
4. Assess the role of divergence and vorticity fields associated with subinertial and wind-driven flows and their net impact on submesoscale dynamics;

5. Expand the internal waves into baroclinic modes to determine cross-shelf wave propagation of nonlinear internal wave packets derived from the KdV equation;
6. Estimate the internal wave strain rates in the subsurface internal wave currents measured at high-resolution and relate them to the surface current signatures;
7. Examine the frequency-wavenumber spectra and compare them to the GM75 spectra in an effort to examine the shallow-water internal wave field in relationship to deep ocean conditions; and,
8. Examine current sections for coherent structures and relate them to forcing mechanisms.

3.3.4 Accomplishments

The experimental portion of the research was conducted in June and July 1999 as part of the South Florida Ocean Measurement Center (SFOMC) program. Below is a brief synopsis of the strategy used to address the objectives with an emphasis on current variability with sufficient coverage of the stratification to allow analyzing its effect on the circulation.

3.3.4.1 OSCR Measurements: The OSCR radar system was deployed in the vicinity of the SFTF range, offshore Dania Beach and Hollywood, Florida, for a four-dimensional ocean current experiment starting on 25 June and ending 10 August 1999. During this period, a 29-day continuous time series of vector surface currents were acquired starting on 9 July and ending 7 August 1999 at 20-min intervals. The system consisted of two Very High Frequency (VHF) radar transmit/receive stations operating at 49.9 MHz that sensed the electromagnetic signals scattered from surface gravity waves with wavelengths of 3 m. The VHF radar system mapped coastal ocean currents over a 7.5 km X 8 km domain with a horizontal resolution of 250 m at 700 grid points (Figure 2.3.1). Radar sites were located in John Lloyd State Park (next to the US Navy Surface Weapons Center Facility) (Master) and an oceanfront site in Hollywood Beach FL (Slave). This equated to a baseline distance of about 7 km. Each site consisted of a four-element transmit and thirty-element receiving array oriented at an angle of 37° (SW-NE at Master) and 160° (SE-NW at Slave) over a distance of 85 m (Haus *et al.*, 1995). The manufacturer's cited accuracy of the radial and the vector speeds are 2 and 4 cm s⁻¹, respectively, and the directional resolution is 5°. In previous experiments, *RMS* differences have been found to be about 7 cm s⁻¹ in a 75 cm s⁻¹ current (Shay *et al.*, 1998a).

To illustrate the marked variability in the surface currents, on 26 June starting at 0120 GMT (Figure 2.3.2), a submesoscale ring was located along the southern part of the VHF-radar domain just inshore of the Florida Current. Surface currents within the submesoscale ring ranged between 20 to 30 cm s⁻¹ at a diameter of about 1 to 1.25 km from the ring's center. Along the inshore edge, surface currents were directed towards the south at 20 cm s⁻¹. A large fraction of this variability was perhaps due to a buoyant outflow from Port Everglades due to excessive rainfall of more than 40 cm during June. Profiles of the density structure from ship-based CTD measurements indicate strong stratification in the near-surface layers over the inner to mid-shelf. Thus, it is likely that a buoyancy-driven current may have been generated by this fresh water influx. Subsequently, the center of the ring moved about 2 km northward, and the diameter of the submesoscale vortex remained about the same about one hour later. By 0400 GMT, the ring moved 3.5 km northward

from its original position, and surface currents increased to about 50 cm s^{-1} at a radius of 1.5 km from its center. As the feature interacted with the coastal current (Figure 2.3.2), the vortex began to develop an asymmetry in its horizontal structure. The ring was located at the northern part of the radar domain by 0520 GMT.

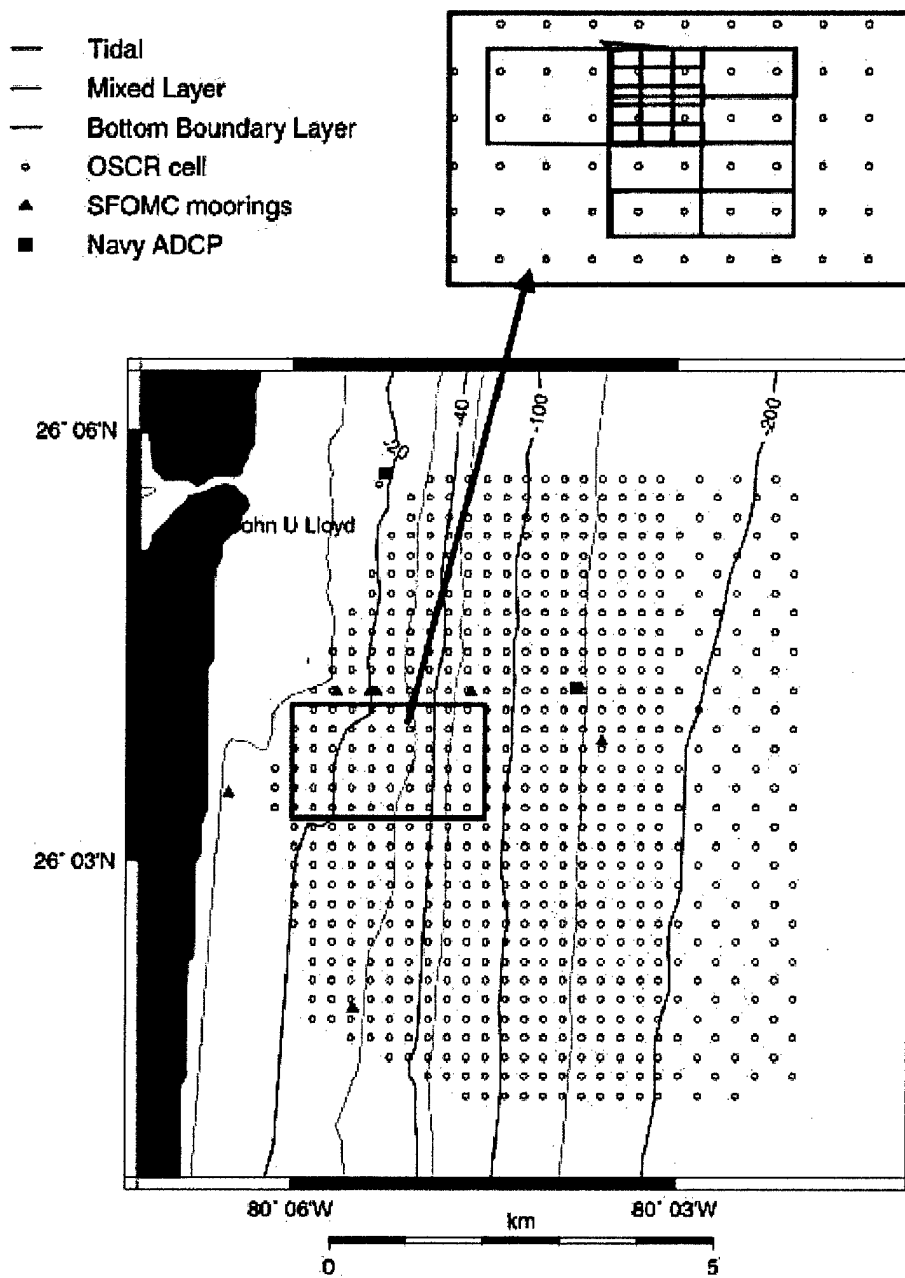


Figure 3.3.1. Multiple-nested measurement domain embedded with the OSCAR grid (circles) for the SFOMC 4-D Current Experiment relative to bottom topography in meters. Master and slave sites are located at John Lloyd State Park and Hollywood Beach, respectively. Inset provide the high-resolution sampling patterns for AUV measurements relative to OSCAR Cells for the Mixed Layer, Bottom Boundary Layer, and Tidal Missions described in Table 3.3.1. The ship track was located 1-2 OSCAR cells removed from the AUV-missions.

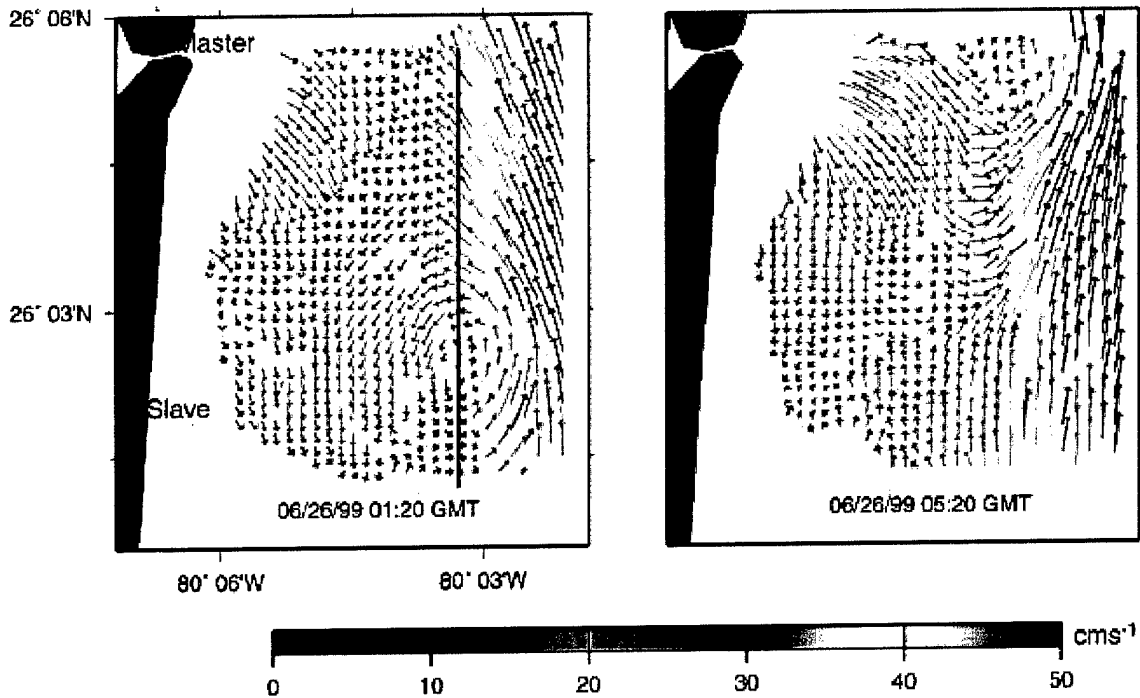


Figure 3.3.2. Surface current images from the SFOMC 4-D Current Experiment on 26 June: at 0120 GMT (left panel) and 0520 GMT (right panel). The black solid line represents a transect described below.

3.3.4.2 AUV-based Measurements: The AUV-based measurements involved an FAU Ocean Explorer (OEX) to map the high-resolution, three-dimensional ocean currents for a continuous period of 12 and 24 hours within the SFOMC range. The purpose of the AUV-based measurements was to profile velocity vectors in vertical and horizontal sections at high resolution over nested grids in the OSCR domain. Measurements of the 3D current vector from a pair of synchronized RDI upward- and downward- looking 1.2 MHz ADCPs were the most important component of observations with the AUV. The sampling rate of the AUV was every second (60Hz), which resolved horizontal scales of about 3 m in several OSCR cells. Note that for these measurements the upward-looking ADCP was programmed to have 0.5 m bins for the Mixed Layer (4D01) and Tidal (4D03) Missions and 1.5 m bins in the downward-looking direction. For the Bottom Boundary Layer (4D02) Mission, higher resolution bins were programmed in the downward-looking ADCP. The downward-looking ADCP performs bottom-tracking thereby providing underwater navigation, and a Falmouth Scientific Instrument CTD allows us to orient the AUV velocity measurements with respect to the background density field. Technical considerations were energy capacity needed to complete the missions and verification of minimal cross-talk interference between two ADCPs.

To extend the energy capacity up to 24 hours, a parallel mid-section was designed and built within which a large number of Alkaline D cells were tightly packed. The use of such primary batteries is justified in that the required survey speed was low at which these batteries are very efficient. Similarly, onboard secondary batteries in the tail section were replaced during the 24 h missions. The resulting OEX configuration increased its energy capacity to approximately 6kWh. A rough estimate of typical vehicle power consumption at 1.25 m s^{-1} was 250W, suggesting that the mission duration was achievable.

In May, several *in situ* tests were conducted to characterize the level of cross-talk interference between the two 1.2MHz ADCPs. Due to limited resources, an existing OVII shell was used instead to house the ADCPs. Spatial separation and operating vehicle depth profile were matched as close as possible to those realized in the test. Results indicated no distinguishable interference in the test experiments. This was believed to be due to the shadowing effect introduced by the vehicle shell and the high-frequency signals that attenuate rapidly in the water column.

Missions: As shown in Table 3.3.1, three different types of missions were conducted in the 4-D Current Experiments over various time scales. During all missions, scientific and vehicle data acquired by the OEX include time, water temperature, salinity, currents, AUV position (latitude, longitude, depth, altitude), and motion parameters (velocity, acceleration, angular rate and attitude). The OEX was acoustically tracked from a launch/chase boat using its onboard Trackpoint II system where acoustic tracking data were integrated into the boat's GPS and flux-gate compass using software running on a portable PC. Tracking information was monitored in real time onboard the boat and archived in files for post-mission analyses of the AUV navigation accuracy. The chase boat followed behind the OEX at a separation distance of 200 to 300 m. In addition, the FAU R/V Stephan cruised outside of the AUV-mission area while acquiring current profile data using a 600kHz ADCP.

Mixed Layer Experiment (4D01): As shown in Figure 3.3.1, the OEX sampled a 500 m x 500 m grid (OSCR Cells), and was programmed to map subsurface current velocities in water depths ranging from about 20 to 35 m, while maintaining a constant depth of about 9 m at a speed of 1.25 m s⁻¹. The upward-looking ADCP was configured only in water profiling mode whereas the downward looking ADCP was configured in both the bottom-track and water profiling modes (alternately with one another). For both ADCPs, only the raw data were collected (no ensemble average)

This mission was conducted on 9 July starting 11:47 GMT for a total of 6 h and 15 min, and again on 27 July from 13:52 GMT time for 12 hours (including a turbulence package as part of the payload). The AUV pre-programmed lawn-mower pattern was repeatedly executed until its battery energy was depleted. During the mission, the OEX occasionally surfaced to obtain differential GPS (DGPS) fixes that bound positional errors to within the required level (25-50 m). The OEX proceeded in directions shown toward succeeding waypoint numbers. The total time to complete one complete pattern was approximately 1.5 hours. Note that in the first mixed layer run, NiCad batteries were used instead (as the Alkaline section was not ready), and thus the mission duration was less than that expected. An example of the velocity sections from the OEX from the 4D01a mission is shown in Figure 3.3.3.

Bottom Boundary Layer Mission (4D02): This mission, second to be accomplished, acquired repeated cross-shelf velocity transects over of 1 km (5 OSCR Cells) separated by 500 m (2 OSCR Cells). The bottom boundary layer mission was conducted once on 12 July, starting at 14:22 GMT for approximately 6 h and 40 min. The mission was broken into two segments because of unexpected low NiCad battery power after about 3.5 hours. Once the batteries were fully charged, the mission continued at 18:30 until 21:20 GMT. As noted above, the ADCPs were switched to provide high-resolution velocity measurements in the bottom boundary layer in water

depths ranging from about 20 to 50 m while maintaining a constant altitude of 9 m and vehicle speed of 1.25 m s^{-1} . The AUV continued profiling as it climbed to the surface to acquire another GPS fix at the pre-programmed waypoints. As it reached the original start position, the OEX started another pattern, and repeated until its energy was exhausted. Two GPS fixes were obtained in each of these patterns.

| Mission Name | Mission Type | Date July 99 | Time (GMT) | Ship Duration h | Auv Duration h |
|--------------|------------------------|--------------|-------------|-----------------|----------------|
| 4DT | ship test | 6 | 14:30-19:00 | 5 | 0 |
| 4D01T | mixed layer test | 7 | 13:45-20:50 | 7 | 8 (CTD bad) |
| 4D01a | mixed layer | 9 | 11:45-23:15 | 11 | 6 |
| 4D02 | bottom boundary layer | 12 | 13:00-23:50 | 11 | 7 |
| 4D03a | tidal | 15-16 | 20:40-23:00 | 26 | 15 |
| 4D03b | tidal | 23-24 | 13:00-16:40 | 27 | 26 |
| 4D01b | mixed layer/turbulence | 27-28 | 12:30-01:35 | 12 | 12 |

Table 3.3.1: Summary of AUV-Ship based missions during the 4-D Current Experiment. The 4D01c mission was in collaboration with the FAU Turbulence Group (Manhar Dhanak and Ken Hollappa)

Tidal Current Experiment (4D03): During the tidal mission, the OEX sampled the velocity structure over an area of 1 km (4 OSCAR Cells) \times 1 km (4 OSCAR Cells) in water depths from about 20 to 35 m for a continuous period of 24 hours while maintaining a constant depth of 9 m and speed of 1.25 m s^{-1} . Bin settings for the ADCP were similar to those used in the mixed layer mission (4D01). The total time to complete one complete pattern was approximately 3 hours. Two tidal missions were conducted, and in both missions, alkaline batteries were used to supply the required energy for the vehicle.

The first 24-hour mission was conducted on 01:05 GMT 16 July for approximately 15 hours. However, this mission was not continuous due to interruption by a number of technical problems, including a broken shaft on the bottom rudder and software bug in the drop weight. The second tidal mission was started at 16:20 GMT 23 July and continued over 25.5 h. The mission ran uninterrupted for 14 hours until the AUV collided with a mooring line that had been previously left by divers. This caused the vehicle to dive below its set maximum depth and thus automatically stop the mission. A new drop weight was installed and the mission was restarted.

3.3.4.3 Ship-board Measurements: Ship-based ADCP measurements of horizontal current profiles with a 5-beam 600-kHz broadband ADCP and of the stratification with CTDs from the R/V *Stephan* accompanied AUV operations (Table 3.3.1). The ADCP was deployed over the starboard side using a mount designed by RSMAS and FAU personnel. Shipborne CTD and ADCP measurements were acquired on a grid pattern spaced 1-2 OSCAR cells outward from the AUV grid, and thus on a slightly larger scale. The pattern was taken along rectangular boxes aligned with the cardinal directions which enclosed the AUV area of operation. The eastern North-South leg of the ship track was positioned beyond the shelf break (coincident with the *Third Reef*) because high horizontal and vertical shear tended to occur just beyond (east) of the shelf break. The typical ship speed was 1.5 m s^{-1} such that ship track boxes took 1.5-3 hours to complete. As shown in Figure 3.3.4, the ADCP was set at 1-m bins, producing a vertical range of

about 35 m depth. Bottom tracking was possible at depths up to about 85 m. Note that all observations (15-s ensemble averages) have valid bottom tracking. DGPS navigation data were logged along with the ADCP output. In addition, CTD profiles were acquired at the corners of the ship-track pattern using a high-resolution Ocean Sensors OS500 CTD. Unfortunately, the temperature-conductivity (TC) sensor assembly broke during 4D03a, and a Seacat CTD was used in the remainder of the experiment.

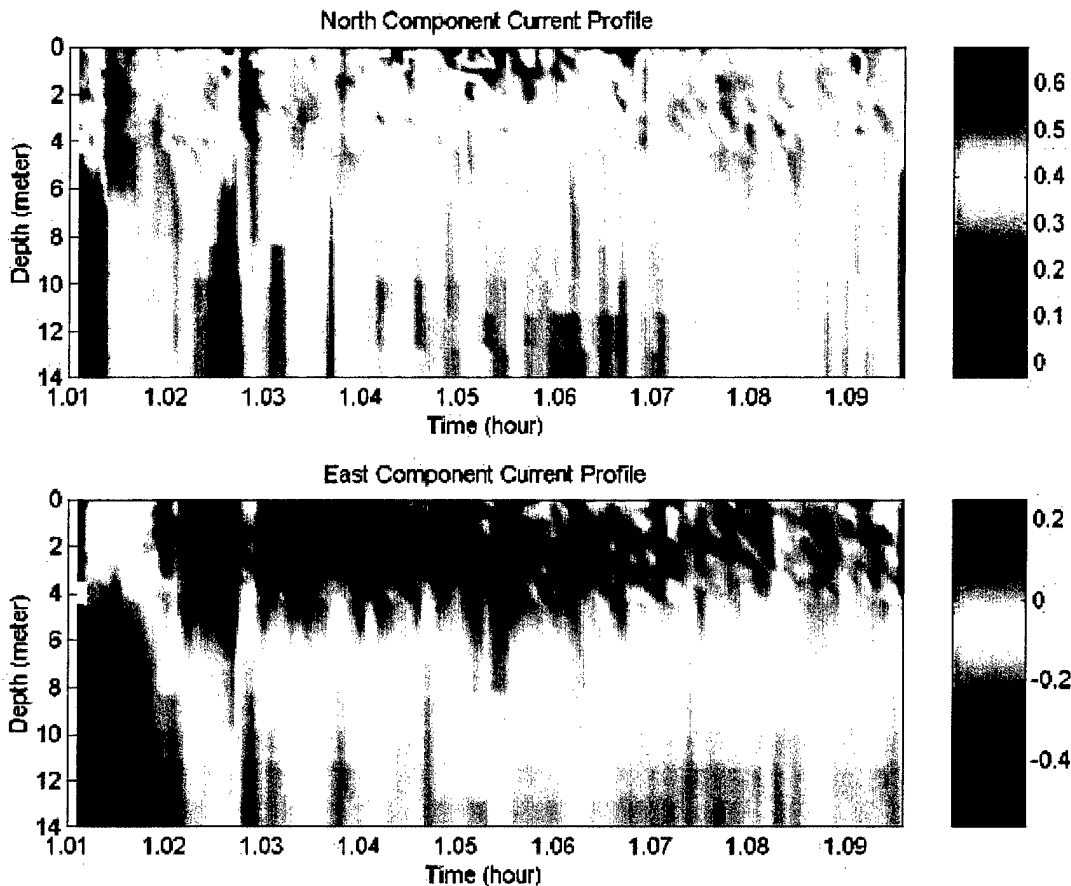


Figure 3.3.3: Velocity profiler transects for the along-shelf component (top panel) and east component (lower panel) acquired by the AUV during the mixed layer mission (4D01a).

3.3.4.4 Moored Measurements: The Cyclesonde Autonomous Profiler (Van Leer, 1980), an instrument designed to acquire repeated vertical profiles along a taut-wire subsurface mooring according to a preset schedule, was deployed in the center of the NOVA/USF array and in the core of the OSCAR domain. A newer and improved version of the Cyclesonde was built, tested and deployed adjacent to the shallow water MUX. This system featured the same valve, sensors and telemetry format as the previous commercial version of the instrument including a new microprocessor based data sampling and recording system built around the Data Logger/Controller Engine. All functions were tested and the CTD sensors were calibrated in the lab and the ballasting tank. A longer-life battery was also installed for a one-month deployment to profile at half-hourly intervals with a 2.5 sec sampling rate. The Cyclesonde successfully communicated

to shore through the MUX/cable system during the experiment, and the data are now being processed. In addition, these data provided useful diagnostic information to assess the performance of the shallow water MUX box built by FAU. Four upward-looking ADCPs, (one US Navy, three NOVA/USF), also sampled the velocity structure at high resolution in the OSCR domain.

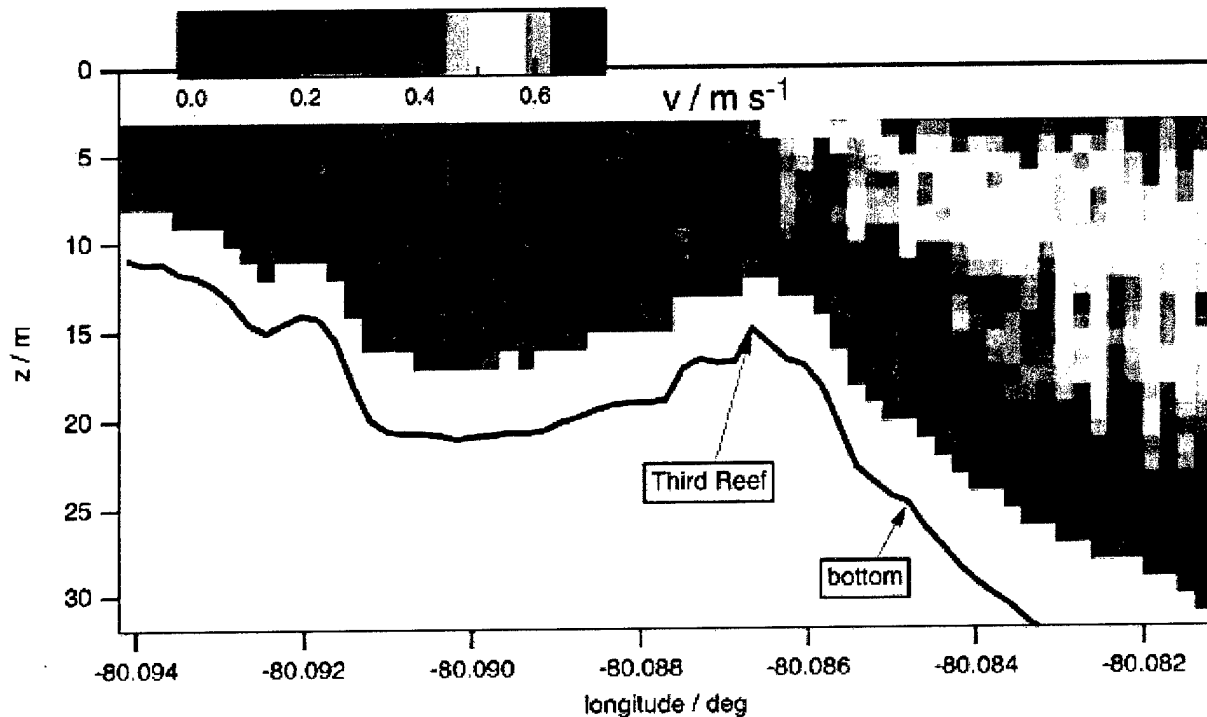


Figure 3.3.4: Cross-shelf section of the along-shelf current observed from the 600kHz ADCP on the R/V Stephan on 1704-1719 GMT 9 July 99. Northward current prevailed over this section with maximum currents near to the surface.

3.3.5 Results:

Preliminary results indicate considerable variability in the coastal ocean currents and stratification even during quiescent conditions that prevailed during June and July. As shown in Figures. 3.3.2 - 3.3.4, surface currents reveal submesoscale rings, frontal lobe-like structures, subsurface current maxima, and Florida Current intrusions over the shelf break. Given the richness of this data set, new insights will be gained from analyzing the data sets acquired during the experiment (Smith *et al.*, 1997). By combining filtered and objectively analyzed data sets, a fairly complete view of tidal, subinertial and wind-driven 3-dimensional currents can be constructed from the OSCR, AUV, ship, and moored measurements.

Comparisons: Initial comparisons of the surface to subsurface currents have been made to the NOVA/USF ADCP mooring in 10 m of water (Figure 3.3.5). Generally, along-shelf currents revealed very similar trends, however at certain times subsurface currents were larger than surface values over the 29-day time series. Similar subsurface current maxima were found in the OSCR measurements off Cape Hatteras (Shay *et al.*, 1995). This is consistent with the ship and AUV

cross-shelf transect data. By contrast, the cross-shelf currents were of similar magnitudes (Figure 3.3.6). Over the time series, the current shear between the surface and subsurface layer (over ~ 2 -m layer) were $O(10^{-2} \text{ s}^{-1})$. Surface currents were highly correlated at levels of > 0.8 to those at 2 m beneath the surface. Notice that the negative phase suggests a predominant clockwise-veering of the current with depth over the time series. We plan to apply such analyses to all data sets to assess *RMS differences* and determine what the surface current measurement means in terms of the mixed layer current structure particularly with respect to a real versus time average from AUV and ship-based ADCP data.

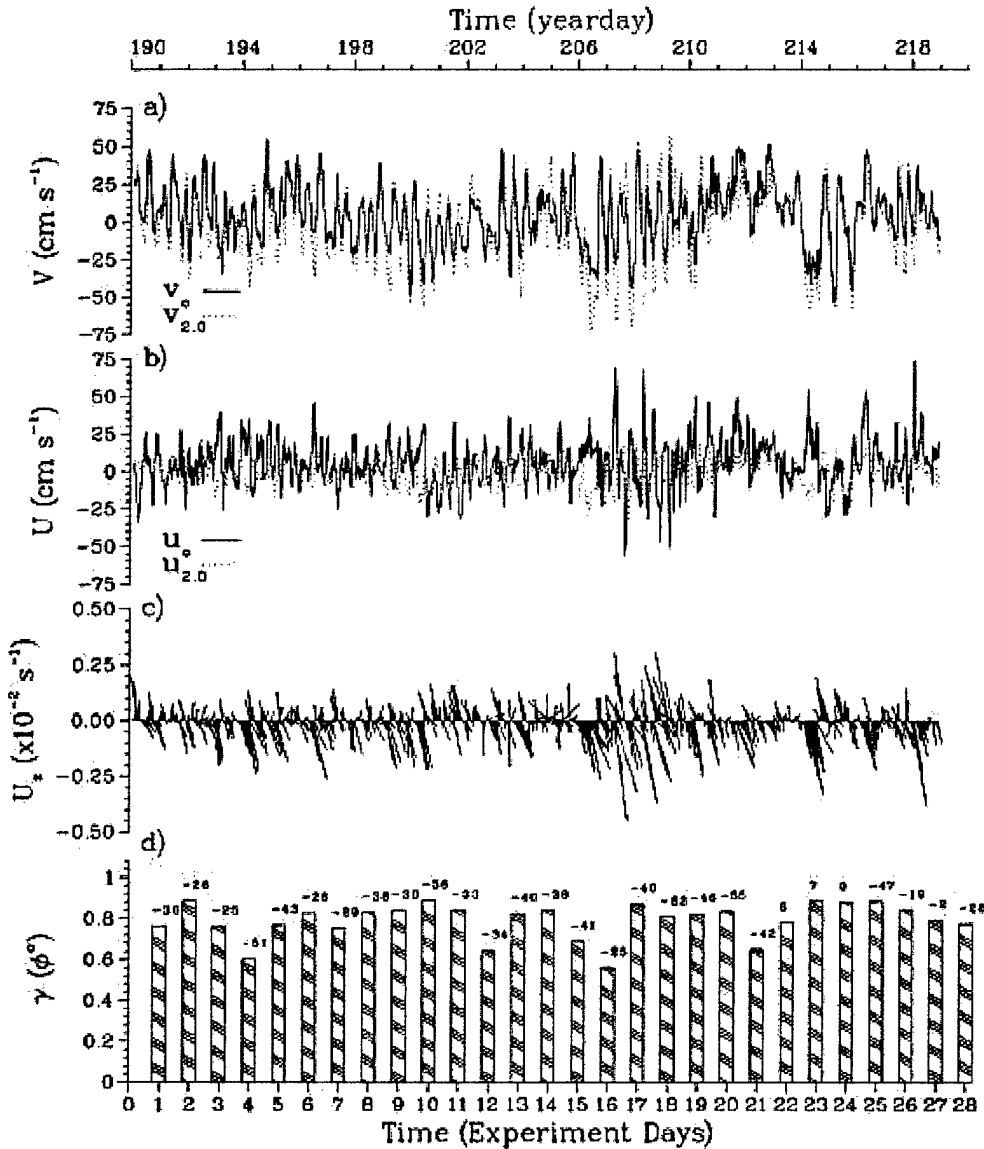


Figure 3.3.5: Comparison of OSCR-derived surface and subsurface current time series at the 10 m mooring deployed by NOVA and USF for the a) v-component (cm s^{-1}), b) u-component (cm s^{-1}), c) current vector shear ($\times 10^{-2} \text{ s}^{-1}$), and d) daily complex correlation coefficients (and phases) relative to the surface velocity. A negative phase implies a clockwise veering of the current with depth. The subsurface data was provided by Alexander Soloviev (NOVA) and Robert Weisberg and Mark Luther (USF).

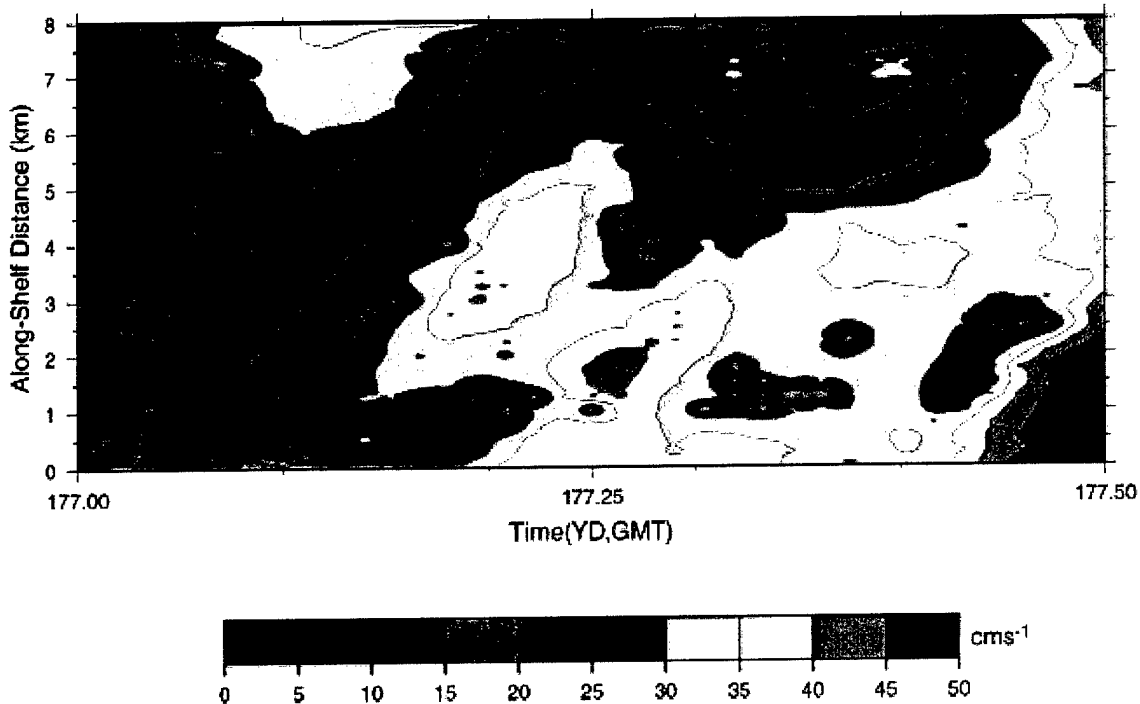


Figure 3.3.6: Along-shelf time section of surface current speed for a 12 h period on 26 June following the ring through the VHF domain. The path of the ring, as depicted by the near-zero current speed, has an approximate slope of 30 cm s^{-1} with the current speed scale (color bar) as in Fig. 2.

Feature Propagation: To examine the translation of the submesoscale ring in Figure 3.3.2, a latitude time plot on the 26 June is constructed over a 12-hour time interval (Figure 3.3.6). The ring's northward displacement of about 6 km, as depicted by the small current speed, occurred over a 5 hour period. This translation speed of about 30 cm s^{-1} is roughly consistent with the propagation speed of spin-off eddies (Lee and Mayer, 1977) and near-inertial motions trapped and advected by the vorticity of the Florida Current (Shay *et al.*, 1998b). However, these features have larger horizontal scales compared to those found here.

The horizontal structure of the depth-averaged currents detected by the AUV during the mixed layer mission (4D01a) is shown in Figure 3.3.7. In the first two realizations, the current vectors indicate a northward flow at a maximum of 30 cm s^{-1} aligned with the bottom topography. Subsequently, the flows reverse (3 hours later) in the inner domain and flow westward in the outer part of the domain at speeds of about 20 cm s^{-1} . Finally, in the 4.5-6 hour map, the current vectors all tend to flow southward. One possibility here is that a large fraction of this variability was due to the tidal currents, which has the approximate time scale of the M_2 tidal current. This is now being explored with the data set.

Tidal Flows: Surface observations have been analyzed using harmonic analysis over the time series to isolate the M_2 and K_1 tidal current constituents following Foreman (1977). To minimize leakage effects between the various constituents, analyses have been performed one constituent at a time. The calculations include tidal ellipse parameters and Greenwich phase lags from horizontal current measurements based on Godin (1972). The package uses a least-squares fit method

coupled with nodal modulation for resolvable constituents with respect to a given Rayleigh criterion. Generally, the diurnal tidal currents were more energetic than the semidiurnal tidal currents. There is a clear enhancement of tidal current amplitudes with bottom topographical changes, which suggests a baroclinic or internal tide perhaps generated by the barotropic tide. Little is known about their behavior and impact on acoustic signal propagation in areas such as the SFTF range where stratification and topography are highly variable.

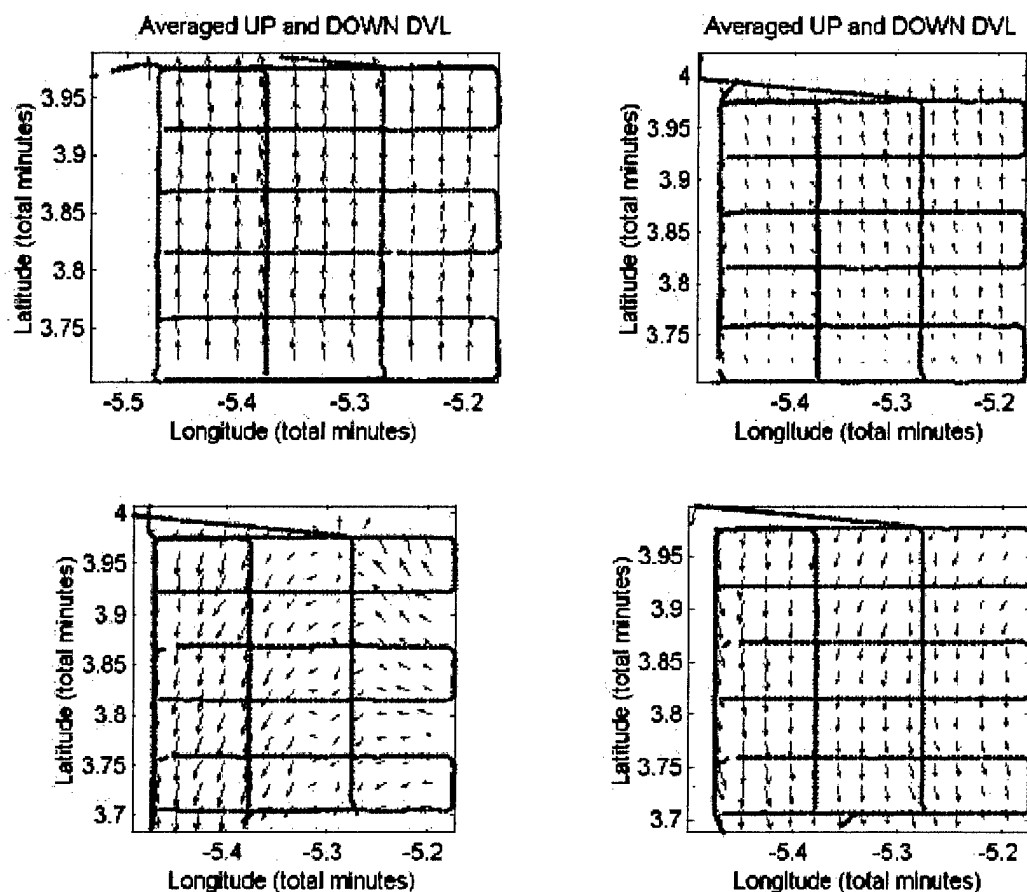


Figure 3.3.7: Four maps of the depth-averaged current vectors acquired from the ADCPs on the AUV during the 4D01a mission a) 0-1.5 h, b) 1.5-3 h, c) 3-4.5 h, and d) 4.5-6 h. Each map represents one realization over about 1.5 h to complete the lawn-mower pattern (AUV-tracks are solid) over a 500 m x 500 m grid.

Objective Analysis: Velocity data from OSCR are being space-time interpolated, using the parameter matrix objective analysis algorithm (Mariano and Brown, 1992), to a regular high resolution space-time grid, 100 m in the horizontal and 15 minutes in time, and to the locations of the AUV, ADCP and Cyclesonde near-surface velocity data. Difference statistics will be tabulated between all the different observing platforms to document the error characteristics for each measurement. Three-dimensional correlation functions are being analyzed to determine dominant phase speeds, space and time scales as a function of distance offshore. The next step is to

calculate high-resolution maps of relative vorticity and horizontal divergence for the purpose of determining the vorticity dynamics of coastal phenomena.

3.3.6. Summary

For the first time, the experiment demonstrated the relative importance of conducting AUV and ship-based sampling grids within a very high-resolution grid of surface current measurements from OSCAR. During the week of 19 July, three additional turbulence missions were also conducted in the OSCAR domain by the FAU group. These current and turbulence measurements will provide new insights into complex physical processes occurring in a coastal ocean forced by a meandering Florida Current where maximum surface velocities exceeded 2 m s^{-1} . Furthermore, the observations significantly challenge numerical models of coastal circulation. Thus, over the next year the synthesis and analysis of these observations will provide data required not only to assess AUV performance in a highly variable ocean, but will systematically address the scientific objectives in section 3.3.3 in pursuit of the long-term goal of the study.

REFERENCES

- An, E., M. Dhanak, L. K. Shay, S. Smith, J. Van Leer, 1999: Coastal oceanography using autonomous underwater vehicles. *J. Atmos. Oceanogr. Tech.*, (Revised and Resubmitted)
- Clarke, A. J., 1991: The dynamics of barotropic tides over the continental shelf and slope. In *Tidal Hydrodynamics*, ed. Bruce Parker, John Wiley and Sons, New York, New York, 79-108.
- Foreman, M.G.G., 1977: Manual for tidal currents analysis and prediction. Pacific Marine Science Report 78-6, Institute of Ocean Sciences, Patricia Bay, Victoria, B.C. 57pp.
- Lee, T. N. and D. A. Mayer, 1977: Low-frequency variability and spin-off eddies along the shelf off southeast Florida. *J. Mar. Res.*, **35**, 193-220.
- Mariano, A. J., and O. B. Brown, 1992: Efficient objective analysis of heterogeneous and nonstationary fields via parameter matrix. *Deep -Sea Res., Part A*, **39**, 1255-1271.
- Prandle, D., 1987: The fine-structure of nearshore tidal and residual circulations revealed by HF radar surface current measurements. *J. Phys. Oceanogr.*, **17**, 231-245.
- Shay, L. K., H. C. Graber, D. B. Ross, and R. D. Chapman, 1995: Mesoscale ocean surface current structure detected by HF radar. *J. Atmos. and Ocean. Tech.*, **12**, 881-900.
- Shay, L. K., S. J. Lentz, H. C. Graber, and B. K. Haus, 1998a: Current structure variations detected by high frequency radar and vector measuring current meters. *J. Atmos. Oceanogr. Tech.*, **15**, 237-256.
- Shay, L. K., T. N. Lee, E. J. Williams, H. C. Graber, and C. G. H. Rooth, 1998b: Effects of low frequency current variability on submesoscale near-inertial vortices. *J. Geophys. Res.* **103**, 18,691-18,714.

Shay, L. K., T. M. Cook, B. K. Haus, J. Martinez, H. C. Graber, and Z. Hallock, 1999: The strength of the M_2 tidal current at the mouth of the Chesapeake Bay. *J. Phys. Oceanogr.* (Revised and resubmitted).

Smith, S., E. An, J. Park, L. K. Shay, H. Peters, and J. Van Leer, 1998: Submesoscale coastal ocean dynamics using autonomous underwater vehicles and high frequency radar. 2nd Conference on Coastal Atmospheric and Oceanic Prediction. 78th Annual Meeting of the American Meteorological Society, 10-16 January 1998, Phoenix, AZ, 143-150.

Stewart, R. H. and J. W. Joy, 1974: HF radio measurements of surface currents. *Deep-Sea Res.*, **21**, 1039-1049.

Van Leer, J. C., 1980: An automatic radiosonde/rawinsonde for coastal oceanography. 2nd Conference on Coastal Meteorology. American Meteorological Society, Boston, MA.

3.4 Environmental Array and Data Analysis (Experiment 4)

PIs: (McCreary, Soloviev (NSU)), (Weisberg, Luther (USF))

Scientific Justification

NSU and USF scientists deployed a three-dimensional mooring array coordinated with the OSCR with acoustic Doppler current profilers (ADCP) and a combination of recording temperature and temperature/ salinity sensors on each mooring. In addition to providing necessary monitoring of the physical-oceanographic environment for the SFTF Range, the array provides data useful for understanding a variety of scientific questions. These questions include: What are the dominant modes of interaction between the nearby Gulf Stream and the shelf/nearshore circulation? Are these events driven by the wind, Gulf Stream Meanders, propagating continental shelf waves, or near-shore eddies? What is the structure and temporal variability of the internal-wave field within the Range. Describing and mapping phenomena like this, and identifying the processes that cause them, is the underlying scientific justification for the proposed array.

Main Accomplishments

The Environmental Array, deployment schemes, and data acquisition software are developed at the USF Marine Science Department. The electronics packages are developed at the NSU Oceanographic Center (in consultation with USF). The design of the array meets two objectives: It is able to provide data that can answer questions like those posed above, and it also satisfies the monitoring needs of the other experiments.

The NSU/USF Environmental Array is implemented into the SFOMC range plan. The Environmental Array including one bottom mooring (NW) and two surface moorings (NE and SW) has been built, tested and deployed at the SFOMC range. Some changes regarding the SE mooring were done to adjust the array and our schedule to the modified plans of our SFOMC partners.

Additional details about the status of the moorings are given below:

(a) NW bottom mooring

The bottom mooring consists of the concrete anchor, SeaGauge Wave and Tide Recorder SBE-26 (Sea-Bird Electronics, Inc.), WH Sentinel 300kHz ADCP, and a junction box. The concrete anchor is manufactured at the USF marine shop. The purpose of the junction box is to adapt the SeaGauge and ADCP units to the FAU Multiplexer (MUX). The junction box includes an RS232 to RS422 and DC-DC power converters.

The NW bottom mooring was successfully deployed from the R/V "Stephan" (FAU) on June, 25 (just before the actual start of the first SFOMC experiment) at a 11-m isobath (26°04.23 N, 80°05.65 W). The NW mooring was installed in an internal recording mode (MUX had not yet been deployed by that time). Later, we decided to keep the mooring in the autonomous recording mode until the end of the "4D" and "Adverse Weather" experiments (to provide an uninterrupted data set) and to connect it to the MUX in August - immediately after the end of the scientific experiments. However, in August, SFOMC decided to recover the MUX for technical services.

Before the recovery, a test connection was done demonstrating that the MUX was communicating with the NW bottom mooring through the bottom cable.

The NW mooring was recovered on August 10, 1999; the data from all sensors were successfully downloaded. The data description is given in the read-me file (see Section "Data Availability"). After replacing batteries, the NW mooring is currently continuing the data collection at SFOMC range in a self-recording mode.

(b) NE and SW surface moorings

The mechanical construction of surface moorings consists of a surface buoy, three segments of chain, wire rope, and anchor. A downward-looking WH Sentinel 600kHz ADCP measures the vertical ADCP profile. The chain of inductively coupled MicroCat instruments, inter-dispersed with self recording temperature sensors, provides detailed information about the temperature (T), salinity (S), and density (σ_t) fields. There is a Coastal Climate Weatherpack on the NE mooring. The data from the ADCP, inductively coupled MicroCats, and weather-package (NE mooring only) is transmitted with spread-spectrum radios every 15 minutes and stored at the PC in the lab.

The data acquisition system is developed to interface with the WH Sentinel ADCP, Coastal Climate Weather-pack, and a Seabird Electronics Inductive Modem (IM) Micro-Cat. Communication to these instruments is via a 900 MHz Freewave radio modem. The software is based on a PC running the Red Hat LINUX operating system. Separate programs are developed to acquire data from each of the instruments. The computers are hooked up to the network, which provides the real time remote access to the system; also, the ftp message containing the recent data is mailed out every 15 minutes.

The data acquisition system has been accommodated temporarily at the NSU Oceanographic Center. After the end of hurricane season (sometime in October), the data acquisition system will be relocated to its permanent place in the Range House at the South Florida Testing Facility (SFTF).

The NE and SW surface moorings were successfully deployed from the R/V "Stephan" on 14 July 1999 (using the first available window in the SFOMC ships schedule). The NE mooring was deployed at 26°04.170'N, 80°04.610'W (50-m isobath); the SW mooring at 26°01.96'N, 80°05.51'W (20-m isobath). During the NE mooring deployment, the ship had to tow the chain with MicroCat instruments for about 1 mile (to compensate for the ship drift) that resulted in a shift of the position of some instruments on the cable. This shift will be accounted for later by interpolating the signals to the original depths.

The moorings are transmitting data in real time via the radio channels. The data are stored in the NSU computers, USF network, and internally on the moorings. The data are available in real time for all SFOMC participants from the following ftp sites: 137.52.16.116 (NE mooring) and 137.52.16.115 (SW mooring). In the second half of August, an unknown object hit the NE mooring, partially damaging the wind monitor of the Weather Package and one of the two solar panels. The repairs of Weather Package on the NE mooring and a solar panel voltage regulator on the SW mooring have been scheduled for the week of September 20.

(c) SE mooring

The NSU/USF environmental array was limited to the deployment of three moorings upon reevaluation of the SE location. Four issues were considered: 1) engineering concerns regarding the maintenance of a mooring in a high current and wave regime with the intended equipment, 2)

a scientific reevaluation based on the recognition that the density field may have considerable alongshore variability over the scales of the University of Miami acoustic array, 3) overall programmatic budget considerations, and 4) the status of telemetry by underwater cabling and the delays associated with this. Instead of a mooring we opted to provide the University of Miami with two inductively coupled Seabird Microcats for use on their acoustic mooring. When deployed in late 1999 this will provide for a single integrated system without the added risk of a separate mooring.

Data Availability

The data from all moorings have been stored internally. The data subsets from the surface moorings are transmitted by radio and stored internally at the lab computer.

NW bottom mount (11 m):

- 1) ADCP velocity profile with 0.5-m vertical resolution and 15-min sampling interval, starting from June 25, 1999.
- 2) WaveGauge p, T, S, and s_t time series at the bottom, starting from June 25, 1999.

NE surface mooring (50 m):

Measured parameters:

- 1) ADCP velocity profile with 1-m vertical resolution and 15-min sampling interval, starting from 15 July 1999.
- 2) MicroCats T, S and σ_t profiles, starting from 15 July 1999.
- 3) Meteorology including air and water temperature, atmospheric pressure, air humidity, wind speed and direction.

SW surface mooring (20 m):

Measured parameters:

- 1) ADCP velocity profile with 0.5-m vertical resolution and 15-min sampling interval, starting from 14 July 1999.
- 2) MicroCats T, S and σ_t profiles, starting from 14 July 1999.

The preliminary data set data are available from the anonymous ftp site:

ftp ocg6.marine.usf.edu (or 131.247.138.76)

login: anonymous

password: <your name>

cd pub/SFOMC

get README

Preliminary Data Analysis

During the 4D and Adverse Weather SFOMC experiments, practically uninterrupted data set was obtained from the Environmental Array moorings. The data include: vertical ADCP profiles, T and S profiles, surface wave parameters, meteorological parameters. Figures 3.4.1 and 3.4.2 show the vertical profile at the 11m isobath mooring: Figure 3.4.3 gives an example of the temperature, salinity, and density profiles at the 50m isobath mooring over an eight-day period in July 199. Figure 3.4.4 shows the velocity and density co-variability over a two-day period in more

detail. Figure 3.4.5 shows the surface wave and sea level variations during the SFOMC experiments in July 1999.

The data demonstrates subtidal reversals in current from north to south at about two knots. Future analysis will be aimed at determining the cause of these substantial current variations while preliminary analysis suggests that these low frequency motions are not locally wind driven. In addition, simple estimates using a logarithmic layer approximation show that the vertical momentum flux due to bottom friction is at least several times larger than the local wind stress. This information will be useful for the analysis of the Adverse Weather Experiment performed by the FAU SFOMC group in July 1999.

Along with the subtidal variations, there are equally strong supertidal oscillations. Their central period of about 8-10 hours is distinctly different from the surface elevation period, and going offshore into deeper water from the 11 m to 50 m isobaths, they appear to be of baroclinic nature. A working hypothesis is that these oscillations are induced by baroclinic motion in stratified layers of the shelf break and may be related to the spin-off eddies generated along the shelf off Southeast Florida. The relationship between the supertidal (and subtidal motions) and the Florida Current via spin-off eddies and the generation of shelf break modes remains to be determined.

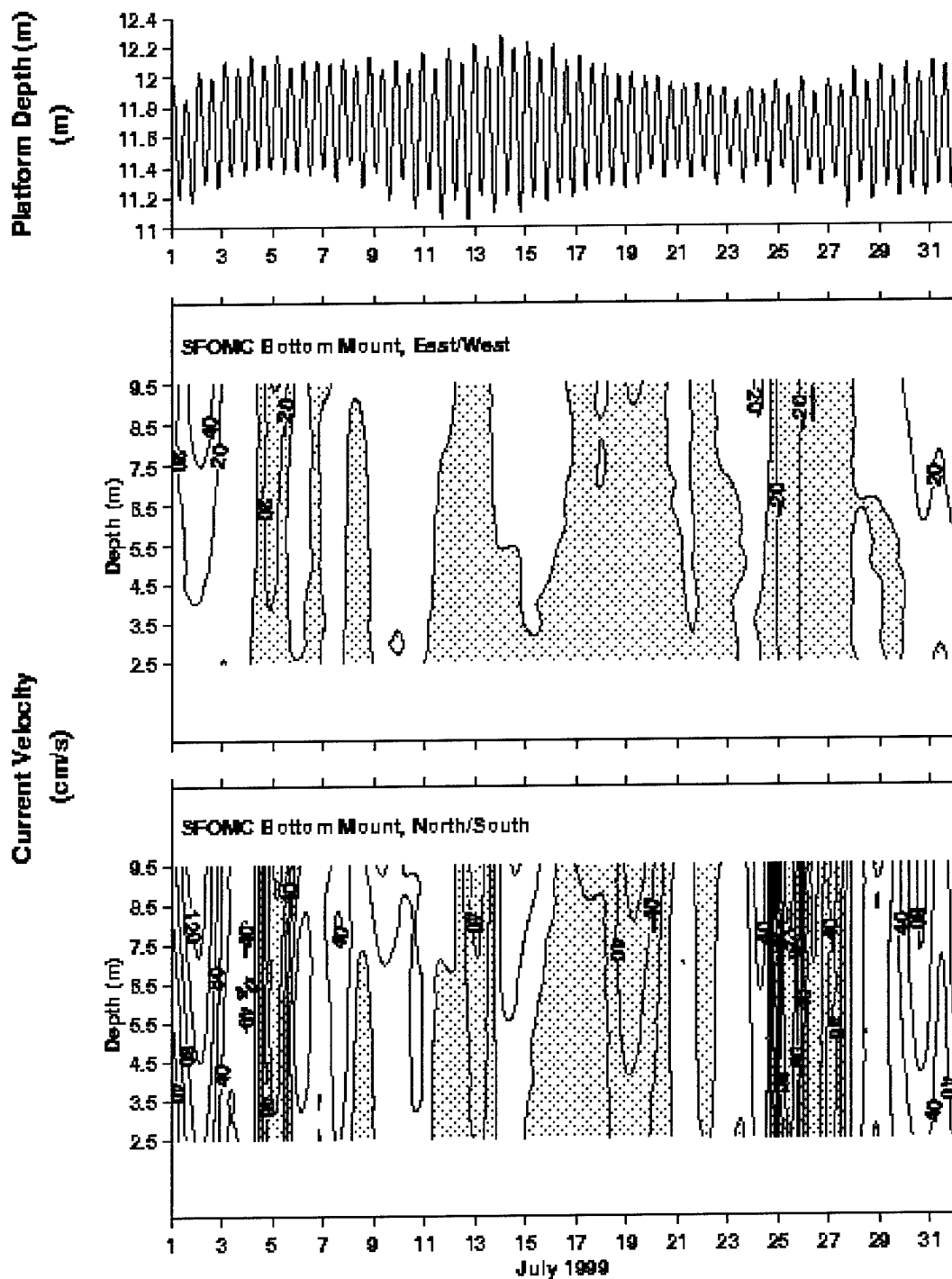
Further joint analysis with other SFOMC partners will provide a 4D description of these energetic subtidal and supertidal current variations. In particular, combining the horizontal distribution at the surface observed from the OSCAR measurements by the UM group (Nick Shay) with the vertical profiles of velocity and density at different isobaths measured by the NSU/USF Environmental Array will provide the temporal structure of these motions. An encouraging factor in this analysis will be the fact that the OSCAR and ADCP records appear to be well correlated.

Conference Presentations:

- 1) The deployment plans were discussed at several meetings including the NSF Sponsored Workshop at SeaTech FAU in February 1999.
- 2) Abstract has been submitted to Special Session "Global Ocean Observatories" (OS05): M. Luther, R. Weisberg, A. Soloviev, and J. McCreary, Environmental Array in the South Florida Ocean Measurement Center (SFOMC) and Data Analysis. 1999 AGU Fall Meeting in San Francisco.

Acknowledgments:

We are grateful to our colleagues, Rick Cole, Jeff Donovan, and David Burwell (USF), Terry Thompson and Laszlo Nemeth (NSU), who provided the top level technical support on the project. The R/V "Stephan" (FAU) and R/V "Researcher" (NSU) operations were excellent, and special thanks to Doug Briggs (FAU), Dave Gilliam and Lance Robinson (NSU). SFTF personnel were also very helpful with the mooring operations. The NSU Oceanographic Center provided substantial administrative help for the project.



July 1999 isochrones of east-west and north-south components of currents and time series of depth measured at the SFOMC buoy. The velocities were 36-hour low-pass filtered and the depth is unfiltered hourly data.

Figure 3.4.1. The velocity field in the SFOMC range in July 1999 (a 11-m isobath)

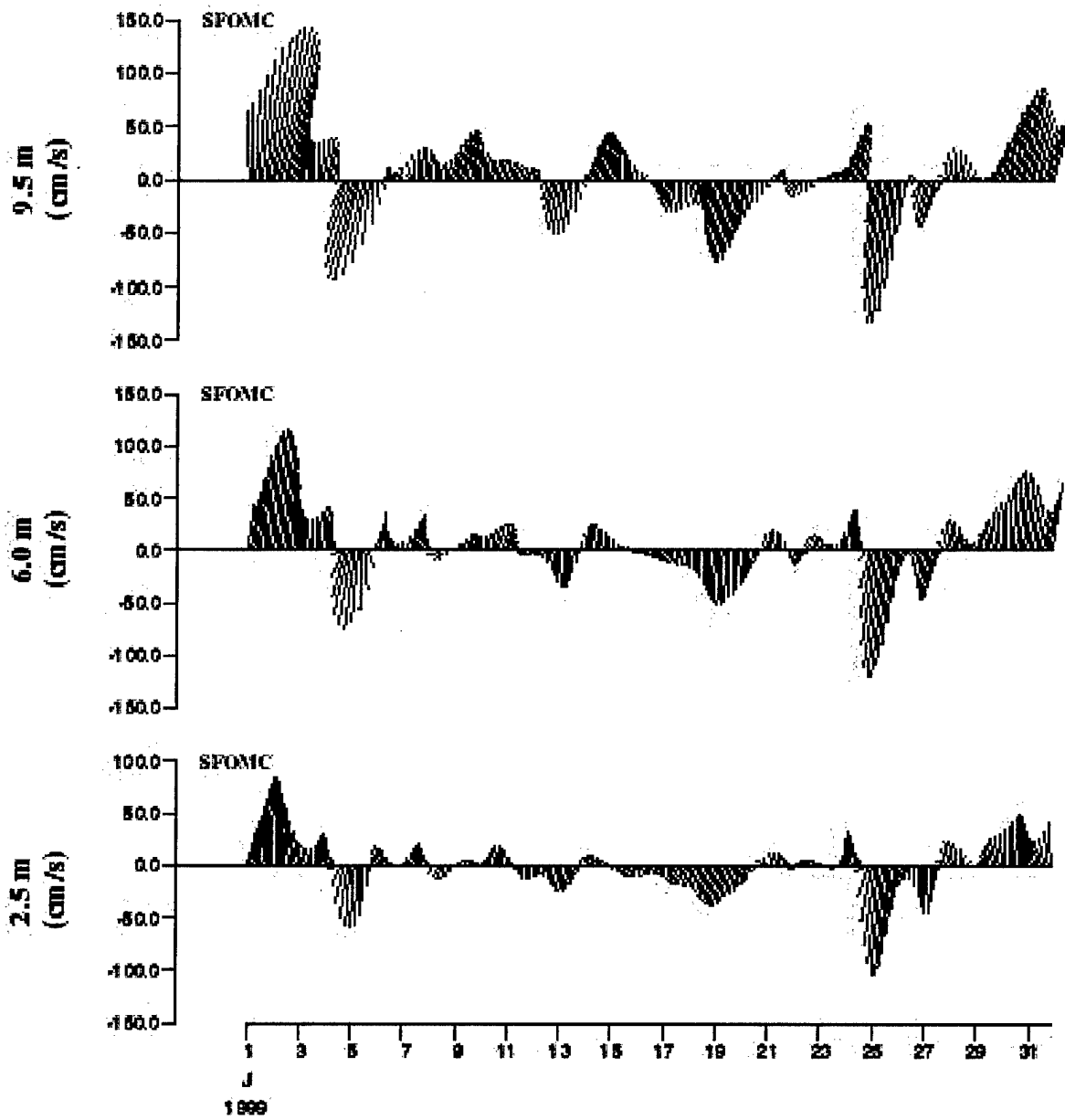


Figure 3.4.2. The velocity vectors on three different heights above the bottom in July 1999 (a 11-m isobath).

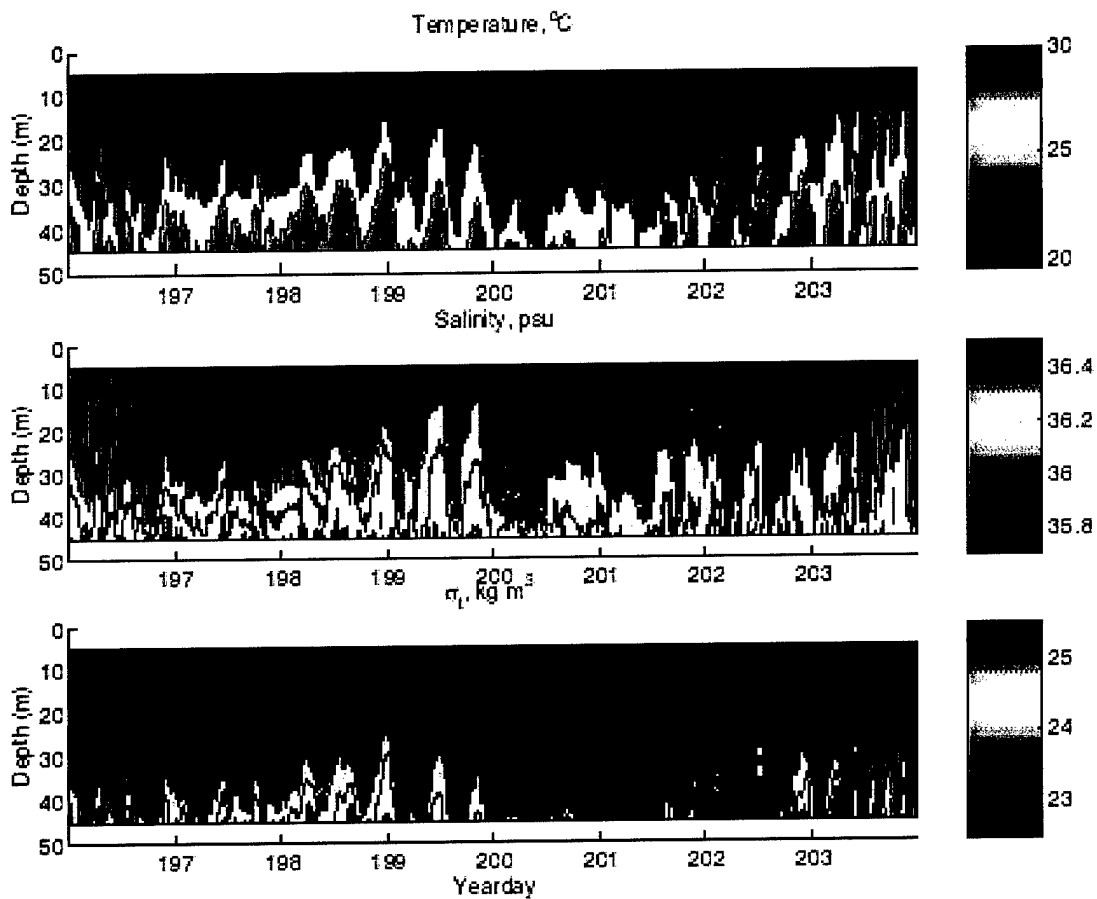


Figure 3.4.3. An example of the temperature, salinity, and density variability in the SFOMC range from the NE mooring (subject to correction after interpolation to the original instruments depths).

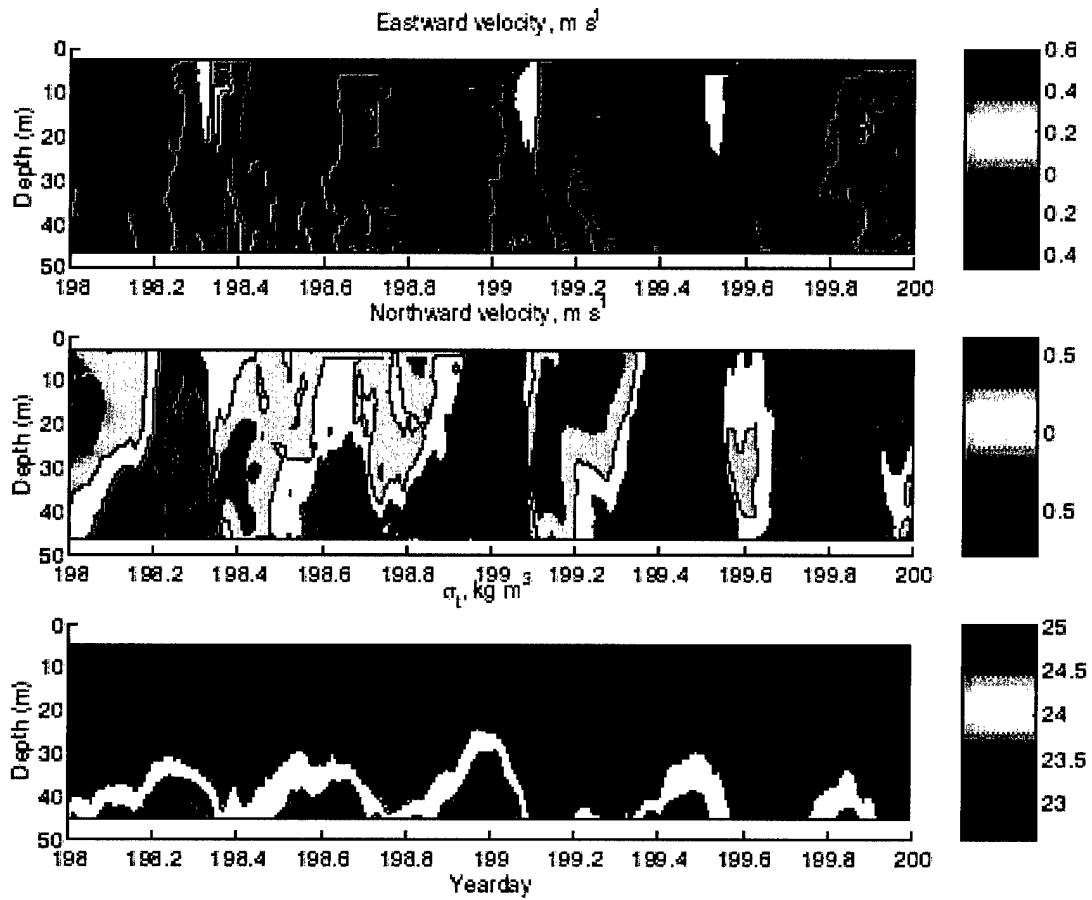


Figure 3.4.4. An example of the velocity and density variability in the SFOMC range from the NE surface mooring (the density field is subject to correction after interpolation to the original instruments depths).

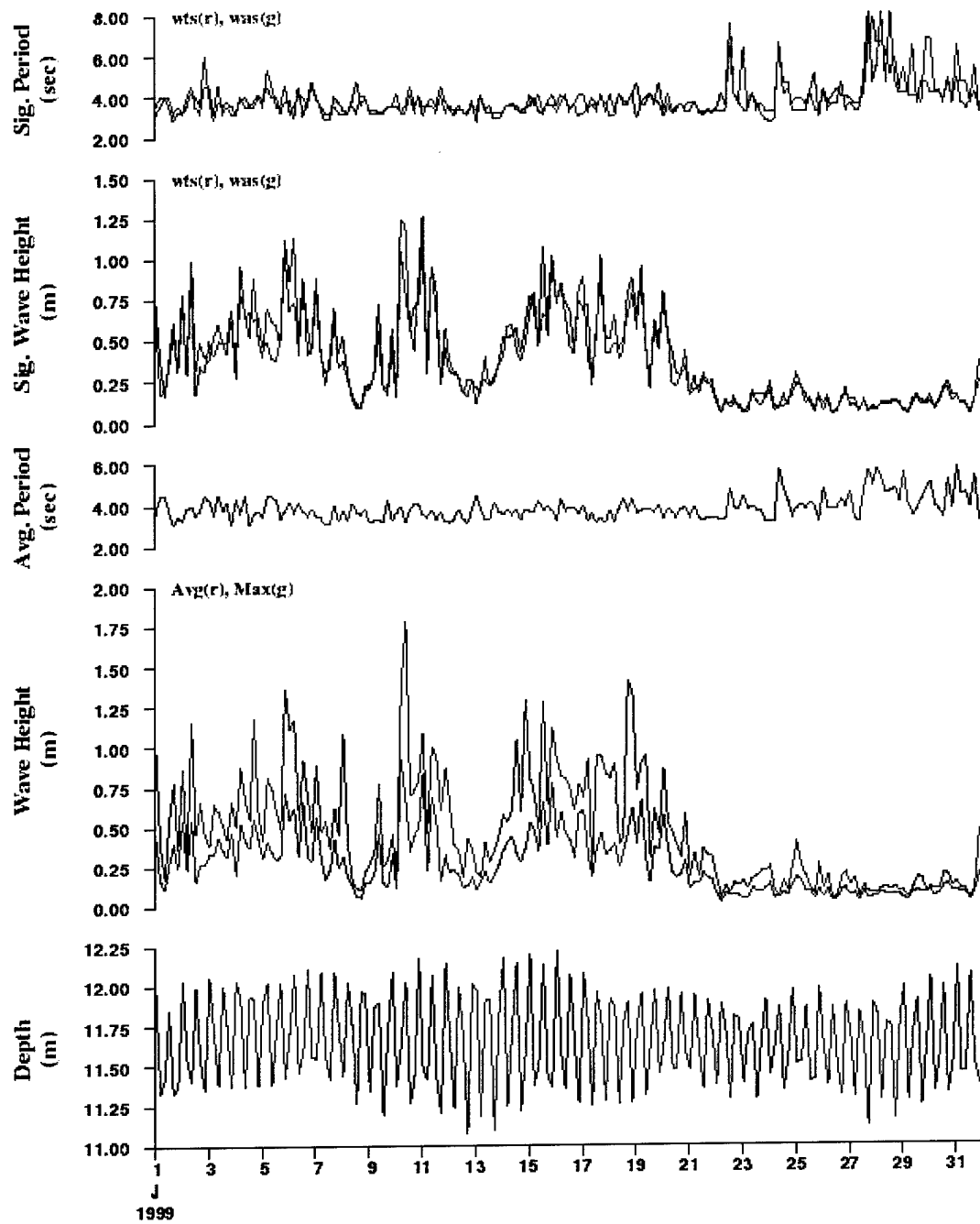


Figure 3.4.5. Surface wave parameters in the SFOMC range in July 1999.

3.5 Development of a Natural Laboratory for the Study of Low Frequency Shallow Water Acoustic Propagation, Reverberation and Ambient Noise (Experiment 5)

H.A. DeFerrari and H.B. Nguyen (UM), W.A. Venezia (SFTF)

Introduction:

A shallow water natural laboratory for the study of acoustic propagation and reverberation is under development. The acoustic measurements are concerned with basic scientific issues about underwater acoustic propagation over a wide range of frequencies. The studies emphasize the focusing effects of wave-guides, especially on the mid-frequencies, a topic that is not well understood. The results will be of practical interest and relevance for active sonar applications in shallow oceans.

The centerpiece of the natural laboratory is a set of three receiver arrays, two horizontal, 500 m in length, and one vertical array that is suspended in 145 m of water. A total of 96 hydrophones are processed *in-situ* and data are transmitted to shore via fiberoptics cable. The system is engineered for a ten-year lifetime and all components can be easily raised from the seafloor for servicing and repair.

The arrays will be used to receive transmissions from a moored source. An over-view of the experimental site is shown in Figure 3.5.1. The ASREX source will be moored at each of 6 ranges tentatively set at 10,20,40,60,80 and 100 km from the receiving array. The source will then transmit m-sequences at each of 6 center frequencies, 100,200,400,800,1600, and 3200 Hz. The bandwidth is 25% of the center frequencies. The transmissions will continue for 14 days, long enough to resolve diurnal components and tides. Four separate moorings, placed between source and receiver, will measure the temperature vs. depth profile at 12 depths to be used for the estimation of the sound speed profile. The bathymetry and geo-acoustic properties of the bottom and sub-bottom will be measure along a 7-km swath around the 200m contour between Miami and Palm Beach - a distance of 100 km.

The limiting factors in the performance Navy sonar are nearly always the result of the very complicated acoustic environment of shallow water. The natural laboratory approach seeks to define that environment in order to understand its influence. Surveys of the bathymetry and geo-acoustic properties of the bottom and sub-bottom, including cores, are planned. Observations of the sound speed profiles along the propagation path during the measurements will be accomplished with moored arrays of self-recording thermisters and CTD's.

At the time of this writing, an environmental impact study has been completed and approved. The study includes evaluations of the effects of acoustic transmission on marine mammals, sea turtles and human divers. For all cases, the acoustic experiments are shown to have negligible effect. A Finding of No Significant Impact (FONSI) was recently issued by NAVSEA.

Accomplishments during the past year are described in the following pages. The main thrust has been the design and fabrication and installation of the receiver arrays. The system design and installation could not have been accomplished without the close partnership with the SFTF-a group that has a unique capability for engineering and operations at sea. Also discussed are acoustic propagation model results used for planning the experiments, the anticipated scientific results and the preparation and groundwork for the rest of the experimental program.

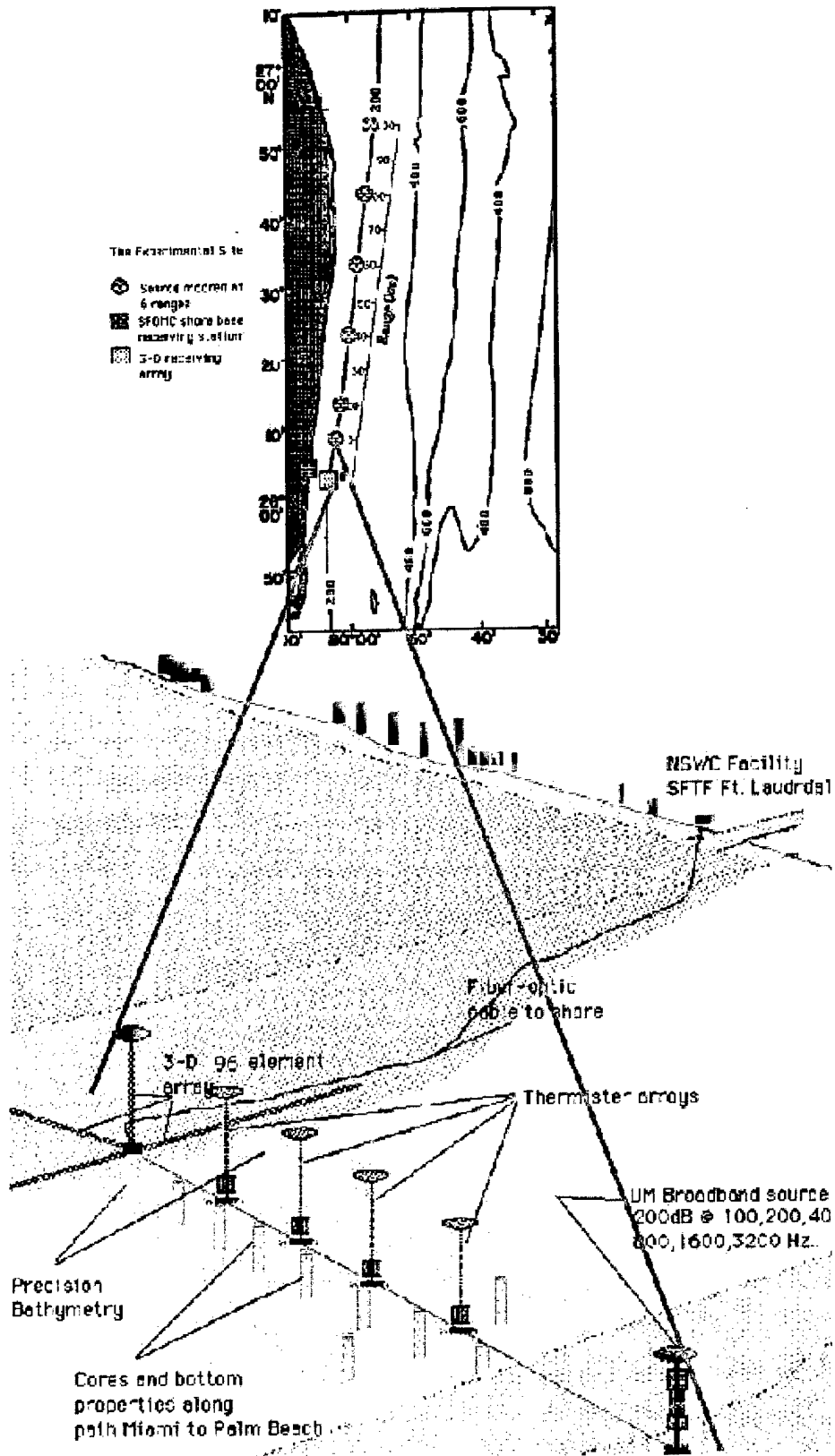


Figure 3.5.1. The SFOMC Acoustic Propagation Range

Apart from the basic research considerations, the new experimental capabilities have uses for NAVSEA codes 6.2 and 6.3 applied programs. One such project is funded and underway at present and other proposals are under consideration. The natural laboratory setting enables the transitioning of basic research findings to more applied topics.

Scientific issues

Shallow water acoustic wave-guides have complicated and irregular boundaries and sound speed fields that vary in time and space. The effects of the wave-guide on the sound field are also complicated and not well understood. Usually, real sound channels tend to randomize the sound field with increasing range of transmission and higher frequency of transmission. But in some cases the wave-guide may attenuate random fluctuations and focus the sound field and thereby accentuate coherent features of signals.

Most studies of shallow water acoustic propagation employ normal mode theory. Normal mode theory is most appropriate for low frequency or shallow channels, i.e. low depth-to-wavelength ratio, D/L , and is computationally efficient for propagation that can be described by a few modes. Such channels are of interest for the problem of passive surveillance. However, active sonar in shallow water uses much higher frequencies that can only be described by many modes – perhaps hundreds to thousands depending on frequency and bandwidth.

Modes are difficult to observe experimentally. Mode separation measurements require spatial filters, i.e. hydrophone arrays. Further, the problem may become intractable for large numbers of modes. On the other hand, “arrival patterns” or channel pulse responses are easily observed with a single hydrophone by recording the arrival time history of a broadband pulse. Generally, most of the received signal energy can be described by a small number of arrivals. The arrival pattern becomes more structured with higher D/L . In the high frequency limit, ray theoretical assumptions are valid and the arrival pattern has a simple interpretation of signals arriving along identifiable paths through the ocean determined by refraction and reflections from channel boundaries. Under such conditions propagation may be considered to be “Deep Ocean” even though the channel may be shallow in depth.

A topic of concern for this research is the D/L region in between those that can be described by a few modes or by a few rays. It is in this region that the wave-guide effects of the channel have a profound influence on the arrival pattern and on the signal coherence and predictability. This is also an area of basic research that has not been systematically studied nor is it well understood.

The shallow water acoustic wave-guide, defined by the sound speed profile, bathymetry and composition of the bottom and sub-bottom, determines the sound field by two influences. First the wave-guide sets the composition and amplitude of the individual modes and second it controls the mode combinations and sums to produce the sound field. Mode prediction is a mature subject and numerous validated normal modes are available. For lower D/L , and narrow band signals, accurate mode the interference pattern amongst a few modes is uncomplicated. But for high D/L and broadband signals, the pulse response of the channel is composed of the coherent summation of hundreds of modes. The recombination of modes produces a structured sound field. At any receiving point the structure produces an arrival pattern for a pulse transmission. A general observation is that most of the signal energy is contained in a small number of distinct arrivals. The one or two most intense arrivals are interesting since they carry

most all of the signal energy and are the only signal detectable at long ranges. Also, they appear to be more stable, coherent and predictable compared with other sound field features.

The most intense arrivals come about from focusing by the wave-guide. Many modes combine in a phase coherent and reinforcing summation. The transition between a low frequency mode interpretation and a high frequency ray field contains structures and patterns of intense sound that are predictable with full wave models. Some of these patterns have associated ray paths but there exist other phase stationary arrivals that do not have legitimate rays. Previous experiments in the Florida straits found sets of stable and persistent precursor arrivals associated with a surface duct that had no identifiable ray equivalent.

Hot spots in the sound field are formed at ray caustics. The concept of ray-mode equivalence defines such caustics and foci as "Phase Stationary" mode summations. At long ranges, when many randomizing effects are at play, caustics and foci form and decay in a random manor that is well beyond the predictive capability of existing theories and models.

Ray arrivals observed in the deep ocean are thought to be 200 times more coherent than the individual modes that comprise the ray. Likewise, we anticipate that the intense arrivals that occur in ducted transmission are much more stable and coherent than a single mode.

Model Predictions for the Planned Propagation.

The model results that follow illustrate the distribution of focused structured in the sound field and their dependence on frequency, wave-guide parameters and source-receiver geometry. An Monterrey-Miami Parabolic Equation (MMPE) model is used for the predictions and typical summer and winter sound speed profiles (Figure 3.5.2) are from archival data recorded near the experimental site during the Subtropical Atlantic Climate (STACS) program. The summer profile is downward refracting from surface to bottom and generally occurs from June through September. Summer heating extends the thermocline to the surface. After the passage of the first cold front, sometime in late October or November, a combination of upwelling, mixing from winds and cooling produces a mixed and constant temperature layer that extend to a depth of 100 m or more. This is a one-time event and after the mixed layer is formed it takes several months of heating and calm weather before the summer condition is restored. As a result, the 100 meter mixed layer is a consistent feature for about 8 months a year.

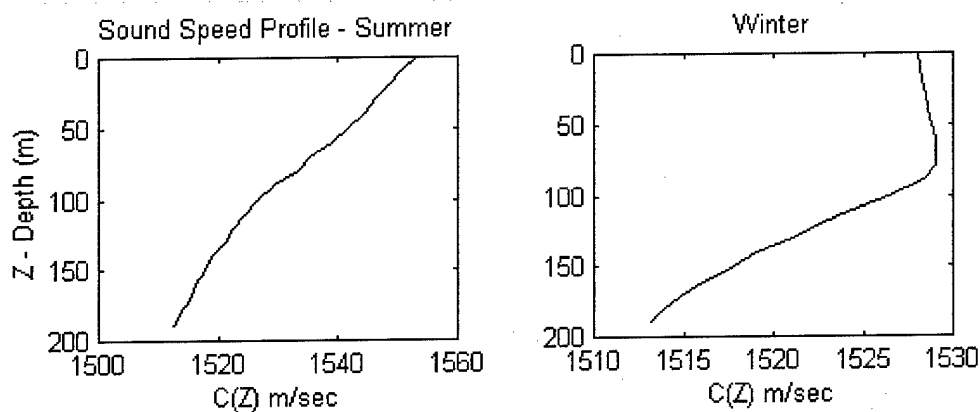


Figure 3.5.2. Summer and Winter Sound Speed Profiles

Pulse arrival structure for all signals to be transmitted during the first leg of the experiment have been predicted using a PE model. The source will be moored at a depth of 170 meters or 12 meters above the bottom.

Figures 3.5.3,a –c, Summer Profile, and 3.5.4 a-c, Winter Profile, show model predictions for the CW carrier line for the 200,400 and 800 Hz. pulse (actually m-sequence) transmissions. The display of CW sound field gives some insight about the channeling of sound and the strength of the wave-guide effects but provides only limited information about pulse arrival features along ‘eigenray” paths. Below 100 Hz the transmission is determined by a few modes and the effect of the wave-guide is minimal. The resultant sound field is readily computed as the interference of the modes and has nondescript shapes without strong focusing. For 200 Hz and above the influence of the wave-guide becomes apparent path structures and ray like features begin to form. The 800 Hz. plots reveals Refracted-Bottom Reflected (RBR) paths that bounce along the bottom. If the sound speed gradient is constant, then the height of each path apex above the bottom will be inversely proportional to the number of bottom interactions. Also, Surface –Reflected, Bottom Reflected (SRBR) paths show up for 800 Hz and higher. Lower frequencies penetrate the bottom and have large losses so that the SRBR paths are not present. The summer profile “paths” that are the result of bottom trapped modes but they extend to near the surface. The winter profile has less trapping near the bottom and surface duct trapping is faintly evident in the 800Hz plot. The duct depth is not sufficiently large to trap the 400 Hz. transmission. The only evident effect on lower frequencies is to have the sound fill the entire channel rather than being concentrated near the bottom. As will be shown this leads to a spreading of the arrival pattern.

The wave-guide determines how modes combine and sum to give an arrival pattern. Arrival patterns as a function of range are computer for broadband transmissions with a bandwidth of 25% of the center frequency (i.e. 25 Hz bandwidth for 100 Hz center frequency, 50 Hz for 200, and so on.) These signals are exactly the same as those that will be used in the experiments. Figure 3.5.5a-b, 3.5.6a-b and 3.5.7a-b are for 200,400 and 800 Hz summer (a) and winter (b) conditions. In each case, the source and receiver are placed 12 meters above the bottom in a 182-m channel. Figure 3.5.8 a-b, is for the 800 Hz transmission but with the receiver at mid depth - 100 m. Reduced time refers to a larger number for faster travel time and hence earlier arrival – that is pulses to the right arrive earlier than pulses to the left.

The 200 Hz pulses have an amorphous arrival pattern with little structure. An intense arrival ridge between 1 and 2 km range corresponds to the direct first surface reflection. The peak arrival, late in the pattern, is the sum of modes trapped at or below the depth of the source and receiver. This is for all frequencies the most intense arrival. From ray considerations the “late peak” results from a caustic formed at the depth of the transmitter. Since the source and receiver depth are at the same for these plots, the receiver always lies directly on a focus point for all pulse receptions and all ranges. The entire pulse response drops by nearly twenty dB at ranges of approximately 2,4, 6 and 8 km. This is the mode interference pattern of two principle modes that carry a large proportion of the total pulse energy. The only observable difference between summer and winter conditions a slight broadening of the overall pulse pattern.

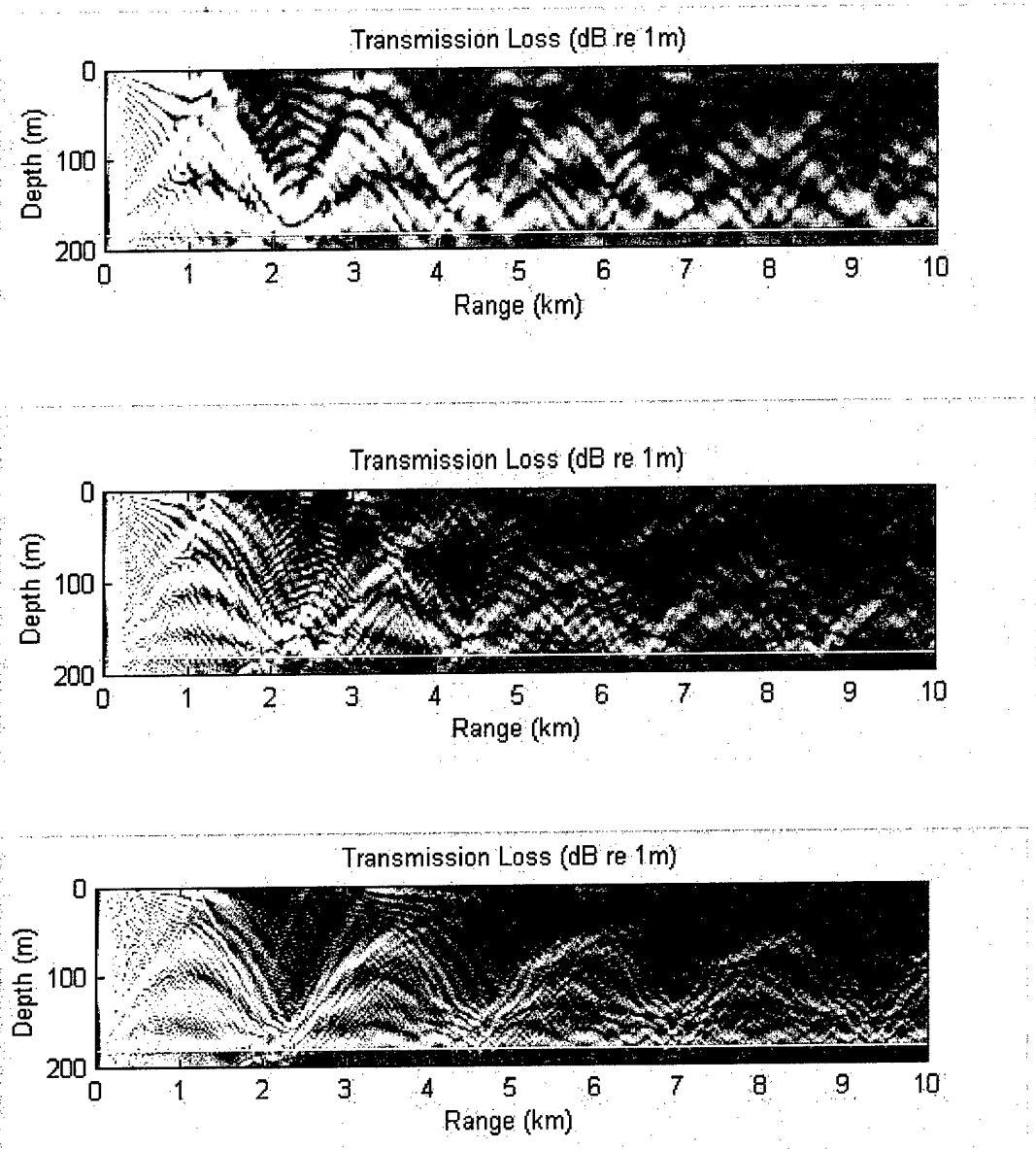


Figure 3.5.3 a-c Sound Field For Center Frequencies – Summer Profile.

- a. 200 Hz - (top)
- 3. 400 Hz - (middle)
- c. 800Hz - (bottom)

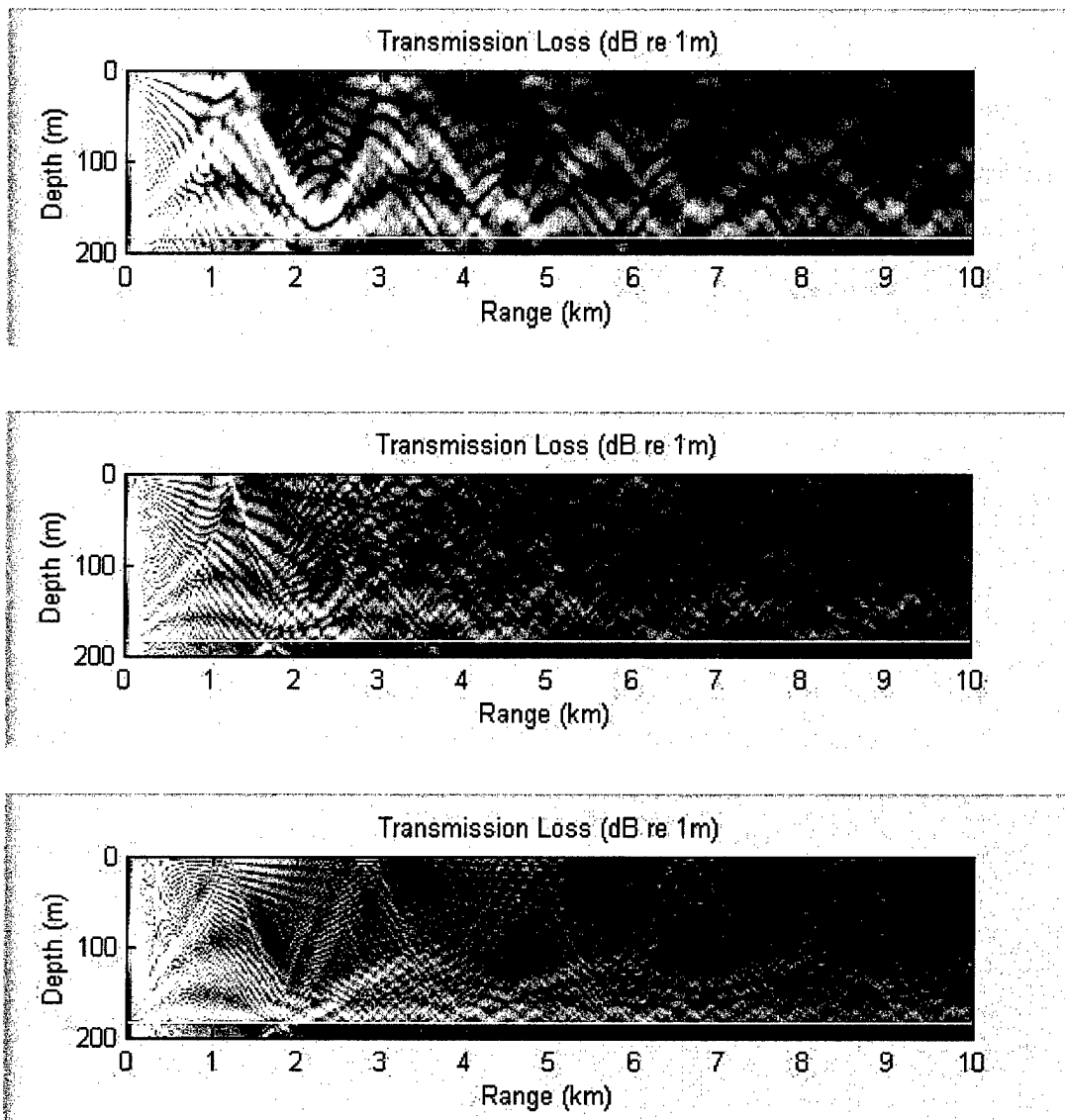


Figure 3.5.4 a-c Sound Field For Center Frequencies – Winter Profile.

- a. 200 Hz - (top)
- b. 400 Hz - (middle)
- c. 800Hz - (bottom)

As the frequency increases to 400 Hz., more of the sound is contained in the channel and the pulse response begins to show structure. Distinct and resolvable arrivals are present at all ranges. Orderly refraction patterns are resolved that can be interpreted as RBR paths. The total number of arrivals at the ten-km range is 5 for the weaker winter profile compared with 4 for the summer. The late peak is even more focused and intense, at least 20 dB higher than other arrivals. Still there is no manifestation of SRBR arrivals other than the first surface reflection paths. The 400 Hz. frequency transmissions are just barely contained within the wave-guide. Slight change in model parameters for the bottom or sub-bottom properties will produce a large effect.

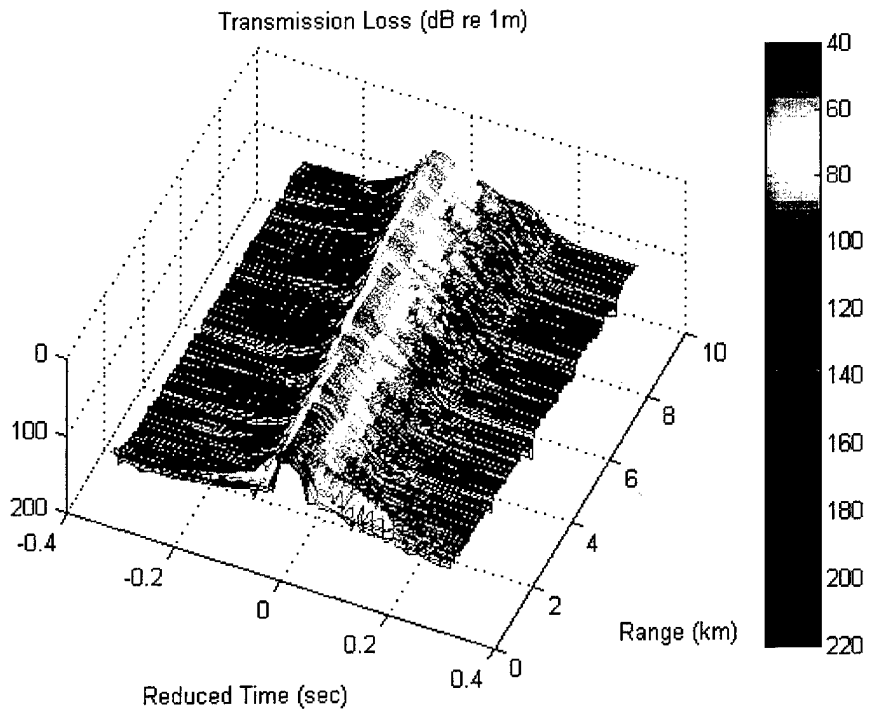
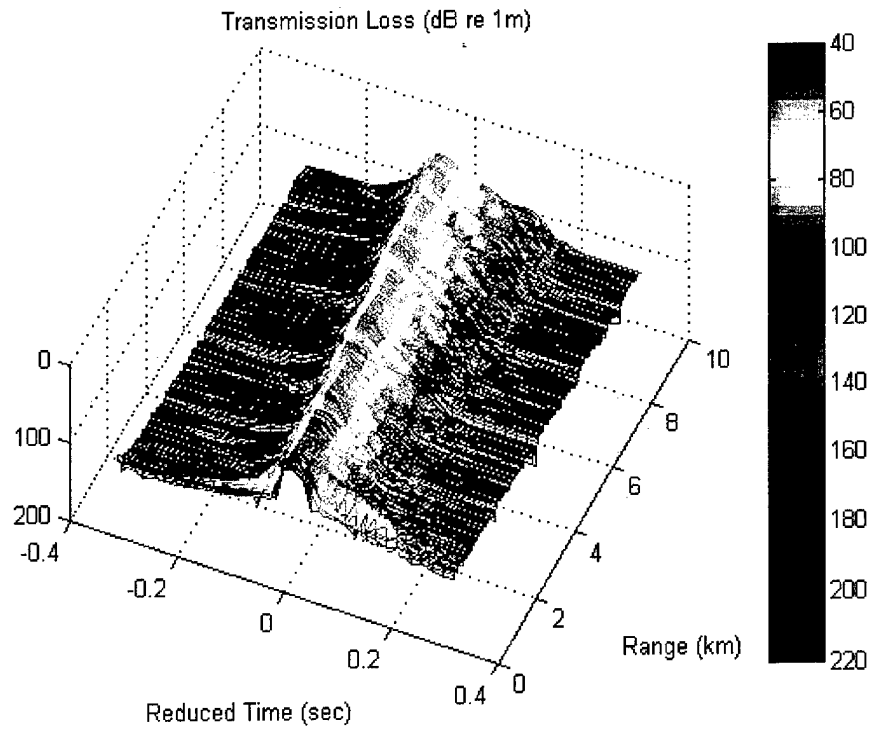


Figure 3.5.5 . Pulse Response. 200 Hz, Depth =182 m, Source 170 m, Receiver 170 m.
 Top (a) - Summer Profile --- Bottom (b) - Winter Profile

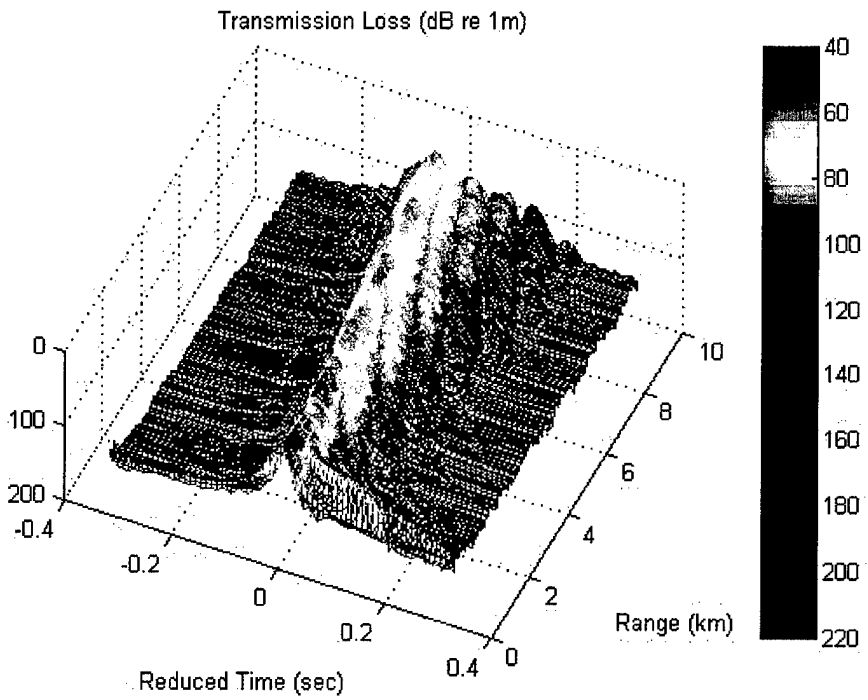
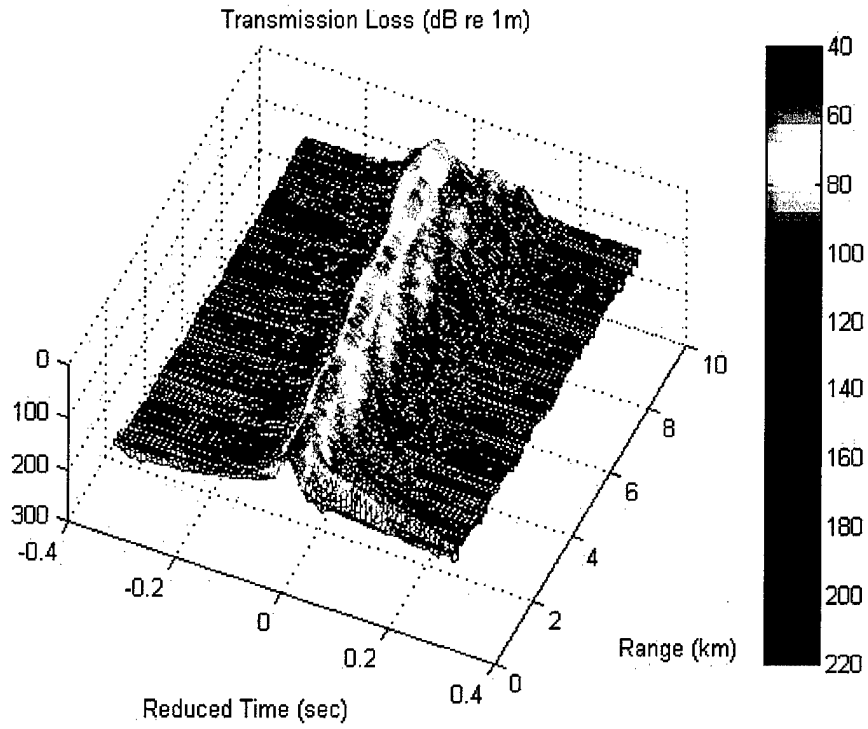


Figure 3.5.6 . Pulse Response. 400 Hz, Depth 182m, Source 170 m, Receiver 170 m

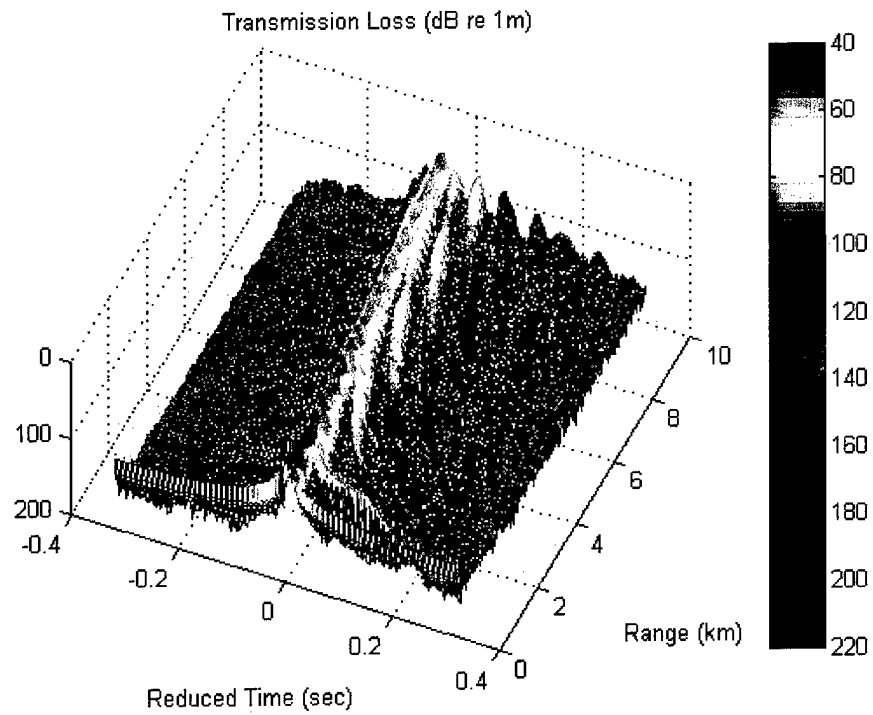
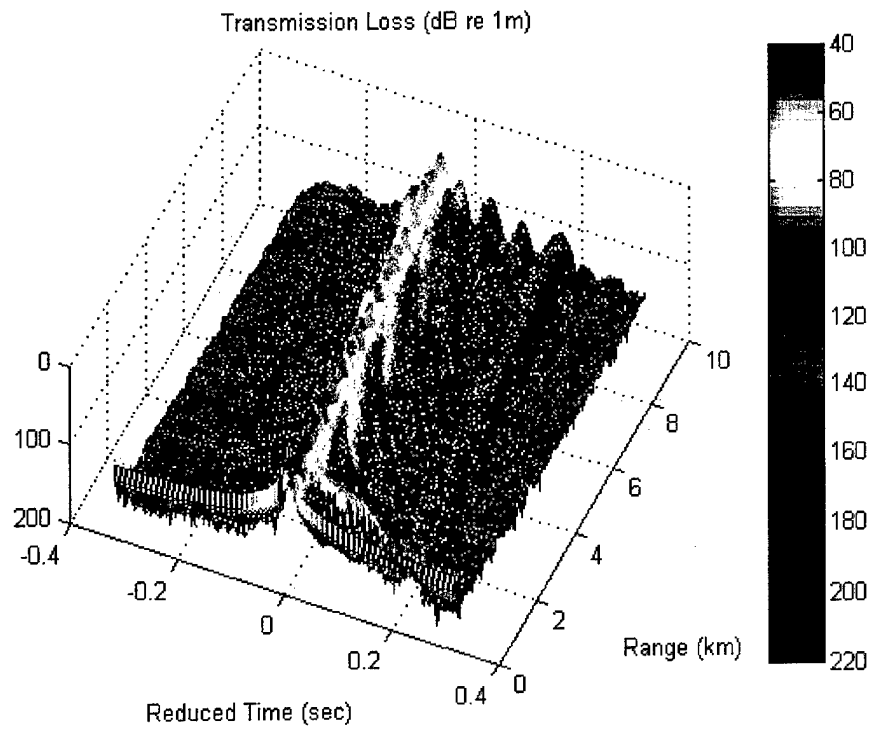


Figure 3.5.7. Pulse Response. 800 Hz, Depth 182 m, Source 170 m, Receiver 170 m
 Top (a) - Summer Profile --- Bottom (b) - Winter Profile

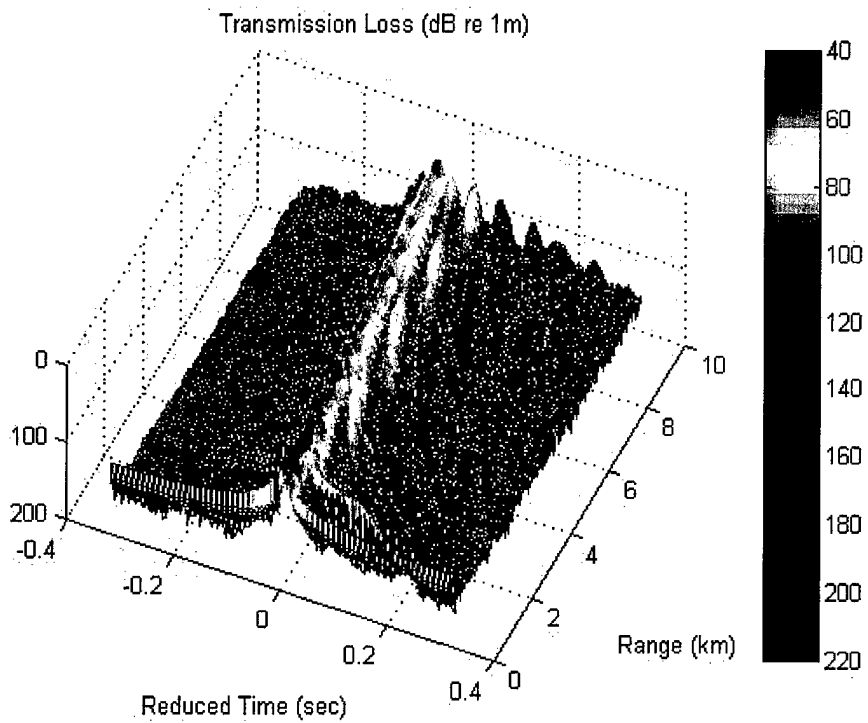
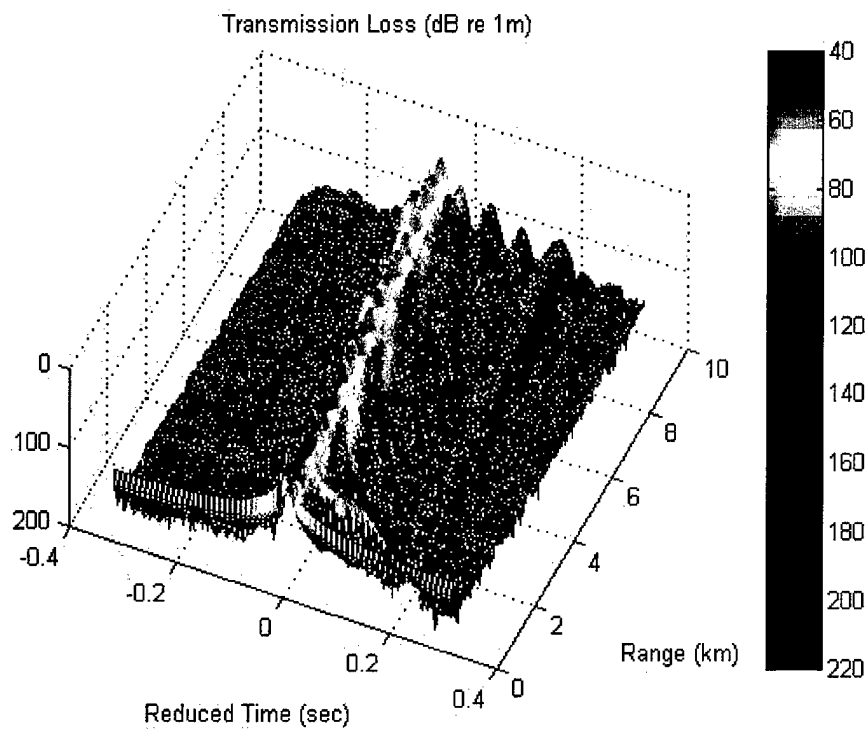


Figure 3.5.8. Pulse Response. 800 Hz, Depth 182 m, Source 170 m, Receiver 100 m
 Top (a) - Summer Profile --- Bottom (b) - Winter Profile

The 800 Hz pulses are far more distinct and structures. An early arrival, from an SRBR, path is clear at all ranges. Another “extra bounce” surface arrival is appears as a late and weak double arrival. As with the 400mHz case, there is one additional arrival for the winter profile than for the summer condition. The surface duct begins to hold the 800 Hz signal and a set of early ducted arrivals are visible. These are refracted pates that are trapped near the surface, and as a result they travel in relatively fast water and arrive early. Although they are ducted near the surface they leak and permeate the entire channel and are sensed by the deep receiver. These interesting and peculiar packets are the ‘Ducted Precursors’ studied by Monjo. As for the lower frequencies, the “late Peak is sharply focused and very intense. Also, there appears to be some periodic focusing with range for the first refracted arrival.

For all the previous examples, the source and receiver are near the bottom so that up-going and down-going arrivals are not separable. As a final example, the 800 Hz. pulse transmission is received at approximately mid-depth – 100 m. The net effect is to double the number of refracted arrivals. In fact, all arrivals are doubled and the focusing and intensity of the late peak is diminished. Clearly source/receiver geometry has influence on arrival structure and signal intensity.

Scientific Objectives and Anticipated Results

After long range transmission through the real ocean the usable level of a signal depends on the signal intensity and the signal processing gain. In turn, the gain depends on the signal coherence in space and time. Signal coherence translates into equivalent signal intensity levels of several tens of dB. Models can predict the intensity in the form of a pulse arrival pattern, as shown above. However, prediction of the coherence is orders of magnitude more difficult and well beyond capabilities of existing theories and models.

Coherence depends on physical properties of the channel parameters such as bottom irregularities and fluctuations of sound speed in the water column. But, for a given set of physical conditions, the coherency will vary with frequency and range of transmission. The coherence,

$$Coh_{r,f}(s,t) = \langle A(s,t) * A(s + \Delta s, t + \Delta t) \rangle / \sqrt{(I(s,t) * I(s + \Delta s, t + \Delta t))} \quad (1)$$

will be computed for each range and for each of the 6 center frequencies of the transmission. The variable, s, is a spatial descriptor in the x, y or z direction corresponding to the three arrays, x – along the path of propagation, y- perpendicular and z –vertical. From equation 1, a de-correlation distance and time can be estimated at each range and frequency. Combining that information with the measured transmission losses determines the obtainable signal level for coherent processing.

The approach here will be to examine the coherence and transmission loss for all of the recognizable features of the pulse response. Arrivals can be separated by time-gating of the pulse response measurements and then the coherence can be computed for the “late peak”, refracted arrivals, surface arrivals or even the “ducted precursors”. By sorting the arrivals the physical effect of the channel should be more easily understood. For example, surface ducted arrivals do not interact strongly with the bottom and may be more coherent at long ranges.

One hypothesis, to be investigated, is that the most intense arrivals will also be the most coherent. This follows from the observation that focused arrivals are usually the sum of a great many modes each contributing in a phase coherent sense. The resultant can be much more stable than the individual modes.

After the recognizable features of the pulse response are extracted for study, the coherence of the residual field can also be studied. These random like features result from forward reverberation and should have different coherence characteristics than the direct paths. Coherence of reverberation is of practical interest, since it may be possible to adaptively process to remove reverberation and become noise limited for sonar applications. Coherent processing always performs better in noise limited environments as opposed to reverberation limited backgrounds.

Results During the Past Year

The principle accomplishment during the past year has been the design, engineering and deployment of three, 32 element receiving arrays in 145m of water. They are connected to a shore station via fiber optic cable. The wet end has *in-situ* processors that are programmable from shore. Gain, filter characteristics and sampling frequency are controllable from shore. Two arrays are horizontal, 500m in length, and the third is vertical.

The Receiver Electronics

System architecture - The University of Miami underwater acoustic arrays developed as part of the South Florida Ocean Measurement Center (SFOMC) program is constructed as a local area network (LAN) of computers divided into two sub-nets. One is deployed on the bottom of the ocean in 145 m depth off Dania Beach, the other sub-net is placed on shore at the range house of the South Florida Testing Facility (SFTF). Two pairs of 12-km single mode fiber optics links the two sub-nets. (Figure 3.5.9.)

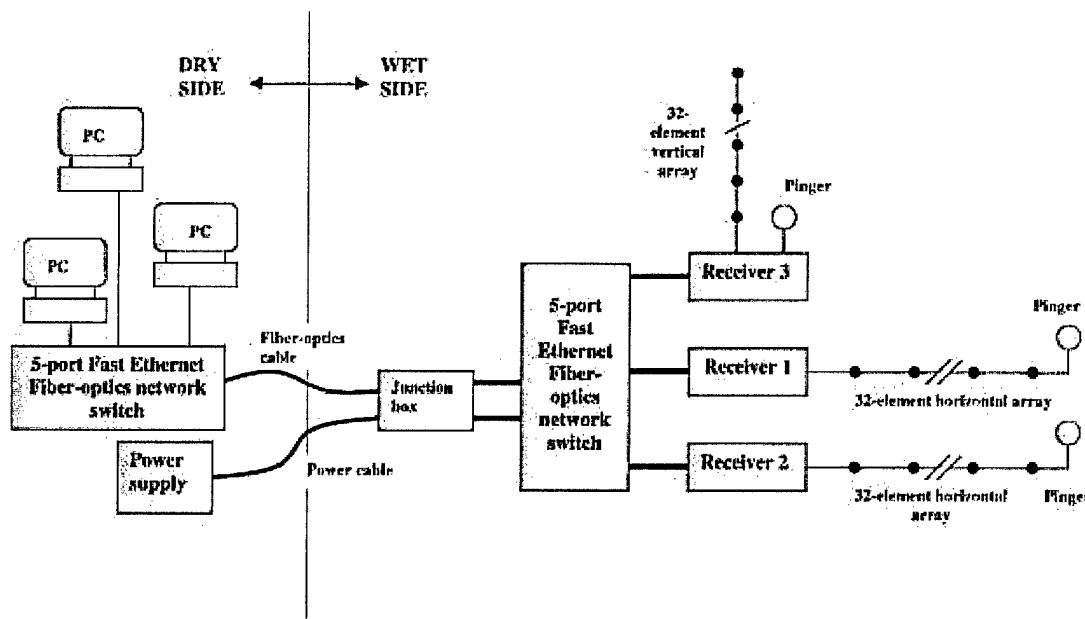


Figure 3.5.9. System block diagram

The system was designed with the following basic goals:

- The system should be flexible. Important experimental parameters should be programmable to adapt to changes in the environment and experiments goals.
- The system should be versatile to accommodate a wide range of experiments.
- The system should be as simple as possible to increase reliability and reduce system cost.
- Standard off-the-shelf components should be used wherever possible to minimize lead times and cost.

The underwater network - The underwater network consists of a network hub and three computers connected in a star configuration using single mode fiber optics cables whose main features are:

- Physical medium: 1300 nm single-mode fiber optics.
- Transmission standard: Fast Ethernet (100 Mbps).
- Transmission protocol: TCP/IP.

The network hub is a 5-port 100 Mbps dedicated active network switch designed to operate with fiber optics links longer than the 2-km limit specified by the fast ethernet standard. Its main function is to direct network traffic between the underwater computers and those of the shore side network. Two of the five ports are connected to the two pairs of fiber optics links to the shore side network. The remaining three ports are connected to three on site computers, also by fiber optics cables.

The physical connections between the network hub and the computers are made with special underwater electro-optical cables. Each is approximately 400 m long and contains three single-mode optical fibers and three conductors. Only two fiberoptic lines are needed for the data link. Two conductors carry electrical power from shore to power the entire network. The third conductor is used to carry a signal that synchronizes the operations of the acoustic receivers.

The physical connection between the network hub and shore is a bit more complicated and consists of two segments. The first segment runs from the hub to a junction box and has two 500 m long electro-optical cables. Each connects to one port of the hub. At the junction box, these two cables are spliced onto the second segment, which consists of separate power and fiber optics cables leading to shore. The power cable running from the junction box to shore also has a third conductor that is used to carry the synchronization signal.

Each of the three nodes of the underwater network is a computer designed to be an acoustic receiver. Each receiver is connected to a 32-hydrophone array. Two arrays are 500 m long and placed on the bottom, one runs eastward from its receiver, the other runs southward. The third array is a vertical array, spanning from the bottom to within 17 m of the surface. Detailed descriptions of the receivers and the arrays are given in separate sections of this report.

The shore side network - The shore side network is located at the SFTF range house where all the undersea cables are terminated. It also consists of a network hub and three computers in the usual star configuration. Two ports of the network hub connect directly to the fiber optics cables leading to the underwater network. Two computers on the network run the

Linux operating system. Each has a digital linear tape recorder (DLT) with 35 GB capacity per tape cartridge for data storage. The third computer runs Windows 95 and provides access to hardware modules inside the receivers whose software tools (assembler, linker, etc...) require Windows 95 compatibility.

Power supply - A separate three-conductor underwater cable running from the range house to the experiment site is used to provide power and synchronization signal to the underwater network. A junction box constructed by SFTF combines the fiber optics cable and power cable at the sea end and re-distributed them into two separate electro-optical cables, each cable has three conductor and three fibers (only two fibers in each cable are used). These 2 cables are approximately 500 m long and terminated with special fiber/copper connectors for plugging directly into the pressure vessel housing the network hub. The power from one of these two connector is re-distributed inside this housing to three identical bulkhead connectors. Each of these connects to a 400 m electro-optical cable leading to each receiver.

Synchronization signal - Since the timing of data packets through the network is not deterministic, that is, it can not be predicted with accuracy, a separate means of synchronizing the receivers is needed. The third copper wire in the power cable accomplishes this. A synchronizing signal generator in the range house sends a square wave to the interrupt circuit of the digital signal processors (DSP) in all receivers through the third copper wire. In this way, the sampling time of all 96 hydrophones can be synchronized. Because the synchronization signal conductor shares a common conductor with the power supply, coupling transformers are used at both ends of the cables to completely isolate the high voltage supply from the synchronization signal circuit.

The Receiver - All three receivers are identical in construction except for receiver 3 which is attached to the vertical array. This array is shorter (110 m) and has a pressure sensor at the top of the array. As shown in Figure 3.5.10, the receiver consists of three modules:

- **The CPU module.** The CPU module is a 450 MHz Pentium II single board computer (SBC) installed in a chassis with a PCI backplane to accommodate 2 additional peripheral boards: a network interface card and a SCSI controller card. The network interface card together with a fiber-optics transceiver is the physical link to the network. The SCSI controller provides high speed interface between the CPU module and the digital signal processor (DSP) module.

The system disk is a 17.2 GB hard disk where Read Hat 5.2 release of the Linux operating system is installed. It is also used to buffered data to be sent to the shore stations. Linux was chosen for the following reasons:

- High reliability.
 - Built-in network support.
 - Flexibility and robustness.
- **The digital signal processor module (DSP).** This module consists of a digital signal processor board and two 16-channel amplifier-filter-A/D boards. Signal coming from the hydrophones is amplified with selectable gain of 30 dB, 50 dB, 60 dB, or 80 dB. The amplifier has a fixed low frequency cut-off at 80 Hz with a 12 dB/octave roll off.

The high frequency cut-off is programmable from 1 kHz to 25 kHz. A 1/3 octave 6th order band pass switched capacitor filter can also be selected by the controlling program. It should be noted that the programmable gain and filter characteristics are applied uniformly across all channels. Each channel has its own dedicated analog-to-digital converter with built-in sample-and-hold circuit and up to 18-bit precision. The maximum conversion rate of the A/D converter is 200 kHz, which is much higher than necessary since the highest cut-off frequency is 25 kHz.

The DSP board controls all the amplifiers, filters and A/D functions. It also accepts digital outputs from the A/D converters, processes and transfers the results to the CPU module through the SCSI controller. The DSP board also connects to the CPU through a serial port where program code that operates the DSP is downloaded.

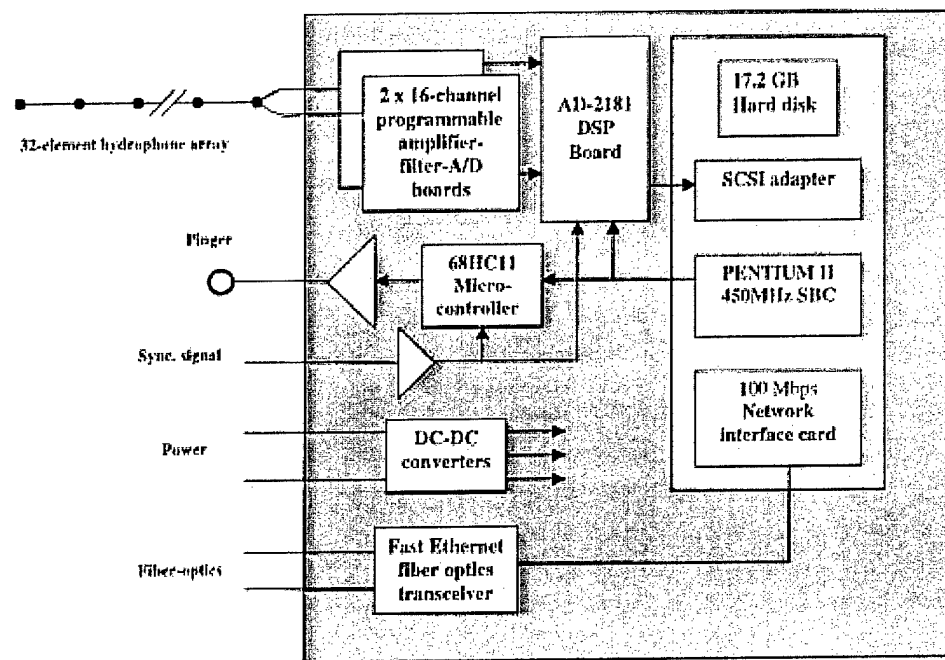


Figure 3.5.10. Receiver block diagram

The synchronization signal is wired to the interrupt circuit of the DSP, which can be programmed to respond instantly to this signal, making it possible for all receivers on the network to operate on one common time base.

- **The pinger module.** Each receiver is equipped with a low-level acoustic transducer, referred to as a “pinger”, capable of generating a programmable signal which is received by all hydrophones. Once the positions of the pingers are known, then the positions of the individual hydrophones can be determined from the timing of the received signals. An 8-bit micro-controller (Motorola 68HC11) is programmed to generate the pinger signal. This signal is amplified by a switching amplifier and applied to the pinger through a step-up transformer and an impedance matching circuit.

An experiment has been planned with the purpose of fixing the positions of the pingers using a surface boat equipped with a DGPS (Differential Global Positioning System) receiver and an acoustic receiver. By recording the pingers signals simultaneously with the positions of the boat over a long period and along different boat tracks, the pingers positions can be calculated and their accuracy evaluated.

In addition to driving the pinger, the micro-controller on receiver #3 can also record the output of a pressure sensor located at the top end of the vertical array.

Array Element Spatial Distribution

The hydrophone arrays were built to satisfy a number of design criteria. Among the most important was to space the hydrophones to allow for a large number of inter-element spatial intervals for the coherence measurements, while permitting a certain degree of redundancy to allow for failure of individual hydrophones. Nuttall presents a set of minimal redundancy intervals that optimize the number of unique inter-element intervals that can be realized with a given number of elements. Given a fundamental interval of interest, such as one wavelength at 3200 Hz, and 8 elements several optimal spatial distributions can be determined. Placement of elements at multiples of the fundamental interval equal to 0, 1, 2, 14, 18, 21, 24, 27, and 29 will yield integer separations at all distances between 0 and 29 (as well as redundant intervals at 1, 2, 3, 6, 13, and 27). This can be seen by taking differences of the various element locations, i.e. $21-18=3$, $18-14=4$, etc. Nuttall provides the source for a FORTRAN computer program to calculate the intervals in the appendix of his report. One disadvantage of Nuttall's scheme is that the loss of a single element may result in the loss of a number of intervals that that element is required for. Some of this redundancy can be added back by using multiple groupings of optimized intervals, i.e. two groups of 8 optimized elements instead of a single optimized group of 16. We have 32 elements to place in each of our 3 hydrophone arrays. They were positioned in groups of 8 elements, with inter-group intervals chosen based on a 4 element Nuttall scheme. This permitted increased redundancy while also increasing the number of possible element intervals over a linear scheme. A histogram of the element intervals for the vertical and horizontal arrays appears in Figure 3.5.11.

One other important criterion that was used in our final distribution scheme was the ability to cover a maximum aperture. The maximum aperture was limited by water depth and range location restrictions in the case of the vertical array and budgetary constraints for the horizontal arrays (i.e. cost per meter of the array electromechanical cable). (At the South Florida Testing Facility the acoustic range is just east of our vertical array location and a vertical array further east (and deeper) than our current location would hamper range operations.) Final aperture values were 105 m for the vertical arrays and 480 m for the horizontal arrays.

The coherence experiment that the arrays were designed for spans a range in frequency from 100 Hz to 3200 Hz. Wavelengths associated with these frequencies, at nominal sound speeds of 1500 m/s, range from about 0.5 m to 15 m (see Table 3.5.1). Fortunately, the frequencies were chosen at octave intervals so that element distribution optimized for higher frequencies (shorter wavelengths) could also be used for lower frequencies (higher wavelengths)-especially if the inter-group intervals are chosen with care.

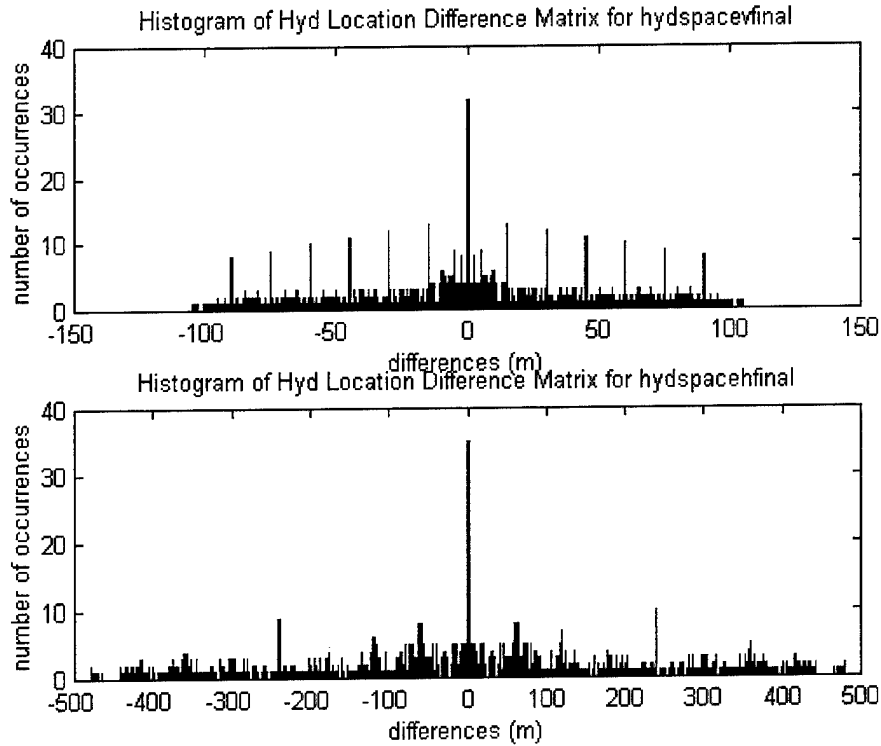


Figure 3.5.11 Histogram of hydrophone element intervals for vertical (top) and horizontal (bottom) arrays

Table 3.5.1 Frequencies and wavelengths of interest in the acoustic array design

| Frequency (Hz) | Wavelength (m) | Half wavelength (m) |
|----------------|----------------|---------------------|
| 100 | 15.00 | 7.50 |
| 200 | 7.50 | 3.75 |
| 400 | 3.75 | 1.88 |
| 800 | 1.88 | 0.94 |
| 1600 | 0.94 | 0.47 |
| 3200 | 0.47 | 0.23 |

The final element distribution for the vertical and horizontal arrays is given in Tables 3.5.2 and 3.5.3. The 3200 Hz wavelength was used as the fundamental interval for all 4 groups in the vertical array, because water depth limitations wouldn't permit use of higher frequency wavelengths. Inter-group distribution, however, uses the 100 Hz wavelength as its fundamental. An "extra" hydrophone was added at 45 m to enhance beamforming capabilities. (It is considered

“extra” because a duplication in the spacing requirements allowed one phone to serve a position in both the 8 element pattern and the inter-group pattern.) The horizontal arrays use a variety of wavelengths for the fundamental intervals in the four groups and group spacing was chosen with a 60 meter fundamental (4 x 100 Hz wavelength) primarily to increase the aperture to an affordable 480 meters.

Table 3.5.2 Vertical hydrophone array element distribution

| hyd # | multiplier | A1 position (m) | A2 position (m) | A3 position (m) | A4 position (m) | Extra hyd position (m) | Fundamental distribution freq (sub-group) | subgroup distribution (m) | hyd # |
|-------|------------|-----------------|-----------------|-----------------|-----------------|------------------------|---|---------------------------|-------|
| 1 | 0 | 0.00 | | | | | 3200 Hz | 0.00 | 1 |
| 2 | 1 | 0.47 | | | | | | 0.47 | 2 |
| 3 | 4 | 1.88 | | | | | | 1.88 | 3 |
| 4 | 9 | 4.22 | | | | | | 4.22 | 4 |
| 5 | 15 | 7.03 | | | | | | 7.03 | 5 |
| 6 | 20 | 9.38 | | | | | | 9.38 | 6 |
| 7 | 22 | 10.31 | | | | | | 10.31 | 7 |
| 8 | 32 | 15.00 | | | | | | 15.00 | 8 |
| dup | 0 | | 15.00 | | | | 3200 Hz | 0.00 | dup |
| 9 | 1 | | 15.47 | | | | | 0.47 | 9 |
| 10 | 4 | | 16.88 | | | | | 1.88 | 10 |
| 11 | 9 | | 19.22 | | | | | 4.22 | 11 |
| 12 | 15 | | 22.03 | | | | | 7.03 | 12 |
| 13 | 20 | | 24.38 | | | | | 9.38 | 13 |
| 14 | 22 | | 25.31 | | | | | 10.31 | 14 |
| 15 | 32 | | 30.00 | | | | | 15.00 | 15 |
| 16 | | | | | | 45.00 | | 30.00 | 16 |
| 17 | 0 | | | 60.00 | | | 3200 Hz | 0.00 | 17 |
| 18 | 1 | | | 60.47 | | | | 0.47 | 18 |
| 19 | 4 | | | 61.88 | | | | 1.88 | 19 |
| 20 | 9 | | | 64.22 | | | | 4.22 | 20 |
| 21 | 15 | | | 67.03 | | | | 7.03 | 21 |
| 22 | 20 | | | 69.38 | | | | 9.38 | 22 |
| 23 | 22 | | | 70.31 | | | | 10.31 | 23 |
| 24 | 32 | | | 75.00 | | | | 15.00 | 24 |
| 25 | 0 | | | | 90.00 | | 3200 Hz | 0.00 | 25 |
| 26 | 1 | | | | 90.47 | | | 0.47 | 26 |
| 27 | 4 | | | | 91.88 | | | 1.88 | 27 |
| 28 | 9 | | | | 94.22 | | | 4.22 | 28 |
| 29 | 15 | | | | 97.03 | | | 7.03 | 29 |
| 30 | 20 | | | | 99.38 | | | 9.38 | 30 |
| 31 | 22 | | | | 100.31 | | | 10.31 | 31 |
| 32 | 32 | | | | 105.00 | | | 15.00 | 32 |

Table 3.5.3 Horizontal hydrophone array element distribution

| hyd # | multiplier | A1 position (m) | A2 position (m) | A3 position (m) | A4 position (m) | Fundamental distribution freq (sub-group) | subgroup distribution (m) | hyd # |
|-------|------------|-----------------|-----------------|-----------------|-----------------|---|---------------------------|-------|
| 1 | 0 | 0.00 | | | | 3200 Hz | 0.00 | 1 |
| 2 | 1 | 0.47 | | | | | 0.47 | 2 |
| 3 | 4 | 1.88 | | | | | 1.88 | 3 |
| 4 | 9 | 4.22 | | | | | 4.22 | 4 |
| 5 | 15 | 7.03 | | | | | 7.03 | 5 |
| 6 | 20 | 9.38 | | | | | 9.38 | 6 |
| 7 | 22 | 10.31 | | | | | 10.31 | 7 |
| 8 | 32 | 15.00 | | | | | 15.00 | 8 |
| 9 | 0 | | 60.00 | | | 1600 Hz | 0.00 | 9 |
| 10 | 1 | | 60.94 | | | | 0.94 | 10 |
| 11 | 4 | | 63.75 | | | | 3.75 | 11 |
| 12 | 9 | | 68.44 | | | | 8.44 | 12 |
| 13 | 15 | | 74.06 | | | | 14.06 | 13 |
| 14 | 20 | | 78.75 | | | | 18.75 | 14 |
| 15 | 22 | | 80.63 | | | | 20.63 | 15 |
| 16 | 32 | | 90.00 | | | | 30.00 | 16 |
| 17 | 0 | | | 120.00 | | 400 Hz | 0.00 | 17 |
| 18 | 1 | | | 123.75 | | | 3.75 | 18 |
| 19 | 4 | | | 135.00 | | | 15.00 | 19 |
| 20 | 9 | | | 153.75 | | | 33.75 | 20 |
| 21 | 15 | | | 176.25 | | | 56.25 | 21 |
| 22 | 20 | | | 195.00 | | | 75.00 | 22 |
| 23 | 22 | | | 202.50 | | | 82.50 | 23 |
| 24 | 32 | | | 240.00 | | | 120.00 | 24 |
| 25 | 0 | | | | 360.00 | 400 Hz | 0.00 | 25 |
| 26 | 1 | | | | 363.75 | | 3.75 | 26 |
| 27 | 4 | | | | 375.00 | | 15.00 | 27 |
| 28 | 9 | | | | 393.75 | | 33.75 | 28 |
| 29 | 15 | | | | 416.25 | | 56.25 | 29 |
| 30 | 20 | | | | 435.00 | | 75.00 | 30 |
| 31 | 22 | | | | 442.50 | | 82.50 | 31 |
| 32 | 32 | | | | 480.00 | | 120.00 | 32 |
| | | | | | | | | |

Ocean Engineering and Installation at Sea

NSWC has a well established capability at the SFTF to install and maintain instruments on the ocean seafloor. The proven technique combines dynamic positioning of a surface support vessel with the tethered remote sled called “TONGS” (Television Observed Nautical Grappling System). Since the mid 1960s, the SFTF has maintained the ability to pluck the end of a marine cable from the ocean floor, attach an instrument and then place the instrument package at a precise location back on the ocean floor – usually within a one or two day period. With this capability it becomes possible to maintain and service instruments indefinitely. The equipment to be installed is shown in the schematic of Figure 3.5.12.

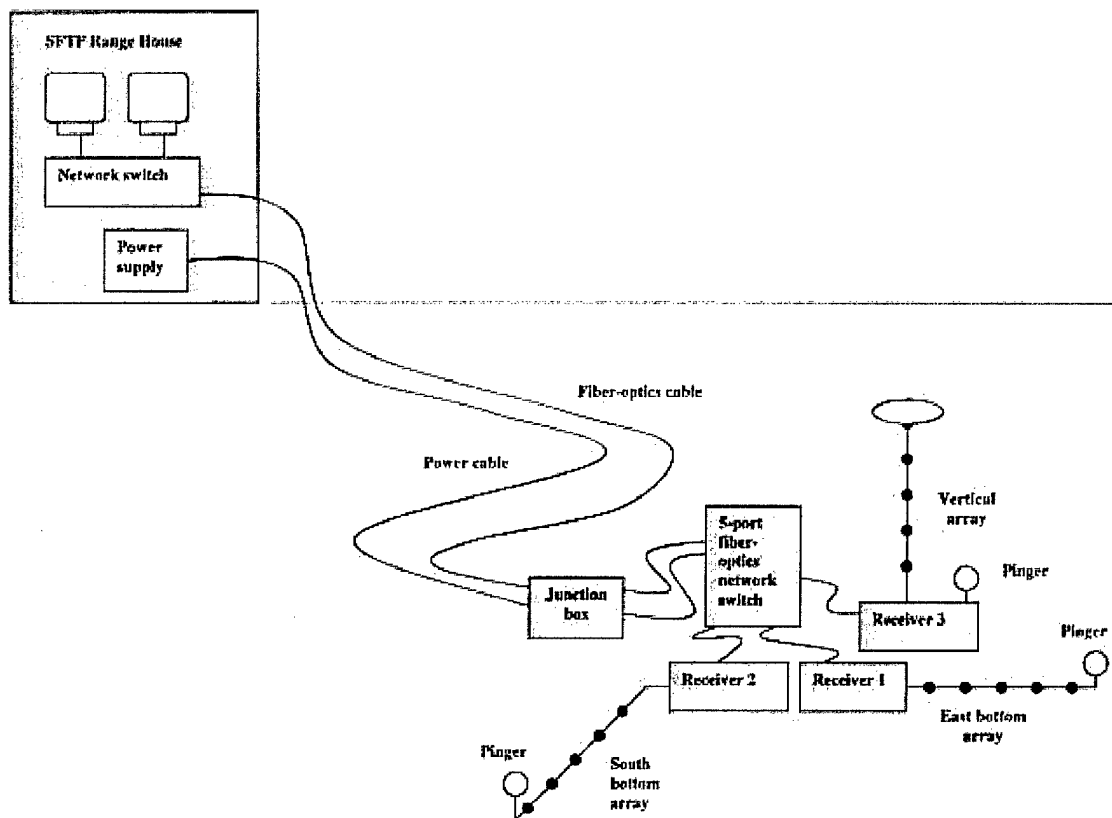


Figure 3.5.12 University of Miami Acoustic Arrays at South Florida Ocean Measurements Center.

The R/V Seward Johnson was used for the first time on the range for installation of the acoustic arrays. The dynamic positioning system and deck equipment proved well suited for the operation. The ship’s position was measured with a local DGPS and was resolvable to within 1m. After some preliminary preparations to recondition an existing fiber optic cable the acoustic multiplexer was connected and placed on the bottom. This operation required that the R/V Seward Johnston hold position within a few meters for a continuous period of three days. During most of the time, the end of the fiber optic cable was attached to the deck.

The center hub of the wet end instrumentation is shown in Figure 3.5.13. The shore cable is connected to the main multiplexer located in the center of the frame, Figure 3.5.14. The three

baskets hold coiled fiber optic cables that connect each of the three array receivers to the main multiplexer. After the entire package is placed on the ocean floor, the cables in the baskets are extracted and paid out loosely on the bottom. Then, in turn, each of the three cable ends is picked up and brought to the surface to be connected to one of the array receivers.



Figure 3.5.13 The Multiplexer Bail with Receiver Cable Baskets

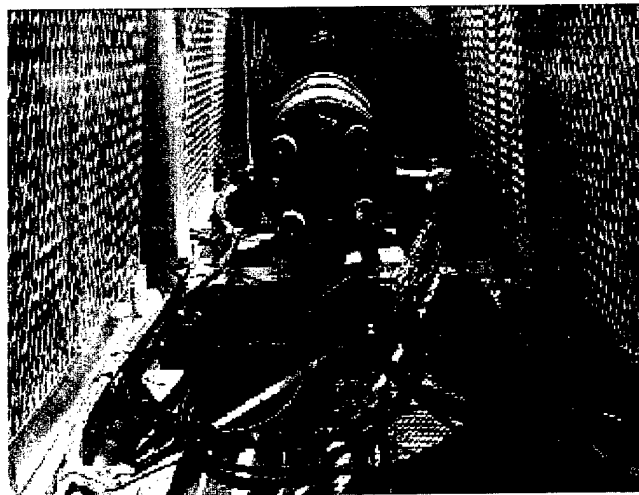


Figure 3.5.14 The Multiplexer Pressure Housing

Figure 3.5.15 Array Receivers. Each of the three umbilicals connects to a receiver and as does one of the hydrophone arrays. The other end of the array is attached to a pick-up bail as shown in Figure 3.5.16. One of three pingers is located on each pick-up bail the pingers are used to measure the position of hydrophones in the arrays. The pick-up bail serves to anchor the array end and as an attachment point for retrieving the array and receiver for maintenance.

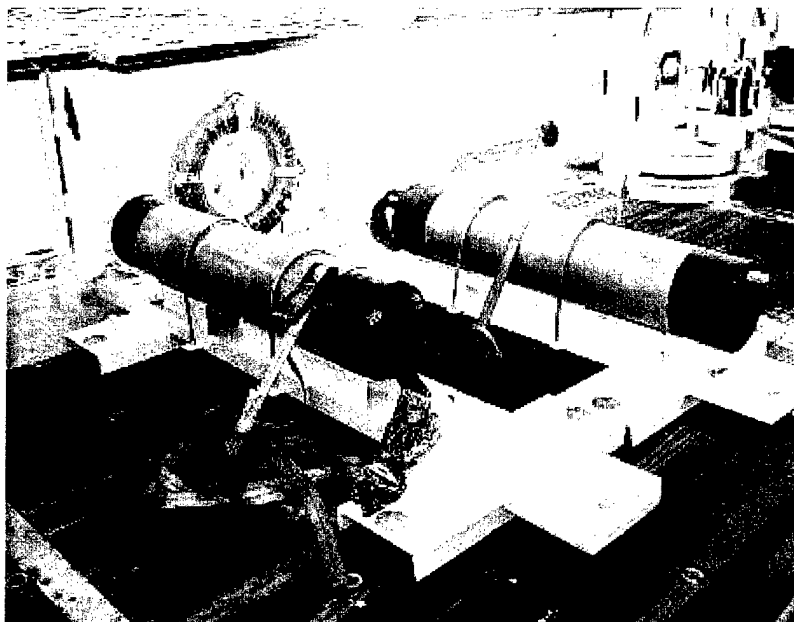


Figure 3.5.15 Receiver Pressure Housings.

The vertical array is deployed with the same procedure. A cable to the multiplexer is brought to the surface and connected to the vertical array receiver and anchor, Figure 3.5.17. The flotation and the array are paid out from the deck and then the anchor is lowered to the bottom.

At the time of this writing all three arrays are in position on the ocean floor. The central multiplexer and two of the arrays are working as designed. The third array-, horizontal, west to east, is not responding to shore commands and must be retrieved and repaired or replaced. A back-up receiver system is ready. The schedule for the R/V Seward Johnson is full and, at present, and we await a two day window to complete the repairs.

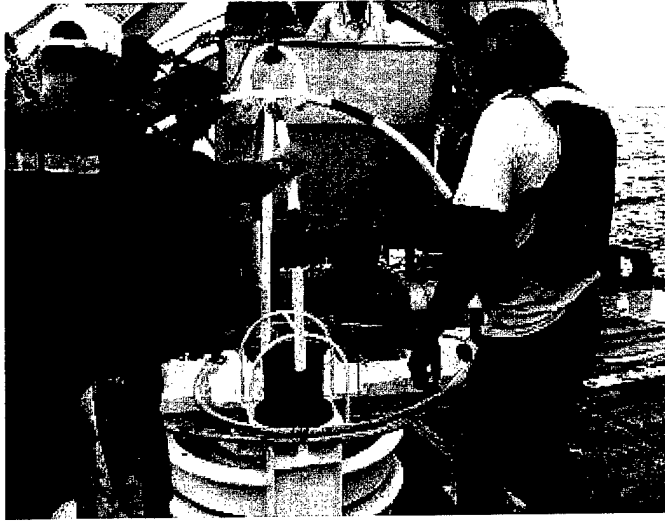


Figure 3.5.16. Pick-up Bail for the End of Bottom Arrays



Figure 3.5.17. Vertical Array Deployment

3.6 Bio/Geological Inventory and Assessment (Experiment 6)

Drs. Richard Dodge, David Gilliam, Richard Spieler, and Charles Messing

3.6.1 Introduction

Nova Southeastern University Oceanographic Center (NSUOC) is developing a shallow water biodiversity inventory, performing associated biogeological assessments, and planning a monitoring program of range environmental assets for the SFTF range. For this specific offshore area, it is important that biogeological stewardship be maintained. This requires a biogeological baseline be accomplished for many reasons:

1) The Navy, as owner of the SFTF range, should have a complete and accurate catalogue of biological and geological characteristics and parameters to enhance its role of environmental stewardship.

2) The availability of such data will preclude the need for collecting fresh data for each project, thereby making use of the SFOMC more cost efficient.

3) Historical biogeological data will serve as benchmarks against which new data (either physical or biogeological) may be examined for change, proof of consistency, and the like.

4) Existing and developing AUV operations and technology provides an opportunity to gather (and develop new gathering methods for obtaining) biogeological data in a cost-effective and innovative fashion, in some cases extending currently available assessment methodologies.

3.6.2. Environmental (Biological/Geological) Goals

The goals of this project were purposed to be:

1) Develop an environmental (biological and geological) map of a portion of the shallow water SFTF range.

2) Develop a monitoring plan for biogeological range resources.

3) Conduct preliminary experiments to gauge the potential for the use of AUV's in quantitative coral reef assessment.

These goals are compatible with overall SFOMC project goals in that they will document aspects of range biology, geology, and ecology for environmental stewardship of the range and will investigate AUV usage for biogeological assessment.

To accomplish these initial goals, NSU OC identified several associated tasks.

1) Baseline for Environmental Stewardship: Relevant biology and geology of a portion of the range shallow water (in less than 100' depth) environments, including coral community hardgrounds (reefs), and sand plains will be mapped. Mapping methods include the use of air photographs, scientific literature, and *in situ* diving for ground-truthing. More detailed biological characterization involve ecological parameter data collections of certain organisms or organism groups including fish, stony corals, soft corals, sponges, macroalgae, other epi- and infaunal invertebrates.

A standard bathymetric chart of the range will serve with air photographs as the basemap for overlaying the results of biological and geological inventories, assessments, and for monitoring planning. Bathymetry of all or a portion of the range is anticipated in 2000 as a data product from US Navy participation. Bathymetry will be integrated as possible into a GIS data base. (The range area of interest for this study is that area, or a smaller subset, bounded approximately between the Port Everglades jetty to the north and Dania Pier to the south and from shore to depths of less than 100'.)

2) A long-term biological monitoring plan is being developed, utilizing the information generated from our mapping and investigations. The monitoring will include consideration of integrating biologic assessment over time with the physical data collection obtained by the remote sensors of the range.

3) A study in conjunction with FAU will be initiated to evaluate the potential for AUV's to collect data relevant for rapid reef assessment.

3.6.3. Project Tasks

This is a progress report of accomplishments made during the first year of work.

3.6.3.1. Baseline for Environmental Stewardship

3.6.3.1.1 Overview of the Shallow Water Habitats within the Range

The seafloor within the range exhibits two major habitats: hard bottom and unconsolidated sediment. Hard bottom habitats consist chiefly of three narrow limestone reefs that run parallel to the coast and support assemblages dominated among invertebrates by sponges (Demospongiae), hard corals (Scleractinia) and soft corals (Alcyonaria), plus a variety of macroalgae. The three habitats are generally referred to, with increasing depth and distance from shore, as the first (4-8 m depth, about 2,000 ft from shore), second (7-18 m, 4,500 ft) and third reefs (+12 m, 8,000 ft) (Raymond 1972, Lighty *et al.* 1978 and unpublished NSU OC staff observations). An additional hard bottom community, which may be a part of the second reef, exists between the second and third reefs and slopes from 45 to 65 ft deep and is generally 6,000 ft offshore (unpublished NSU OC staff observations). The three reefs are actually relict Holocene reefs. According to Lighty (1977), at least the outermost of these has not actively accreted for about 6000 years. Actively growing hard corals generally account for no more than 7% of cover (Raymond & Antonius 1977, Dodge *et al.* 1991), and the habitats are often referred to as coral communities or hardground assemblages rather than coral reefs. The low coral cover and lack of active reef accretion underscore the location of the inventory site 1) north of the northernmost inshore actively accreting coral reef on the eastern U.S. continental shelf (Fowey Light, about 16 km southeast of Miami) (Marszalek *et al.* 1977, Jaap 1984, Voss 1988) and 2) within a segment of coastline (Monroe to Palm Beach County) characterized by significant decreases in richness and abundance of corals and associated organisms (Goldberg 1973, Marszalek 1981).

Additional hard substrates may occur immediately adjacent to the shoreline (<50 m) in the form of hard sand mounds accreted by the sabellariid polychaete worm, *Phragmatopoma lapidosa*. Such worm mounds have not yet been reported within the area covered by this

inventory, but do occur within 2.5 km of the southern boundary. Organisms such as littorinid and neritid gastropod mollusks, normally found on intertidal hard substrates (e.g., rocks lining the Port Everglades Inlet) have not been included in the macroinvertebrate inventory.

Unconsolidated sediments, or soft bottoms, found from the shoreline to the first reef and between successive hard bottoms consist of mixed silica and skeletal carbonate sands (Raymond 1972). They support diverse assemblages of chiefly infaunal invertebrates dominated by polychaete worms, peracarid crustaceans and bivalve mollusks.

3.6.3.1.2 Macroinvertebrate Inventory

3.6.3.1.2.1 Introduction

The accompanying dataset (Appendix Table A3.6.3.1) represents a preliminary inventory of benthic (bottom-dwelling) macroinvertebrates found within the shallow part of the SFOMC range from the shoreline to 2.4 km offshore at a depth of approximately 23 m, and from the Port Everglades Inlet south jetty to the Dania Fishing Pier, an area of approximately 13.6 km². The dataset represents a compilation of all data currently available for the area and is based chiefly on information collected during two beach renourishment assessments—John U. Lloyd State Recreation Area (1989-1990) (Dodge *et al.* 1991) and Hollywood/Hallandale (1990-2, 1994) (Dodge *et al.* 1995)—plus additional data collected for this compilation in 1998 and 1999.

3.6.3.1.2.2 Methods

3.6.3.1.2.2.1 Sites

During the John U. Lloyd and Hollywood/Hallandale beach renourishment projects, fifteen hard bottom sites and fourteen soft bottom sites were selected for detailed biological assessment of benthic communities. Five first reef sites were located in 3-6 m depth; five second reef sites in 9-15 m, and five third reef sites in 14-23 m. Ten soft bottom sites were chosen approximately 90 m seaward of the then current shoreline in depths of about 2.4 m (8 ft). Four additional sites were chosen between the second and third reefs in approximately 18 m (Dodge *et al.* 1991, 1995).

Of these sites, six hard bottom and six soft bottom fall within the boundaries of the area treated in this inventory. However, because of the close proximity and similar environmental conditions of the other sites relative to the study area, species recorded only at sites outside the range have also been included, but are noted as such in Appendix Table A3.6.3.1.

Additional general collection and survey dives were made randomly within the range during 1998 and 1999. Species recorded during these dives are also distinguished in the inventory table.

3.6.3.1.2.2.2 Belt Quadrat Transects

Following an initial cross-section survey of each site with a recording fathometer, a 4m² weighted PVC frame was deployed over the side of the survey vessel at the crest of the reef in the survey area. Metal stakes (rebar) were driven into the reef to define 2 x 2-m quadrats and 20-m transects along the reef surface. Transects were oriented in an approximate north-south direction. One corner stake of the 2 x 2-m quadrat served as the initial stake of each transect. Another stake was placed at 10 m and a final stake at 20 m and a tape measure, graduated in centimeters (cm), was secured between the stakes. Scleractinian corals (plus *Millepora* spp. hydrozoan fire corals) were inventoried along each transect by counting and identifying all colonies larger than 1 cm

within a 0.75 m² quadrat placed sequentially along first one side and then the opposing side of the 20 m transect line, so inspecting a total area of 30 m² per transect.

3.6.3.1.2.2.3 Quadrats

At each of the 15 quadrat stations, the four metal stakes described above defined the corners of each 2 x 2 m quadrat. SCUBA divers tied a length of yellow polypropylene line around the stakes to define the quadrat perimeter. Macroepibenthic organisms were identified and counted *in situ*. When specific identifications could not be made, samples of the same organisms from outside the quadrat were collected, transferred to plastic bags, preserved in 70% ethanol or fixed in 10% borate-buffered formalin, and transported to the laboratory for subsequent identification.

3.6.3.1.2.2.4 Cores

On unconsolidated bottoms, divers using a cylindrical hand-held coring apparatus 8-cm across and 14-cm deep collected sediment samples containing infauna. Each station at which infauna was sampled consisted of 15 replicate cores for the Hollywood/Hallandale project and 18 for the John U. Lloyd project (Dodge *et al.* 1991 1995). Each sediment sample was transferred underwater to a plastic bag and fixed on deck in 10% borate-buffered formalin containing Rose Bengal. In the laboratory, each core sample was washed separately with seawater through a 0.5-mm mesh Nalgene screen. Organisms and sediment retained on the screen were decanted into 70% ethanol and stored in glass jars for sorting. Organisms were sorted initially to phylum or general morphological form (e.g., Mollusca, Crustacea, "worm", "other") and subsequently to lowest recognizably distinct taxa. Only organisms apparently alive at the time of collection were counted (i.e., dead bryozoan colonies and mollusk shells were not considered). Nova Southeastern University staff and various taxonomic specialists undertook specimen identifications.

The term macroinvertebrate refers herein to invertebrates retained on the 0.5-mm mesh screen with the omission of nematodes and harpacticoid copepods. Although some specimens of each of these two groups were collected, they are normally treated as components of the meiofauna and have not been included in this inventory. None were identified.

3.6.3.1.2.2.5 Survey dives

Both beach renourishment projects mandated that sampling on hard-bottom assemblages quantitatively assess sessile macroinvertebrates within narrowly drawn quadrats and transects. Survey dives thus attempted to add qualitatively to the inventory any additional sessile macroinvertebrates and all vagile (mobile) benthic macroinvertebrates as well. Species were either identified *in situ* or specimens were collected by hand and brought to the laboratory for identification by Nova Southeastern University staff and various taxonomic specialists.

3.6.3.1.2.3 Results

The macroinvertebrate inventory list currently includes 708 species with the taxonomic groups to which they belong (Appendix Table A3.6.3.1). Species are distinguished by major habitat and general location. "Reef" refers to species found on the first through third reefs. For species collected on unconsolidated sediments, "inshore" refers to samples taken about 90 m from the shoreline in about 2.4 m depth. "Offshore" refers to samples taken between the second and third

reef terraces in about 18 m. Species recorded during renourishment monitoring projects are indicated with an X in Appendix Table A3.6.3.1 if collected within the SFTF range boundaries treated herein, with an H if recorded only to the south off Hollywood Beach, and by an O if found within the range area on subsequent survey dives. Designations followed by an asterisk indicate species found on inshore hardgrounds. As noted above, species recorded off Hollywood Beach have been included in the range inventory because of the combination of close proximity and similar environments relative to the range.

The most diverse groups on hard bottoms are sponges (39 species), alcyonarians (soft corals) (25) and scleractinians (hard corals) (28). The most diverse groups on unconsolidated bottoms are polychaete worms (235 species), peracarid crustaceans (amphipods, isopods, tanaids, cumaceans and mysids) (80), bivalve mollusks (46), gastropod mollusks (38), nemertine worms (31), oligochaete worms (25) and decapod crustaceans (23). These numbers refer only to those species found in the specified habitat. Members of any group may also be found on either major habitat. For example, the chiefly reef-dwelling Scleractinia includes the solitary *Sphenotrochus* sp., which occurs on sand bottoms. Bivalves and polychaete worms, though most diverse on unconsolidated bottoms, include families characteristic of hard bottoms (e.g., arcid and pteriid bivalves, serpulid polychaetes).

In order to gauge variability among reefs, mean numbers of individual sponges, gorgonians, and scleractinians in the quadrates were graphed and are presented in Figure 3.6.3.1. It is apparent from these data that there was high variability among sites. Number of sponge individuals are highest on the third reef, intermediate on the second reef, and lowest on the first reef. For gorgonians, numbers are highest on the first reef. These are all small individuals, probably relatively ephemeral. For scleractinians, numbers per 2 m² quadrat are roughly evenly distributed among reefs with high variability.

As noted above, this inventory represents a preliminary effort. The narrow quantitative focus of sampling methodologies employed during the beach renourishment assessments omitted or severely limited recovery of several macrofaunal components. Hard bottom assessment focussed on sessile macrofauna. As a result, the vagile fauna of these communities has been greatly undersampled so far. A substantial diversity of decapod crustaceans (notably caridean shrimps, hermit crabs and allies, and brachyuran crabs), gastropod mollusks, peracarid crustaceans, polychaete worms, hydrozoans and bryozoans remains to be inventoried. Thorough recording of these faunal elements will require additional collecting using different methodologies such as night diving, trapping and deployment and recovery of three-dimensional settlement panel arrays. Similarly, the core sampling of unconsolidated sediment habitats in the previous projects omitted or severely limited recovery of large or deeply burrowing taxa. Current understanding of regional faunas suggest that, in particular, a substantial diversity of sediment-dwelling gastropod and bivalve mollusks remains to be inventoried within the SFTF range (Abbott 1974). These faunal components can be recovered via night diving, trawling, and examination of fresh shoreline storm deposits.

3.6.3.1.3 Fish Inventory

3.6.3.1.3.1 Introduction

This survey characterized the reef fishes within the SFTF range in water from 3 to 30 m along a 5 nautical mile section of the coastline extending south from Port Everglades inlet (N 26° 5.50' to N 26° 0.50'). Width of the survey area was determined by the westernmost edge of the first reef (closest to shore) to the easternmost edge of the third reef; this distance varies but is about one nautical mile. The dataset presented (Appendix Table A3.6.3.2) will be part of a larger dataset sponsored by the National Marine Fisheries Service to characterize the reef and reef-associated fishes of Broward County.

3.6.3.1.3.2 Methods

The survey consisted of a non-destructive, visual census using the stationary visual census technique of Bohnsack and Bannerot (1986). This method has been statistically verified and is in wide use nationally and internationally on coral reefs. In brief, the technique is a stationary point count of fishes in a 15 m diameter cylinder. A diver, using SCUBA and at a selected point on, or directly above, the substrate, recorded all fish species identified within a 7.5 m radius around the point during a 5 min period. After the 5 min species-count was completed, the number of fish per species and the minimum, maximum and mean total length of each species was also

recorded along with depth and bottom features of the census station. The diver carried a 1 m PVC rod with a ruler attached at one end of the rod in a T-configuration to aid in fish length estimation. Fish total length estimates allowed for post-census calculation of fish biomass using

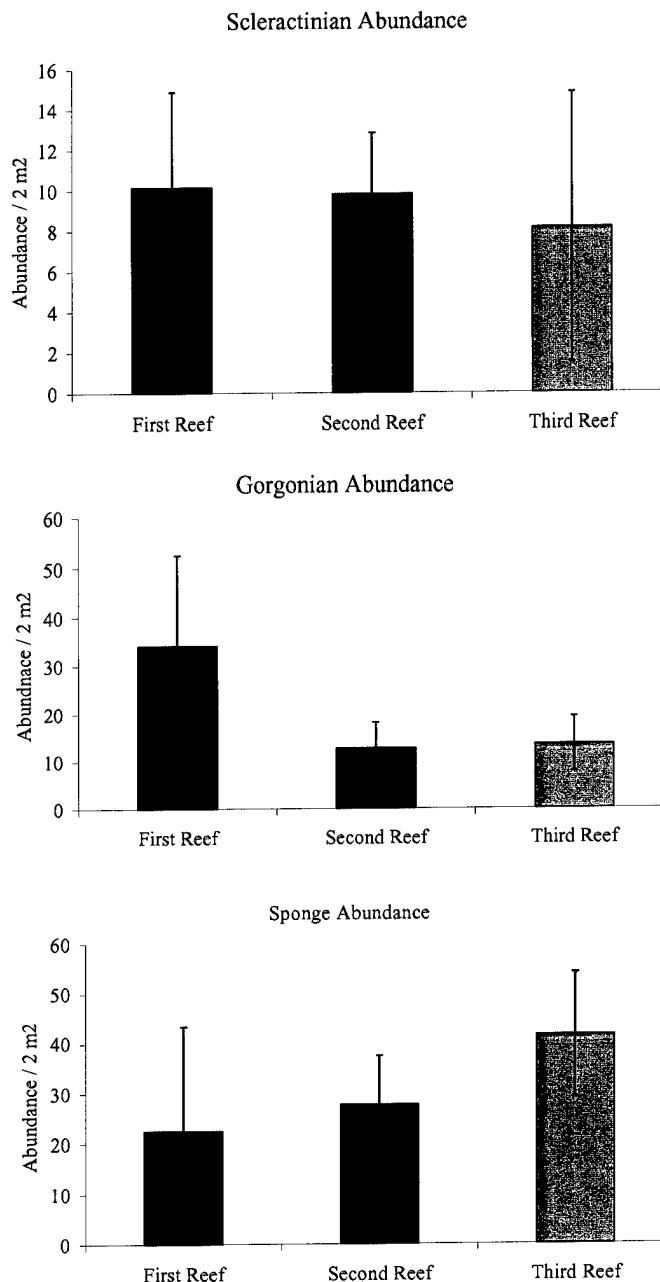


Figure 3.6.3.1: Scleractinian, gorgonian, and sponge abundance (mean \pm 1 SE) for each of the three reefs within the range.

length-weight equations published by Bohnsack and Harper (1988). When a length-weight equation for an identified species was not available, the equation for a congeneric was used.

The census stations (180 total) were arranged in a grid pattern: a series of nine stations on an east-west line (determined by DGPS) were done every 0.25 nautical mile of the coastline. Each series of nine stations was divided into three per reef, one station at the easternmost edge, one at the westernmost edge and one at the crest of each reef. The sites were selected by motoring west to east on the correct line of latitude and determining the western and eastern edges of a reef tract with a paper-recording, depth sounder. These edges were buoyed and a third buoy was deployed at the shallowest depth between the two edges. With the exception of five stations which inadvertently were censused two (or in one case three) times, each station was censused once. Data were analyzed with non-parametric analysis of variance techniques using Statistical Analysis Systems (SAS) software (PROC GLM of ranked data \approx Kruskal-Wallis k-sample test, and a Student-Newman-Keuls test between means).

3.6.3.1.3.3 Results

Fish censuses were completed between August of 1998 through May 1999. One-hundred and eighty-one sites were surveyed. Three sites on the third reef were not sampled because of an apparent break in the reef tract and an additional third reef site was inadvertently missed. Five locations on one latitude transect were repeated. However, the DGPS coordinates of the repeated counts differ and therefore the counts were included as separate sites for statistical analysis. A total of 16,746 fish of 139 species (Appendix 3.6 Table A3.6.3.2) were recorded during the quantitative survey. An additional 22 species were identified within the range for a total of 161 species. There were significantly fewer total fish ($p < 0.001$) and fewer species ($p < 0.001$) on the first reef than either on the second or third reefs, which did not differ ($p > 0.05$) (Figure 3.6.3.2 and Appendix 3.6 Table 3.6.3.2). There was also a differences amongst the positions on a reef with the three reef tracts combined. The eastern edge had significantly fewer total fish ($p < 0.001$) than the center and

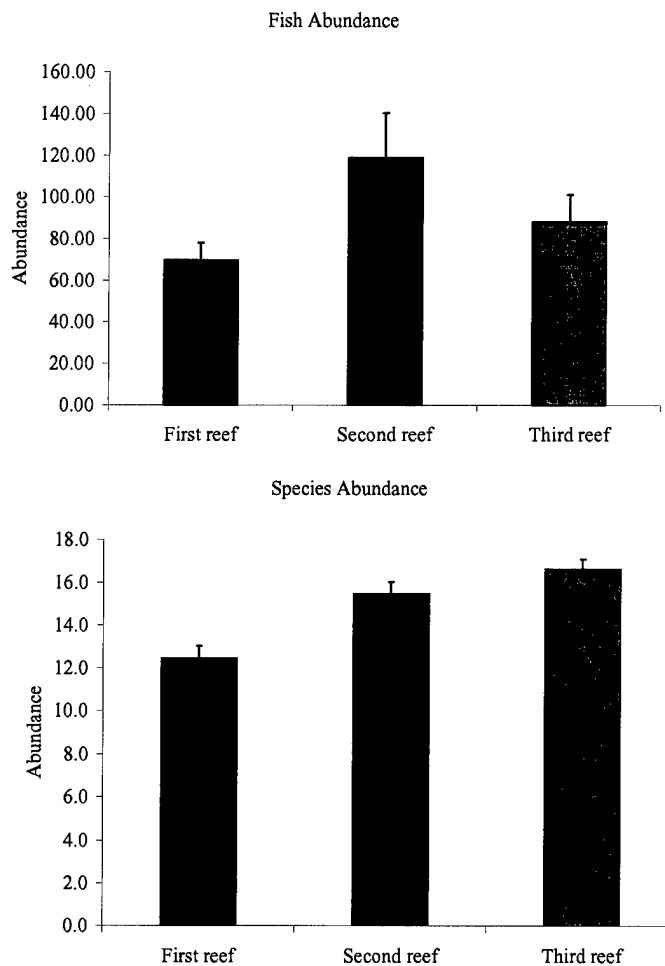


Figure 3.6.3.2: Fish abundance and species (mean \pm 1SE) for each of the three reefs within the range. Letters above columns indicates significant difference between the means ($p < 0.05$, SNK).

western edges (which did not differ significantly, $p > 0.05$). Likewise, there was an edge effect among species with the most species on the western edge of the tracts ($p < 0.01$); center and eastern edges did not differ ($p > 0.05$). There was also an edge/reef tract effect for total fish ($p < 0.05$) but not species (Figure 3.6.3.3).

3.6.3.1.3.4 Discussion

At this time, it appears there are differences in the total number of fish as well as the total number of species between the three reef tracts within the SFTF range. However, these conclusions are based on a relatively low number of counts (181) taken over several seasons. It would, therefore, be premature to assume that the distribution of species noted in this initial inventory is consistent across the entire reef and over time. Nonetheless, the statistical differences noted in fish assemblages among the three reef tracts do cause us to reject the null hypothesis (that total fishes, species and biomass are not different among the three reef tracts) and suggest that a full inventory of the reef fishes within the range and of Broward County will require continued surveying all three reef tracts.

3.6.3.1.3.5 Future Directions

In order to gain some insight into seasonal variation in local fish populations, during July 1999 we censused 45 sites (not included in this report) that were previously censused during the winter months (January-February 1999). In August-September 1999 we intend to re-census 45 sites censused 12 months earlier to gain some insight into annual variation. We also intend to set up a single station that will be repeatedly censused during the year to look at smaller time scale (monthly) variation. An additional 90 point counts, possibly more, will be done at new sites in north of the SFTF range in Broward County.

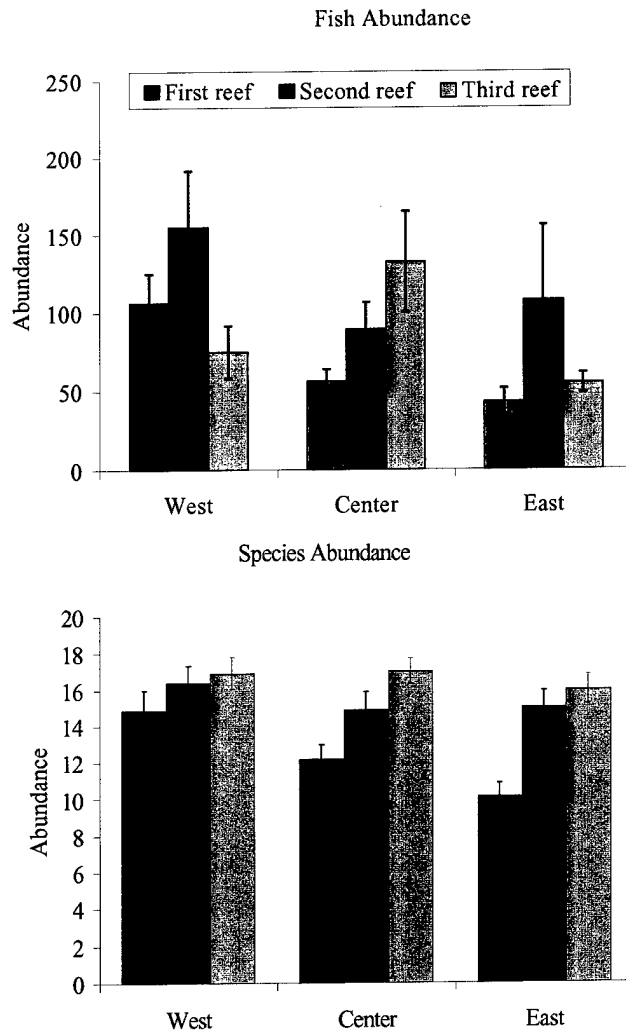


Figure 3.6.3.3: Fish abundance and species (mean \pm 1SE) for each of the three sample locations for each of reefs within the range.

3.6.3.1.4 Benthic Habitat Map

Completion of this task has been hampered by lack of detailed bathymetry and poor quality of preliminary air photography. Nevertheless, some progress towards completion has been accomplished.

3.6.3.1.4.1 Bathymetry

Detailed additional bathymetry of the SFTF range has not been accomplished according to project requirements. This bathymetry was originally scheduled to be done by the Navy utilizing the USNS Henson; however, this ship could not be scheduled to accomplish the work in the desired timeframe. We expect high-resolution bathymetry to be provided by the Navy, possibly sometime in late 2000. In the interim, historical sources of bathymetric data have been investigated for utility. An existing USGS 7.5' quadrangle (Figure 3.6.3.4) (Port Everglades, FL 26080-A1-TB-024) contains contoured bathymetry supplied by National Ocean Survey hydrographic surveys including H-4811 in 1928, H-4930 in 1928-29.

Another more promising bathymetry source has been a US Army Corps of Engineers data set taken in 1998 of the Port Everglades area via LIDAR. Unfortunately, the data set does not cover the entire range. Nevertheless, the data goes from shore and past the Third Reef line for a portion of the range.

Figure 3.6.3.5 is a shaded surface plot of the LIDAR data and is illustrative of the density and detail of the data. The horizontal feature is the Port Everglades channel, which descends to a depth of approximately 45 feet.



Figure 3.6.3.4: Portion of USGS quadrangle showing familiar range area from Port Everglades to Dania Pier. Bathymetric contours are provided and illustrate approximate positions of First, Second, and Third Reefs.

3.6.3.1.4.2 New Air Photography

Air photography of the entire range portion of interest from shore to the Third Reef has been accomplished at scales of 1":2500', 1":200' and 1":100'. Prints were made of the 1":200' runs and used to evaluate their usefulness for identification of obvious features of the range habitats. These air photographs were judged to have been not of sufficient quality to provide visualization of features on the Third and the deeper Second Reefs. New air photography is under scheduling and will be designed so that individual overlapping air photographs will provide stereo coverage. In addition, each will be rectified and geo-referenced so that the images can provide a proper basemap for ground truthing. In the interim, we will use 1981 high level NOAA air photography.

Port Everglades USACOE LIDAR bathymetry

January 25, 1998 Lidar Survey of Port Everglades



Figure 3.6.3.5: Shaded surface plot of Port Everglades LIDAR.

3.6.3.1.4.3 Preexisting Air Photography

High-level air photographs from NOAA are available for the range area for a number of years. These were evaluated and the 1981 series provided the most detail of the undersea area.

We have use georeferencing and air photographic techniques to overlay these ir

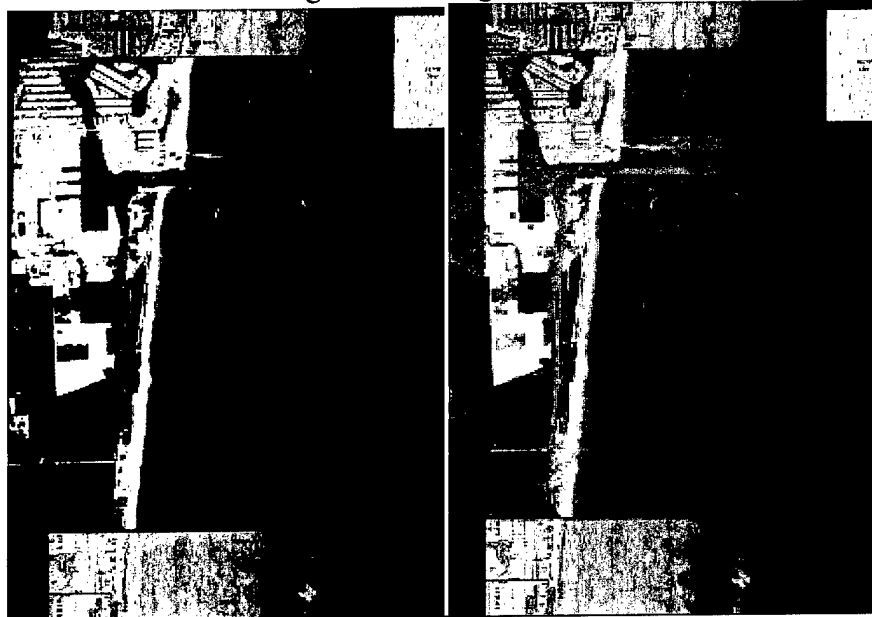


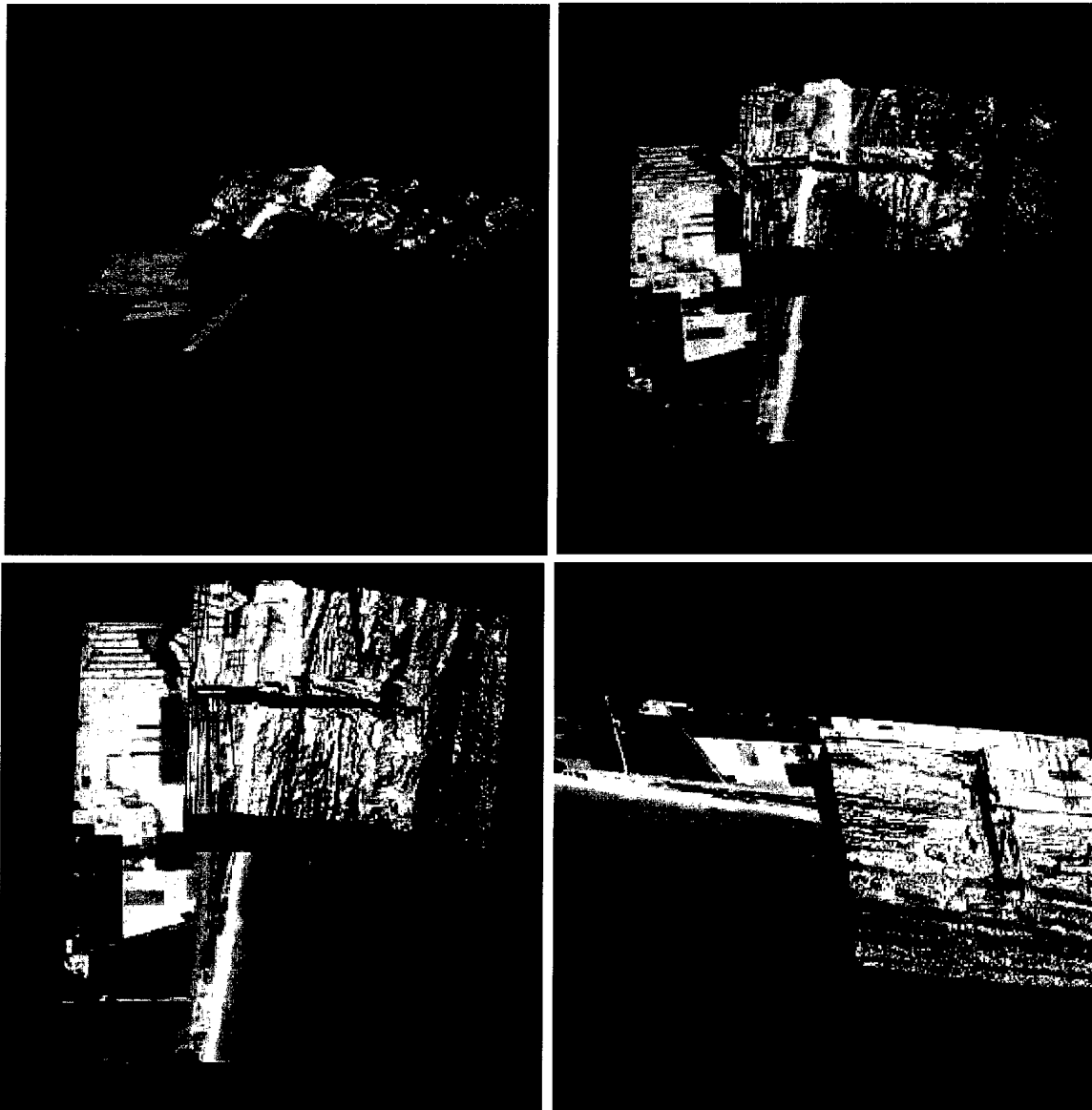
Figure 3.6.3.6: Air photograph, georeferenced, rectified, and overlain on USGS bathymetric map. Panel to the right shows the air photograph partially transparent.

photographs onto the existing USGS bathymetry map in order to best visualize and describe range environments.

Figure 3.6.3.6 shows a 1981 air photograph overlaid upon the USGS map. The first shows the air photograph simply overlain on the map. The second shows the photography as partially transparent. Clearly visible within the photograph are the First and Second Reef lines as well as part of the Third Reef.

3.6.3.1.4.4 Mating of Air Photography and Bathymetry for reef visualization.

Using a GIS based program (ER Mapper) we have combined existing air photography and LIDAR bathymetry to produce three-dimensional relieve images of the portion of the Range area which contains bathymetric data. This has been useful to visualize position of the reef lines, to mate bathymetric relieve with air photograph coloration, and to facilitate mapping of benthic habitat zones. Figure 3.6.3.7 is a collage of various three dimensional views of the data arranged in this way.



Continued next page

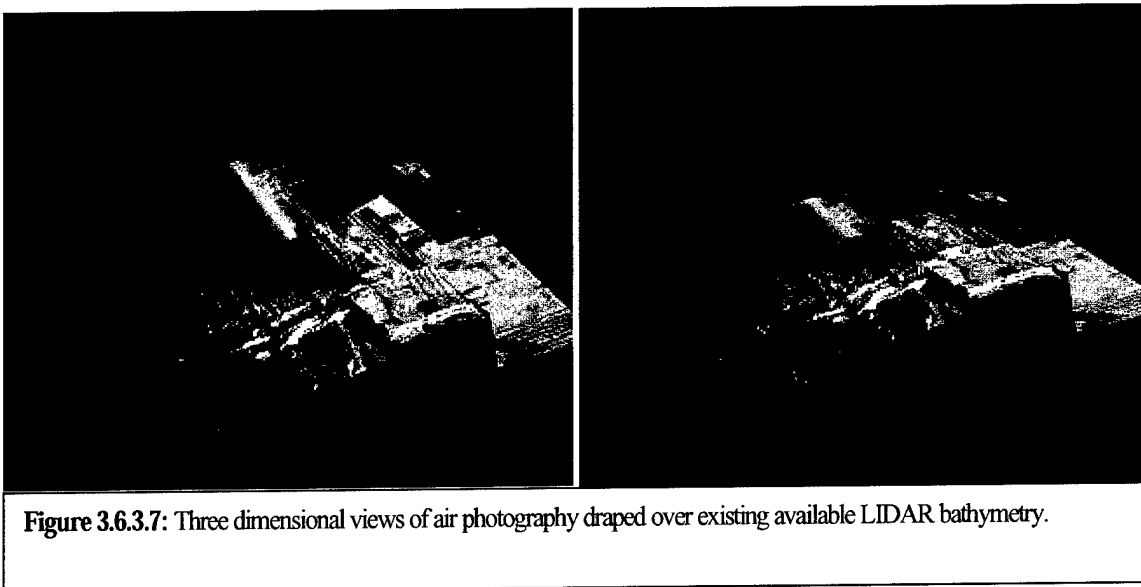


Figure 3.6.3.7: Three dimensional views of air photography draped over existing available LIDAR bathymetry.

3.6.3.1.5 Marine Mammals of Southeast Florida

A description, through a literature search, of the populations and migratory or territorial routes of marine mammals (resident and transient) within the range has been completed and is under review. This task report meets requirements of the Marine Mammal Protection Act as well as the Endangered Species Act. Special attention is given to the potential interaction of low-frequency acoustics with marine mammal populations of the range.

3.6.3.2 Monitoring Plan for Environmental Stewardship

Establish and implement a long-term biological monitoring plan, utilizing the permanent stations (and equipment to the extent possible) established by the other studies of this partnership. The monitoring will involve an integration of biologic assessment over time with the physical variables obtained by the remote sensors and AUVs. This portion of our study will be accomplished as more of our biological inventory becomes complete. This will not be accomplished this year but in succeeding years.

3.6.3.3 AUV Applications for Environmental Stewardship

In the next year, we will initiate a study in conjunction with FAU to evaluate the potential for AUV's to collect data relevant for rapid reef assessment. The use of diver operated video assessment for quantifying coral reefs is a rapidly growing methodology. We will investigate the utility of taking this technology to the next level of utilizing AUV platforms to accomplish the data collection.

3.6.3.4 References

- Abbott, R. T. 1974. *American Seashells*. 2nd ed. Van Nostrand Reinhold, NY. 663 pp. + 24 pls.
- Bohnsack, J.A. and S.P. Bannerot. 1986. A stationary visual census technique for quantitatively assessing community structure of coral reef fishes. U.S. Dept. of Commerce, NOAA Technical Report NMFS 41:1-15.
- Bohnsack, J.A. and D.E. Harper. 1988. Length-weight relationship of selected marine reef fishes from southeastern United States. NOAA Technical Memorandum NMFS-SEFC. U.S. Dept. of Commerce.

- Dodge, R. E., Hess, S. and Messing, C. G. 1991. Final report: Biological monitoring of the John U. Lloyd beach renourishment: 1989. Prepared for: Broward Co. Board of County Commissioners, Erosion Prevention District of the Office of Natural Resource Protection, Ft. Lauderdale, FL. iii + 62 pp. + map, figures & tables.
- Dodge, R. E., Goldberg, W., Messing, C. G. and Hess, S. 1995. Final report: Biological monitoring of the Hollywood - Hallandale beach renourishment. Prepared for: Broward Co. Board of County Commissioners, Dept. Natural Resources Protection, Biological Resources Division, Ft. Lauderdale, FL. 153 pp.
- Goldberg, W. 1973. The ecology of the coral-octocoral communities off the southeast Florida coast: geomorphology, species composition, and zonation. *Bull. Mar. Sci.* 23:465-488.
- Jaap, W. C. 1984. The ecology of the south Florida coral reefs: a community profile. U. S. Fish & Wildlife Service FWS/OBS - 82/08. 138 pp.
- Lighty, R. G. 1977. Relict shelf-edge Holocene coral reef: southeast coast of Florida. pp. 215-221 IN: Taylor, D. L. (ed.) *Proc. 3rd Internatl. Coral Reef Symposium*, Miami. Rosenstiel School of Marine and Atmospheric Science, Univ. Miami, vol. 2.
- Lighty, R. G., MacIntyre, I. G. and Stuckenrath, R. 1978. Submerged early Holocene barrier reef south-east Florida shelf. *Nature* 276:59-60.
- Marszalek, D. S. 1981. Impact of dredging on a subtropical reef community, southeast Florida, U.S.A. pp. 147-153 IN: Gomez, E. D., Birkeland, C. E., Buddemeier, R. W., *et al.* (eds.) *The Reef and Man, Proc. 4th Internatl. Coral Reef Symposium*, Manila, Marine Sci. Ctr., Univ. Philippines, vol. 1.
- Marszalek, D. S., Babashoff, Jr., G., Noel, M. R. & Worley, D. R. 1977. Reef distribution in south Florida, pp. 224-229 IN: Taylor, D. L. (ed.) *Proc. 3rd Internatl. Coral Reef Symposium*, Miami. Rosenstiel School of Marine and Atmospheric Science, Univ. Miami, vol. 2.
- Raymond, W. F. 1972. A geologic investigation of the offshore sands and reefs of Broward County, Florida. Florida State University, Unpublished M. S. Thesis, vi + 95 pp.
- Raymond, W. F. & Antonius, A. 1977. Final Report: Biological monitoring project, John U. Lloyd Restoration Project, Broward County Erosion Prevention Division, Environmental Quality Control Board, Broward Co., FL. Contract No. 6-76-32-F. 41 pp. + 11 pls.
- Robins, R.C. and G.C. Ray. 1986. A field guide to Atlantic coast fishes of North America. Houghton Mufflin Co. Boston. pp354.
- Sherman, R.L., D.S. Gilliam and R.E. Spieler. (In Press). A preliminary examination of depth associated spatial variation in fish assemblages on small artificial reefs. *Jour. Of Appl. Ichth.*
- Voss, G. L. 1988. *Coral Reefs of Florida*. Pineapple Press, Sarasota, FL. 80 pp. + plates.

4. SUMMARY

At the SFOMC Workshop held in February 1999, international participants from the ocean community pointed out the strategic importance of the SFTF range for oceanographic and ocean engineering studies related to the Gulf Stream and air-sea interactions. The participants recognized the wealth of talent and expertise within the center and the synergy among its scientists and engineers. Much interest was shown in the efforts that are already underway in establishing SFOMC as a center for continuous ocean observation and as an in-water laboratory in the 21st century. The achievements within the past year, including the completion of six major experimental efforts, related to Mine Counter Measures (MCM) operations, physical oceanography, ocean acoustics and bio/geological assessments, reiterates the commitments of the partners in developing a center of excellence.

The centerpiece of the in-water laboratory at the SFTF range is a shallow water multiplexer (MUX) which provides power to the various instruments and relays data in real time to shore via a fiber-optic communication. The MUX was designed, fabricated and installed on the range. It provides power and shore-based communication link to the instruments during the experiments.

The experiments carried out in the SFTF range addressed issues of importance to scientific and engineering aspects of AUV development as well as enhancements of the infrastructure in the SFTF range. Capabilities for autonomous ocean sampling technology involving AUVs and oceanographic sensors have been demonstrated.

The MCM Experiment demonstrated the versatility of AUVs fitted with side-scan sonars in detecting buried objects. Significant experience has been gained from the experiment and will be utilized to make refinements in identifying targets. The experiment was also useful in establishing procedures for environmental assessment and for post processing information.

In the Adverse Weather Experiment, a successful, well-coordinated effort was able to capture a cold front event during Fall, 1998. The effort demonstrated the nature of process-oriented experiments that are possible at SFOMC and how AUVs can be utilized for profiling, and making *in-situ* CTD and small-scale turbulence measurements. Measurements using a 5-head ADCP, CTD casts from the support ship and the atmospheric data from the local C-MAN buoys provided the background information necessary to put the small-scale measurements in their proper context. Detailed analysis of the data is underway and will address issues relating to the energy budgets in the physical processes in a shallow water environment.

The ambient noise sonar, the PEACOCK, demonstrated the ability to operate and collect data ambient noise over a 24hr period. Analysis of the noise data is in progress to identify the various major sources of noise that have been detected on the range. The work will help in assessing the noise environment on the range.

The design and preliminary tests have been completed in the development of the Docking Station. The SBL system has performed well, and the simulation work is ongoing to model and optimize this system. A docking station, when completed will be of immense importance in operating during storms.

Two underwater acoustic modems, Mills-Cross and General Purpose Modem, designed and built for acoustic communication during the development of the Docking Station, have been successfully tested at sea. The modems will be attached to the MUX.

The 4-D current experiment during summer 1999, demonstrated, for the first time, the relative importance of conducting AUV and ship-based sampling grids within a very high-resolution grid of surface current measurements from OSCAR. Detailed analysis of current and turbulence measurements will provide new insights into complex physical processes occurring in a coastal ocean forced by a meandering Florida Current where maximum surface velocities exceeded 2 m s^{-1} . Furthermore, the observations significantly challenge numerical models of coastal circulation.

The 3-D Environmental Array is now in place and continuously collected current, salinity, temperature, density and wave data over the range during the 4-D Current Experiment and beyond. Data was also collected during Hurricane Floyd and will be of significant importance. Detailed analysis of the data will be carried out during the next year and will provide important characterization of the SFTF range. In the long run, the gathered information will be valuable in studying the impact of the Florida Current meanders on coastal processes, for example.

During the year, the design, fabrication and installation of the receiver arrays for the Acoustic Propagation Study (Experiment 5) were completed and model acoustic propagation results, for planning the experiments, have been obtained. An environmental impact study (FONSI) has been completed and approved by NAVSEA.

A number of Bio/Geological Surveys have been completed to characterize the biodiversity of the in-water laboratory. The surveys suggest that there are differences in the total number of fish as well as the total number of species between the three reef tracts within the SFOMC range. More data is required to confirm this and to determine seasonal variations. A detailed bathymetric survey of the range is required.

A number of enhancements and further collaborative adverse weather experiments are expected next year. At the February workshop, participants suggested visitor programs be set up, whereby scientists from other laboratories could come to SFOMC for studying pertinent processes on a range equipped with the instruments installed in this phase of the project. Further, a new initiative has been proposed to form a consortium of East Coast Observatories, involving WHOI, LEO-15, Duck, SABSOON and SFOMC. Such a consortium would co-ordinate efforts to monitor synoptic scale events as well share ideas and resources.

APPENDICES

- Appendix 2.7** Shallow Water Multiplexer (MUX)
- Appendix 3.2.3** AUV Docking/Navigation Missions
- Appendix 3.6.1** Macroinvertebrate Inventory Table
- Appendix 3.6.2** Fish Inventory Table

Appendix 2.7

A2.7 Shallow Water Multiplexer (MUX) Installation

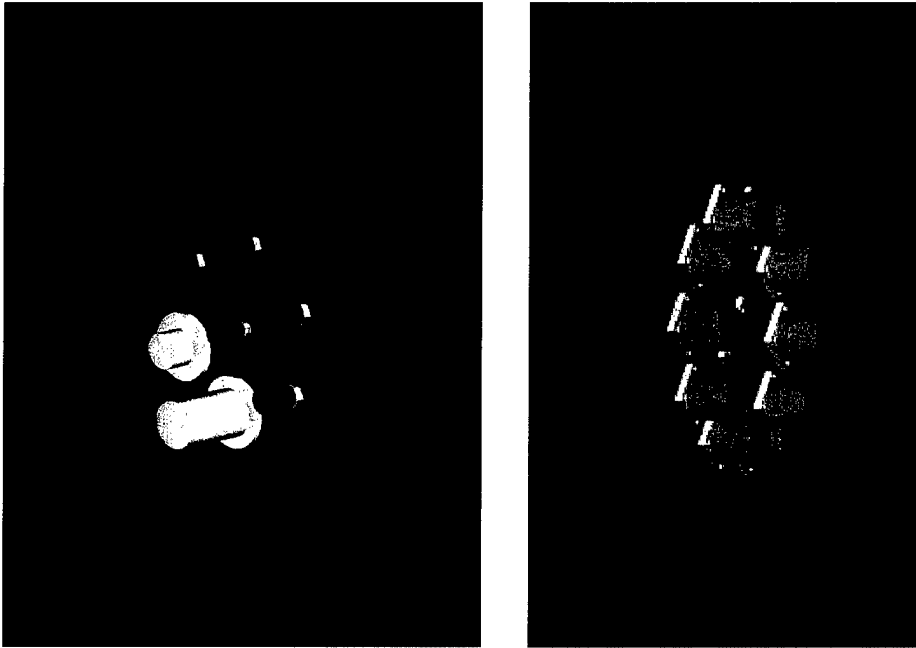


Figure 2.7.4 SFOMC MUX endcaps

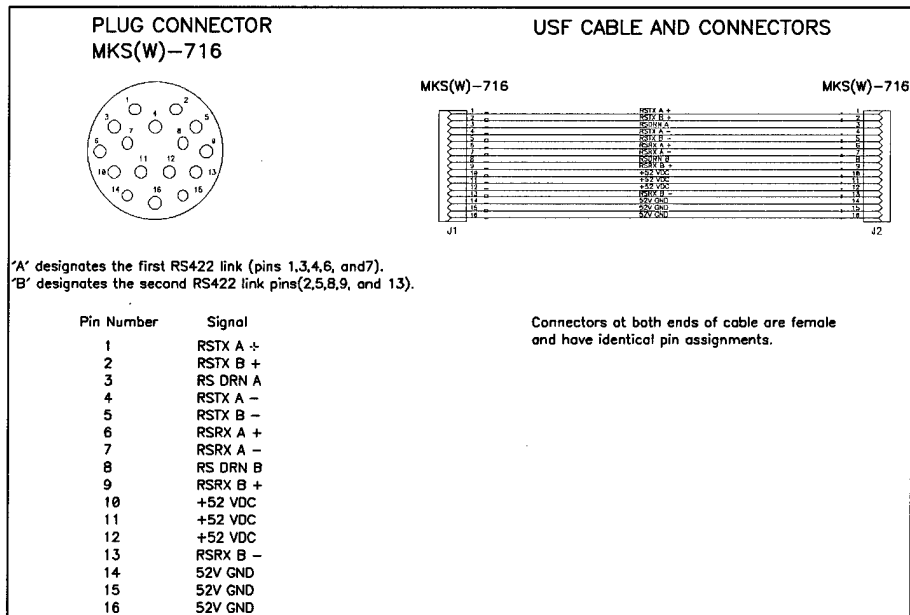


Figure 2.7.5 USF environmental array cable/connector pinouts

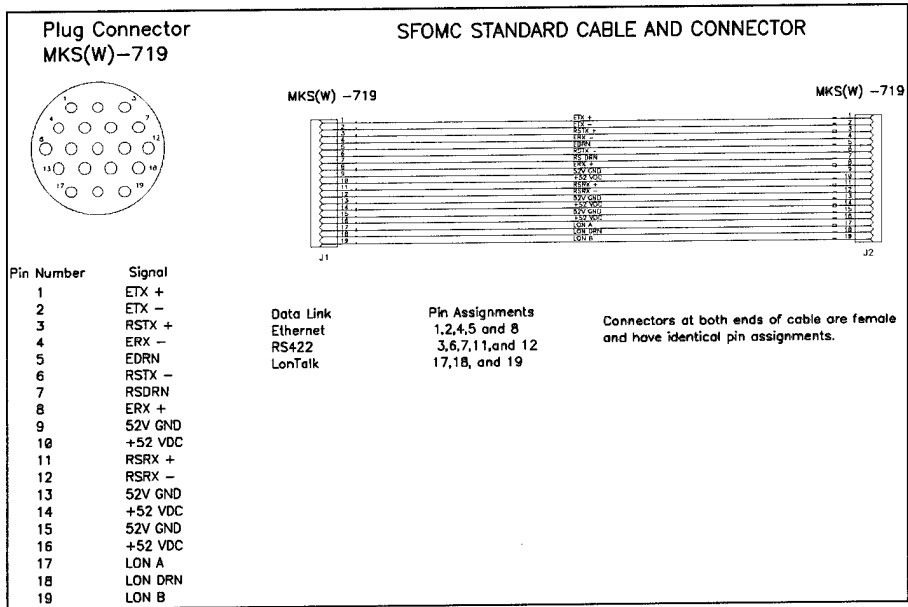


Figure 2.7.6 Generic instrument cable/connector pinouts

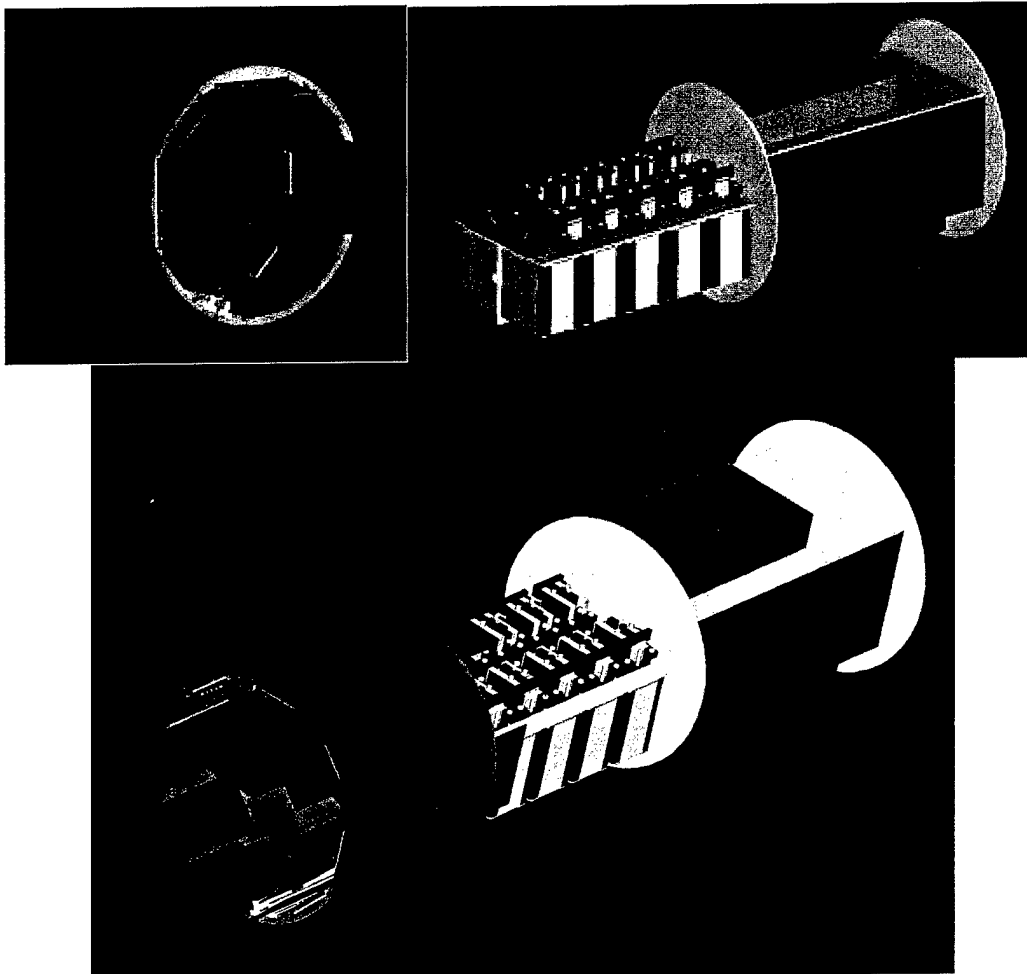


Figure 2.7.7 MUX internal mechanical assembly

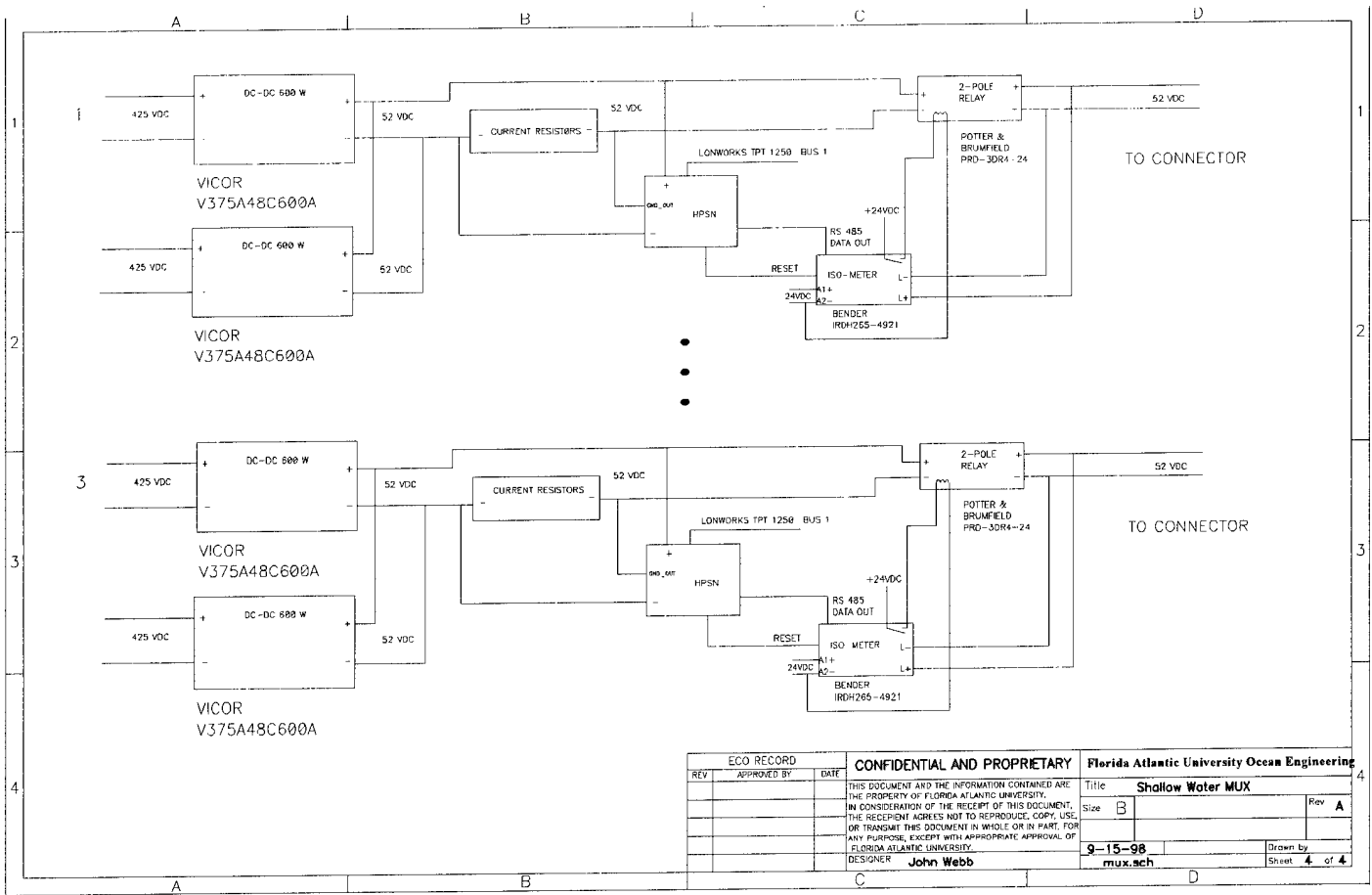


Figure 2.7.10 Power board layout for one of the AUV docks

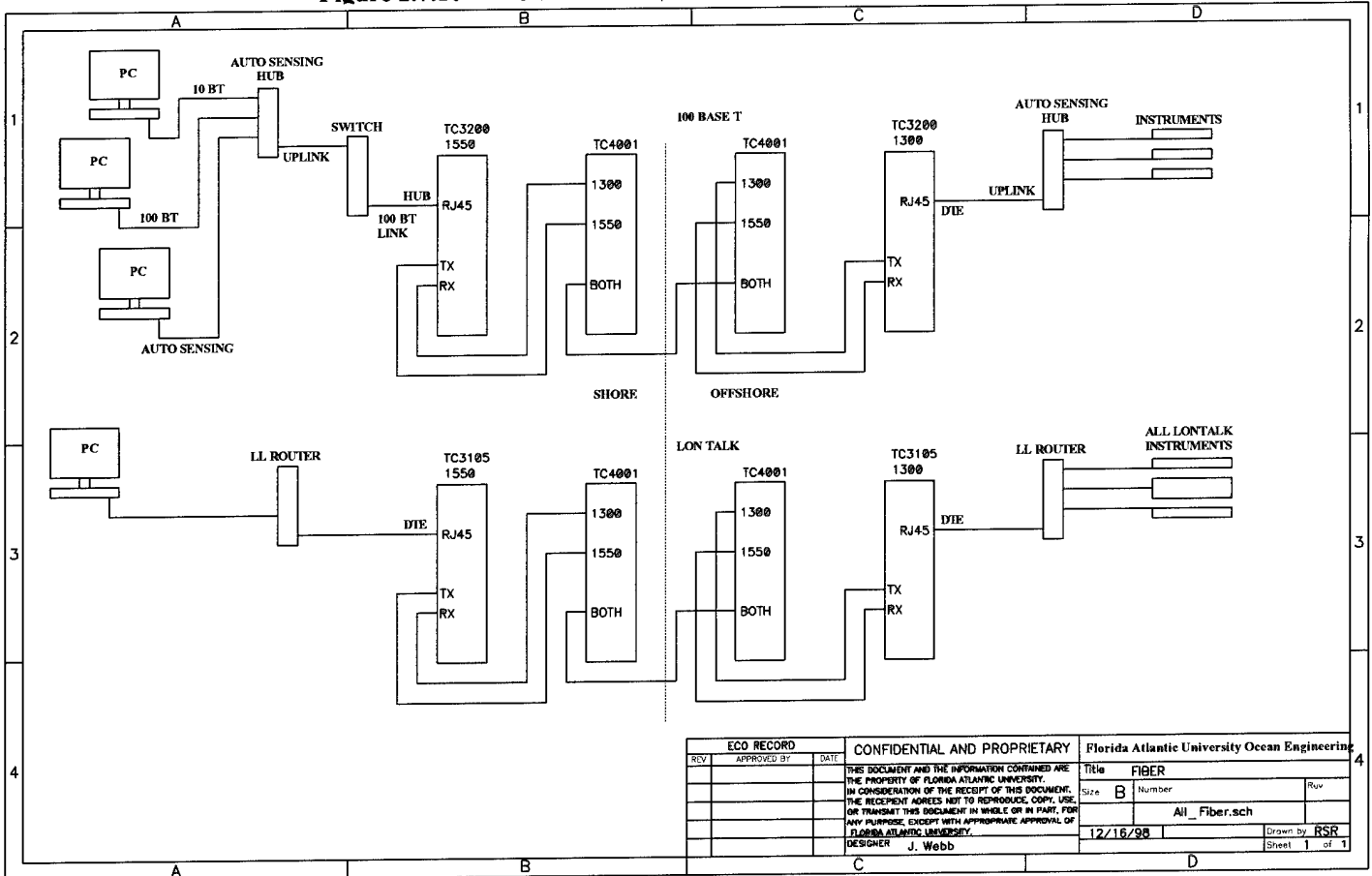


Figure 2.7.11 Fiber-optic Ethernet transceiver connection

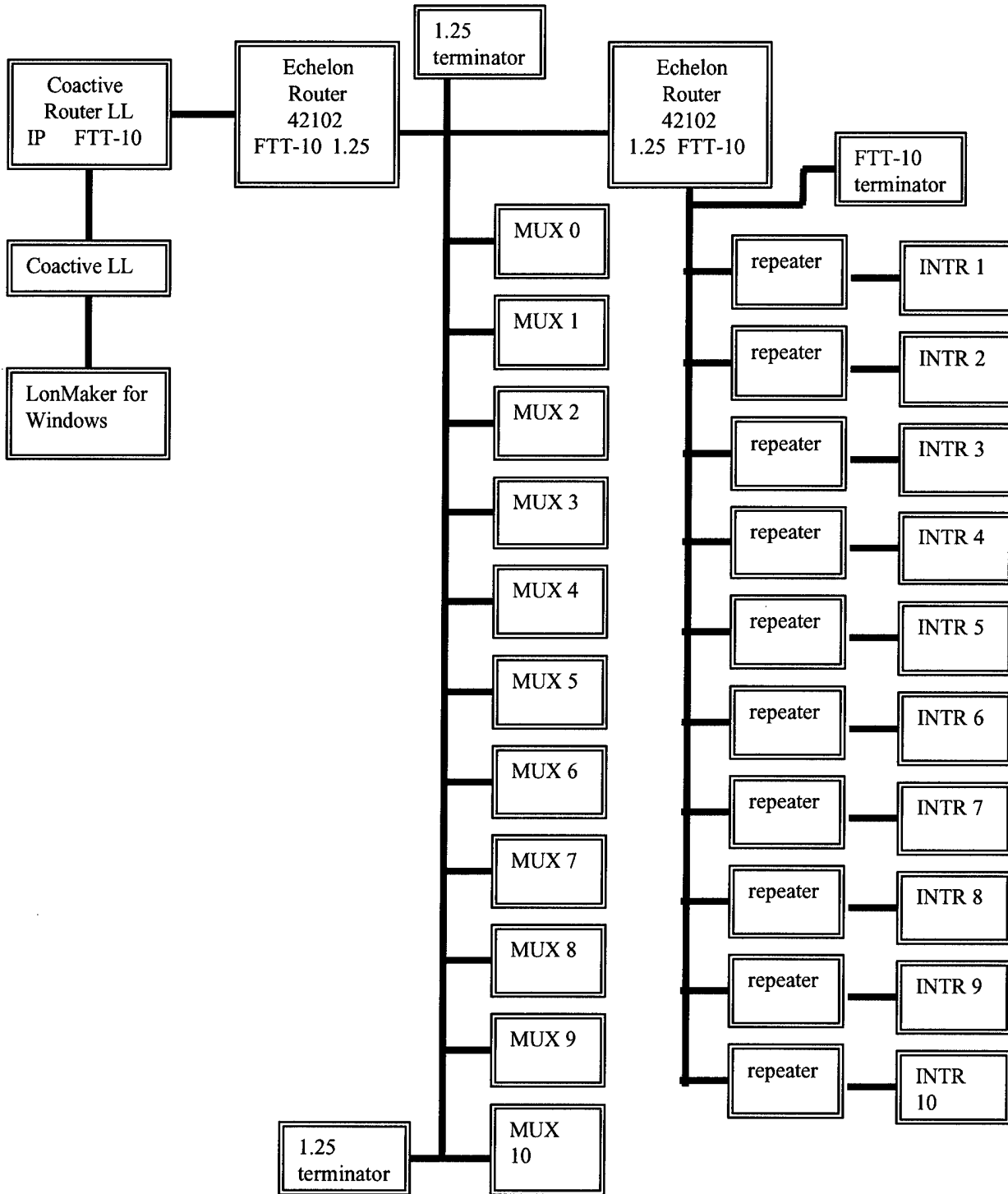


Figure 2.7.12 A block diagram of LonTalk connection

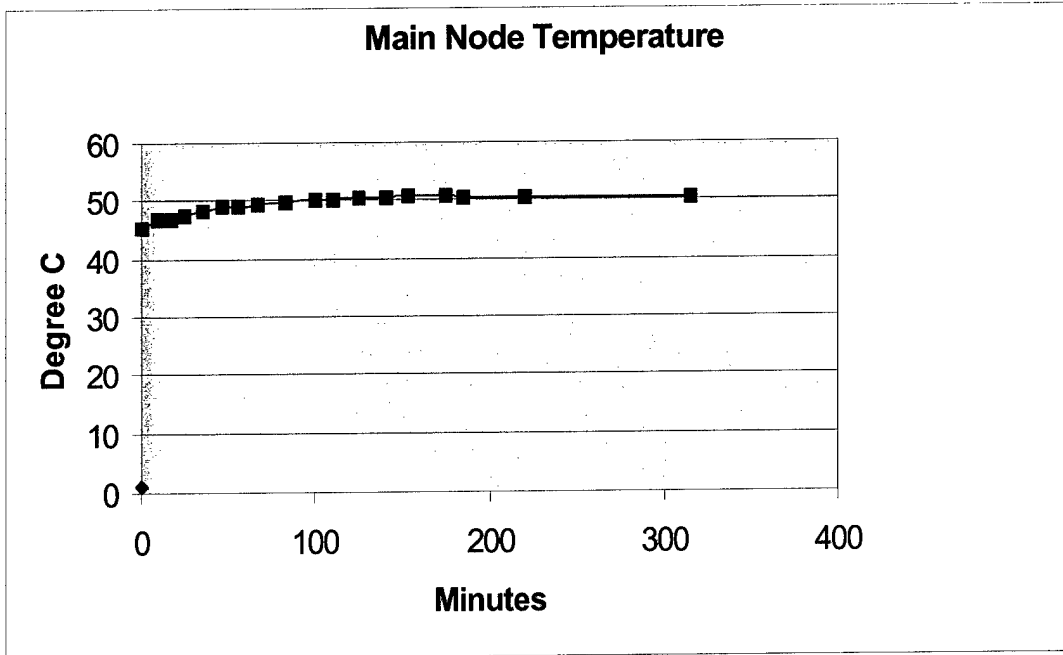
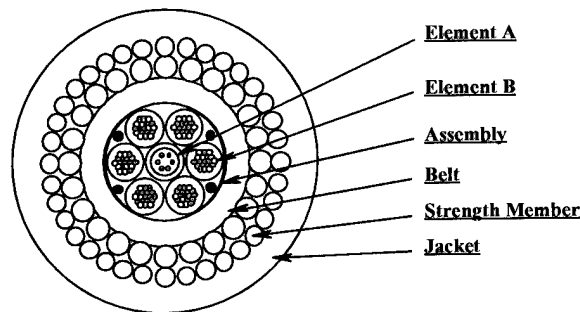


Figure 2.7.13 Internal MUX temperature fluctuation when subjected to close to 100% of maximum power load

Cabling and Connectors

Shore To Mux. Box Electro-Optic Cable: The double steel armored electro-optic cable that will run from the NSWCCD site to the MUX will be 14,000ft long and will be laid on the sea floor. This cable is being fabricated by The Rochester Corporation to the following specifications;



Element A: Optic Core (1)

| | |
|---|-------|
| Fiber: 8.3/125/245 μm SM | .010" |
| Six color-coded optical fibers inside gel filled hermetic stainless steel tube. | .094" |
| Belt: HPDE | .115" |

Element B: Power Singles (6)

| | |
|------------------|-------|
| Cdr: # 14 AWG Cu | |
| Insl: HPDE | .110" |

Assembly

| | |
|--|-------|
| Core: Element A | .115" |
| Layer #1; 6 Element A's with 4 drain wires (#20 AWG Cu) in interstices. Void filled and bound with AL/Polyester tape. | .346" |

Belt

| | |
|------|-------|
| HDPE | .469" |
|------|-------|

Strength Member

| | |
|--------------------------|-------|
| Layer #1; 24/ .062" GIPS | .593" |
| Layer #2; 36/ .051" GIPS | .695" |

Jacket

| | |
|------|-------|
| HPDE | .845" |
|------|-------|

CABLE CHARACTERISTICSMETRICENGLISH

(Nominal Values @ 20 °C)

Physical

| | | |
|---------------|-------------|------------|
| Weight in Air | 1,161 kg/km | 780 lb/kft |
|---------------|-------------|------------|

| | | |
|--------------------|-----------|------------|
| Weight in Seawater | 790 kg/km | 531 lb/kft |
|--------------------|-----------|------------|

| | | |
|------------------|-----|-----|
| Specific Gravity | 3.2 | 3.2 |
|------------------|-----|-----|

Mechanical

| | | |
|-------------------|--------|------------|
| Breaking Strength | 147 kN | 33,000 lbf |
|-------------------|--------|------------|

| | | |
|-------------------|-------|-----------|
| Installation Load | 33 kN | 7,500 lbf |
|-------------------|-------|-----------|

| | | |
|-------------------------|-------|-----------|
| Recommended Bend Radius | 43 cm | 17 inches |
|-------------------------|-------|-----------|

Electrical

| | | |
|---------------------------|-----------|-----------|
| Voltage Rating: Element B | 600 Volts | 600 Volts |
|---------------------------|-----------|-----------|

| | | |
|----------------------------------|-------------|---------------|
| Insulation Resistance: Element B | 3,000 MΩ.km | 10,000 MΩ.kft |
|----------------------------------|-------------|---------------|

| | | |
|--------------------------|----------|-----------|
| dc Resistance: Element B | 9.2 Ω/km | 2.8 Ω/kft |
|--------------------------|----------|-----------|

Optical

Attenuation Rate: Element A

| | | |
|-----------|------------|----|
| @ 1310 nm | 0.40 dB/km | -- |
|-----------|------------|----|

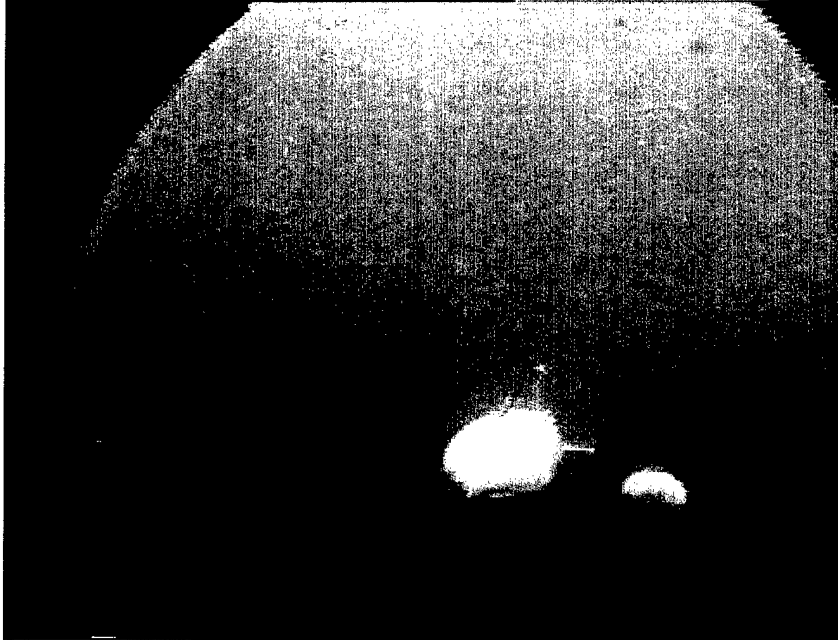
| | | |
|-----------|------------|----|
| @ 1550 nm | 0.25 dB/km | -- |
|-----------|------------|----|

Table A.2.7..1 Summary of Cables and Connectors

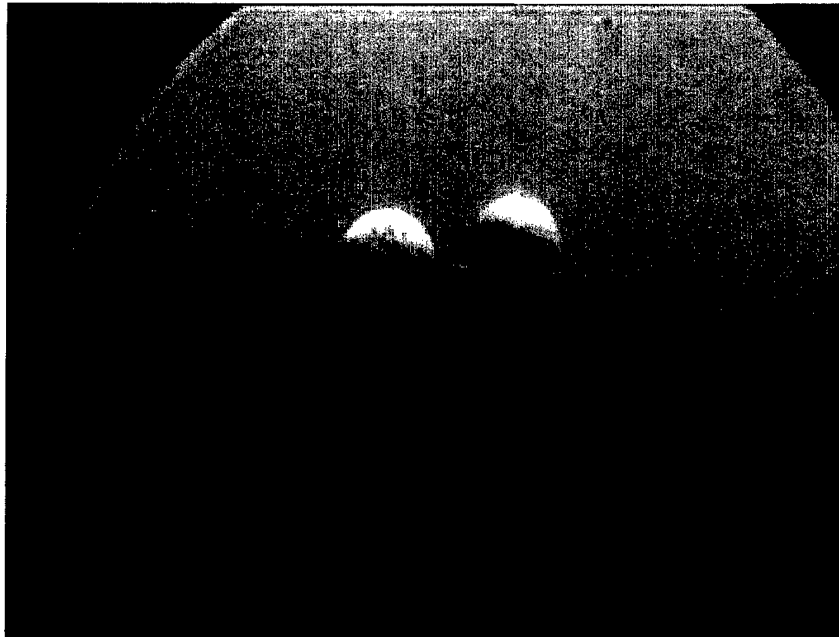
| Sensor | MUX Connector | Cable | Length in feet |
|--------------------------|---|---|----------------|
| USF ADCP | Impulse Titan Series MKS(W) -716 | Power: 6 #14 AWG Data: 4 #24 AWG TSP | 2000 |
| Peacock | Impulse Titan Series MKS(W) - 719 | Power: 6 #14 AWG Data: 5 #24 AWG TSP | 350 |
| Cyclesonde | Impulse Titan Series MKS(W) - 719 | Power: 6 #14 AWG Data: 5 #24 AWG TSP | 100 |
| 5-Head ADCP | Impulse Titan Series MKS(W) - 719 | Power: 6 #14 AWG Data: 5 #24 AWG TSP | 650 |
| Acoustic Modem Source | Impulse Titan Series MKS(W) - 719 | Power: 6 #14 AWG Data: 5 #24 AWG TSP | 800 |
| AUV Dock | Connector 1 Impulse Titan Series MKS(W) - 719 Connector 2 Impulse HD-4 | Cable 1 Power: 6 #14 AWG Data: 5 #24 AWG TSP Cable 2 Power: 4 #12 AWG | 300 |

Appendix 3.2.3

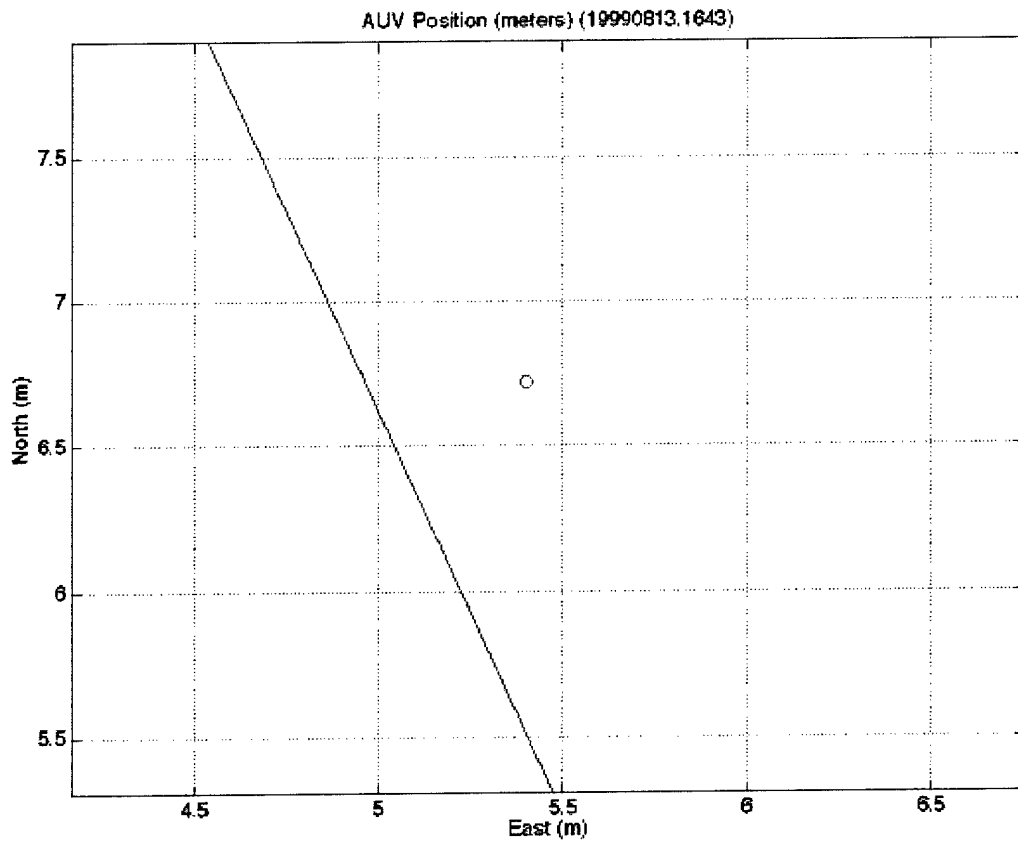
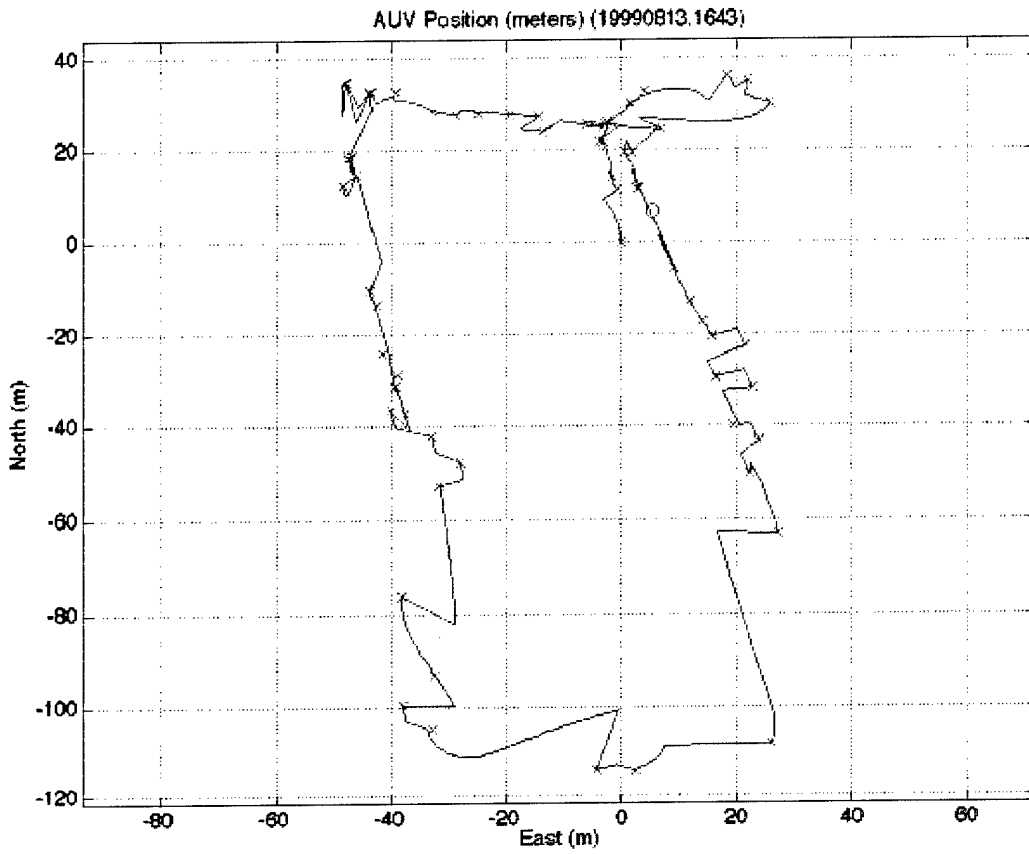
AUV Docking/Navigation Missions



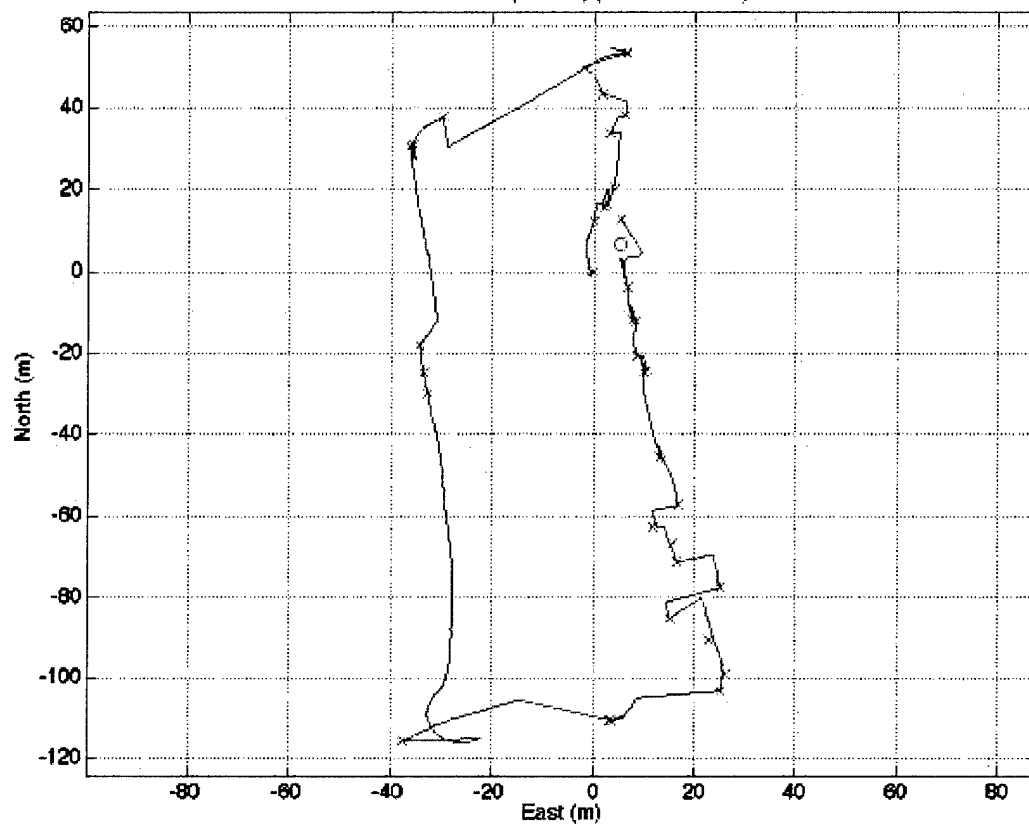
MISSION 1728



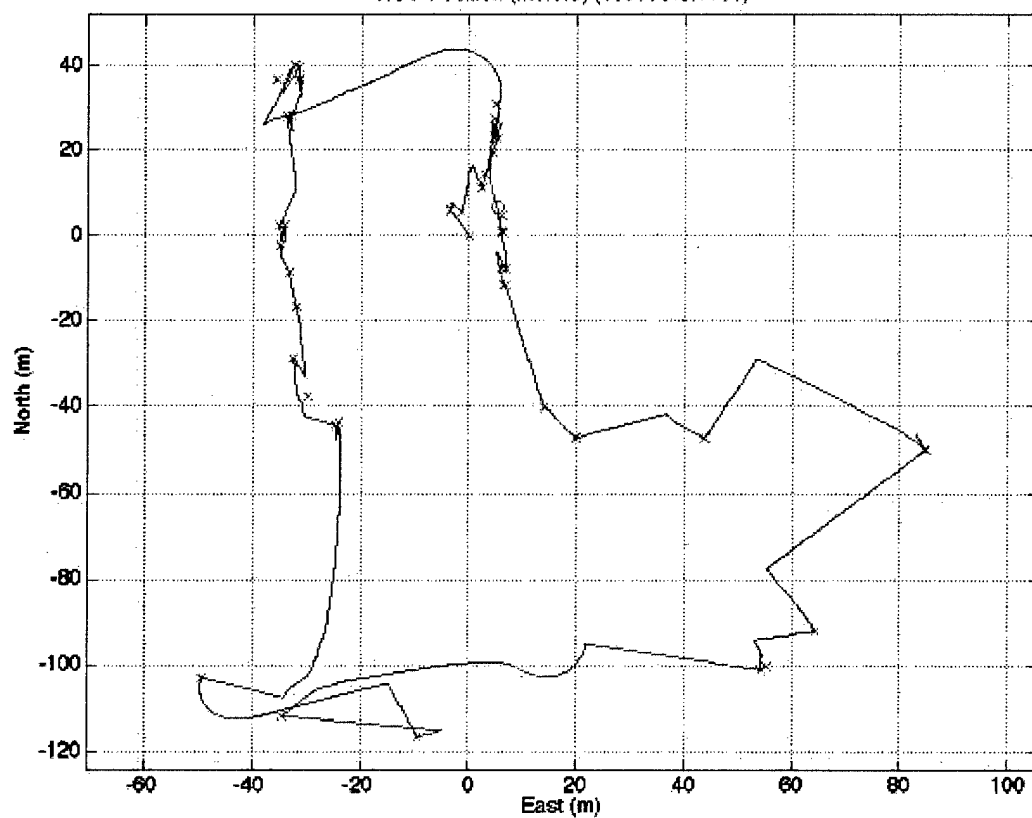
MISSION 1756



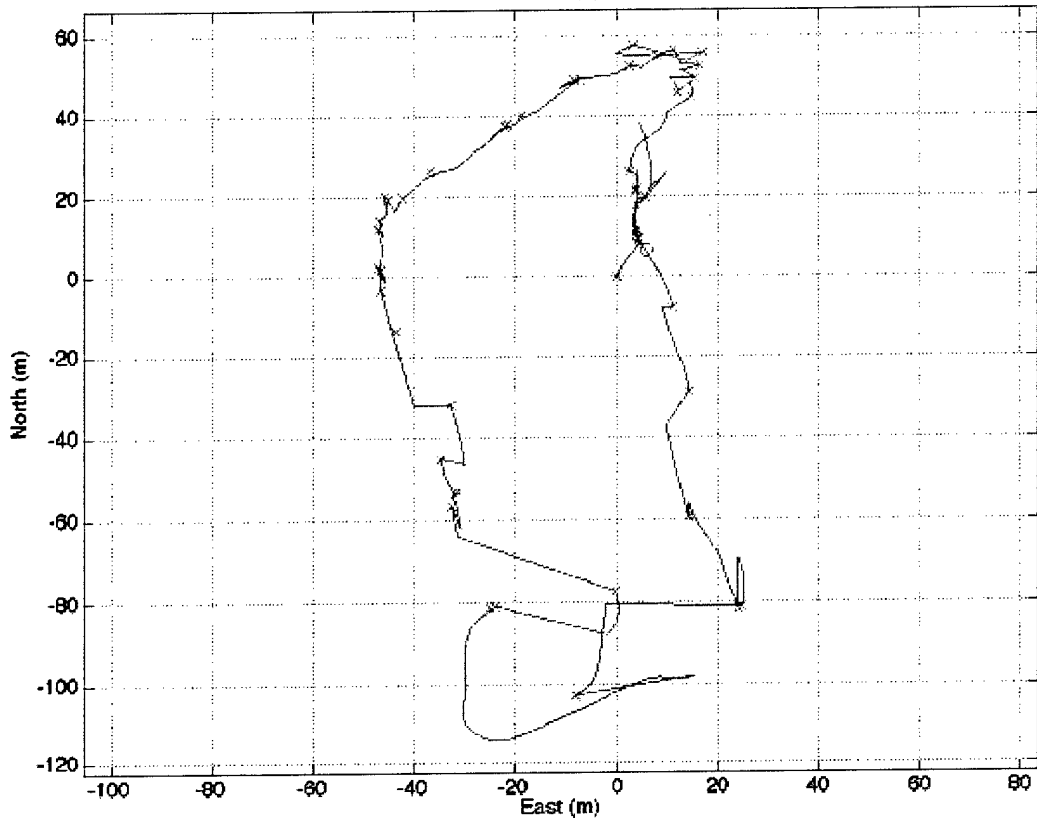
AUV Position (meters) (19990813.1653)



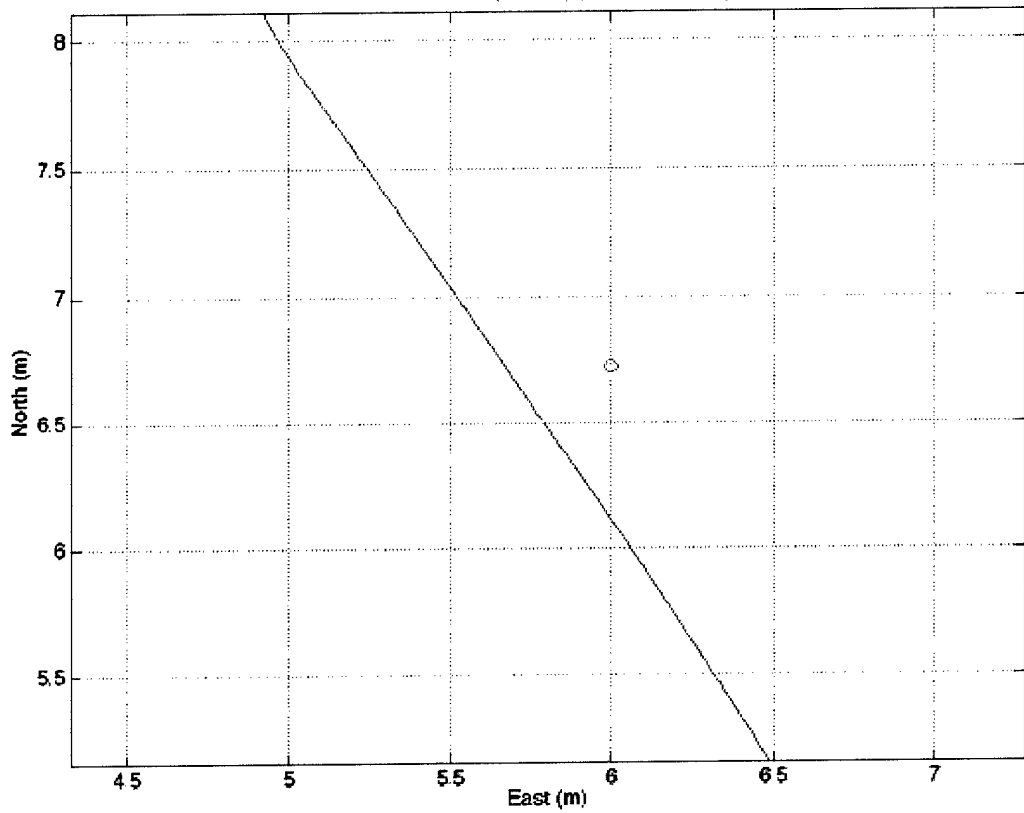
AUV Position (meters) (19990813.1701)

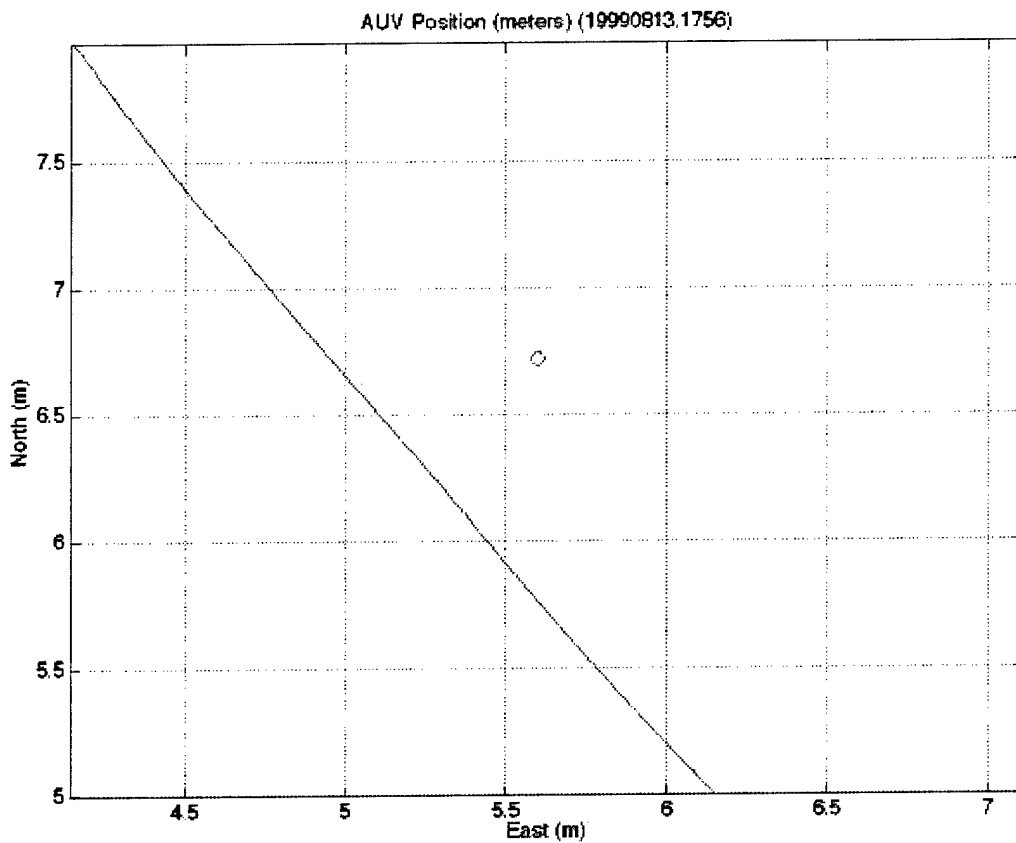
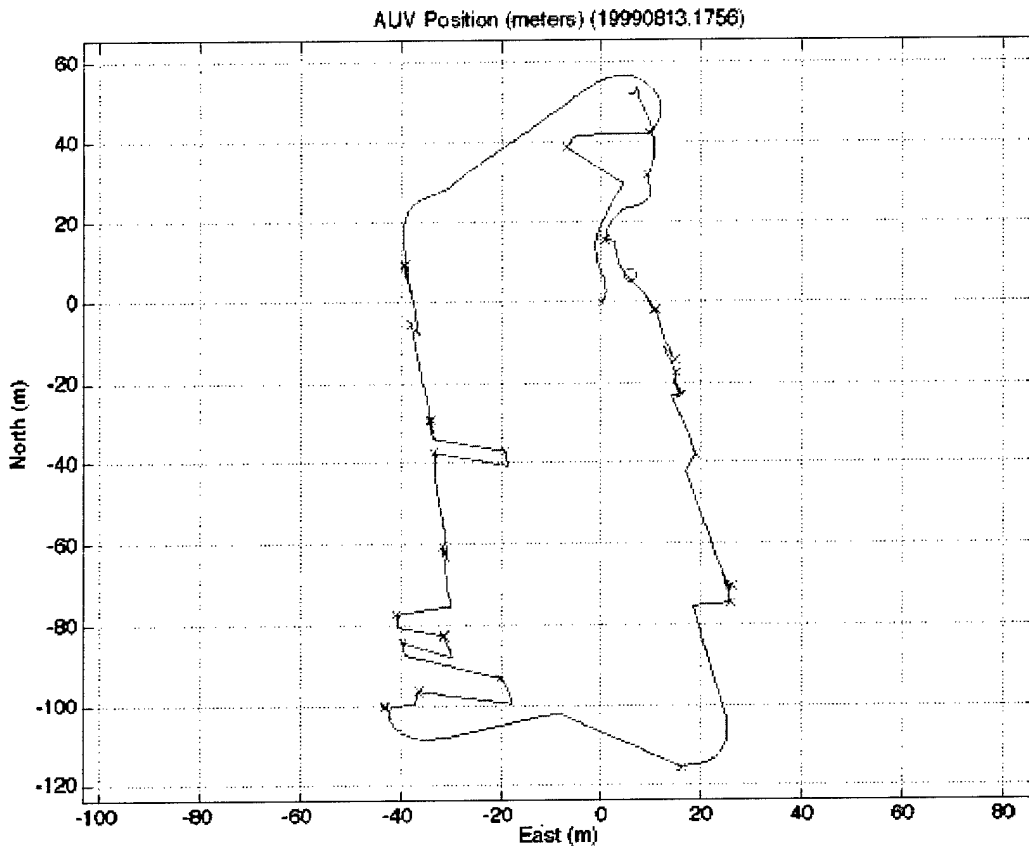


AUV Position (meters) (19990813.1728)

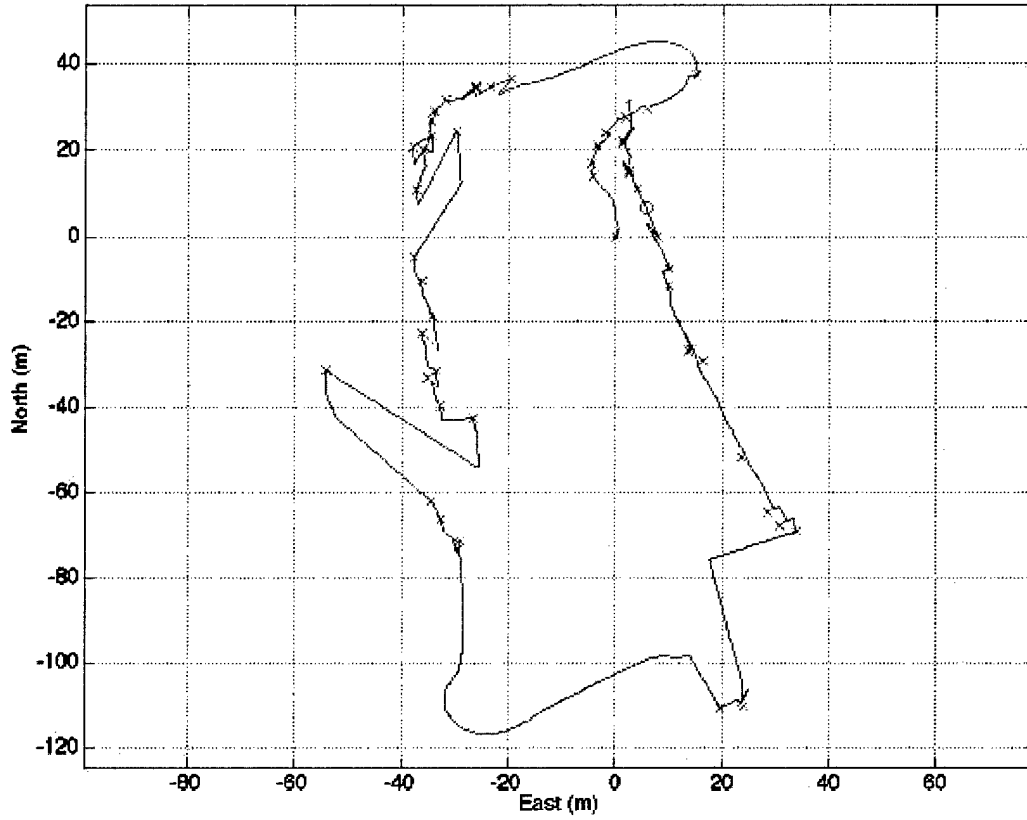


AUV Position (meters) (19990813.1728)

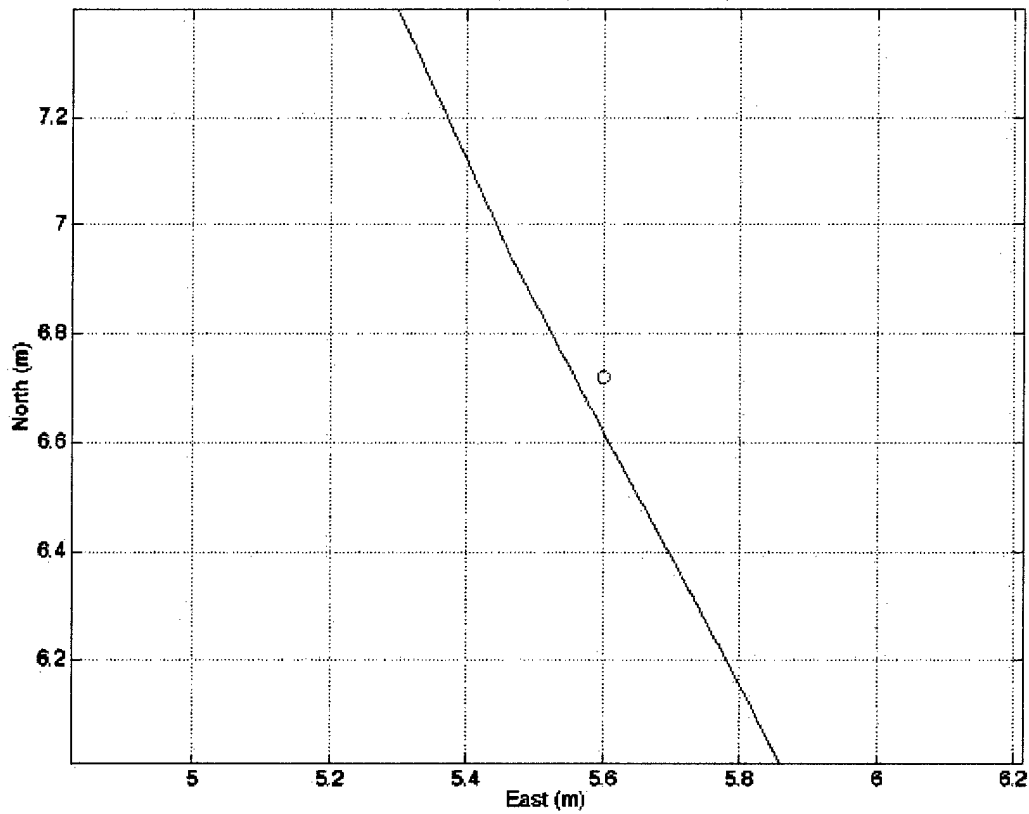




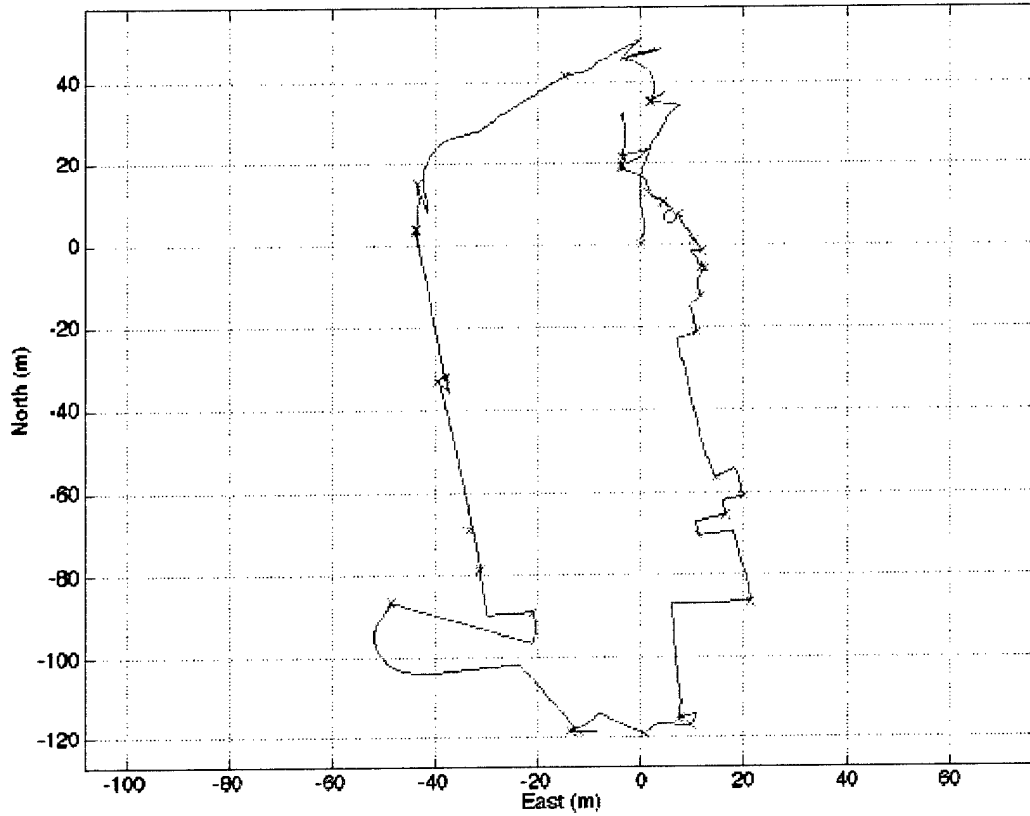
AUV Position (meters) (19990813.1812)



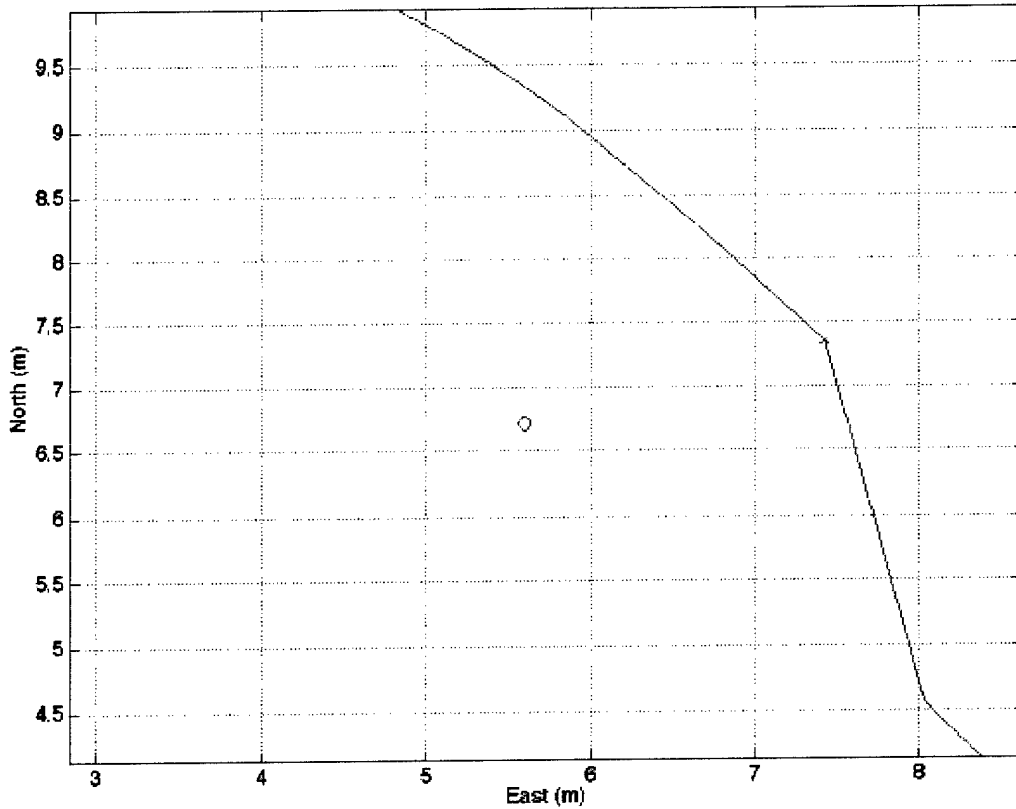
AUV Position (meters) (19990813.1812)



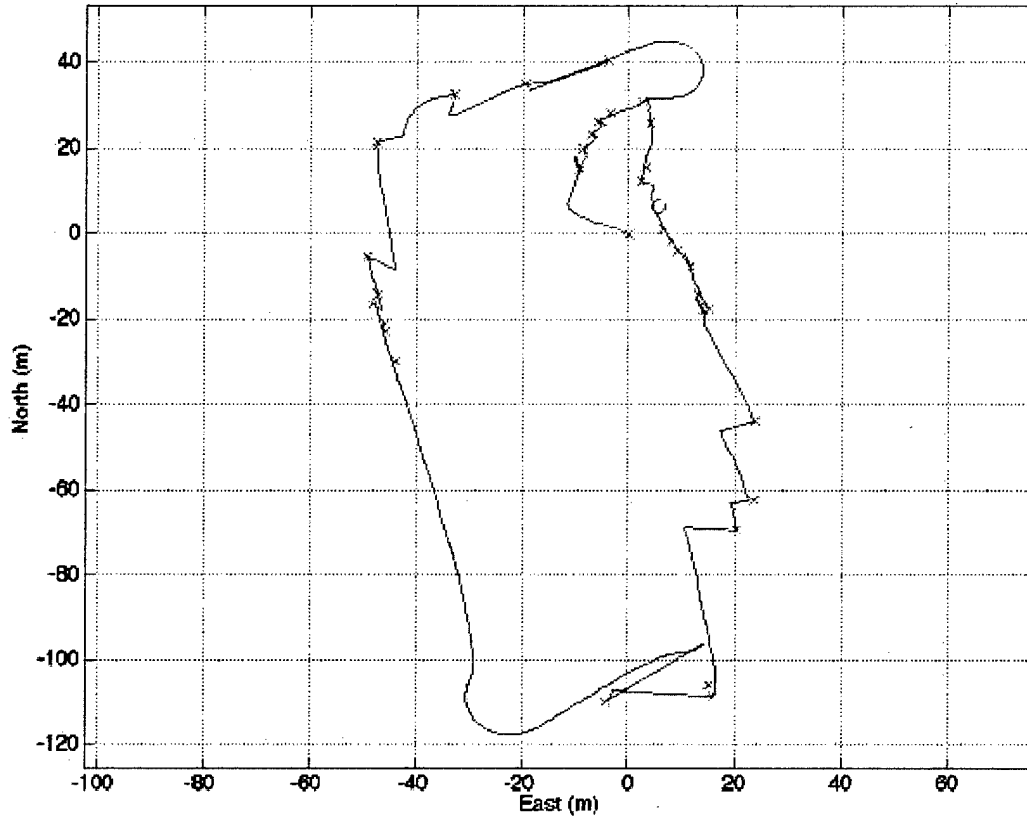
AUV Position (meters) (19990813.1844)



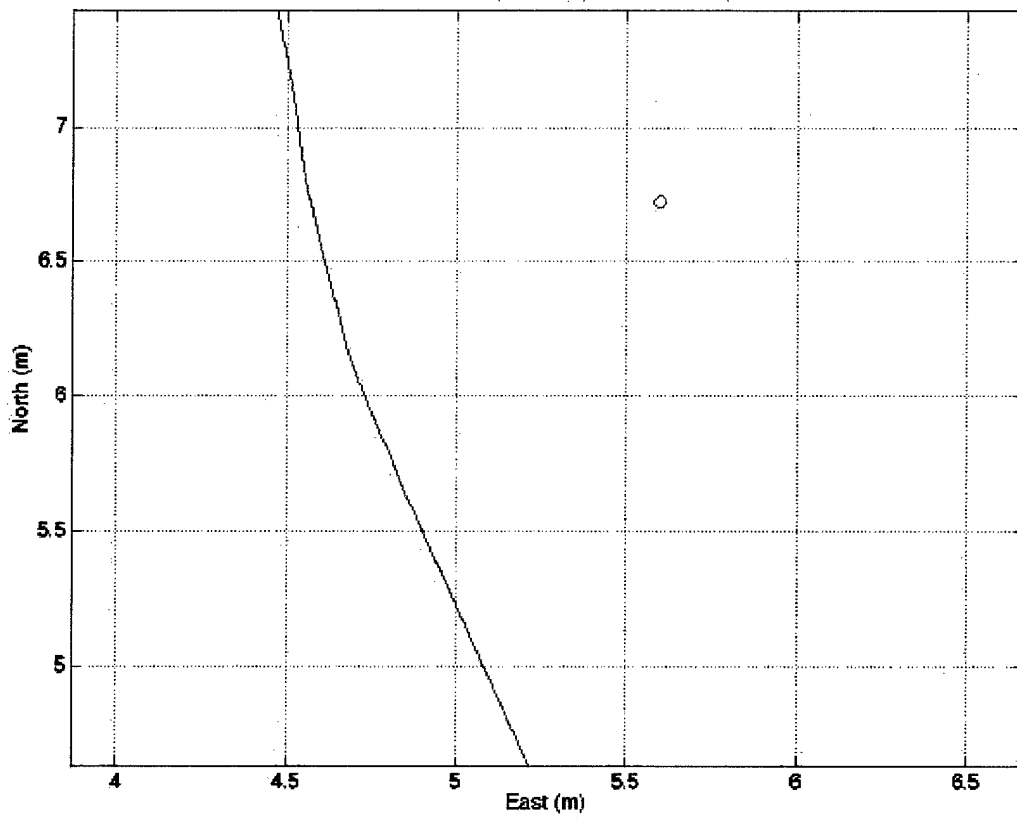
AUV Position (meters) (19990813.1844)



AUV Position (meters) (19990813.1853)



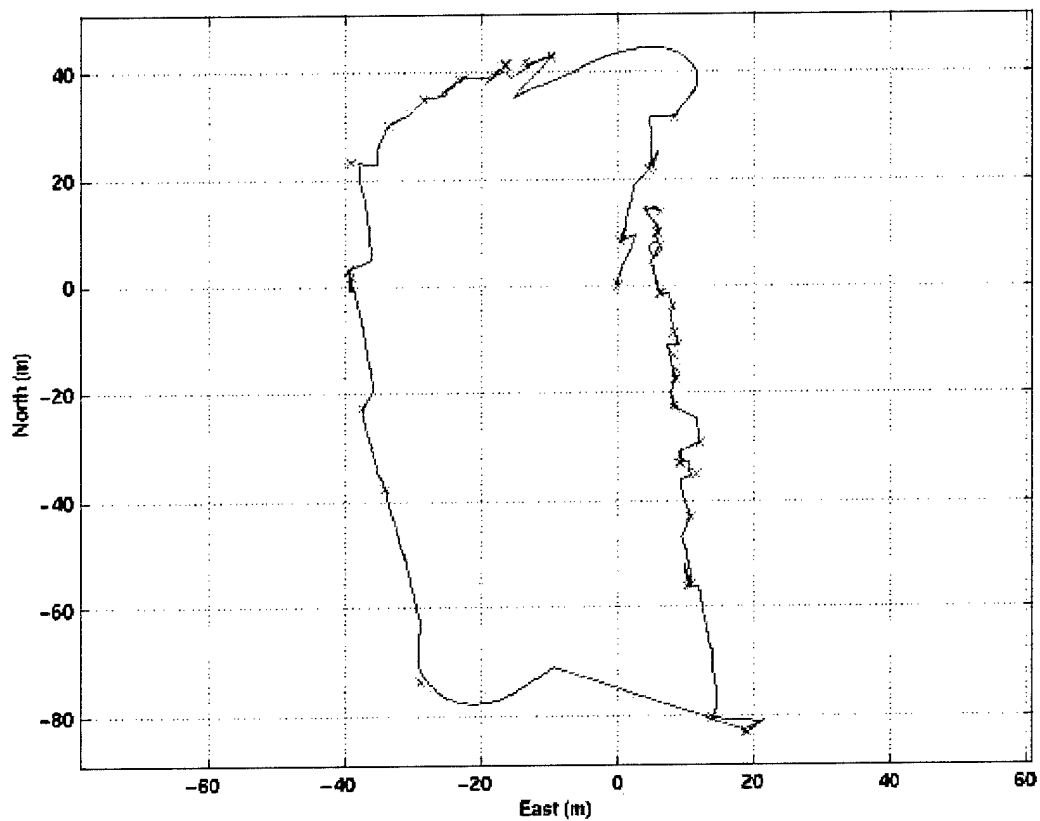
AUV Position (meters) (19990813.1853)



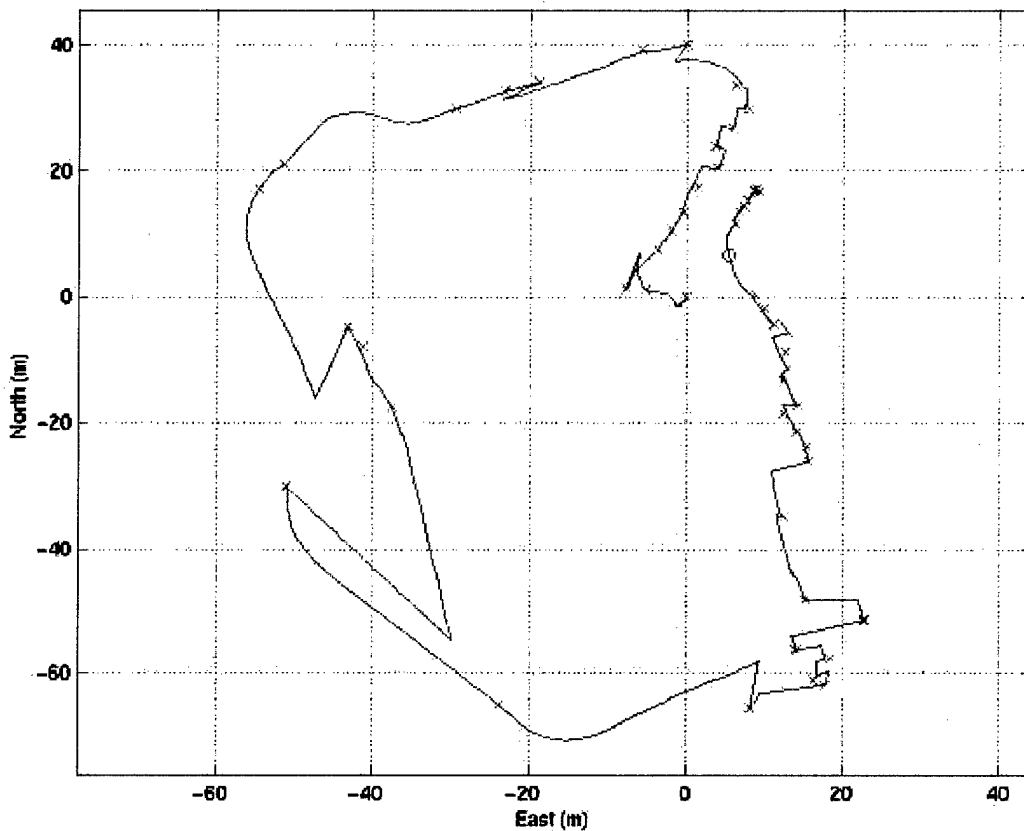
AUV Position Mission 1828



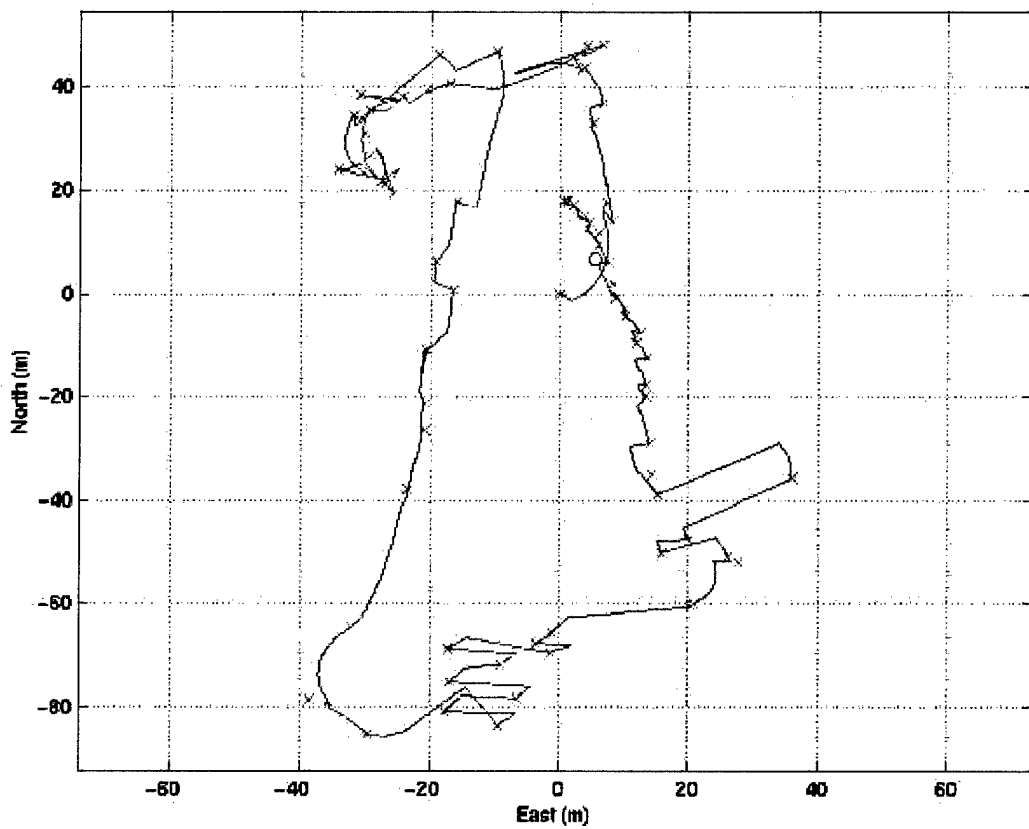
AUV Position Mission 1837



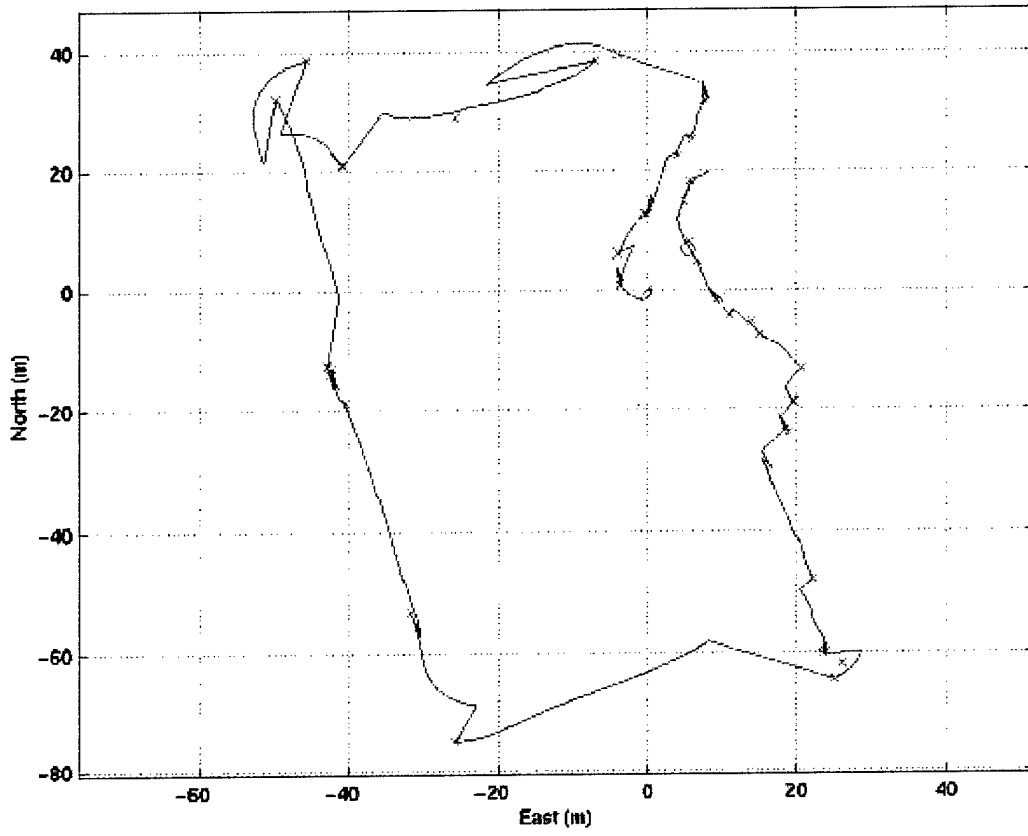
AUV Position Mission 1847



AUV Position Mission 1855



AUV Position Mission 1906



Appendix 3.6

A3.6.1. Macroinvertebrate Inventory Table

Inventory table of the benthic macroinvertebrates found within the SFOMC range. ("X" indicates taxa found within range during renourishment projects; "O" during survey dives; "H" found off Hollywood Beach; "FL" off Ft. Lauderdale; and "*" on shoreline hardgrounds.)

| Taxon | Sediment | | Taxon | Sediment | |
|---------------------------------------|----------|----------|----------------------------------|----------|----------|
| | inshore | offshore | | inshore | offshore |
| Phylum PORIFERA | | | <i>Aplysina fulva</i> | O | |
| Class DEMOSPONGIAE | | | <i>Aplysina lacunosa</i> | X | |
| <i>Cinachyra alloclada</i> | H | | <i>Verongula rigida</i> | O | |
| <i>Anthosigmella varians</i> | X | | <i>Pseudoceratina crassa</i> | H | |
| <i>Cliona delitrix</i> | O | | <i>Agelas clathrodes</i> | H | |
| <i>Spirastrella coccinea</i> | X | | <i>Agelas conifera</i> | X | |
| <i>Terpios aurantiaca</i> | O | | Phylum CNIDARIA | | |
| ? <i>Timea</i> sp. | X | | Class HYDROZOA | | |
| <i>Chondrilla nucula</i> | X | | <i>Eudendrium</i> sp. A | O | |
| <i>Chondrosia reniformis</i> | H | | <i>Eudendrium</i> sp. B | O | |
| <i>Didiscus</i> sp. | H | | <i>Campanularia</i> sp. | O | |
| <i>Ectyoplasia ferox</i> | O | | <i>Millepora alcicornis</i> | X | |
| <i>Dictyonella (=Ulosa) ruetzleri</i> | X | | Class SCYPHOZOA | | X |
| <i>Pseudaxinella lunaecharta</i> | X | | <i>Scyphistoma polyyps?</i> | | |
| <i>Teichaxinella morchella</i> | X | | Class OCTOCORALLIA | | |
| <i>Homaxinella rudis</i> | X | | <i>Erythropodium caribaeorum</i> | X | |
| <i>Iotrochota birotulata</i> | X | | <i>Iciligorgia schrammi</i> | O | |
| <i>Desmapsamma anchorata</i> | H | | <i>Briareum asbestinum</i> | X | |
| <i>Strongylacidon</i> sp. | O | | <i>Eunicea asperula</i> | X | |
| <i>Mycale</i> sp. | H | | <i>Eunicea calyculata</i> | X | |
| <i>Rhaphidophlus juniperinus</i> | X | | <i>Eunicea clavigera</i> | X | |
| <i>Haliclona</i> sp. | X | | <i>Eunicea fusca</i> | X | |
| <i>Amphimedon compressa</i> | X | | <i>Eunicea knighti</i> | X | |
| <i>Niphates erecta</i> | X | | <i>Eunicea mammosa</i> | X | |
| <i>Niphates digitalis</i> | X | | <i>Eunicea palmeri</i> | H | |
| <i>Callyspongia fallax</i> | X | | <i>Eunicea succinea</i> | X | |
| <i>Callyspongia plicifera</i> | X | | <i>Eunicea tourneforti</i> | X | |
| <i>Callyspongia vaginalis</i> | X | | <i>Muricea muricata</i> | X | |
| <i>Xestospongia muta</i> | X | | <i>Muricea elongata</i> | H | |
| <i>Ircinia campana</i> | X | | <i>Muriceopsis petila</i> | H | |
| <i>Ircinia felix</i> | X | | <i>Plexaurella fusifera</i> | H | |
| <i>Ircinia strobilina</i> | X | | <i>Plexaurella grisea</i> | H | |
| <i>Dysidea etheria</i> | X | | <i>Plexaura flexuosa</i> | X | |
| <i>Aplysina cauliformis</i> | X | | <i>Pseudoplexaura porosa</i> | O | |
| <i>Aplysina fistularis</i> | X | | <i>Gorgonia ventalina</i> | X | |
| | | | <i>Pseudopterogorgia acerosa</i> | X | |

| Taxon | Sediment | | Taxon | Sediment | |
|------------------------------------|----------|----------|------------------------------------|----------|----------|
| | inshore | offshore | | inshore | offshore |
| <i>Pseudopterogorgia americana</i> | X | | Unidentified coelogynopoid | H | |
| <i>Pterogorgia anceps</i> | H | | Unidentified bothrioplanid | H | |
| <i>Pterogorgia citrina</i> | X | | Unidentified monocelidid | H | |
| <i>Pterogorgia guadalupensis</i> | H | | Unidentified nematoplanid | H | |
| Class ZOANTHARIA | | | Unidentified otoplanid | H | |
| <i>Palythoa caribaeorum</i> | X | | Unidentified philosyrtine | X | H |
| <i>Zoanthus sociatus</i> | X | | Unidentified proseriate | X | |
| <i>Parazoanthus swiftii</i> | O | | Unidentified acoel | H | |
| <i>Ricordea florida</i> | X | | Unidentified typhloplanid | H | |
| <i>Acropora cervicornis</i> | X | | Unidentified kalyptorhynchid | X | X |
| <i>Agaricia agaricites</i> | X | | Unidentified polyclad | | |
| <i>Agaricia ?fragilis</i> | O | | Phylum NEMERTINA | | |
| <i>Agaricia lamarcki</i> | X | | Class ANOPLA | | X |
| <i>Leptoseris cucullata</i> | O | | <i>Cephalothrix</i> sp. A | X | H |
| <i>Stephanocoenia michelini</i> | X | | <i>Cephalothrix</i> sp. 114 | X | H |
| <i>Eusmilia fastigiata</i> | X | X | <i>Procephalothrix spiralis?</i> | X | X |
| <i>Sphenotrochus</i> sp. | | X | <i>?Procephalothrix</i> sp. | X | H |
| <i>Colpophyllia natans</i> | O | | <i>Carinoma</i> sp. A | X | |
| <i>Diploria clivosa</i> | X | | <i>Carinoma tremaphoros</i> | X | X |
| <i>Diploria labyrinthiformis</i> | H | | <i>Carinomella lactea</i> | X | X |
| <i>Diploria strigosa</i> | X | | <i>Hubrechtella dubia</i> | X | X |
| <i>Montastrea annularis</i> | X | | <i>Tubulanus pellucidus</i> | X | X |
| <i>Montastrea cavernosa</i> | X | | <i>Tubulanus rhabdotus</i> | | X |
| <i>Montastrea faveolata</i> | O | | Paleonemertean sp. 2 | X | X |
| <i>Montastrea franksi</i> | O | | Paleonemertean sp. 3 | H | X |
| <i>Solenastrea bournoni</i> | X | | Paleonemertean sp. 4 | X | X |
| <i>Solenastrea hyades</i> | H | | Paleonemertean sp. 5 | X | X |
| <i>Dichocoenia stokesi</i> | X | | Paleonemertean sp. 6 | | |
| <i>Meandrina meandrites</i> | X | | Paleonemertean sp. 103 | X | |
| <i>Isophyllia sinuosa</i> | O | | Paleonemertean sp. A | X | H |
| <i>Scolymia</i> sp. | X | | <i>?Cerebratulus lineolatus</i> | X | |
| <i>Oculina diffusa</i> | O | | <i>?Cerebratulus leucopsis</i> | X | X |
| <i>Madracis decactis</i> | X | | <i>Cerebratulus</i> sp. | | X |
| <i>Porites astreoides</i> | X | | <i>Baseodiscus</i> sp. | H | X |
| <i>Porites porites</i> | X | | <i>Micrura</i> sp. | X | |
| <i>Astrangia solitaria</i> | H | | Heteronemertean sp. 2 (juv) | X | X |
| <i>Siderastrea radians</i> | X | | Heteronemertean sp. 3 | | H |
| <i>Siderastrea siderea</i> | X | | Unidentified drepanophorid | | |
| <i>Bartholomea annulata</i> | O | | <i>?Prostomatella enteroplecta</i> | X | H |
| <i>Condylactis gigantea</i> | O | X | <i>Tetrastemma worki</i> | X | |
| Unidentified ?edwardsiid | | | Hoploneimertean sp. 1 | X | X |
| Phylum | | | Hoploneimertean sp. 2 | X | |
| PLATYHELMINTHES | | | Hoploneimertean sp. 3 | X | X |
| Class TURBELLARIA | | X | Hoploneimertean sp. 5 | | H |
| <i>?Coelogynopora</i> sp. | | H | 4-eye Hoplonemertean | X | |

| Taxon | Sediment | | Taxon | Sediment | |
|---------------------------------------|----------|----------|--------------------------------------|----------|----------|
| | inshore | offshore | | inshore | offshore |
| Phylum PRIAPULA | | X | <i>Prionospio steenstrupi</i> | | X |
| <i>Tubiluchus corallicola</i> | X | | <i>Pseudopolydora</i> sp. A | X | |
| Phylum ANNELIDA | | | <i>Scolecopsis acmeceps</i> | X | X |
| Class POLYCHAETA | | X | <i>Scolecopsis squamata</i> | X | X |
| <i>Orbinia riseri</i> | | H | <i>Scolecopsis texana</i> | X | X |
| <i>Scoloplos acmeceps</i> | | X | <i>Spio pettiboneae</i> | X | H |
| <i>Scoloplos capensis</i> | | X | <i>Magelona pettiboneae</i> | | H |
| <i>Scoloplos rubra</i> | | | <i>Magelona</i> sp. B | | X |
| <i>Scoloplos</i> sp. B | X | H | <i>Magelona</i> sp. C | X | H |
| <i>Naineris bicomis</i> | | H | <i>Magelona</i> sp. G | | H |
| <i>Leitoscoloplos fragilis</i> | | X | <i>Magelona</i> sp. H | | X |
| <i>Aricidea</i> cf. <i>catherinae</i> | X | X | <i>Poecilochaetus johnsoni</i> | X | H |
| <i>Aricidea cerrutii</i> | X | X | Unidentified chaetopterid (juv) | | X |
| <i>Aricidea fragilis</i> | X | X | <i>Caulleriella</i> cf. <i>alata</i> | | H |
| <i>Aricidea philbinae</i> | | X | <i>Caulleriella killariensis</i> | | X |
| <i>Aricidea taylori</i> | H | H | <i>Caulleriella</i> sp. A | | X |
| <i>Arcidea suecica</i> | | X | <i>Caulleriella</i> sp. C | | X |
| <i>Arcidea</i> sp. A | | X | <i>Caulleriella</i> sp. D | X | H |
| <i>Arcidea</i> sp. C | | | <i>Chaetozone setosa</i> | | X |
| <i>Cirrophorus branchiatus</i> | X | X | <i>Chaetozone</i> sp. B | | X |
| <i>Cirrophorus lyra</i> | X | X | <i>Cirriiformia</i> sp. A | | H |
| <i>Levinsenia gracilis</i> | | H | <i>Dodecaceria</i> sp. A | | |
| <i>Paraonis fulgens</i> | X | H | <i>Macrochaeta</i> sp. A | X | X |
| <i>Paraonis pygoenigmatica</i> | X | | <i>Monticellina dorsobranchialis</i> | H | H |
| <i>Questa caudicirra</i> | X | X | <i>Tharyx marioni</i> | | X |
| <i>Raphidrilus nemasoma</i> | X | H | <i>Capitella capitata</i> | X | X |
| <i>Ctenodrilus serratus</i> | | | <i>Dasybranchus lunulatus</i> | | X |
| <i>Ctenodrilus</i> sp. A | X | H | ? <i>Decamastus</i> sp. | | H |
| <i>Cossura soyeri</i> | | X | <i>Leiocapitella</i> sp. A | X | X |
| <i>Aonides mayaguezensis</i> | | X | <i>Mastobranchus</i> sp. A | | X |
| <i>Aonides paucibranchiata</i> | X | X | <i>Mastobranchus</i> sp. B | | |
| <i>Apoprionospio dayi</i> | X | | <i>Mediomastus californiensis</i> | X? | H |
| <i>Apoprionospio pygmaea</i> | X | H | <i>Notomastus americanus</i> | | X |
| <i>Dispio uncinata</i> | X | H | <i>Notomastus daueri</i> | | X |
| <i>Malacoceros vanderhorstii</i> | X | X | <i>Notomastus hemipodus</i> | | X |
| <i>Malacoceros</i> sp. A | | X | <i>Notomastus latericeus</i> | H | X |
| <i>Minuspio</i> sp. A | | X | <i>Notomastus tenuis</i> | | X |
| <i>Paraprionospio pinnata</i> | | | <i>Scyphoproctus platyproctus</i> | H | X |
| <i>Polydora cornuta</i> | H | | <i>Axiiothella mucosa</i> | | X |
| <i>Polydora tetrabranchia</i> | H | H | <i>Axiiothella</i> sp. A | X | X |
| <i>Polydora websteri</i> | | X | <i>Boguea enigmatica</i> | X | X |
| <i>Prionospio cristata</i> | X | H | <i>Euclymene</i> sp. | | |
| <i>Prionospio heterobranchia</i> | | X | <i>Arenicola</i> sp. | H | H |
| <i>Prionospio multibranchiata</i> | X | X | <i>Armandia agilis</i> | X | X |
| <i>Prionospio perkinsi</i> | | X | <i>Armandia maculata</i> | X | |

| Taxon | Sediment | | Taxon | Sediment | |
|---------------------------------|----------|----------|--------------------------------------|----------|----------|
| | inshore | offshore | | inshore | offshore |
| <i>Armandia</i> sp. A | X | X | <i>Opisthodonta</i> sp. B | | X |
| <i>Polyophthalmus</i> sp. A | | X | <i>Paraprionosyllis longicirrata</i> | X | X |
| <i>Sclerobregma stenocerum</i> | | X | <i>Pionosyllis gesae</i> | X | |
| <i>Anaitides groenlandica</i> | | X | <i>Plakosyllis quadrioculata</i> | X | |
| <i>Genetyllis castanea</i> | | X | <i>Sphaerosyllis aciculata</i> | X | |
| <i>Genetyllis</i> sp. A | | X | <i>Sphaerosyllis brevidentata</i> | X | X |
| <i>Hesionura elongata</i> | X | H | <i>Sphaerosyllis glandulata</i> | X | H |
| <i>Mystides borealis</i> | | X | <i>Sphaerosyllis longicauda</i> | | X |
| <i>Phyllodoce arenae</i> | X | X | <i>Sphaerosyllis piriferopsis</i> | | X |
| Polynoid genus A | | X | <i>Sphaerosyllis riseri</i> | X | H |
| <i>Fimbriosthenelais minor</i> | | H | <i>Sphaerosyllis taylora</i> | | X |
| <i>Sigalion arenicola</i> | | X | <i>Sphaerosyllis</i> sp. A | | H |
| <i>Sthenelais boa</i> | | X | <i>Streptosyllis pettiboneae</i> | X | |
| <i>Sthenelanella</i> sp. A | | X | <i>Syllides bansei</i> | X | H |
| <i>Thalenessa</i> sp. A | | X | <i>Syllides floridanus</i> | | X |
| <i>Thalenessa</i> sp. B | X | X | <i>Typosyllis amica</i> | | X |
| <i>Bhawania goodei</i> | | H | <i>Typosyllis</i> cf. <i>lutea</i> | H | X |
| <i>Bhawania heteroseta</i> | | H | <i>Typosyllis</i> sp. A | | |
| <i>Gyptis vitatta</i> | | X | <i>Typosyllis</i> sp. G | X | X |
| <i>Hesione</i> sp. | | X | <i>Typosyllis</i> sp. L | | X |
| <i>Heteropodarke lysoni</i> | X | X | <i>Ceratocephale oculata</i> | X | H |
| <i>Heteropodarke formalis</i> | X | X | <i>Ceratonereis irritabilis</i> | X | H |
| <i>Kefersteinia</i> sp. A | | | <i>Ceratonereis longicauda</i> | | X |
| <i>Microphthalmus</i> sp. A | X | X | <i>Ceratonereis mirabilis</i> | | H |
| <i>Podarke obscura</i> | X | X | <i>Ceratonereis oculata</i> | H | H |
| <i>Podarkeopsis levifuscina</i> | X | H | <i>Ceratonereis versipedata</i> | | X |
| <i>Litocorsa</i> sp. A | | X | <i>Ceratonereis</i> sp. A | | |
| <i>Pilargis</i> sp. | | X | <i>Neanthes</i> sp. A | H | |
| <i>Sigambra tentaculata</i> | | X | <i>Neanthes acuminata</i> | X | H |
| <i>Synelmis</i> sp. B | X | X | <i>Nereis falsa</i> | | X |
| <i>Autolytus</i> sp. A | | X | <i>Platynereis dumerilii</i> | | X |
| <i>Brania clavata</i> | | | <i>Glycera abranchiata</i> | X | X |
| <i>Brania swedmarki</i> | X | H | <i>Glycera americana</i> | X | X |
| <i>Brania wellfleetensis</i> | X | X | <i>Glycera</i> sp. A | X | X |
| <i>Brania</i> sp. A | | X | <i>Glycera</i> sp. B | | X |
| <i>Dentatisyllis carolinae</i> | X | X | <i>Glycera</i> sp. C | | |
| <i>Ehlersia cornuta</i> | X | X | <i>Glycinde solitaria</i> | X | H |
| <i>Ehlersia ferrugina</i> | | | <i>Goniada littorea</i> | | X |
| <i>Exogone atlantica</i> | H | X | <i>Goniada maculata</i> | H | X |
| <i>Exogone dispar</i> | | X | <i>Goniada teres</i> | | X |
| <i>Exogone lourei</i> | H | H | <i>Goniadella</i> sp. A | | X |
| <i>Grubeosyllis clavata</i> | | X | <i>Goniadides carolinae</i> | | X |
| <i>Haplosyllis spongicola</i> | H | | <i>Inermonephtys inermis</i> | | |
| <i>Odontosyllis enopla</i> | X | H | <i>Nephtys simoni</i> | X | |
| | | | <i>Pisione remota</i> | X | X |

| Taxon | Sediment | | Taxon | Sediment | |
|------------------------------------|----------|----------|--------------------------------------|----------|----------|
| | inshore | offshore | | inshore | offshore |
| <i>Pisone</i> sp. A | | X | <i>Terebellides stroemi</i> | | X |
| <i>Chloeia viridis</i> | | X | <i>Trichobranchus glacialis</i> | | H |
| <i>Paramphinome</i> sp. B | X | H | <i>Bogoea enigmatica</i> | | H |
| <i>Pseudeurythoe</i> sp. | | H | Unidentified bogueid | | H |
| <i>Eunice</i> sp. A | | H | <i>Branchiomma nigromaculata</i> | | X |
| <i>Lysidice ninetta</i> | | X | <i>Chone</i> cf. <i>americana</i> | X | X |
| <i>Lysidice</i> sp. A | | X | <i>Demonax microphthalmus</i> | | H |
| <i>Marphysa</i> sp. A | | X | <i>Fabricia</i> sp. A | | X |
| <i>Nematonereis hebes</i> | X | H | <i>Fabricinuda trilobata</i> | X | X |
| <i>Diopatra cuprea</i> | | X | <i>Jasmineira</i> sp. | | X |
| <i>Kinbergonuphis</i> sp. A | | X | <i>Megalomma heterops</i> | | X |
| <i>Mooreonuphis pallidula</i> | X | X | <i>Megalomma pigmentum</i> | | X |
| <i>Lumbrinerides dayi</i> | X | | <i>Notaulax nudicollos</i> | | H |
| <i>Lumbrineris latreila</i> | X | | <i>Sabella melanostigma</i> | | X |
| <i>Lumbrineris tetraura</i> | X | X | <i>Sabellastarte magnifica</i> | X | H |
| <i>Lumbrineris tenuis</i> | X | X | <i>Sabellastarte</i> sp. A | | |
| <i>Lumbrineris verillii</i> | | | <i>Filograna huxleyi</i> | O | |
| <i>Lumbrinereis</i> sp. A | X | | <i>Pomatostegus stellatus</i> | X | |
| <i>Arabella multidentata</i> | X | X | <i>Spirobranchus giganteus</i> | X | X |
| <i>Arabella mutans</i> | X | X | <i>Vermiliopsis</i> sp. | | |
| <i>Drilonereis longa</i> | X | | Class OLIGOCHAETA | | X |
| <i>Drilonereis</i> sp. B | H | X | <i>Bathyrilus adriaticus</i> | X | |
| <i>Dorvillea sociabilis</i> | X | X | <i>Bathyrilus ?macroprostatus</i> | X | X |
| <i>Eliberidens forceps</i> | | X | <i>Heterodrilus bulbiporous</i> | X | |
| <i>Pettibonia duofurca</i> | X | X | <i>Heterodrilus paucifascis</i> | X | X |
| <i>Protodorvillea kefersteini</i> | X | H | <i>Heterodrilus pentcheffi</i> | X | X |
| <i>Schistomeringos pectinata</i> | | X | <i>Heterodrilus</i> n. sp. CBC | | X |
| <i>Schistomeringos rudolphi</i> | X | X | <i>Inanidrilus leukodermatus</i> | X | X |
| <i>Galathowenia oculata</i> | | H | <i>Limnodriloides appendiculatus</i> | | H |
| <i>Myriochele oculata</i> | | X | <i>Limnodriloides monotheucus</i> | | |
| <i>Therochaeta</i> sp. A | | | <i>Olavius caudatus</i> | X | |
| <i>Pherusa inflata</i> | | H | <i>Olavius longissimus</i> | X | X |
| <i>Phragmatopoma lapidosa</i> | H* | H | <i>Olavius tenuissimus</i> | X | H |
| <i>Pectinaria gouldii</i> | | X | <i>Olavius imperfectus</i> | H | X |
| <i>Amphicteis scaphobranchiata</i> | | X | <i>Olavius</i> sp. A | | H |
| <i>Samytha</i> sp. A | | H | <i>Olavius</i> sp. T | X | H |
| <i>Ameaena trilobata</i> | | X | <i>Olavius/Inanidrilus</i> sp. | X | |
| <i>Glossothelopsis</i> sp. A | | X | <i>Pectinodrilus molestus</i> | X | |
| <i>Pista cristata</i> | | H | <i>Phalldrilus acochlearis</i> | X | X |
| <i>Pista quadrilobata</i> | | X | <i>Phalldrilus sabulosus</i> | | H |
| <i>Polycirrus carolinensis</i> | X | X | <i>Smithsonidrilus luteolus</i> | | H |
| <i>Polycirrus plumosus</i> | X | H | <i>Smithsonidrilus marinus</i> | | H |
| <i>Polycirrus</i> sp. B | | H | <i>Tectidrilus bori</i> | | |
| <i>Scionella</i> sp. A | | X | <i>Tectidrilus squalidus</i> | X | |

| Taxon | Sediment | | Taxon | Sediment | |
|---|----------|----------|----------------------------------|----------|----------|
| | inshore | offshore | | inshore | offshore |
| <i>Tectidrilus verrucosus</i> | | X | <i>Amphithalamus vallei</i> | | X |
| <i>Grania</i> sp. A | | X | <i>Aclis</i> sp. | | X |
| Phylum PHORONA | | | <i>Bermudaclis</i> sp. | | X |
| <i>Phoronis architecta</i> | | | <i>Polygyreulima</i> sp. | | X |
| Phylum SIPUNCULA | | | <i>Calyptraea centralis</i> | | |
| <i>Siphonosoma</i> cf. <i>cumanense</i> | | | <i>Cypraea cervus</i> | O | |
| <i>Sipunculus nudus</i> | | | <i>Cyphoma gibbosum</i> | O | H |
| Unidentified golfingiid (juv) | | | Unidentified naticid (juv) | | |
| <i>Phascolion</i> sp. A | H | X | <i>Murex pomum</i> | | O |
| ? <i>Phascolosoma</i> sp. (juv) | | X | <i>Pleuroploca gigantea</i> | | |
| <i>Apionsoma misakiana</i> | | | <i>Olivella mutica</i> | | H |
| <i>Aspidosiphon albus</i> | X | | <i>Vasum muricatum</i> | O | X |
| <i>Aspidosiphon fischeri</i> | X | X | <i>Granulina ovuliformis</i> | | X |
| <i>Aspidosiphon</i> cf. <i>parvulus</i> | | X | <i>Marginella apicina</i> | | X |
| <i>Aspidosiphon</i> sp. A | X | X | <i>Marginella eburneola</i> | | X |
| <i>Aspidosiphon</i> sp. B | X | X | <i>Marginella hartleyana</i> | | X |
| <i>Aspidosiphon</i> sp. C | | X | <i>Marginella lavalleana</i> | | X |
| <i>Paraspidosiphon</i> sp. | | X | <i>Kurtziella atrostyla</i> | | X |
| <i>Centrosiphon</i> sp. | | | ? <i>Cryoturris</i> sp. | | X |
| Phylum MOLLUSCA | | | <i>Vitricythara metria</i> | | X |
| Class POLYPLACOPHORA | | | <i>Acteocina candei</i> | | X |
| <i>Acanthochitona</i> sp. | | H | <i>Acteocina inconspicua</i> | | X |
| <i>Lepidozona</i> sp. | | X | <i>Atys sandersoni</i> | | X |
| Class SCAPHOPODA | | | <i>Atys riiseana</i> | | |
| <i>Dentalium calamus</i> | X | X | ? <i>Haminoea</i> sp. | | X |
| <i>Dentalium laqueatum</i> | | X | <i>Retusa sulcata</i> | | X |
| <i>Cadulus tetrodon</i> | | | <i>Volvulella persimilis</i> | | X |
| Class GASTROPODA | | | <i>Cylindrobulla beauui</i> | | X |
| <i>Diodora cayenensis</i> | O | | <i>Cylichnella bidentata</i> | | H |
| <i>Diodora listeri</i> | O | | <i>Hypselodoris bayeri</i> | O | |
| <i>Diodora sayi</i> | O | X | <i>Hypselodoris edenticulata</i> | O | |
| <i>Fissurella</i> sp. | | X | Class BIVALVIA | | X |
| <i>Arene tricarinata</i> | | | <i>Solemya occidentalis</i> | | |
| <i>Tricolia affinis</i> | X | O | <i>Arcopsis adamsi</i> | O | |
| <i>Architectonica nobilis</i> | | H | <i>Barbatia cancellaria</i> | O | |
| <i>Cerithiopsis emersoni</i> | | | <i>Barbatia candida</i> | | X |
| <i>Cerithium litteratum</i> | H | X | <i>Barbatia domingensis</i> | | X |
| <i>Finella dubia</i> | | | <i>Branchiodontes modiolus</i> | | H |
| <i>Teinostoma clavium</i> | X | X | <i>Lithophaga antillarum</i> | O | |
| <i>Caecum imbricatum</i> | | H | <i>Modiolus americanus</i> | | O |
| <i>Caecum pulchellum</i> | X | H | <i>Pteria colymbus</i> | O | |
| <i>Meioceras cubitatum</i> | | X | <i>Pinctada imbricata</i> | O | |
| <i>Meioceras nitidum</i> | | X | <i>Spondylus americanus</i> | X | |
| <i>Vermicularia knorri</i> | O | | <i>Lima scabra</i> | O | |
| | | | <i>Lima lima</i> | O | |

| Taxon | Sediment | | Taxon | Sediment | |
|---------------------------------|----------|----------|-------------------------------------|----------|----------|
| | inshore | offshore | | inshore | offshore |
| <i>Limatula hendersoni</i> | | X | Phylum BRYOZOA | | X |
| <i>Lopha frons</i> | O | | <i>Cupuladria</i> sp. | X | |
| <i>Chione cancellata</i> | | X | Phylum BRACHIOPODA | | H |
| <i>Chione</i> sp. A | | X | <i>Lingula</i> sp. | | |
| <i>Gouldia cerina</i> | | H | Phylum ARTHROPODA | | |
| <i>Parastarte triquetra</i> | | H | Subphylum CHELICERATA | | |
| <i>Pitar simpsoni</i> | | | Class PYCNOGONIDA | | X |
| <i>Tivela floridana</i> | | X | Unidentified pycnogonid | | |
| <i>Transennella cubaiana</i> | | X | Class ARACHNIDA | | H |
| <i>Parvilucina multilineata</i> | | | Unidentified acarine | X | |
| <i>Lucina</i> sp. | | | Subphylum CRUSTACEA | | |
| <i>Diplodonta semiaspera</i> | | | Class OSTRACODA | | X |
| <i>Chama</i> sp. | | | <i>Actinoseta chelisparsa</i> | | X |
| Unidentified sportellid | | H | <i>Asteropella punctata</i> | | |
| Unidentified leptonid | | | <i>Parasterope muelleri</i> | X | H |
| <i>Cyclocardia</i> sp. | | | <i>Prionotoleberis salomani</i> | X | X |
| <i>Pleuromeris tridentata</i> | | X | <i>Harbansus paucichelatus</i> | X | X |
| <i>Pteromeris perplana</i> | | X | <i>Rutiderma darbyi</i> | X | X |
| <i>Carditopsis smithi</i> | | X | <i>Rutiderma mollitum</i> | | |
| <i>Crassinella dupliniana</i> | | X | <i>Euryphlus rousei</i> | X | X |
| <i>Americardia media</i> | | X | <i>Bairdia</i> sp. | | |
| <i>Laevicardium</i> sp. | | | Class MALACOSTRACA | | X |
| <i>Ervilia concentrica</i> | | X | <i>Nannosquilla schmitti</i> | | X |
| ? <i>Solen</i> sp. | | | <i>Alima hyalina</i> | | X |
| <i>Strigilla mirabilis</i> | | X | <i>Eurysquilla plumata</i> | | |
| <i>Tellina consobrina</i> | | | <i>Gonodactylus oerstedii</i> | O | X |
| <i>Tellina fausta</i> | | O | <i>Caprella pentantis</i> | | H |
| <i>Tellina gouldi</i> | | X | <i>Ampelisca abdita</i> | | X |
| <i>Tellina iris</i> | | X | <i>Ampelisca agassizi</i> | | X |
| <i>Tellina listeri</i> | | O | <i>Ampelisca bicarinata</i> | | |
| <i>Tellina ?probina</i> (juv) | | | <i>Amphilocheus neopolitanus</i> | X | |
| <i>Tellina promera</i> | | | <i>Anamixis cavitura</i> | FL | H |
| <i>Tellina sybaritica</i> | | | <i>Acuminodeutopus</i> sp. | | X |
| <i>Tellina texana</i> | | | <i>Amphideutopus</i> | | X |
| <i>Tellina versicolor</i> | | | <i>dolichocephalus</i> | | |
| <i>Cumingia tellinoides</i> | | H | <i>Amphideutopus</i> sp. A | | X |
| <i>Semele bellastrata</i> | | | <i>Bemlos unifasciatus reductus</i> | | X |
| <i>Corbula krebsiana</i> | | | <i>Batea catharinensis</i> | X | |
| <i>Varicorbula oporculata</i> | | | <i>Carinobatea catharinensis</i> | H | |
| <i>Spengleria rostrata</i> | | | <i>Cerapus</i> sp. | X | |
| <i>Bushia elegans</i> | | | <i>Chevalia</i> sp. | FL | H |
| <i>Verticordia ornata</i> | | | <i>Grandidierella bonnieroides</i> | | H |
| <i>Teinostoma clavium</i> | | H | Unidentified corophiid n.sp. | | |
| | | | <i>Hoplophenoides obesa</i> | FL | X |
| | | | <i>Tethygenia</i> sp. | | |

| Taxon | Sediment | | Taxon | Sediment | |
|----------------------------------|----------|----------|--|----------|----------|
| | inshore | offshore | | inshore | offshore |
| <i>Elasmopus balkomanus</i> | FL | | <i>Microcharon</i> sp. | | X |
| <i>Elasmopus levis</i> | | | <i>Epicaridium carva</i> | | X |
| <i>Maera</i> sp. | | | <i>Cyclaspis bacescui</i> | | X H |
| <i>Acanthohaustorius pansus</i> | | X | <i>Cyclaspis</i> cf. <i>longipes</i> | | X H |
| <i>Bathyporeia parkeri</i> | | X H | <i>Cyclaspis</i> cf. <i>pustulata</i> | | X H |
| <i>Haustorius</i> n. sp. A | | X | <i>Cyclaspis unicornis</i> | | H |
| <i>Panahaustorius holmesi</i> | | X X | <i>Cyclaspis</i> cf. <i>varians</i> | | X |
| <i>Chevalia aviculae</i> | | | <i>Cyclaspis</i> cf. <i>striata/bacescui</i> | | X |
| <i>Chevalia carpenteri</i> | | | <i>Cyclaspis</i> sp. A | | X X |
| <i>Erichthonius brasiliensis</i> | FL | | <i>Cyclaspis</i> sp. B | | X X |
| <i>Lysianassa cubensis</i> | | X X | <i>Cyclaspis</i> sp. C | | H |
| <i>Gibberosus myersi</i> | | X X | <i>Cyclaspis</i> sp. D | | X |
| Neomegamphopidae sp. A | | | <i>Cyclaspis</i> n. sp. E | | X H |
| Neomegamphopidae sp. B | | | Bodotriid new genus A | | X |
| Neomegamphopidae sp. G | | | <i>Campylaspis</i> sp. A | | X |
| <i>Curidia debrogania</i> | FL | | <i>Cumella</i> sp. A | | X |
| <i>Monoculodes nyei</i> | | | <i>Cumella</i> sp. B | | |
| <i>Synchelidium americanum</i> | | | <i>Cumella</i> sp. C | | X X |
| <i>Paraphinotus seclusus</i> | FL | | <i>Nannastacus</i> sp. | | X |
| <i>Metharpinia floridana</i> | | X | <i>Leptochelia forresti</i> | | X? X |
| <i>Eudevanopus honduranus</i> | | X | <i>Leptochelia rapax</i> | | |
| <i>Polocerus kleidus</i> | FL | | <i>Tanaissus</i> sp. | | X H |
| Unidentified stenothoid | FL | | <i>Apseudes</i> sp. A | | X |
| <i>Synopia caraibica</i> | | X X | <i>Apseudes</i> sp. B | | X |
| <i>Tiron biocellatus</i> | | | <i>Apseudes</i> sp. C | | X |
| <i>Tiron triocellatus</i> | | X X | <i>Cirratodactylus floridensis</i> | | X X |
| <i>Amakusanthura magnifica</i> | | | <i>Kalliapseudes</i> sp. | | X X |
| <i>Apanthura cracenta</i> | | X X | Unidentified mysid | O | X X |
| <i>Apanthuretta signifca</i> | | | Unidentified penaeid (juv) | | |
| <i>Haliophasma</i> sp. | | | <i>Sicyonia dorsalis</i> | | X H |
| <i>Mesanthura pulchra</i> | | | <i>Solenocera</i> sp. | | |
| <i>Mesanthura reticulata</i> | | | <i>Stenopus hispidus</i> | O | |
| <i>Gnathia</i> sp. | | | <i>Stenopus scutellatus</i> | O | H |
| <i>Horoloanthura irpex</i> | | | <i>Automate</i> sp. | | |
| <i>Xenanthura brevitelson</i> | | H X | <i>Gnathophylloides mineri</i> | O | |
| <i>Eurydice convexa</i> | | | <i>Ogyrides alphaerostris</i> | | X |
| <i>Eurydice personata</i> | | X | <i>Periclimenes pedersoni</i> | O | X |
| <i>Ancinus braziliensis</i> | | X | <i>Leptochela populata</i> | | |
| <i>Ancinus depressus</i> | | X | <i>Processa</i> sp. | | X H |
| <i>Exosphaeroma diminuta</i> | | X H | Callianassid new genus | | X X |
| <i>Exosphaeroma</i> | | | <i>Upogebia</i> sp. | | H |
| <i>productatelson</i> | | | Unidentified nephropid (juv.) | | |
| ? <i>Paradella</i> sp | | X | <i>Panulirus argus</i> | O | |
| <i>Carpias</i> sp. | | X | <i>Emerita talpoida</i> | | O H |
| | | | <i>Albunea gibbesii</i> | | X |

| Taxon | Sediment | | Taxon | Sediment | |
|---------------------------------|----------|----------|---------------------------------|----------|----------|
| | inshore | offshore | | inshore | offshore |
| <i>Zygopa michaelis</i> | | | <i>Mellita isometra</i> | | O |
| <i>Dardanus venosus</i> | O | X | <i>Meoma ventricosa</i> | O | |
| Unidentified pagurid | | H | Class OPHIUROIDEA | | |
| <i>Cycloes bairdii</i> | | X | <i>Astrophyton muricatum</i> | O | |
| <i>Trapezioplax tridentata</i> | | H | <i>Ophioderma rubicunda</i> | O | |
| <i>Ebalia stimpsonii</i> | | | <i>Ophiactis quinqueradiala</i> | O | |
| <i>Ocypode quadrata</i> | | O | <i>Ophiactis savignyi</i> | O | |
| <i>Batrachonotus fragosus</i> | | X | <i>Ophionereis reticulata</i> | O | |
| <i>Hemus cristulipes</i> | | | <i>Ophiocoma echinata</i> | O | |
| <i>Mithrax holderi</i> | O | | <i>Ophiocoma pumila</i> | O | |
| <i>Pelia mutica</i> | O | | <i>Ophiocoma wendti</i> | O | |
| <i>Stenorhynchus seticornis</i> | O | | <i>Ophiolepis impressa</i> | O | |
| <i>Pinnixa cristata</i> | | X | <i>Ophiothrix angulata</i> | | |
| <i>Pinnixa ?floridana</i> | | X | <i>Ophiothrix suensonii</i> | O | |
| <i>Pinnixa gorei</i> | | X | Class HOLOTHUROIDEA | | O |
| Subphylum HEXAPODA | | | <i>Astichopus multifidus</i> | | |
| Class INSECTA | | X | Phylum CHORDATA | | |
| <i>Pontomyia</i> sp. | | | Subphylum | | |
| Phylum HEMICHORDATA | | | UROCHORDATA | | |
| Class ENTEROPNEUSTA | | X | Class ASCIDIACEA | | |
| Unidentified enteropneust | | | <i>Distaplia</i> sp. | X | |
| Phylum | | | Unidentified didemnid | O | |
| ECHINODERMATA | | | <i>Stolonica sabulosa</i> | O | |
| Class ECHINOIDEA | | | Ascidian species A | O | |
| <i>Eucidaris tribuloides</i> | H | | Ascidian species B | O | |
| <i>Diadema antillarum</i> | O | | Ascidian species C | O | |
| <i>Tripneustes ventricosus</i> | O | | Subphylum | | X |
| <i>Echinometa lucunter</i> | H* | | CEPHALOCHORDATA | | |
| <i>Echinometra viridis</i> | O | | <i>Branchiostoma caribbeum</i> | | |
| <i>Leodia sexiesperforata</i> | | O | | | |

A3.6.2. Fish Inventory Table

Inventory table of the fishes identified within the SFOMC range. ("X" indicates species identified within range but not quantitatively sample.)

| Common Name | Taxon Scientific Name | Reef | | | |
|------------------------|---------------------------------|-------|-------|--------|-------|
| | | Total | First | Second | Third |
| FAMILY: CARPET SHARK | RHINCODONTIDAE | | | | |
| Nurse Shark | <i>Ginglymostoma cirratum</i> | 4 | 2 | 1 | 1 |
| FAMILY: GUITARFISH | RHINOBATIDAE | | | | |
| Atlantic Guitarfish | <i>Rhinobatos lentiginosus</i> | 1 | 1 | | |
| FAMILY: STINGRAY | DASYATIDAE | | | | |
| Southern stingray | <i>Dasyatis americana</i> | 1 | | 1 | |
| Yellow Stingray | <i>Urolophus jamaicensis</i> | 14 | 5 | 6 | 3 |
| FAMILY: MORAY EELS | MURAENIDAE | | | | |
| Green Moray | <i>Gymnothorax funebris</i> | X | | | |
| Purplemouth Moray | <i>Gymnothorax vicinus</i> | X | | | |
| Spotted Moray | <i>Gymnothorax moringa</i> | 1 | | | 1 |
| FAMILY: SQUIRRELFISHES | HOLOCENTRIDAE | | | | |
| Squirrelfish | <i>Holocentrus adsensionis</i> | 58 | 4 | 37 | 17 |
| Blackbar Soldierfish | <i>Myripristis jacobus</i> | 2 | | | 2 |
| FAMILY: CORNETFISHES | FISTULARIDAE | | | | |
| Bluespotted Cornetfish | <i>Fistularia tabacaria</i> | 1 | | 1 | |
| FAMILY: TRUMPETFISHES | AULOSTOMIDAE | | | | |
| Trumpetfish | <i>Aulostomus maculatus</i> | 13 | 4 | 7 | 2 |
| FAMILY: TILEFISHES | MALACANTHIDAE | | | | |
| Sand Tilefish | <i>Malacanthus plumieri</i> | 11 | | 4 | 7 |
| FAMILY: REMORA | ECHENEIDIDAE | | | | |
| Sharksucker | <i>Echeneis naucrates</i> | 1 | | 1 | |
| FAMILY: HERRINGS | CLUPEIDAE | | | | |
| Scaled Sardine | <i>Harengula jaguana</i> | 1500 | | 1000 | 500 |
| FAMILY: SEA BASSES | SERRANIDAE | | | | |
| Black Grouper | <i>Mycteroperca bonaci</i> | 4 | | 4 | |
| Scamp | <i>Mycteroperca phenax</i> | 1 | 1 | | |
| Gag | <i>Mycteroperca microlepis</i> | 3 | | 2 | 1 |
| Yellowfin Grouper | <i>Mycteroperca venenosa</i> | X | X | | |
| Red Grouper | <i>Epinephelus morio</i> | 17 | 8 | 6 | 3 |
| Graysby | <i>Epinephelus cruentatus</i> | 11 | | | 11 |
| Red Hind | <i>Epinephelus guttatus</i> | 3 | 1 | | 2 |
| Rock Hind | <i>Epinephelus adscensionis</i> | 2 | | | 2 |
| Coney | <i>Epinephelus fulvus</i> | X | | | |
| Sand Perch | <i>Diplectum formosum</i> | 25 | 8 | 16 | 1 |
| Black Hamlet | <i>Hypoplectrus nigricans</i> | X | | | |
| Butter Hamlet | <i>Hypoplectrus unicolor</i> | 90 | 3 | 53 | 34 |
| Barred Hamlet | <i>Hypoplectrus puella</i> | 1 | | 1 | |
| Blue Hamlet | <i>Hypoplectrus gemma</i> | 2 | | 1 | 1 |

| Common Name | Taxon Scientific Name | Reef | | | |
|-----------------------------|---------------------------------|-------|-------|--------|-------|
| | | Total | First | Second | Third |
| Banks Sea bass | <i>Centropristis ocyurus</i> | 8 | 6 | | 2 |
| Lantern Bass | <i>Serranus baldwini</i> | 12 | | | 12 |
| Tobaccofish | <i>Serranus tabacarius</i> | 170 | 1 | 64 | 105 |
| Chalk Bass | <i>Serranus tortugarum</i> | 241 | 25 | 120 | 96 |
| Harlequin Bass | <i>Serranus tigrinus</i> | 81 | 1 | 25 | 55 |
| Tattler | <i>Serranus phoebe</i> | 3 | | | 3 |
| FAMILY: BIGEYES | PRIACANTHIDAE | | | | |
| Bigeye | <i>Priacanthus arenatus</i> | | | | |
| FAMILY: CARDINALFISHES | APOGONIDAE | | | | |
| Flamefish | <i>Apogon maculatus</i> | 1 | | | 1 |
| Twospot Cardinalfish | <i>Apogon pseudomaculatus</i> | X | | | |
| Barred Cardinalfish | <i>Apogon binotatus</i> | X | X | | |
| FAMILY: JACKS | CARANGIDAE | | | | |
| Amberjack | <i>Seriola dumerili</i> | X | | | |
| Horse-Eyed Jack | <i>Caranx latus</i> | X | | | |
| Blue Runner | <i>Caranx crysos</i> | 56 | 5 | 37 | 14 |
| Bar Jack | <i>Caranx ruber</i> | 121 | 47 | 58 | 16 |
| Round Scad | <i>Decapterus punctatus</i> | 6 | 5 | 1 | |
| FAMILY: Flyingfish/Halfbeak | EXOCOETIDAE | | | | |
| Ballyhoo | <i>Hemiramphus brasiliensis</i> | 100 | | 100 | |
| FAMILY: SNAPPERS | LUTJANIDAE | | | | |
| Yellowtail Snapper | <i>Ocyurus chrysurus</i> | 32 | 18 | 12 | 2 |
| Schoolmaster | <i>Lutjanus apodus</i> | 3 | 1 | 2 | |
| Gray Snapper | <i>Lutjanus griseus</i> | 24 | 13 | 11 | |
| Lane Snapper | <i>Lutjanus synagris</i> | 1 | 1 | | |
| Mutton Snapper | <i>Lutjanus analis</i> | 13 | 3 | 6 | 4 |
| FAMILY: MOJARRAS | GERREIDAE | | | | |
| Yellowfin Mojarra | <i>Gerres cinereus</i> | 2 | | 2 | |
| FAMILY: GRUNTS | HAEMULIDAE | | | | |
| Cottonwick | <i>Haemulon melanurum</i> | 31 | 4 | | 27 |
| White Grunt | <i>Haemulon plumieri</i> | 413 | 236 | 115 | 62 |
| Tomtates | <i>Haemulon aurolineatum</i> | 295 | 270 | 20 | 5 |
| French Grunt | <i>Haemulon flavolineatum</i> | 1038 | 614 | 403 | 21 |
| Bluestripe Grunt | <i>Haemulon sciurus</i> | 149 | 34 | 61 | 54 |
| Smallmouth Grunt | <i>Haemulon chrysargyreum</i> | X | | | |
| Spanish Grunt | <i>Haemulon macrostomum</i> | X | | | |
| Sailors Choice | <i>Haemulon parrai</i> | 3 | 2 | 1 | |
| Grunt Sp. | <i>Haemulon sp.</i> | 549 | 539 | 10 | |
| Black Margate | <i>Anisotremus surinamensis</i> | 1 | | 1 | |
| Porkfish | <i>Anisotremus virginicus</i> | 64 | 24 | 20 | 20 |
| FAMILY: PORGIES | SPARIDAE | | | | |
| Pinfish | <i>Lagodon rhomboides</i> | X | | | |

| Common Name | Taxon Scientific Name | Reef | | | |
|-------------------------|----------------------------------|-------|-------|--------|-------|
| | | Total | First | Second | Third |
| Spottail Pinfish | <i>Diplodus holbrooki</i> | 6 | 5 | 1 | |
| Silver Porgy | <i>Diplodus argenteus</i> | 1 | 1 | | |
| Saucereye Porgy | <i>Calamus calamus</i> | 19 | 6 | 4 | 9 |
| Sheepshead Porgy | <i>Calamus penna</i> | 9 | | 9 | |
| Porgy Sp. | <i>Calamus sp.</i> | 13 | 1 | 12 | |
| FAMILY: DRUMS | SCIAENIDAE | | | | |
| Reef Croaker | <i>Odontoscion dentex</i> | 1 | | 1 | |
| Highhat | <i>Equetus acuminatus</i> | 42 | 14 | 27 | 1 |
| Jackknife fish | <i>Equetus lanceolatus</i> | 3 | 2 | 1 | |
| Spotted Drum | <i>Equetus punctatus</i> | X | | | |
| FAMILY: SWEEPER | PEMPHERIDAE | | | | |
| Glassy Sweeper | <i>Pempheris schomburgki</i> | 3 | | 3 | |
| FAMILY: GOATFISHES | MULLIDAE | | | | |
| Spotted Goatfish | <i>Pseudupeneus maculatus</i> | 62 | 16 | 10 | 36 |
| Yellow Goatfish | <i>Mulloidichthys martinicus</i> | 20 | | 20 | |
| FAMILY: SEA CHUBS | KYPHOSIDAE | | | | |
| Bermuda Chub | <i>Kyphosus sectatrix</i> | 4 | 4 | | |
| FAMILY: SPADEFISHES | EPHIPPIDAE | | | | |
| Spadefish | <i>Chaetodipterus faber</i> | 3 | 1 | 2 | |
| FAMILY: BUTTERFLYFISHES | CHAETODONTIDAE | | | | |
| Spotfin Butterflyfish | <i>Chaetodon ocellatus</i> | 39 | 1 | 12 | 26 |
| Reef Butterflyfish | <i>Chaetodon sedentarius</i> | 183 | 3 | 52 | 128 |
| Foureye Butterflyfish | <i>Chaetodon capistratus</i> | 30 | | 11 | 19 |
| Banded Butterflyfish | <i>Chaetodon striatus</i> | 20 | | 2 | 18 |
| FAMILY: ANGELFISHES | POMACANTHIDAE | | | | |
| Queen Angelfish | <i>Holocanthus ciliaris</i> | 12 | 1 | 4 | 7 |
| Blue Angelfish | <i>Holocanthus bermudensis</i> | 24 | 5 | 1 | 18 |
| Rock Beauty | <i>Holocanthus tricolor</i> | 48 | | 7 | 41 |
| French Angelfish | <i>Pomacanthus paru</i> | 63 | 5 | 45 | 13 |
| Gray Angelfish | <i>Pomacanthus arcuatus</i> | 75 | 21 | 28 | 26 |
| Cherubfish | <i>Centropyge argi</i> | 1 | | | 1 |
| FAMILY: DAMSELFISHES | POMACENTRIDAE | | | | |
| Sergeant Major | <i>Abudefduf saxatilis</i> | 96 | 11 | 80 | 5 |
| Dusky Damsel fish | <i>Stegastes fuscus</i> | 24 | 14 | 7 | 3 |
| Threespot Damsel fish | <i>Stegastes planifrons</i> | 30 | 28 | 2 | |
| Longfin Damsel fish | <i>Stegastes diencaeus</i> | 2 | | 2 | |
| Cocoa Damsel fish | <i>Stegastes variabilis</i> | 324 | 136 | 175 | 13 |
| Beaugregory | <i>Stegastes leucostictus</i> | 58 | 27 | 24 | 7 |
| Bicolor Damsel fish | <i>Stegastes partitus</i> | 1251 | 12 | 387 | 852 |
| Yellowtail Damsel fish | <i>Microspathodon chrysurus</i> | 20 | 3 | 16 | 1 |
| Sunshinefish | <i>Chromis insolatus</i> | 14 | | | 14 |
| Purple Reef fish | <i>Chromis scotti</i> | 12 | | 2 | 10 |

| Common Name | Taxon | Total | Reef | | |
|------------------------|----------------------------------|-------|-------|--------|-------|
| | Scientific Name | | First | Second | Third |
| Brown Chromis | <i>Chromis multilineatus</i> | 2 | 1 | 1 | |
| Blue Chromis | <i>Chromis cyanis</i> | 209 | | 2 | 207 |
| FAMILY: HAWKFISHES | CIRRHITIDAE | | | | |
| Redspotted Hawkfish | <i>Amblycirrhitus pinos</i> | X | | | |
| FAMILY: WRASSES | LABRIDAE | | | | |
| Hogfish | <i>Lachnolaimus maximus</i> | 28 | | 9 | 19 |
| Spotfin Hogfish | <i>Bodianus pulchellus</i> | 2 | | | 2 |
| Spanish Hogfish | <i>Bodianus rufus</i> | 15 | 1 | 7 | 7 |
| Creole Wrasse | <i>Clepticus parrai</i> | 138 | | 1 | 137 |
| Green Razorfish | <i>Hemipteronotus splendens</i> | 8 | 2 | 6 | |
| Rainbow Wrasse | <i>Halichoeres pictus</i> | 2 | 2 | | |
| Clown wrasse | <i>Halichoeres maculipinna</i> | 47 | 28 | 18 | 1 |
| Slippery Dick | <i>Halichoeres bivittatus</i> | 663 | 323 | 288 | 52 |
| Yellowcheek wrasse | <i>Halichoeres cyanocephalus</i> | 23 | | 8 | 15 |
| Puddingwife | <i>Halichoeres radiatus</i> | 10 | 2 | 3 | 5 |
| Yellowhead wrasse | <i>Halichoeres garnoti</i> | 328 | | 118 | 210 |
| Bluehead Wrasse | <i>Thalassoma bifasciatum</i> | 2023 | 474 | 931 | 618 |
| FAMILY: PARROTFISHES | SCARIDAE | | | | |
| Blue Parrotfish | <i>Scarus coeruleus</i> | 1 | | | 1 |
| Striped Parrotfish | <i>Scarus croicensis</i> | 326 | 112 | 122 | 92 |
| Princess Parrotfish | <i>Scarus taeniopterus</i> | 265 | 58 | 117 | 90 |
| Rainbow Parrotfish | <i>Scarus guacamaia</i> | 1 | | 1 | |
| Parrotfish | <i>Scarus sp.</i> | 5 | | 4 | 1 |
| Red tail Parrotfish | <i>Sparisoma chrysopterygum</i> | 30 | 4 | 21 | 5 |
| Redfin Parrot | <i>Sparisoma rubripinne</i> | 10 | 2 | 7 | 1 |
| Stoplight Parrotfish | <i>Sparisoma viride</i> | 96 | 28 | 41 | 27 |
| Greenblotch Parrotfish | <i>Sparisoma atomarium</i> | 3 | | | 3 |
| Redband Parrot | <i>Sparisoma aurofrenatum</i> | 820 | 177 | 359 | 284 |
| Parrotfish | <i>Sparisoma sp.</i> | 130 | 31 | 51 | 48 |
| FAMILY: BARRACUDAS | SPHYRAENIDAE | | | | |
| Barracuda | <i>Sphyraena barracuda</i> | 7 | 1 | | 6 |
| FAMILY: JAWFISH | OPISTHOGNATHIDAE | | | | |
| Yellowhead Jawfish | <i>Opisthognathus aurifrons</i> | 79 | | 43 | 36 |
| FAMILY: BLENNIES | BLENNIDAE | | | | |
| Roughhead Blenny | <i>Acanthemblemaria aspera</i> | X | | | |
| Redlip Blenny | <i>Ophioblennius atlanticus</i> | X | | | |
| Seaweed Blenny | <i>Parablennius marmoratus</i> | 2 | 2 | | |
| Sailfin Blenny | <i>Emblemaria pandionis</i> | 17 | 10 | | 7 |
| Saddled Blenny | <i>Malacoctenus triangulatus</i> | 1 | 1 | | |
| Rosy Blenny | <i>Malacoctenus macropus</i> | 2 | 2 | | |
| FAMILY: GOBIES | GOBIIDAE | | | | |

| Common Name | Taxon Scientific Name | Reef | | | |
|---------------------------|--|--------------|-------------|-------------|-------------|
| | | Total | First | Second | Third |
| Neon Goby | <i>Gobiosoma oceanops</i> | 24 | 21 | 3 | |
| Bridled Goby | <i>Coryphopterus glaucofraenum</i> | 287 | 120 | 112 | 55 |
| Goldspot Goby | <i>Gnatholepis thompsoni</i> | 3 | | 1 | 2 |
| Seminole Goby | <i>Microgobius carri</i> | 2 | 2 | | |
| Blue Goby | <i>Ioglossus calliurus</i> | 97 | 5 | 60 | 32 |
| Glass/masked Goby | <i>Coryphopterus personatus/hyalinus</i> | 1761 | 36 | 1505 | 220 |
| FAMILY: SURGEONFISHES | ACANTHURIDAE | | | | |
| Ocean Surgeon | <i>Acanthurus bahianus</i> | 1004 | 402 | 437 | 165 |
| Doctorfish | <i>Acanthurus chirurgus</i> | 154 | 64 | 28 | 62 |
| Blue tang | <i>Acanthurus coeruleus</i> | 64 | 27 | 23 | 14 |
| FAMILY: MACKERELS | SCOMBRIDAE | | | | |
| Cero | <i>Scomber regalis</i> | 1 | | 1 | |
| Spanish Mackerel | <i>Scomberomorus maculatus</i> | X | | | |
| FAMILY: SCORPIONFISH | SCORPAENIDAE | | | | |
| Spotted Scorpionfish | <i>Scorpaena plumieri</i> | 10 | 5 | 3 | 2 |
| FAMILY: Lefteye Flounders | BOTHIDAE | | | | |
| Eyed Flounder | <i>Bothus ocellatus</i> | X | | | |
| Gulf Flounder | <i>Paralichthys albigutta</i> | X | | | |
| FAMILY: LEATHERJACKETS | BALISTIDAE | | | | |
| Scrawled Filefish | <i>Aluterus scriptus</i> | 8 | 1 | 1 | 6 |
| Orangespotted Filefish | <i>Cantherhines pullus</i> | 13 | 1 | 5 | 7 |
| Fringed Filefish | <i>Monocanthus ciliatus</i> | X | | | |
| Slender Filefish | <i>Monocanthus tuckeri</i> | X | | | |
| Planehead Filefish | <i>Monocanthus hispidus</i> | 10 | 1 | 4 | 5 |
| Gray Trigger | <i>Balistes capriscus</i> | 139 | 30 | 67 | 42 |
| Queen Trigger | <i>Balistes vetula</i> | 2 | | 1 | 1 |
| Ocean Trigger | <i>Canthidermis sufflamen</i> | 1 | | | 1 |
| FAMILY: BOXFISHES | OSTRACIIDAE | | | | |
| Scrawled cowfish | <i>Lactrophrys quadricornis</i> | 4 | | 3 | 1 |
| Smooth trunkfish | <i>Lactrophrys triquetter</i> | 9 | 2 | 5 | 2 |
| Spotted Trunkfish | <i>Lactrophrys bicaudalis</i> | 1 | | | 1 |
| FAMILY: PUFFERS | TETRAODONTIDAE | | | | |
| Sharpnose Puffer | <i>Canthigaster rostrata</i> | 136 | 7 | 36 | 93 |
| Bandtail Puffer | <i>Sphoeroides spengleri</i> | 11 | 1 | 2 | 8 |
| Checkered Puffer | <i>Sphoeroides testudineus</i> | 4 | | | 4 |
| FAMILY: SPINY PUFFERS | DIODONTIDAE | | | | |
| Porcupinefish | <i>Diodon hystrix</i> | 2 | 2 | | |
| Balloonfish | <i>Diodon holocanthus</i> | 9 | 8 | 1 | |
| Striped Burrish | <i>Chilomycterus schoepfi</i> | X | | | |
| FAMILY: OCEAN SUNFISHES | MOLIDAE | | | | |
| Ocean Sunfish | <i>Mola mola</i> | X | | | X |
| Total Species | | 161 | 90 | 107 | 99 |
| Total Abundance | | 16746 | 4199 | 7613 | 4934 |

REPORT DOCUMENTATION PAGE

Form Approved
OMB No. 0704-0188

Public reporting burden for this collection of information is estimated to average 1 hour per response, including the time for reviewing instructions, searching data sources, gathering and maintaining the data needed, and completing and reviewing the collection of information. Send comments regarding this burden estimate or any other aspect of this collection of information, including suggestions for reducing this burden to Washington Headquarters Service, Directorate for Information Operations and Reports, 1215 Jefferson Davis Highway, Suite 1204, Arlington, VA 22202-4302, and to the Office of Management and Budget, Paperwork Reduction Project (0704-0188) Washington, DC 20503.

PLEASE DO NOT RETURN YOUR FORM TO THE ABOVE ADDRESS.

| | | | | | |
|---|------------------|--------------------------------------|----------------------------|--|--|
| 1. REPORT DATE (DD-MM-YYYY) 30-09-1999 | | 2. REPORT DATE September 30, 1999 | | 3. DATES COVERED (From - To) 20-07-98 to 30-09-99 | |
| 4. TITLE AND SUBTITLE Final Technical Report for the enhancement of autonomous marine vehicle testing in the South Florida Testing Facility Range. | | | | 5a. CONTRACT NUMBER | |
| | | | | 5b. GRANT NUMBER N00014-98-1-0861 | |
| | | | | 5c. PROGRAM ELEMENT NUMBER | |
| 6. AUTHOR(S) South Florida Ocean Measurement Center (SFOMC) Partners | | | | 5d. PROJECT NUMBER | |
| | | | | 5e. TASK NUMBER | |
| | | | | 5f. WORK UNIT NUMBER | |
| 7. PERFORMING ORGANIZATION NAME(S) AND ADDRESS(ES) South Florida Ocean Measurement Center (SFOMC) 101 North Beach Road Dania Beach, FL 33004 | | | | 8. PERFORMING ORGANIZATION REPORT NUMBER | |
| 9. SPONSORING/MONITORING AGENCY NAME(S) AND ADDRESS(ES) Office of Naval Research (Code 3320M) Ballston Centre Tower One 800 North Quincy Street Arlington, VA 22217-5660 | | | | 10. SPONSOR/MONITOR'S ACRONYM(S) ONR | |
| | | | | 11. SPONSORING/MONITORING AGENCY REPORT NUMBER | |
| 12. DISTRIBUTION AVAILABILITY STATEMENT Approved for public release; distribution is unlimited | | | | | |
| 13. SUPPLEMENTARY NOTES | | | | | |
| 14. ABSTRACT The purpose of this grant was to carry out the six scientific experiments on the South Florida Testing Facility (SFTF) Range. In addition to the enhancements to the range, work was performed on all six with some being successfully completed while research continues on the long term tasks. | | | | | |
| 15. SUBJECT TERMS SFOMC, AUV | | | | | |
| 16. SECURITY CLASSIFICATION OF: | | | 17. LIMITATION OF ABSTRACT | 18. NUMBER OF PAGES 190 | 19a. NAME OF RESPONSIBLE PERSON Dr. Stanley E. Dunn, P.I. |
| a. REPORT U | b. ABSTRACT U | c. THIS PAGE U | | | 19b. TELEPHONE NUMBER (Include area code) (954) 924-7265 |